THESIS CONTAINS CD/DVD

Metal alkoxides as transesterification catalysts

James E. Hobson

A thesis submitted for the degree of Doctor of Philosophy

University of York,
Department of Chemistry

September 2004

In Loving Memory

Thomas David Hobson

28th August 1946 - 20th March 2000

Marjorie Hudson

24th April 1919 - 21st December 2002

Abstract

A range of mononuclear metal alkoxide complexes have been prepared as catalysts for transesterification reactions. Cobalt (II) and zinc (II) complexes of the type $[M(TCT)(OR)]BAr_4$ were prepared (where M = Co: R = Ph, Et; Ar = Ph, 3,5-$(CF_3)_2$-C_6H_3; and where M = Zn, R = Ph; Ar = Ph, 3,5-$(CF_3)_2$-C_6H_3 (or Ar^F); TCT = *N,N',N''-cis,cis*-1,3,5-*tris*(cinnamylideneamino)cyclohexane). Three neutral titanium complexes of the type Ti(L)(O^{i}Pr) have been prepared, where L is either *tris*(2-phenoxyl)amine (TPA), *tris*({2-oxy-3,5-dimethyl}benzyl)amine (TDMA) or *tris*({2-oxy-3,5-di-*tert*-butyl}benzyl)amine (TDBA); the ligands vary in the amount of steric shielding that they provide around the titanium centre.

The complexes were tested as catalysts for transesterification, using the conversion of 2-phenyl acetic acid ethyl ester to 2-phenyl acetic acid benzyl ester, in the presence of an excess of benzyl alcohol, as a standard test reaction. The most active catalyst under the standard conditions was the complex $[Co(TCT)(OPh)]BAr^F_4$, with a turnover frequency (TOF) of 65 [±3] h^{-1} at 373 K. However, additional experiments showed that the titanium complex Ti(TDBA)(O^{i}Pr) had increased TOF values (55 [±1] h^{-1}) at lower concentration (0.05 mol%), suggesting that aggregation of the catalyst occurs at the higher concentrations.

Mechanistic studies have suggested that the transesterification reaction is catalysed by a concerted reaction between ester and alcohol at the metal centre; the metal acts as a Lewis acid, activating the carbonyl group of the ester, whilst the alkoxide ligand acts as a base, deprotonating the alcohol, allowing it to attack the carbonyl function by nucleophilic attack. Testing the mononuclear complexes as catalysts for an interesterification reaction showed no catalytic effect. Addition of small amounts of alcohol to the reaction resulted in slow conversion *via* successive transesterification reactions. This lack of activity suggests that binuclear metal complexes are necessary to catalyse the interesterification reaction.

Investigation of the reactivity of the cobalt complexes towards CO_2 has shown that the arylcarbonate absorptions in the infra-red region are shifted substantially in different solvents, providing direct spectroscopic evidence for the presence of a bound solvent molecule in the arylcarbonate complexes formed by insertion of CO_2 into the Co – OR bond.

List of contents

		Page
Abstract		3
List of contents		4
Lists of figures, schemes & tables		11
Acknowledgements		20
Author's declaration		21
Chapter 1	**Introduction**	22
1.1	Aims	22
1.2	Metal alkoxides	22
1.2.1	Bonding in metal alkoxide species	24
1.2.2	Synthesis of metal alkoxides	26
1.2.3	General aspects of metal alkoxide chemistry	28
1.2.4	Applications of metal alkoxides	30
1.2.4 a	Sharpless asymmetric epoxidation	30
1.2.4 b	Lactide polymerisation	32
1.2.4 c	CO_2 / epoxide copolymerisation	34
1.2.4 d	Polyurethane synthesis	35
1.2.4 e	Liver alcohol dehydrogenase (metal alkoxides in nature)	36
1.2.4 f	Metal oxide films	39
1.2.4 g	Sol-gel preparation of ceramics and glasses	39
1.3	Esterification processes and the use of metal alkoxides	40
1.3.1	Transesterification	40
1.3.2	Interesterification	42
1.3.3	Polyesterification	43
1.4	Lactamase enzymes	44
1.5	Fats and lipids	46
1.5.1	Fatty acids	47
1.5.2	Triglycerides	48
1.5.3	Other classes of lipids	48

1.5.4	Fats and human health	49
1.6	Commercial uses of triglyceride interesterification	49
1.7	Lipase enzymes	51
1.8	Approach	53
1.9	References	54
Chapter 2	**Synthesis and characterisation of metal complexes**	58
2.1	Ligand preparation	58
2.1.1	Amino-*tris*-phenol ligands	58
2.1.1 a	*Tris*(2-methoxyphenyl)amine	59
2.1.1 b	*Tris*(2-hydroxyphenyl) amine (TPA-H_3)	59
2.1.1 c	*Tris*{(2-hydroxy-3,5-dimethyl)benzyl}amine (TDMA-H_3)	60
2.1.1 d	*Tris*{(2-hydroxy-3,5-di-*tert*-butyl)benzyl}amine (TDBA-H_3)	60
2.1.2	Synthesis of alternative ligands for titanium complexes	61
2.1.2 a	Synthesis of *tris*{(2-benzylamino)ethylene}amine (H_3-Bz_3TREN)	61
2.1.3	Synthesis of ligands utilising *cis,cis*-1,3,5-triaminocyclohexane (TACH) as a backbone	62
2.1.3 a	*Cis,cis*-1,3,5-*tris*(cinnamylideneamino)cyclohexane (TCT)	63
2.1.3 b	*Cis,cis*-1,3-diamino-5{(4-*tert*-butyl)benzylamino}cyclohexane (BzTACH)	64
2.1.3 c	*Cis,cis*-1,3-*bis*-{(2-hydroxy-3,5-di-*tert*-butyl)benzylideneamino} -5-{(4-*tert*-butyl)benzylamino}cyclohexane ({^{t}Bu$_2$Sal-H}$_2$BzTACH)	65
2.2	Titanium complexes	65
2.2.1	Ti(TPA)(O^{i}Pr) – synthesis and characterisation	66
2.2.2	Ti(TDMA)(O^{i}Pr) – synthesis and characterisation	66
2.2.3	Ti(TDBA)(O^{i}Pr) – synthesis and characterisation	69
2.2.4	[Ti({^{t}Bu$_2$Sal}$_2$BzTACH)(O^{i}Pr)]BPh_4 – synthesis and characterisation	69
2.2.5	Ti(Bz_3TREN)(O^{n}Bu) – synthesis and characterisation	70
2.3	Cobalt complexes	70
2.3.1 a	[Co(TCT)(NO_3)]BAr_4 – synthesis and characterisation	73

2.3.1 b	$[Co(TCT)(NO_3)]BAr^F_4$ – crystallography	73
2.3.2 a	$[Co(TCT)Cl]BAr_4$ – synthesis and characterisation	75
2.3.2 b	$[Co(TCT)Cl]BAr^F_4$ – crystallography	75
2.3.3 a	$[Co(TCT)(OEt)]BAr_4$ – synthesis and characterisation	76
2.3.3 b	$[Co(TCT)(OEt)]BAr_4$ – crystallography	80
2.3.4 a	$[Co(TCT)(OPh)]BAr_4$ – synthesis and characterisation	82
2.3.4 b	$[Co(TCT)(OPh)]BAr^F_4$ – crystallography	84
2.3.5	$[Co(TCT)(OBz)]BPh_4$ – synthesis and characterisation	86
2.3.6	$[Co(\{^tBu_2Sal\}_2BzTACH)]$	88
2.4	Zinc complexes	88
2.4.1 a	$[Zn(TCT)(NO_3)]BAr_4$ – synthesis and characterisation	88
2.4.1 b	$[Zn(TCT)(NO_3)]BAr_4$ – crystallography	89
2.4.2 a	$[Zn(TCT)(OPh)]BAr_4$ – synthesis and characterisation	90
2.4.2 b	$[Zn(TCT)(OPh)]BAr_4$ – crystallography	92
2.5	Conclusions	95
2.6	References	96
Chapter 3	**Catalytic experiments**	100
3.1	Transesterification	100
3.1.1	Standard test reaction	103
3.1.2	Activities of catalysts for test reaction	104
3.1.3	Additional catalytic experiments	105
3.1.3 a	Adjusting catalyst concentration	106
3.1.3 b	Adjusting the ester / alcohol ratio	107
3.1.3 c	Moisture stability test	109
3.1.4	Mechanistic investigations	110
3.1.4 a	Interaction between metal centre and carbonyl function	110
3.1.4 b	Interaction between metal centre and alcohol	114
3.1.5	Proposed mechanism	116
3.2	Interesterification	118
3.2.1	Standard test reaction	122
3.2.2	Additional reactions	125

3.3	Discussion	125
3.3.1	Titanium complexes	125
3.3.2	Cobalt complexes	127
3.3.3	Zinc complexes	128
3.3.4	Mechanism	130
3.4	Conclusions	132
3.5	References	132
Chapter 4	**Reactivity of metal complexes towards CO_2 and CO**	135
4.1	Reactivity of metal alkoxides and related species with CO_2	135
4.2	Reaction of cobalt alkoxides with CO_2	138
4.2.1	Background – Human Carbonic Anhydrase	138
4.2.2	UV/vis spectroscopic study	142
4.2.3	Solution FTIR spectroscopic study	144
4.2.4	Attempts to isolate the carbonated species	146
4.3	Attempted reaction of titanium alkoxides with CO_2	147
4.4	Attempted reaction of cobalt alkoxides with CO	147
4.5	Conclusions	148
4.6	References	148
Chapter 5	**Future work**	151
5.1	Titanium catalysts	151
5.2	Cobalt catalysts	152
5.3	Ligand design	153
5.4	Binuclear complexes	154
5.5	Lactide polymerisation	154
5.6	References	155

Chapter 6	**Experimental**	156
6.1	General considerations	156
6.2	Instrumentation	156
6.3	Synthesis of ligand precursors	157
6.3.1	*Tris*(2-methoxyphenyl)amine	157
6.3.2	*Cis,cis*-1,3,5-cyclohexane-*tris*(benzyl carbamate)	158
6.3.3	*Cis,cis*-1,3,5-triaminocyclohexane.3HBr (TACH.3HBr)	158
6.3.4	*Cis,cis*-1,3,5-triaminocyclohexane.3CF_3SO_3H (TACH.3HOTf)	159
6.3.5	Synthesis of benzyl-TACH ligand precursor	159
6.3.5 a	*Cis,cis*-1,3,5-*tris*({4'-*tert*-butyl}benzylideneamino) cyclohexane (TBT)	159
6.3.5 b	{R-1-[(*Z*)-{4'-*tert*-butyl}benzylideneamino]-3,5-diamino cyclohexane}$Ni^{II}(NO_3)_2$ [Ni(MBT)$(NO_3)_2$]	160
6.3.5 c	(1-{(4'-*tert*-butyl)benzylamino}-3,5-diaminocyclohexane) $Ni^{II}(NO_3)_2$ [Ni(BzTACH)$(NO_3)_2$]	160
6.3.5 d	*Cis,cis*-1-{(4'-*tert*-butyl)benzylamino}-3,5-diamino cyclohexane (BzTACH)	160
6.4	Synthesis of ligands	161
6.4.1	*Tris*{(2-hydroxy)phenyl}amine (TPA-H_3)	161
6.4.2	*Tris*{(2-hydroxy-3,5-dimethyl)benzyl}amine (TDMA-H_3)	161
6.4.3	*Tris*{(2-hydroxy-3,5-di-*tert*-butyl)benzyl}amine (TDBA-H_3)	162
6.4.4	*Tris*{(2-benzylamino)ethylene}amine (H_3-Bz_3TREN)	162
6.4.5	Attempted synthesis of *tris*{(2-mercapto-3,5-dimethyl) benzyl}amine (TDMMA-H_3)	163
6.4.6	*Cis,cis*-1,3,5-*tris*(*E,E*-cinnamylideneamino)cyclohexane (TCT)	163
6.4.7	Synthesis of *cis,cis*-1,3-*bis*-cinnamylideneamino-5-{(4-*tert*-butyl)benzylamino}cyclohexane (Cin_2BzTACH)	164
6.4.8	*Cis,cis*-1,3-*bis*{(2-hydroxy-3,5-di-*tert*-butyl)benzylideneamino} -5-{(4-*tert*-butyl)benzylamino}cyclohexane ({$^tBu_2$Sal-H}$_2$BzTACH)	164
6.5	Synthesis of titanium complexes	165
6.5.1	Ti(TPA)(O^iPr)	165

6.5.2	Ti(TDMA)(O^iPr)	165
6.5.3	Ti(TDBA)(O^iPr)	166
6.5.4	[Ti({$^tBu_2Sal$}$_2$BzTACH)(O^iPr)]BPh_4	166
6.5.5	$TiCl_3(O^nBu)$	167
6.5.6	Ti(Bz_3TREN)(O^nBu)	167
6.6	Synthesis of cobalt complexes	168
6.6.1	[Co(TCT)(NO_3)]BPh_4	168
6.6.2	[Co(TCT)Cl]BPh_4	168
6.6.3	[Co(TCT)(OEt)]BPh_4	169
6.6.4	[Co(TCT)(OPh)]BPh_4	170
6.6.5	[Co(TCT)(OBz)]BPh_4	170
6.6.6	[Co(TCT)(NO_3)]$BAr^F{}_4$	171
6.6.7	[Co(TCT)Cl]$BAr^F{}_4$	172
6.6.8	[Co(TCT)(OEt)]$BAr^F{}_4$	172
6.6.9	[Co(TCT)(OPh)]$BAr^F{}_4$	173
6.6.10	[Co({$^tBu_2Sal$}$_2$BzTACH)]	174
6.7	Synthesis of zinc complexes	174
6.7.1	[Zn(TCT)(NO_3)]BPh_4	174
6.7.2	[Zn(TCT)(OPh)]BPh_4	175
6.7.3	[Zn(TCT)(NO_3)]$BAr^F{}_4$	176
6.7.4	[Zn(TCT)(OPh)]$BAr^F{}_4$	176
6.8	Preparation of $NaBAr^F{}_4$	177
6.9	Catalytic experiments	178
6.9.1	Sample procedure for titanium-catalysed interesterification	178
6.9.2	Sample procedure for cobalt-catalysed transesterification	178
6.10	CO_2 sequestration experiments	179
6.10.1	Reversible reaction of CO_2 with [Co(TCT)(OEt)]BPh_4	179
6.10.2	Reaction of CO_2 with [Co(TCT)(OPh)]BPh_4 in CD_3CN	179
6.11	References	179

Appendix	**Crystallographic data**	181
A1	Crystal data and structure refinement for [Co(TCT)(NO_3)] $BAr^F_4 \cdot CH_2Cl_2 \cdot 1½\ c\text{-}C_6H_{12}$.	205
A2	Crystal data and structure refinement for [Co(TCT)Cl]BAr^F_4.	216
A3	Crystal data and structure refinement for [Co(TCT)(OEt)] $BPh_4 \cdot ½$ EtOH.	226
A3 a	Personal communication from Dr. Stephen J. Archibald – concerning the structure of the [disordered] solvent molecule.	232
A4	Crystal data and structure refinement for [Co(TCT)(OPh)]BAr^F_4.	233
A5	References	239

Publications 217

"Preparation of cationic cobalt phenoxide and ethoxide complexes and their reversible reaction with carbon dioxide", Stephen J. Archibald, Simon P. Foxon, Jonathan D. Freeman, James E. Hobson, Robin N. Perutz and Paul H. Walton, *J. Chem. Soc., Dalton Trans.*, 2002, 2797. 218

Definitions 221

List of abbreviations 221

Journal abbreviations 226

Supplementary Data

A compact disc containing complete crystallographic data, additional appendices and an electronic version of this thesis is provided in a pocket on the front inside cover.

Lists of figures, schemes & tables

List of figures

Chapter 1

Figure 1.1: Schematic of different bonding characters possible for metal alkoxides (terminal alkoxide ligand).

Figure 1.2: Bonding modes observed for metal alkoxides.

Figure 1.3: Bridging modes for alkoxide ligands.

Figure 1.4: Schematic diagram showing the structure of a dimeric cobalt (II) alkoxide and titanium tetra-alkoxides.

Figure 1.5: Range of insertion reactions displayed by metal alkoxides.

Figure 1.6: Examples of reactivity exhibited by $W_2(OR)_6$ species.

Figure 1.7: Chiral ligand used for Sharpless asymmetric epoxidation.

Figure 1.8: Enantiofacial selectivity of Sharpless epoxidation catalyst.

Figure 1.9: Example of specificity for allylic alkene functions.

Figure 1.10: Common lactide monomers and their associated polymers.

Figure 1.11: Lactide polymerisation catalyst, and proposed mechanism, from M. H. Chisholm & N. W. Eilerts, *Chem. Commun.*, 1996, 853.

Figure 1.12: CO_2 / epoxide copolymerisation mechanism proposed by Darensbourg.

Figure 1.13: Formation of generic polyurethane.

Figure 1.14: Conversion of ethanol to ethanal, catalysed by LADH.

Figure 1.15: Active site of LADH, showing the preorganisation of NAD^+ for hydride abstraction from ethoxide ligand.

Figure 1.16: Coordination sphere of Zn at the active site of LADH (A), and a structural model by Berreau (B).

Figure 1.17: Structural mimics of LADH by Parkin (A) and Vahrenkamp (B).

Figure 1.18: General transesterification reaction.

Figure 1.19: Transesterification reaction driven by tautomerisation of liberated vinyl alcohol

Figure 1.20: Transesterification of dimethyl terephthalate with ethylene glycol.

Figure 1.21: Nickel aryloxide complexes, one including hydrogen-bonded phenol (B).

Figure 1.22: General interesterification reaction.

Figure 1.23: Formation of poly(ethylene terephthalate).

Figure 1.24: Schematic diagram of the active site of zinc-β-lactamase from *Bacillus cereus*.

Figure 1.25: Proposed global catalytic cycle for zinc-β-lactamase from *Bacillus cereus*.

Figure 1.26: Saturated / unsaturated fatty acids, *cis* vs. *trans* conformation.

Figure 1.27: Tripalmitylglycerolate as an example of a triacylglycerolate.

Figure 1.28: Resulting mixture of triglycerides from random interesterification.

Figure 1.29: Schematic views of lipase enzyme from *Mucor miehei*, showing lid closed (A) and open (B). Adapted from original.

Figure 1.30: Steps in the catalytic cycle of lipase from *Rhizopus oryzae*.

Figure 1.31: Titanium alkoxide complexes using tetradentate ligands; vacant coordination site indicated.

Chapter 2

Figure 2.1: Synthesis of *tris*(2-methoxyphenyl)amine.

Figure 2.2: Synthesis of *tris*(2-hydroxyphenyl)amine (TPA-H_3).

Figure 2.3: Synthesis of *tris*{(2-hydroxy-3,5-dialkyl)benzyl}amine [alkyl = Me (TDMA-H_3), ^{t}Bu (TDBA-H_3)].

Figure 2.4: Synthesis of H_3-Bz_3TREN.

Figure 2.5: Synthesis of TACH.3HOTf.

Figure 2.6: Synthesis of TCT.

Figure 2.7: Synthesis of BzTACH.

Figure 2.8: Synthesis of alternate N_3O_2 ligand using BzTACH as a backbone.

Figure 2.9: Synthesis of Ti(TPA)(O^iPr).

Figure 2.10: Synthesis of Ti(TDMA)(O^iPr) [R = Me] and Ti(TDBA)(O^iPr) [R = ^{t}Bu].

Figure 2.11: ^{1}H NMR spectrum of Ti(TDMA)(O^iPr) in C_6D_6 (300 MHz, 298 K).

Figure 2.12: Fluxional behaviour of Ti(TDMA)(O^iPr) on the NMR timescale.

Figure 2.13: UV/vis spectra of Ti(TDMA)(O^iPr) and Ti(TDBA)(O^iPr) in CH_2Cl_2 / ^{i}PrOH (9:1, *v*/*v*).

Figure 2.14: Synthesis of [Ti(Sal_2BzTACH)(O^iPr)]BPh_4.

Figure 2.15: Synthesis of cobalt-TCT complexes.

Figure 2.16: Cobalt-TCT-alkoxide complexes, as prepared by Freeman.

Figure 2.17: Reactivity displayed by $[Co(TCT)(OEt)]BPh_4$.

Figure 2.18: An ORTEP representation (30% probability ellipsoids) of $[Co(TCT)(NO_3)]BAr^F{}_4$, cation only, H atoms omitted for clarity.

Figure 2.19: An ORTEP representation (30% probability ellipsoids) of $[Co(TCT)Cl]BAr^F{}_4$, cation only, H atoms omitted for clarity.

Figure 2.20: UV/vis spectra of the complexes $[Co(TCT)(OR)]BPh_4$. (a) R = Et, solvent: CH_2Cl_2 / EtOH (9:1, *v/v*). (b) R = Ph, solvent: CH_2Cl_2. (c) R = Bz, solvent = CH_2Cl_2 / BzOH (9:1, *v/v*).

Figure 2.21: Proton labels for $[Co(TCT)(OEt)]^+$ (BPh_4 & $BAr^F{}_4$ analogues).

Figure 2.22: ^1H NMR spectrum of $[Co(TCT)(OEt)]BPh_4$ in CD_2Cl_2 / d_6-EtOH recorded at 295 K and 300 MHz (low chemical shift region).

Figure 2.23: ^1H NMR spectrum of $[Co(TCT)(OEt)]BPh_4$ in CD_2Cl_2 / d_6-EtOH recorded at 295 K and 300 MHz (high chemical shift region).

Figure 2.24: An ORTEP representation (30% probability ellipsoids) of $[Co(TCT)(OEt)]BPh_4$, cation only, H atoms omitted for clarity.

Figure2.25: Proton labels for $[Co(TCT)(OPh)]^+$ (BPh_4 & $BAr^F{}_4$ analogues).

Figure 2.26: ^1H NMR spectrum of $[Co(TCT)(OPh)]BAr^F{}_4$ recorded in CD_2Cl_2 at 295 K and 300 MHz (low chemical shift region).

Figure 2.27: ^1H NMR spectrum of $[Co(TCT)(OPh)]BAr^F{}_4$ recorded in CD_2Cl_2 at 295 K and 300 MHz (high chemical shift region).

Figure 2.28: An ORTEP representation (30% probability ellipsoids) of $[Co(TCT)(OPh)]BAr^F{}_4$, cation only, H atoms omitted for clarity.

Figure 2.29: Proton labels for $[Co(TCT)(OBz)]BPh_4$.

Figure 2.30: ^1H NMR spectrum of $[Zn(TCT)(OPh)]BAr^F{}_4$.

Figure 2.31: An ORTEP representation (30% probability ellipsoids) of $[Zn(TCT)(OPh)]BPh_4$, cation only, H atoms omitted for clarity.

Figure 2.32: ORTEP representation (30% probability ellipsoids) of $[Zn(TCT)(OPh)]BAr^F{}_4$, cation only, H atoms omitted for clarity.

Figure 2.33: View of the crystal lattice for $[Zn(TCT)(OPh)]BPh_4 \cdot ½\ C_6H_{12}$.

Figure 2.34: View of the crystal lattice of $[Zn(TCT)(OPh)]BAr^F{}_4 \cdot C_6H_{12}$.

Chapter 3

Figure 3.1: Proposed transesterification mechanism for distannoxane catalysts.

Figure 3.2: Trans-esterification test reaction.

Figure 3.3: Proton signals used for monitoring transesterification reaction.

Figure 3.4: Reaction profiles for trans-esterification reaction.

Figure 3.5: Dependence of catalyst activity on concentration.

Figure 3.6: Effect of alcohol: ester ratio on catalyst activity.

Figure 3.7: Possible coordination modes between metal centres and carbonyl functions (including bimetallic interactions).

Figure 3.8: Overlaid UV/vis spectra showing the addition of 2-phenyl acetic acid ethyl ester to a solution of $[Co(TCT)(OEt)]BPh_4$ in CH_2Cl_2 / EtOH (9:1, *v/v*).

Figure 3.9: Overlaid UV/vis spectra showing the addition of 2-pentanone to a solution of $[Co(TCT)(OEt)]BPh_4$ in CH_2Cl_2 / EtOH (9:1, *v/v*).

Figure 3.10: Overlaid UV/vis spectra showing the addition of extra solvent to a solution of $[Co(TCT)(OEt)]BPh_4$ in CH_2Cl_2 / EtOH (9:1, *v/v*) – Control experiment.

Figure 3.11: Overlaid UV/vis spectra of $[Co(TCT)(OEt)]BAr^F_4$ dissolved in 9:1, *v/v* mixtures of carbonyl species and ethanol.

Figure 3.12: Overlaid UV spectra of $Ti(TDBA)(O^iPr)$ in CH_2Cl_2, with the addition of 2-phenyl acetic acid ethyl ester and the consequent changes in the bands.

Figure 3.13: Overlaid UV spectra of $Ti(TDBA)(O^iPr)$ in CH_2Cl_2, with the addition of 2-pentanone and the consequent changes in the bands.

Figure 3.14: Alkoxide / alcohol exchange for Ti complexes (two phenolate "arms" abbreviated for simplicity).

Figure 3.15: Proposed intermediate for transesterification reaction as catalysed by metal alkoxide complexes.

Figure 3.16: Proposed catalytic cycle for transesterification reaction as catalysed by metal alkoxide complexes.

Figure 3.17: Possible mechanisms proposed for ester hydrolysis by Zn complex

Mechanism 1: Attack by hydroxide

Mechanism 2: Attack by alkoxide

Figure 3.18: Mechanism for alkali-metal alkoxide catalysed interesterification, proposed by Gagné *et al.*

Figure 3.19: Catalytic cycle for interesterification, intermediates not shown.

Figure 3.20: Interesterification mechanism proposed by Jackman *et al.*

Figure 3.21: Test reaction for interesterification.

Figure 3.22: Proton signals used for monitoring interesterification reaction.

Figure 3.23: Effect of alcohol addition to interesterification reaction.

Figure 3.24: Proposed catalytic cycle for alcohol-assisted interesterification (intermediate species not shown).

Figure 3.25: Hydrophobic cavities provided by Ti(TDMA)(O^{i}Pr) & Ti(TDBA)(O^{i}Pr).

Figure 3.26: Possible route for decomposition of zinc ethoxide complex.

Chapter 4

Figure 4.1: Insertion of CO_2 into the M – N bonds of group 4 & 5 metal amides.

Figure 4.2: Insertion of CO_2 into the M – N bonds of di-tungsten amides.

Figure 4.3: Carboxylative cyclisation of dienes, racemic and enantioselective.

Figure 4.4: σ-bonding (A) and π-bonding (B) modes of coordination between CO_2 and a metal centre.

Figure 4.5: A schematic diagram of the active site of HCA II.

Figure 4.6: Catalytic cycle for the hydration of carbon dioxide by HCA II.

Figure 4.7: Funnel complexes prepared by Reinaud *et al.*

Figure 4.8: Model complex for formation of hydrogen-bonded solvent molecules.

Figure 4.9: Schematic representations of different modes of nitrate binding to cobalt centre, along with hydrogen-bonded solvent chains.

Figure 4.10: Cobalt alkoxide complexes prepared by Freeman, and their reactivity with CO_2.

Figure 4.11: Visible spectra showing reversible reaction of [Co(TCT)(OEt)]BPh_4 with CO_2 in CH_2Cl_2 / EtOH (9:1, *v*/*v*).

Figure 4.12: Coordination modes of alkyl / aryl-carbonate ligand to metal centres.

Figure 4.13: Solution FTIR spectrum of [Co(TCT)(OPh)]BPh_4 in CD_3CN, before and after addition of CO_2.

Figure 4.14: Solution FTIR spectrum of [Co(TCT)(OPh)]BPh_4 + CO_2 in CD_3CN – difference spectrum.

Figure 4.15: Insertion of CO into the M – O bond.

Chapter 5

Figure 5.1: Modification of titanium coordination catalysts to enable immobilisation on a solid support.

Figure 5.2: Possible approaches to the preparation of polymers containing titanium alkoxide functionalities.

Figure 5.3: Proposed method for immobilising metal-TCT alkoxide complexes within a polystyrene support; method developed by Lusby.

Figure 5.4: Hydroxy-acid derivatives used successfully in titanium chemistry; A: diethyl tartrate, B: ammonium lactate, C: sodium citrate.

Figure 5.5: Possible intermediates in the trans-esterification reaction, as catalysed by titanium tetra-alkoxides.

Chapter 6

Figure 6.1: Proton labels for $[Co(TCT)(X)]^+$, X = Cl, NO_3.

Figure 6.2: Proton labels for $[Co(TCT)(OEt)]^+$.

Figure 6.3: Proton labels for $[Co(TCT)(OPh)]^+$.

Figure 6.4: Proton labels for $[Co(TCT)(OBz)]^+$.

Figure 6.5: Proton labels for $[Zn(TCT)(NO_3)]^+$.

Figure 6.6: Proton labels for $[Zn(TCT)(OPh)]^+$.

Appendix

Figure A1.1: An ORTEP representation (30% probability ellipsoids) of $[Co(TCT)(NO_3)]BAr^F_4 \cdot CH_2Cl_2 \cdot 1½\ c\text{-}C_6H_{12}$, cation only, H atoms omitted for clarity.

Figure A1.2: An ORTEP representation (30% probability ellipsoids) of $[Co(TCT)(NO_3)]BAr^F_4 \cdot CH_2Cl_2 \cdot 1½\ c\text{-}C_6H_{12}$, H atoms omitted for clarity.

Figure A2.1: An ORTEP representation (30% probability ellipsoids) of $[Co(TCT)(Cl)]BAr^F_4$, cation only, H atoms omitted for clarity.

Figure A2.2: An ORTEP representation (30% probability ellipsoids) of [Co(TCT)(Cl)]BAr^F_4, H atoms omitted for clarity.

Figure A3.1: An ORTEP representation (30% probability ellipsoids) of [Co(TCT)(OEt)]$BPh_4 \cdot ½$ EtOH, H atoms omitted for clarity.

Figure A3.2: An ORTEP representation (30% probability ellipsoids) of [Co(TCT)(OEt)]$BPh_4 \cdot ½$ EtOH, H atoms omitted for clarity.

Figure A4.1: An ORTEP representation (30% probability ellipsoids) of [Co(TCT)(OPh)]BAr^F_4, cation only, H atoms omitted for clarity.

Figure A4.2: An ORTEP representation (30% probability ellipsoids) of [Co(TCT)(OPh)]BAr^F_4, H atoms omitted for clarity.

List of Schemes

Chapter 3

Scheme 3.1: Suggested aggregation behaviour for titanium species.

Scheme 3.2: Overall interesterification via two successive transesterification reactions.

Chapter 4

Scheme 4.1: Insertion of CO_2 into the M – O bonds of group 2 metal alkoxides.

Scheme 4.2: Amine-catalysed CO_2 fixation.

List of Tables

Chapter 1

Table 1.1: Predicted molecular association of metal alkoxides (adapted from Bradley *et al.*, *J. Chem. Soc.*, 1953, 2025).

Chapter 2

Table 2.1: Selected bond lengths (/ Å) and angles (/ °) for $[Co(TCT)(NO_3)]^+$ in $[Co(TCT)(NO_3)]BAr^F_4 \cdot 1½\ C_6H_{12} \cdot CH_2Cl_2$.

Table 2.2: Selected bond lengths (/ Å) and angles (/ °) for $[Co(TCT)Cl]^+$ species.

Table 2.3: Assignment of ^1H NMR peaks for $[Co(TCT)(OEt)]^+$.

Table 2.4: Selected bond lengths (/ Å) and angles (/ °) for $[Co(TCT)(OEt)]BPh_4$; values for $[Co(TCT)(OPh)]\ BPh_4$ are included for comparison.

Table 2.5: Assignment of ^1H NMR spectra for $[Co(TCT)(OPh)]BAr_4$, recorded at 295 K and 300 MHz in CD_2Cl_2. [*: Hidden under BPh_4 signal]

Table 2.6: Selected bond lengths (/ Å) and angles (/ °) for $[Co(TCT)(OPh)]^+$.

Table 2.7: UV/vis peaks for $[Co(TCT)(OR)]BPh_4$.

Table 2.8: Assignment of ^1H NMR peaks for $[Co(TCT)(OBz)]^+$; assignments for $[Co(TCT)(OPh)]^+$ included for comparison.

Table 2.9: ^1H NMR assignments for $[Zn(TCT)(OPh)]BAr_4$.

Table 2.10: Selected bond lengths (/ Å) and angles (/ °) for $[Zn(TCT)(OPh)]BAr_4$, with data for $[Co(TCT)(OPh)]BPh_4$ presented for comparison.

Chapter 3

Table 3.1: Observed transesterification activities for the standard test reaction.

Table 3.2: Activities for different catalyst concentrations.

Table 3.3: Effect of altering ester / alcohol ration on catalytic activity.

Table 3.4: Observed equilibrium constants for alcohol / alkoxide exchange.

Table 3.5: Catalytic activities for interesterification.

Table 3.6: Effect of addition of alcohol to inter-esterification reaction.

Appendix

Table A1.1: Bond lengths (/ Å) and angles (/ °) for $[Co(TCT)(NO_3)]BAr^F_4 \cdot CH_2Cl_2 \cdot 1½\ c\text{-}C_6H_{12}$.

Table A2.1: Bond lengths (/ Å) and angles (/ °) for $[Co(TCT)Cl]BAr^F_4$.

Table A3.1: Bond lengths (/ Å) and angles (/ °) for $[Co(TCT)(OEt)]BPh_4 \cdot ½\ EtOH$.

Table A4.1: Bond lengths (/ Å) and angles (/ °) for $[Co(TCT)(OPh)]BAr^F_4$.

Acknowledgements

A big thanks to all my family and friends for continued support throughout!

I would like to thank my supervisors Robin Perutz, Paul Walton and Bruno Stengel, and my independent panel member Fran Kerton, for their constant encouragement and helpful suggestions, and also Jon Freeman, whose work formed the foundation for much of this thesis.

Thanks to all the students, post-docs, academics & visitors for making the laboratory and office a pleasant working environment, especially to: Naser, Iman, Anders, Daniele, Meike, Suzanne, Richard, Jake, Libby, Nuria, Eleonora, Jennifer, Rodrigo, Ciara, Sebastien, Marius, Fernando, Beatriz, Phil, Khordad, Cyril, Jenny, Damir, Simon, Chris, Nick, Kirsten, Charlotte, John, Stuart, Anne Duhme-Klair, David, Simon, Helen, Clive, Craig, Matthew, Matt, Mike, Sean, Jane, Jessica, Emma, Laura, Phil Palmer, Dave, Charlotte W, Shohreh, Jason Lynam, Iain, Alistair, Yohann, Pip, Guy, Simon, Peter & Steve. Thanks to Ramon Hendricx for training on the GC. Apologies to anyone I missed!

Thanks to Jan, Callum, Martin, Richard, David, Eric, Graham & everyone else at the Synetix research labs.

Thanks to all of the technical staff: Steve Hau, Derek Barratt, Mike, John & Val (stores), Steve Moehr and Brian Smith (glassblowers), Terry Chamberlain and Chris Mortimer (workshops), Ben Glennie (NMR & mass spectrometry), Trevor Dransfield (mass spectrometry) and Adrian Whitwood (crystallography). Thanks to Heather Fish for the NMR training, and to Stephen Archibald (University of Hull) for additional crystallography whilst we had no diffractometer of our own.

Thanks to the administrative staff: Karen Whiteley, Karen Prescott, Jean Humpherson, Deborah Turner, May Price & Catherine Garcia.

I also wish to acknowledge the Engineering & Physical Sciences Research Council (EPSRC) and Synetix / Johnson Matthey PLC for their financial support of this CASE award studentship.

Author's declaration

Except where specific reference has been made to other sources, the work in this thesis is the work of the author. It has not been submitted, in whole or in part, for any other degree. Some of the results have already been published in a research journal, and have also been presented at conferences in the form of posters, conference proceedings and an oral presentation.

James Hobson

September 2004

Chapter 1: Introduction

1.1 Aims

The aim of this project was to develop a new metal-based industrial catalyst for the interesterification of triglycerides, to be used by Synetix (Johnson-Matthey PLC). Currently, sodium methoxide is the most commonly used metal-based catalyst in industry. Whilst cheap and effective, sodium methoxide gives undesirable side products, which must be removed prior to consumption, adding to production costs. The new catalyst would need to be more selective and, ideally, recoverable. It was also envisaged that such a catalyst might have applications in general transesterification processes, and that mechanistic information might be obtained from the study, thereby increasing understanding of transesterification processes, and aiding in the design of future catalysts. Synetix's expertise in titanium chemistry suggested that titanium alkoxides would be a particularly suitable basis for the new technology. A secondary aim was to engineer the catalyst(s) to give selectivity for exchange at the 1- and 3-positions of triglycerides. This feature would allow the catalyst to compete effectively with lipase enzymes, which must normally be used when selectivity is required.[1]

1.2 Metal alkoxides

Metal alkoxide complexes have been used exclusively for the catalytic investigations described in this thesis. Metal alkoxides are species containing the M – O – C moiety, where C is part of an alkyl or aryl group, and are known for almost all of the transition metals.[2] Many examples of homoleptic metal alkoxides and aryloxides have been prepared; due to the tendency of the alkoxide ligand to form bridges between metal centres, these are frequently polynuclear species, especially in low-valent metals (see Section 1.2.1). For instance, the homoleptic manganese and iron alkoxides $[M\{O(2,4,6\text{-}^tBu_3\text{-}C_6H_2)\}_2]_2$ are dimers despite the significant steric bulk of the aryloxide ligands,[3] as are the cobalt alkoxides discussed below. Increasing the steric bulk around metals of higher valency can enforce a monomeric species, since the metal is more coordinatively congested; for example, $[Ti(OR)_4]$ (where R = Me, Et) is found to be tetrameric in the solid state, whereas the behaviour of $Ti(O^iPr)_4$ depends strongly

upon the solvation conditions; an early study concluded that it is monomeric,[4] whereas a more recent study using IR spectroscopy concluded that it exists as an equilibrium between monomer, dimer and trimer,[5] with association being strongest in the neat material. Bradley proposed a series of rules to predict the molecular association of metal alkoxides,[6] which are summarised in Table 1.1. Heterometallic alkoxides, containing two or more different metals held together by alkoxide bridges, have been recognised since 1924,[7] but it is only quite recently that concerted efforts have been made to investigate their properties and explore their potential as catalysts and structural material precursors.[8]

Metal alkoxide $M(OR)_n$	Coordination number of M	Stereochemistry of M	Minimum degree of association
MOR	2	OMO = 180°	2
	2	OMO = 120°	3
	3	Pyramidal	4
$M(OR)_2$	3	Planar One OMO = 90°	2
	3	Planar, OMO = 120°	3
	4	Tetrahedral	3
	4	Square planar	4
	6	Octahedral	Infinite 3-D polymer
$M(OR)_3$	4	Tetrahedral	2
	4	Square planar	2
	4 and 6	Tetrahedral & Octahedral	4
	6	Octahedral	8
$M(OR)_4$	5	Trigonal bipyramidal	2
	6	Octahedral	3
	8	Cubic	4
$M(OR)_5$	6	Octahedral	2
	8	Cubic	4
$M(OR)_6$	8	Cubic	2

Table 1.1: Predicted molecular association of metal alkoxides (adapted from Bradley *et al.*, *J. Chem. Soc.*, 1953, 2025).

1.2.1 Bonding in metal alkoxide species

The alkoxide ligand, and the related aryloxide ligand, both bear a formal negative charge. The bonding between the alkoxide ligand and the metal centre can be described as somewhere between the extreme cases of ionic bonding and covalent bonding, depending on the formal oxidation state and electropositivity of the metal centre (Figure 1.1).

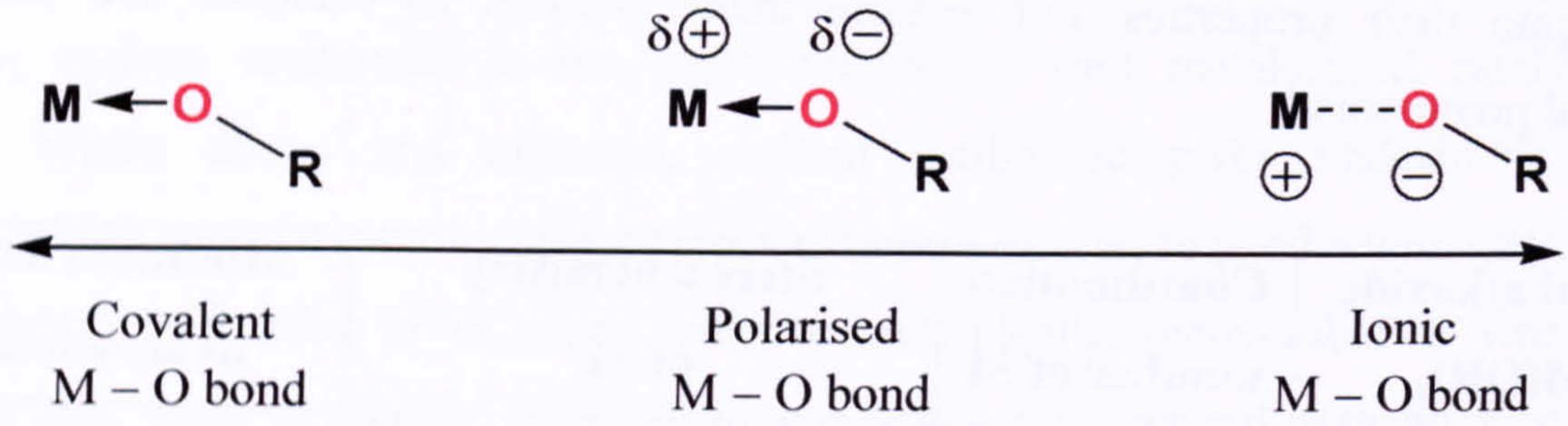

Figure 1.1: Schematic of different bonding characters possible for metal alkoxides (terminal alkoxide ligand).

For instance, titanium tetra-alkoxides, $Ti(OR)_4$, can be considered to have appreciable covalent character in their Ti – O bonds, due to the highly polarising nature of Ti^{IV}. All metal alkoxides, without exception, have polarised M – O bonds, and this is the basis of their reactivity and many of their applications (Section 1.2.4). Despite the polarity of the M – O bond, most metal alkoxides are relatively soluble in nonpolar organic solvents and show a degree of volatility, which is consistent with covalent compounds.

The alkoxide ligand donates two electrons to the metal centre via a σ-interaction, but is also capable of acting as a π-donor,[9] contributing additional electron density to the metal centre through one, or even two, lone pair(s) of electrons in vacant p-orbitals, into vacant metal d-orbitals of appropriate symmetry and energy (Figure 1.2). It should be noted that, in the case of aryloxide ligands, this contribution is limited by the competing effect of the aromatic ring pulling electron density towards it, although electron deficient metals are still capable of inducing strong π-donor character (for instance, Ti – O – C bond angles in $Ti\{OAr\}_4$ can approach 165°).[10] Increase of bond angles toward linear, coupled with a shortening of the M – O bond, are the key indicators of π-donor character; where a metal alkoxide species can be characterised crystallographically, these data can be compared easily with other metal alkoxides. However, this model of bonding has been disputed by Kaltsoyannis *et al.*,[11] particularly

in the case of lanthanide alkoxides; they argue that the bonding is predominantly ionic in nature.

σ- or π-bonding?

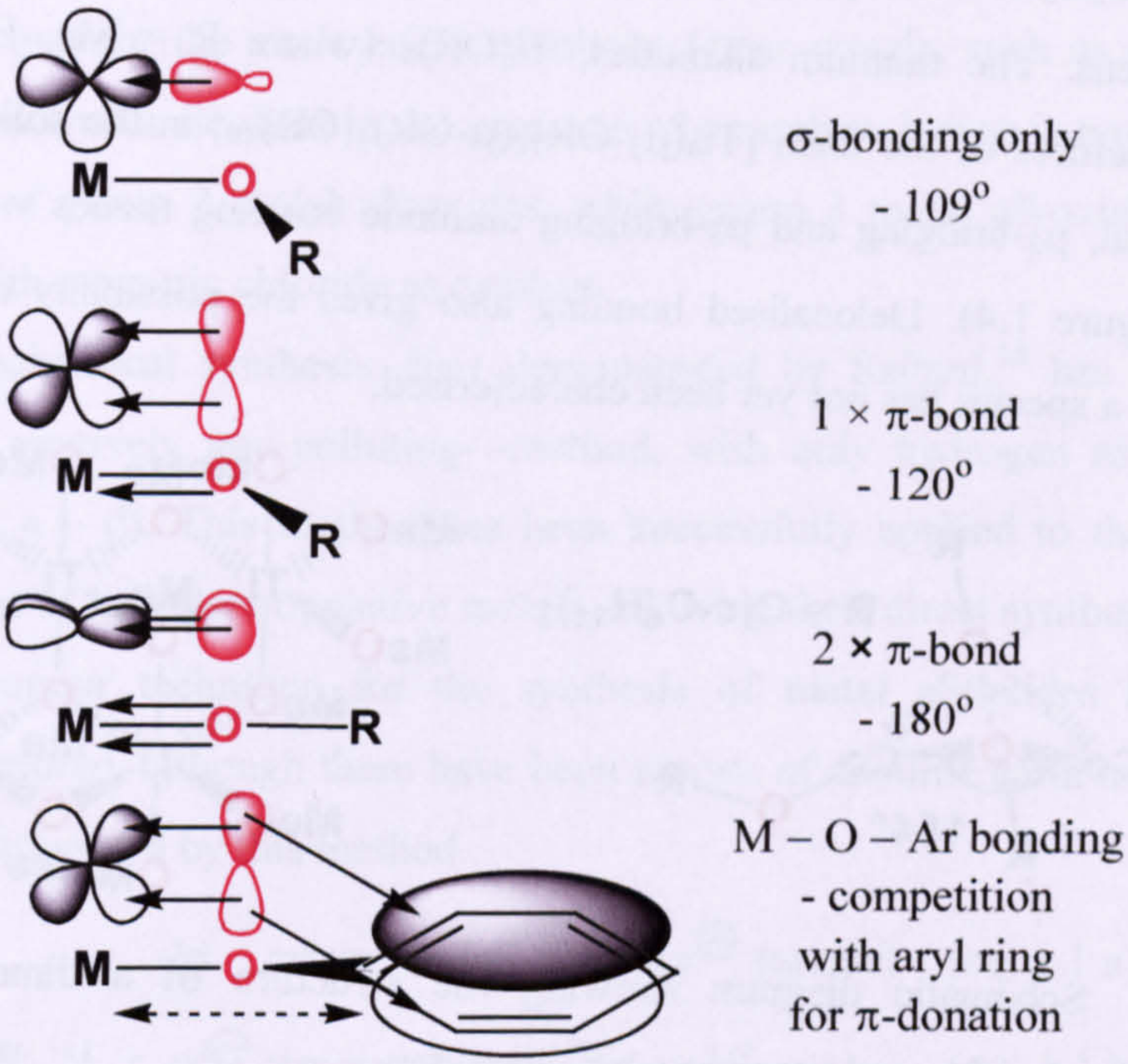

Figure 1.2: Bonding modes observed for metal alkoxides.

Note that the above examples describe the bonding of a *terminal* alkoxide ligand. The alkoxide ligand can also act as a bridging ligand between two or even three metal centres (Figure 1.3). In addition to donating electrons to metal atoms through σ-bonding, an alkoxide ligand bridging between two metal centres can also contribute additional electron density from their filled p-orbitals into available d-orbitals of other metal atoms; these interactions can be localised, giving distinct differences in bond strengths and discernible π-bonding interactions, or the bonding can be delocalised, giving a symmetrical arrangement.

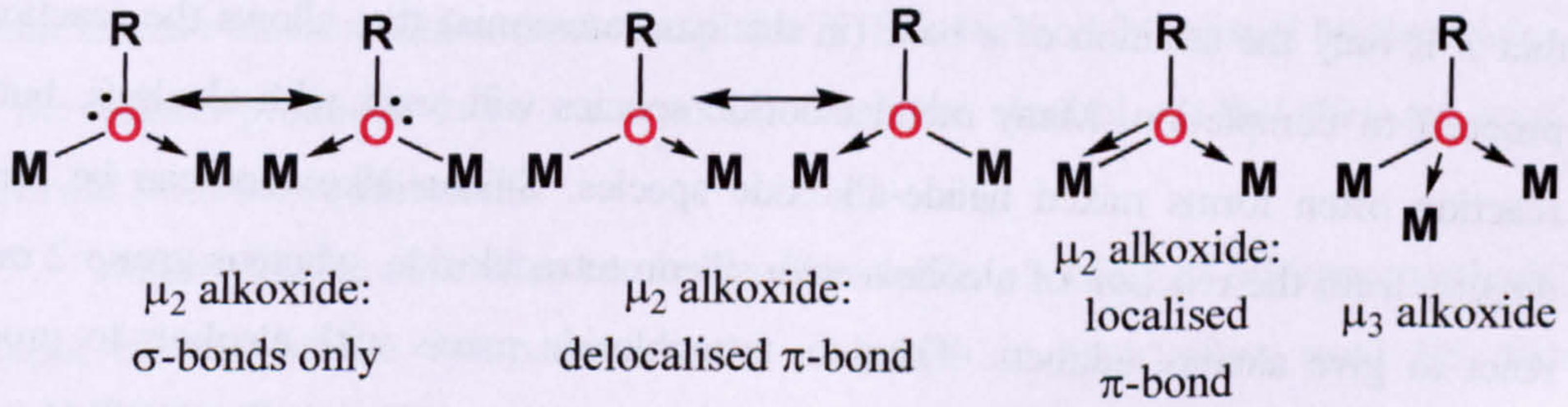

Figure 1.3: Bridging modes for alkoxide ligands.

For example, $[Co(OC\{C_6H_{11}\}_3)(\mu_2\text{-}OC\{C_6H_{11}\}_3)]_2$ displays very little difference in the bond angles between the oxygen and cobalt atoms, suggesting delocalised bonding; the Co_2O_2 core adopts a butterfly conformation, bent along the axis of the two bridging oxygens. The titanium alkoxides, $Ti(OR)_4$ (where R = Me, Et, ^{n}Pr) adopt tetrameric structures of the form $[Ti_4(\mu_3\text{-}OR)_2(\mu\text{-}OR)_4(OR)_{10}]$ in the solid state, which display terminal, μ_2-bridging and μ_3-bridging alkoxide bonding modes within the same aggregate (Figure 1.4). Delocalised bonding also gives the possibility of μ_4-bridging, although such a species has not yet been characterised.

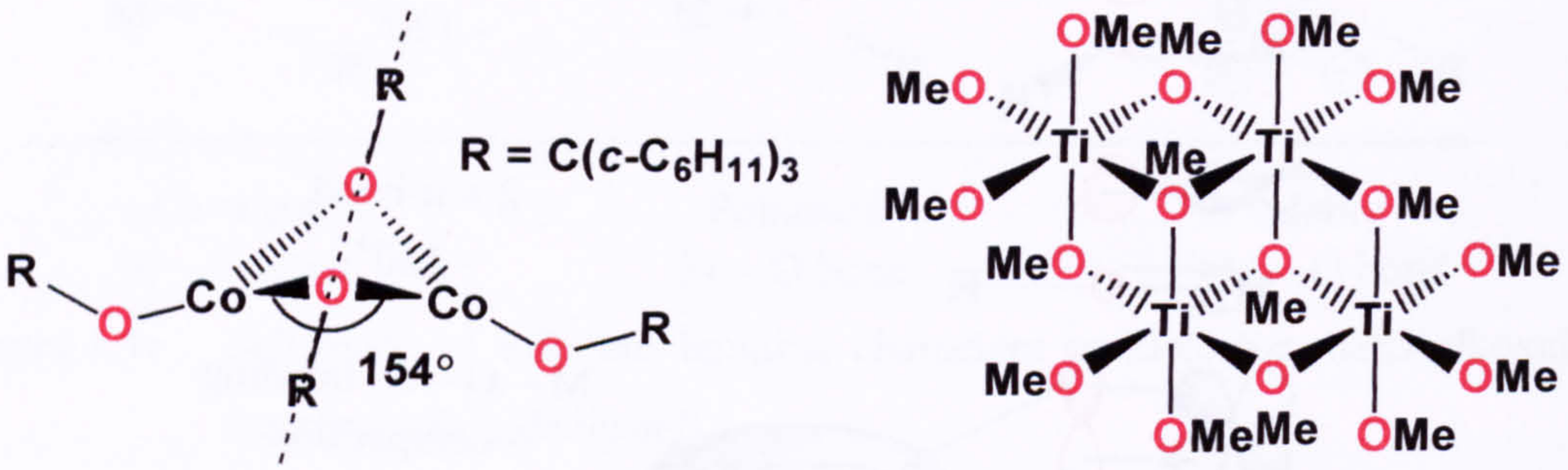

Figure 1.4: Schematic diagram showing the structure of a dimeric cobalt (II) alkoxide and titanium tetra-alkoxides.

1.2.2 Synthesis of metal alkoxides

A variety of methods are known for the synthesis of homoleptic metal alkoxides, some of which are used only for research purposes, whilst others are sufficiently practical and economical for large-scale commercial production. Titanium alkoxides, for instance, can be synthesised on a large scale by the direct reaction between titanium tetrachloride and ethanol, with ammonia bubbled through the reaction mixture to neutralise the liberated HCl; the ammonium chloride byproduct precipitates out of solution, and the volatile titanium alkoxide is purified by distillation. It should be noted that it is only the addition of a base (in this case ammonia) that allows the reaction to proceed to completion. Many metal chloride species will react with alcohols, but the reaction often forms mixed halide-alkoxide species. Silicon alkoxides can be formed directly from the reaction of alcohols with silicon tetrachloride, whereas group 2 metals react to give alcohol adducts. Titanium tetrachloride reacts with alcohols to produce mixed species such as $[TiCl_3(HO^iPr)(\mu\text{-}Cl)]_2$, $[TiCl_2(O^iPr)(HO^iPr)(\mu\text{-}Cl)]_2$ and$[TiCl_2(O^iPr)(HO^iPr)(\mu\text{-}O^iPr)]_2$, depending on the molar ratio of *iso*-propanol

added.[12] The reverse reaction, adding HCl to titanium tetra-alkoxides, also produces mixed chloride alkoxide species. Alkali metals will react directly with alcohols to produce metal alkoxide and hydrogen gas. The reaction is more rapid for the heavier alkali metals, and for the more acidic alcohols. Other metals, such as group 2 and 3 metals, will react with alcohols in the presence of a catalyst; iodine is typically used for the synthesis of group 2 metal alkoxides, while group 3 metal alkoxides are usually synthesised with mercuric chloride as catalyst.

Electrochemical synthesis, first demonstrated by Szilard,[13] has emerged as a reliable—and relatively non-polluting—method, with only hydrogen as a by-product (equations 1.1 a – d). This method has been successfully applied to the synthesis of metal alkoxides of less electropositive metals, allowing their direct synthesis. The use of metal atom vapour technique for the synthesis of metal alkoxides has not been extensively explored, although there have been reports of alkaline earth metal aryloxide compounds synthesised by this method.

$$M \longrightarrow M^{n\oplus} + n\,e^{\ominus} \text{ (anode)} \quad \text{(eq. 1.1 a)}$$

$$n\,ROH + ne^{\ominus} \longrightarrow n\,RO^{\ominus} + n\,H^{\bullet} \quad \text{(eq. 1.1 b)}$$

$$n\,H^{\bullet} \longrightarrow n/2\,H_2 \text{ (cathode)} \quad \text{(eq. 1.1 c)}$$

$$M^{n\oplus} + n\,RO^{\ominus} \longrightarrow M(OR)_n \quad \text{(eq. 1.1 d)}$$

Where there is sufficient driving force, alcoholysis reactions can convert one alkoxide species to another; the alkoxide to be displaced must be less basic than the alkoxide ligand to replace it, or the alcohol produced can be distilled out of the mixture if it has a lower boiling point than the alcohol being added. Transesterification reactions with organic esters can also be used to exchange the alkoxide ligand; this is particularly useful for the synthesis of alkoxides that are sterically hindered (such as *tert*-butoxides), or where the corresponding alcohol (e.g.: silyloxides) is unstable. Reaction of alcohols with the metal dialkylamides can be a successful synthetic route, particularly when the metal is more electropositive (and "oxophilic"). This method is assisted by the tendency of the amines produced to be more volatile than the alcohol, so that they are readily removed from the equilibrium.

Heterometallic alkoxides can be synthesised by a variety of different methods.[14] Simple mixing of the component metal alkoxides is most often used for alkali alkoxometallates, in conjunction with many of the less basic metals. This procedure can be used for many other mixed metal alkoxides, although their formation is often limited by the establishment of an equilibrium with the free components. Although group 2

metal halides do not normally react with alcohols to form metal alkoxide species, the reaction is facile in the presence of another metal alkoxide, producing mixed metal alkoxides (these have also been reported for Al, Ga, Zr, Hf, Nb and Ta). Furthermore, halides and nitrates of other metals will also react with alkali alkoxides and alkoxometallate species to produce mixed metal alkoxides.

1.2.3 General aspects of metal alkoxide chemistry

Metal alkoxides are inherently reactive species. They readily undergo nucleophilic attack, due to the polarity of the metal-oxygen bond and the availability of vacant orbitals at the metal centre. The oxygen atoms are also susceptible to electrophilic attack (i.e.: act as nucleophiles). Hydrolysis of the metal–oxygen bond in metal alkoxides (eq. 1.2) occurs readily *via* initial coordination of the water molecule to the metal centre, and is generally thermodynamically favoured, especially when the resulting hydroxide species then react to form oxo-bridged species (eq. 1.3).

$$M-OH + H_2O \rightleftharpoons M-OH + ROH \quad \text{(eq. 1.2)}$$

$$M-OH + M-OR \rightleftharpoons M-O-M + ROH \quad \text{(eq. 1.3)}$$

This tendency to hydrolyse to metal oxides necessitates careful handling procedures for homoleptic metal alkoxides, but is also the basis of the sol-gel application (Section 1.2.4 g). Controlling the environment around the alkoxide ligand, through use of bulky supporting ligands, can strongly affect the reactivity and stability of the alkoxide ligand. For example, the complex LTi(O^{t}Bu) (where L-H_3 = *tris*{(2-hydroxy-3,5-di-*tert*-butyl)benzyl}amine) is extremely resistant to hydrolysis, only forming the hydoxide species indirectly, by sequential reaction with trifluoroacetic acid and sodium hydroxide;[15] the alkoxide species is reformed by the addition of traces of alcohol. The μ-oxo dimer can be formed by evaporation of solutions of the hydroxide complex, but is readily cleaved by traces of water.

Another route for the decomposition of metal alkoxides is through β-hydride elimination to form aldehydes or ketones – an important example of this reaction is in the enzyme liver alcohol dehydrogenase (Section 1.2.4 e), although in this particular case the reaction is advantageous.

Metal alkoxides show a range of insertion chemistry with unsaturated molecules. In addition to CO_2 (discussed in Chapter 4), a number of species tend to insert, often reversibly, into the metal–oxygen bond. These include species isoelectronic

with CO_2 such as alkyl and aryl isocyanates (RNCO), isothiocyanates (RNCS) and carbodiimides (RNCNR) (Figure 1.5). The insertion of isocyanates is the basis of polyurethane synthesis – see Section 1.2.4 d. Other species that will insert include alkenes, ketenes, carbon monoxide, carbon disulphide and sulphur dioxide. As Lewis acids, they also show a tendency to react with carbonyl functions,[16] which forms the basis of a wide range of specialised catalytic applications.

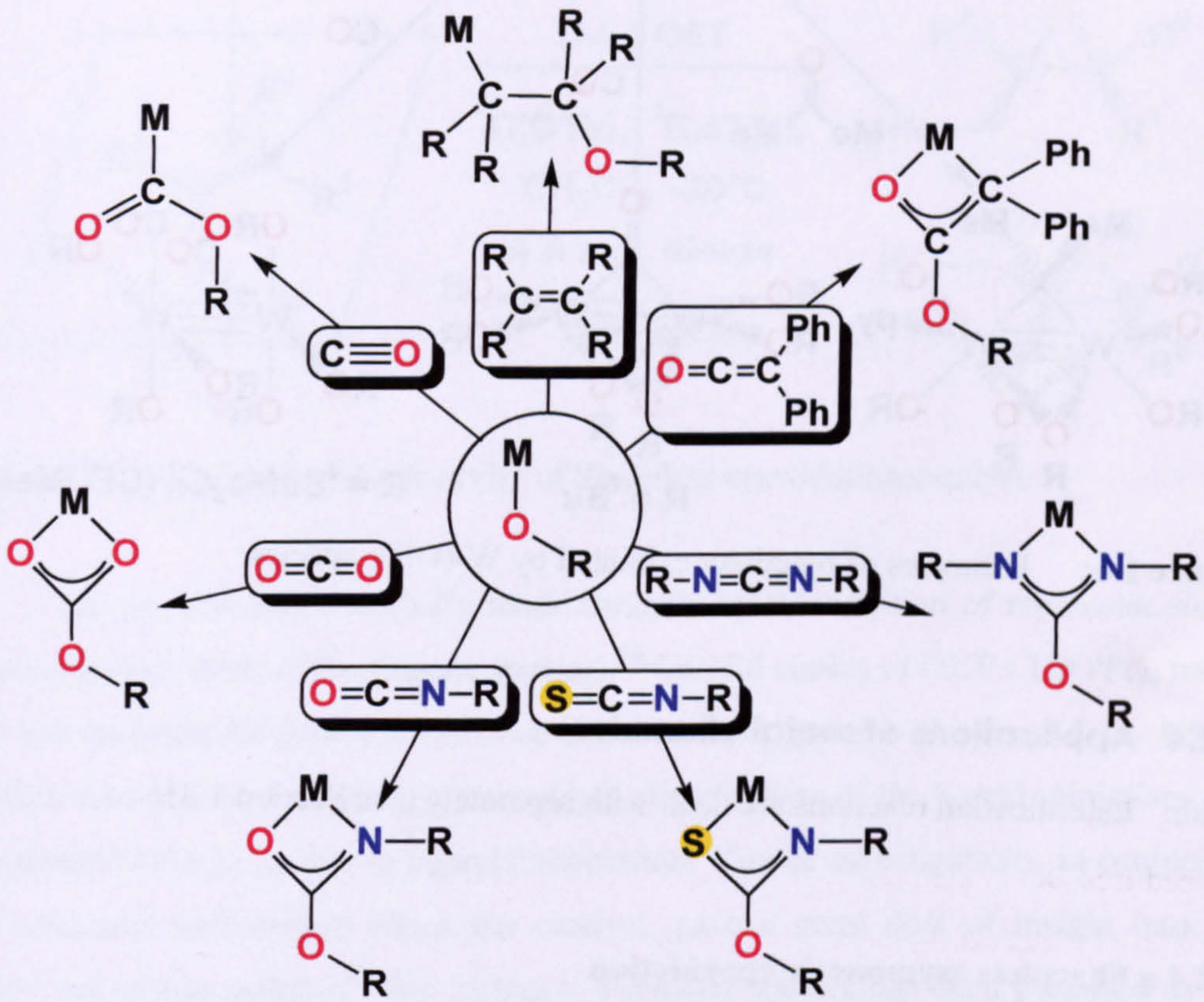

Figure 1.5: Range of insertion reactions displayed by metal alkoxides.

An interesting class of metal alkoxides is the dinuclear, metal-metal bonded species $W_2(OR)_6$.[17] These compounds contain a W – W triple bond, and are members of the family of d^3-d^3 ethane-like dimers. The normal geometry for M_2X_6 dimers involves ligand bridging; due to the electron deficiency of the metal centres in this case, the formation of metal-metal bonds gives a more favourable bonding arrangement, although they require bulky R groups to avoid the formation of tetranuclear species. Their reactivity has been explored in some depth,[18] and is still under investigation. They are known to react with a variety of unsaturated substrates (Figure 1.6), adding either one[19] or two[20] equivalents of carbon monoxide, depending on the nature of the R groups, and cleaving the C = O bonds of aldehydes[21] and ketones,[22] for instance. Carbon dioxide will also insert into the W – O bond – see Chapter 4. Note that some of these reactions

are not common to other metal alkoxides, but occur due to the particular (electron-deficient) nature of the dimers.

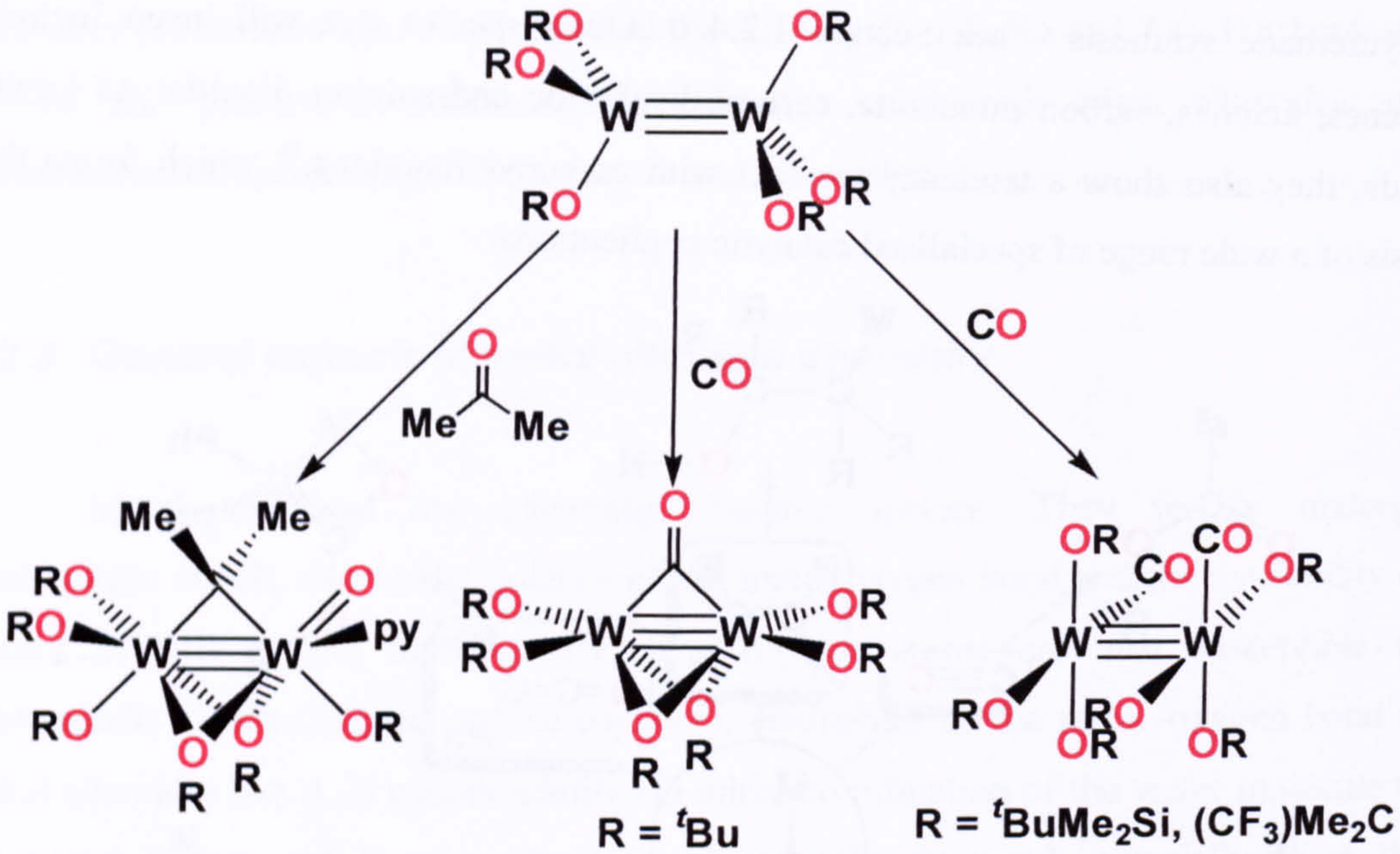

Figure 1.6: Examples of reactivity exhibited by $W_2(OR)_6$ species.

1.2.4 Applications of metal alkoxides

Note: Esterification reactions are dealt with separately (see Section 1.3).

1.2.4 a Sharpless asymmetric epoxidation

The award of a half share in the Nobel Prize for Chemistry 2001 to K. B. Sharpless for his development of enantioselective catalysts for the asymmetric epoxidation of allylic alcohols, makes this one of the most important current applications of metal alkoxides in catalysis. This reaction uses titanium alkoxides in conjunction with the chiral ligand diethyl tartrate (DET, Figure 1.7) with *tert*-butyl hydroperoxide as the stoichiometric oxidant.

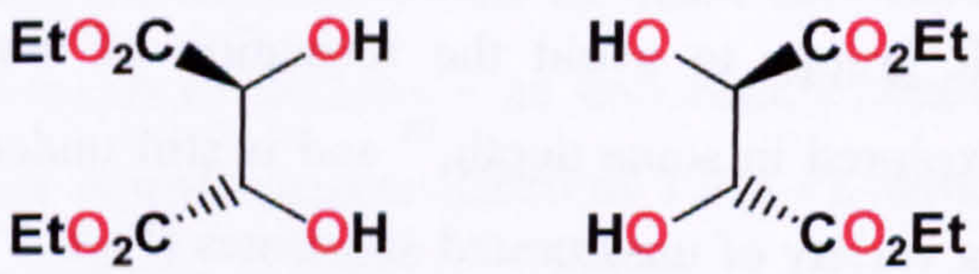

S,*S*-Diethyl tartrate
D-(−)-DET

R,*R*-Diethyl tartrate
L-(+)-DET

Figure 1.7: Chiral ligand used for Sharpless asymmetric epoxidation.

In their initial report,[23] Sharpless and Katsuki detailed the stoichiometric process for a variety of allylic alcohols with different substitution patterns, each substrate being converted to the corresponding epoxide in good yield (70 – 90%) with enantiomeric excesses of 90 – 95%, the choice of enantiomer produced being controlled by the appropriate enantiomer of DET (Figure 1.8).

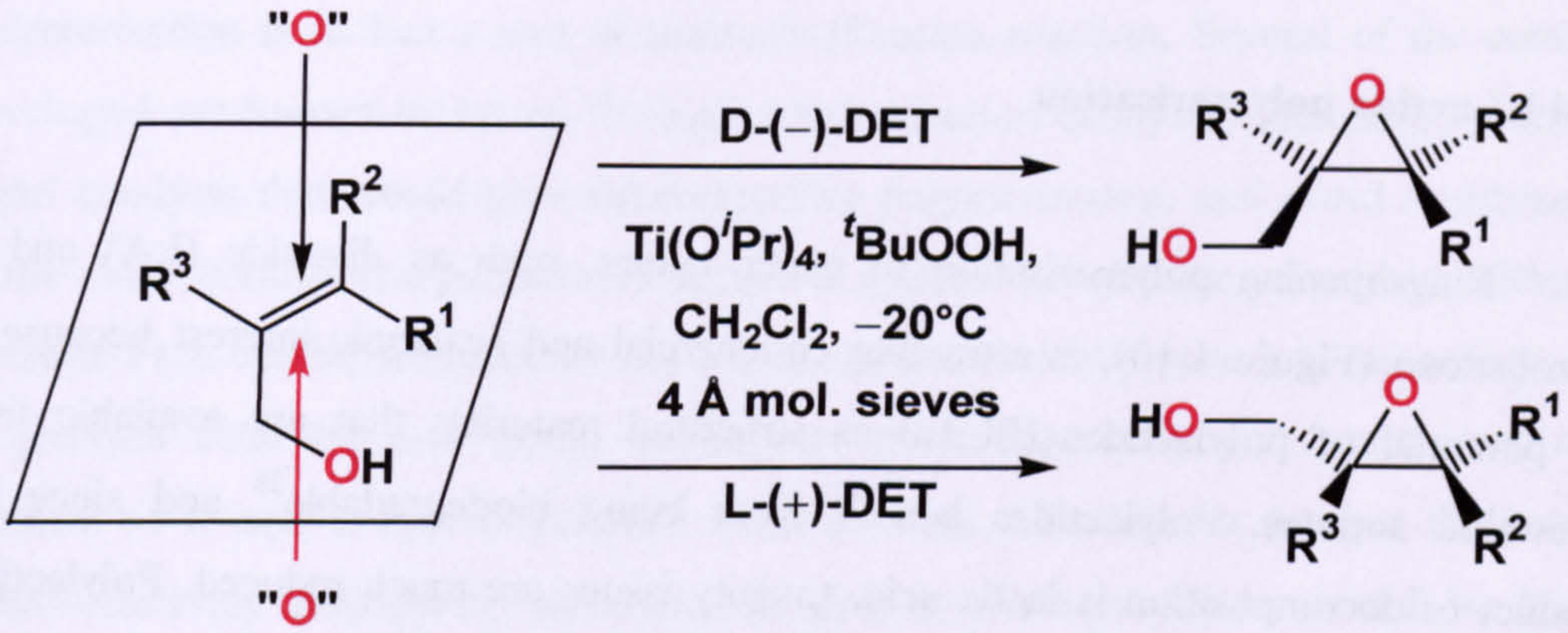

Figure 1.8: Enantiofacial selectivity of Sharpless epoxidation catalyst.

The process was eventually made catalytic by the addition of molecular sieves (to prevent hydrolysis of the titanate species).[24] Careful choice of DET : $Ti(O^iPr)_4$ molar ratio was essential for good performance in the catalytic process (the range 1.2 – 1.5 eq. was found to give best results), presumably a slight excess of the ligand minimises any loss of stereoselectivity due to ligand dissociation. Kinetic investigations, in conjuction with structural information about the catalyst, gave a great deal of insight into the mechanism of this process.[25] For instance, a dimeric species has been proposed as the active catalyst,[26] with dissociation of a carbonyl group providing a free coordination site to enable exchange of the *iso*-propoxide ligands; allylic alcohols readily exchange with *iso*-propoxide to form the corresponding alkoxide and *iso*-propanol, and *tert*-butyl hydro-peroxide exchanges to form a coordinated peroxide ligand, which then uses the vacant coordination site to transfer the oxygen atom to the alkene function. The catalyst can also be used to great effect in the kinetic resolution of racemic allylic alcohols, with relative rates of enantioselective epoxidation of 100 : 1.[27] This process has allowed the efficient production of a wide range of important synthetic targets by use of readily available and relatively cheap reagents. Note that the process only works for allylic alcohols, as it is the alcohol function that enables coordination to the titanium centre; however, this does give the advantage of specificity for allylic alkene functions only (Figure 1.9).

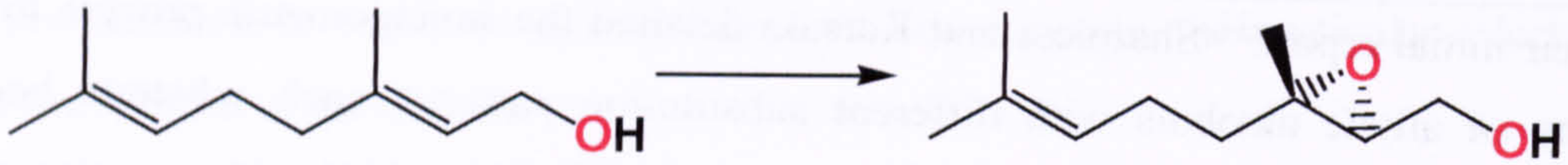

geraniol

Figure 1.9: Example of specificity for allylic alkene functions.

1.2.4 b Lactide polymerisation

Ring-opening polymerisation of cyclic esters, such as dilactide (LA) and ε-caprolactone (Figure 1.10), is attracting commercial and academic interest because of the potential of polylactides (PLAs) as structural materials that are available from renewable sources. Polylactides benefit from being biodegradable[28] and since the product of decomposition is lactic acid, toxicity issues are much reduced. Polylactides have been used as dissolvable sutures, and are being investigated for use as medical implants that can be broken down in the body over time. The starting material, dilactide, is a cyclic diester of lactic acid. Since dilactide units have two chiral centres, there is interest in the different properties of polymers composed of the different forms. The polymerisation of ε-caprolactone and δ-valerolactone are of related interest, due to their structural similarities. Existing catalysts used by industry are often insoluble solids; it has been speculated that the bulk catalysts are inactive themselves, with hydrolysis products being the active species. Additionally, whilst the catalysts are effective, they do not yield much insight into the mechanism, and the lack of structural knowledge inhibits any systematic attempts at development.

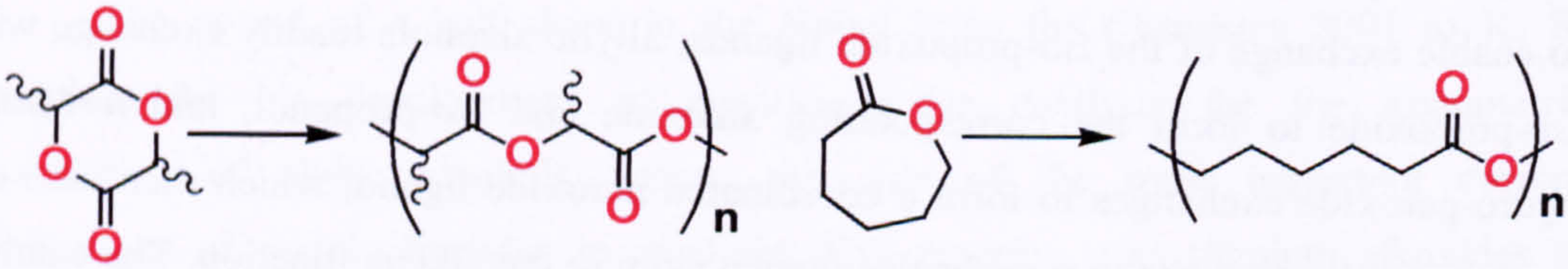

Dilactide Poly(dilactide) ε-Caprolactone Poly(ε-caprolactone)

Figure 1.10: Common lactide monomers and their associated polymers.

Metal species with a terminal alkoxide ligand are under investigation as precatalysts for the lactide polymerisation reaction. High activities are desirable for a useful catalyst, but the relative rates of initiation and propagation are also important; initiation should be faster than propogation to reduce the polydispersity index. The maximum chain length attainable is determined by the rate of the back reaction as the

maximum chain length attainable is determined by the rate of the back reaction as the polymerisation approaches completion and monomer becomes less available. The rate of transesterification, or "back-biting", where the catalyst breaks a growing polymer chain instead of reacting with free dilactide, can increase the polydispersity index, and also compromise the structural integrity of copolymers. It should be noted that lactide polymerisation is in fact a sort of transesterification reaction. Several of the catalysts developed are known to act as "living" polymerisation catalysts. The development of metal catalysts that would give stereoselective polymerisation, and avoid racemisation of the chiral centres, is a particularly attractive goal for coordination chemists. Although isotactic PLA can be produced by the use of enantiomerically pure LA, researchers aim to produce catalysts that would exclusively polymerise only one enantiomer of a mixture of D and L LA, to produce isotactic PLA. Likewise, a catalyst that would stereoselectively polymerise *meso*-LA, to give syndiotactic PLA, would be highly desirable. Recently Gibson *et al.* have reported a series of aluminium catalysts supported by tetradentate aminophenoxide ligands, which give a high degree of stereocontrol in the polymerisation of racemic lactide.[28]

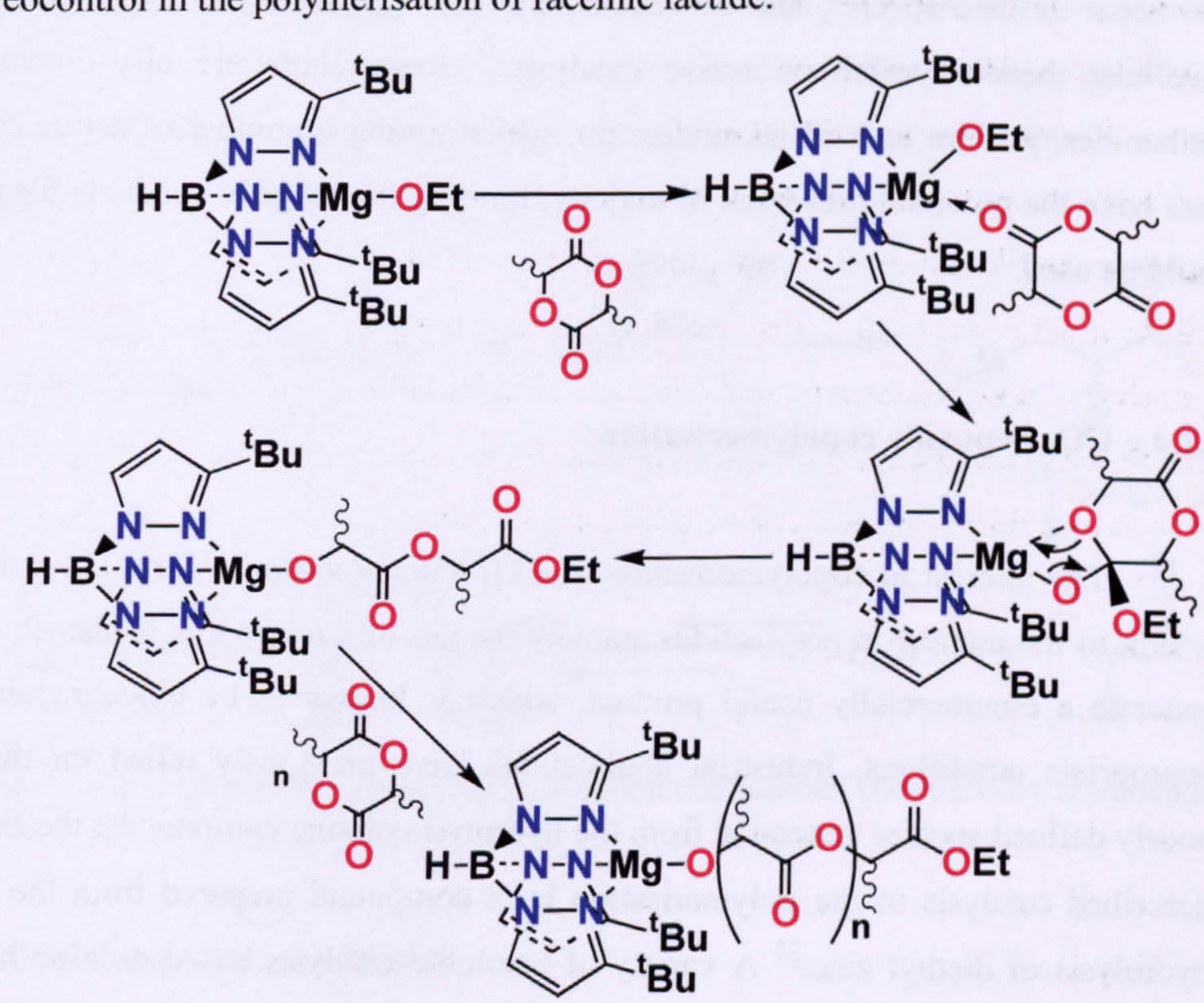

Figure 1.11: Lactide polymerisation catalyst, and proposed mechanism, from M. H. Chisholm & N. W. Eilerts, *Chem. Commun.*, 1996, 853.

Zinc and magnesium are particularly attractive candidates for catalysts as they are biologically benign, thus reducing the impact of catalyst remaining in the end product; they are also cheap, and give low colour. Chisholm *et al.* have developed several highly active catalysts,[29] and have suggested a catalytic mechanism (Figure 1.11).[30] They proposed that a molecule of dilactide coordinates to the metal centre through the acyl oxygen atom, followed by nucleophilic attack by the alkoxide ligand (the growing polymer chain) at the acyl carbon atom. The authors suggest a four-membered cyclic transition state, which ring-opens to regenerate the alkoxide chain, with an ester end-group. Evidence for this mechanism was provided by ^{1}H NMR spectroscopy, which revealed the presence of ester end groups, as opposed to ether end groups, which would have been observed if a different mechanism were operating.

More recently, Verkade and co-workers have tested titanium alkoxide complexes as catalysts for polymerisation of lactides.[31] They reported high activities for complexes bearing the triethanolamine ligand. Iron alkoxides have shown some promise as catalysts; the initial reports of ferric alkoxides ($Fe\{OEt\}_3$) prompted investigation into better-defined species, and iron alkoxides bearing a variety of supporting ligands have also been reported as active catalysts.[32] Researchers are also interested in lanthanides, yttrium and tin alkoxides; tin, whilst giving a number of active catalysts, does have the potential drawback of toxicity, limiting the range of products for which it could be used.

1.2.4 c CO_2 / epoxide copolymerisation

The interest in copolymerisation of CO_2 and epoxides, to form polycarbonates, is akin to the interest in polylactides, namely the use of a renewable feedstock (CO_2) to generate a commercially useful product, which is known to be biodegradable under appropriate conditions. Industrial applications have previously relied on the use of poorly defined species generated from the hydrolysis of zinc compounds; the first report described catalysis of the polymerisation by a compound prepared from the selective hydrolysis of diethyl zinc.[33] A variety of insoluble catalysts based on zinc have been prepared, the most active of which are prepared by the addition of carboxylic acids to zinc hydroxides or oxides.[34] Soluble catalysts based on the reaction of zinc oxides with acid anhydrides in alcohol solvents are somewhat more attractive due to the ease of separating catalyst from the product. Catalysts based on double metal cyanide units,

such as [CpFe(μ-CN)2Zn(X)(THF)](μ-dppp),[35] where X = I or phenolate and dppp = *bis*-1,3-diphenylphosphinopropane, have also shown activity for the polymerisation, but these present some environmental hazards. Whilst these groups of catalysts are sufficiently active for commercial use, the lack of information regarding the catalyst structure or the mechanism of action makes future development an uncertain process.

Researchers interested in understanding the mechanism of polymerisation, and probing the relationships between structure and activity of catalysts are studying well-defined mononuclear metal complexes because they allow the fine control over the active site that is necessary for such investigations. Mononuclear metal species containing a terminal alkoxide or aryloxide ligand have been proposed as suitable precatalysts for this application, and indeed a number of active catalysts have been generated accordingly. The research groups of Darensbourg[36] and Coates[37] have synthesised and tested successful catalysts for this reaction. They have also proposed a mechanism for the process; the epoxide coordinates to the metal centre, and one of the strained ring carbons undergoes nucleophilic attack by the alkoxide ligand, opening the ring and forming a new alkoxide group, whilst CO_2 can insert into metal alkoxide bonds (Figure 1.12). Note that the reaction often produces ether linkages in addition to carbonate linkages, since the epoxide can insert into either a carbonate or an ether linkage.

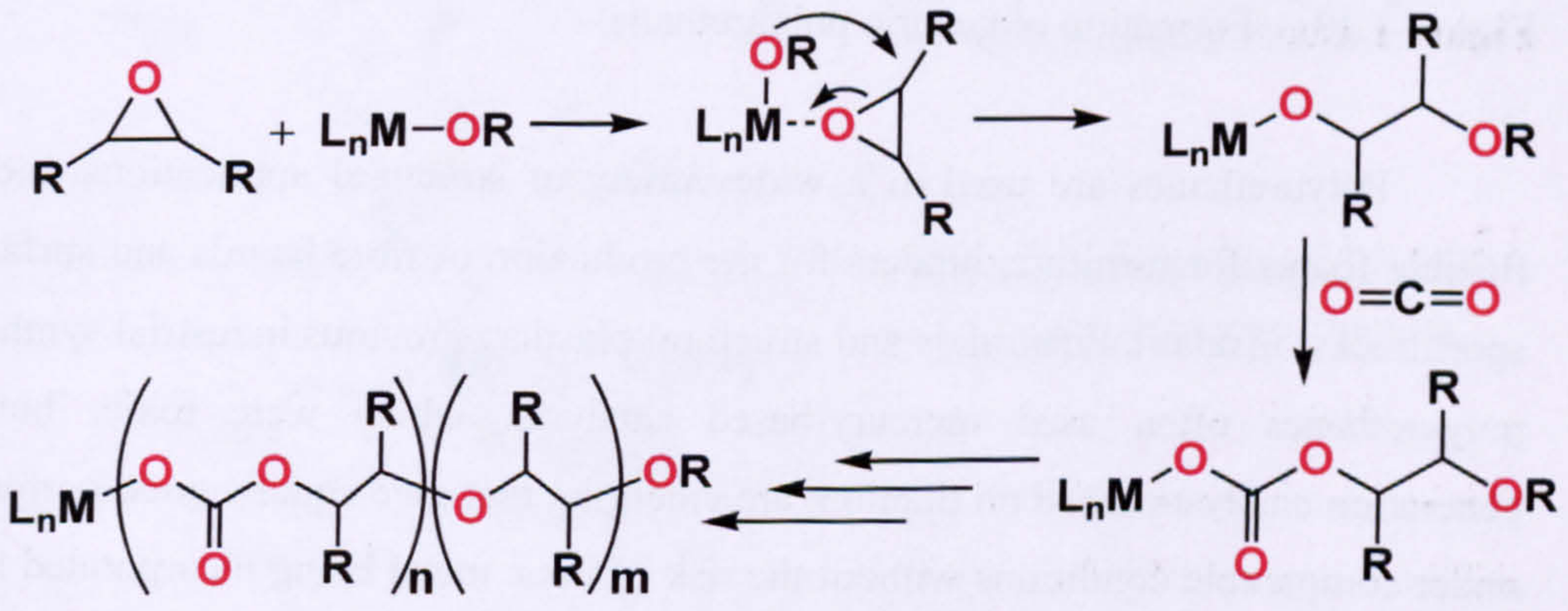

Figure 1.12: CO_2 / epoxide copolymerisation mechanism proposed by Darensbourg.

1.2.4 d Polyurethane synthesis

The ability of metal alkoxides to insert unsaturated molecules into the M – O bond is the basis of some catalytic applications. For instance, the formation of polyurethanes by the condensation of polyols and poly-*iso*-cyanates (Figure 1.13) can

be catalysed by metal alkoxide species such as $Ti(OR)_4$. The nature of the linker group and the polyol will determine the properties of the end polymer. Aromatic di-*iso*-cyanates are more often used than aliphatic di-*iso*-cyanates. Cross-linking of the polymer, to produce a more rigid substance, can be achieved by the use of tri- or tetra-*iso*-cyanates and / or tri- or tetra-ols, although it is more often the polyol that is used as a branching site. An alternative synthesis uses carbamic esters and diols in a transesterification reaction to produce the polyurethane. This synthesis depends on the ready availability of the carbamic ester, which can be synthesised by the reaction of the appropriate nitrobenzene with CO and alcohol. Currently, it is used only on relatively small scales.

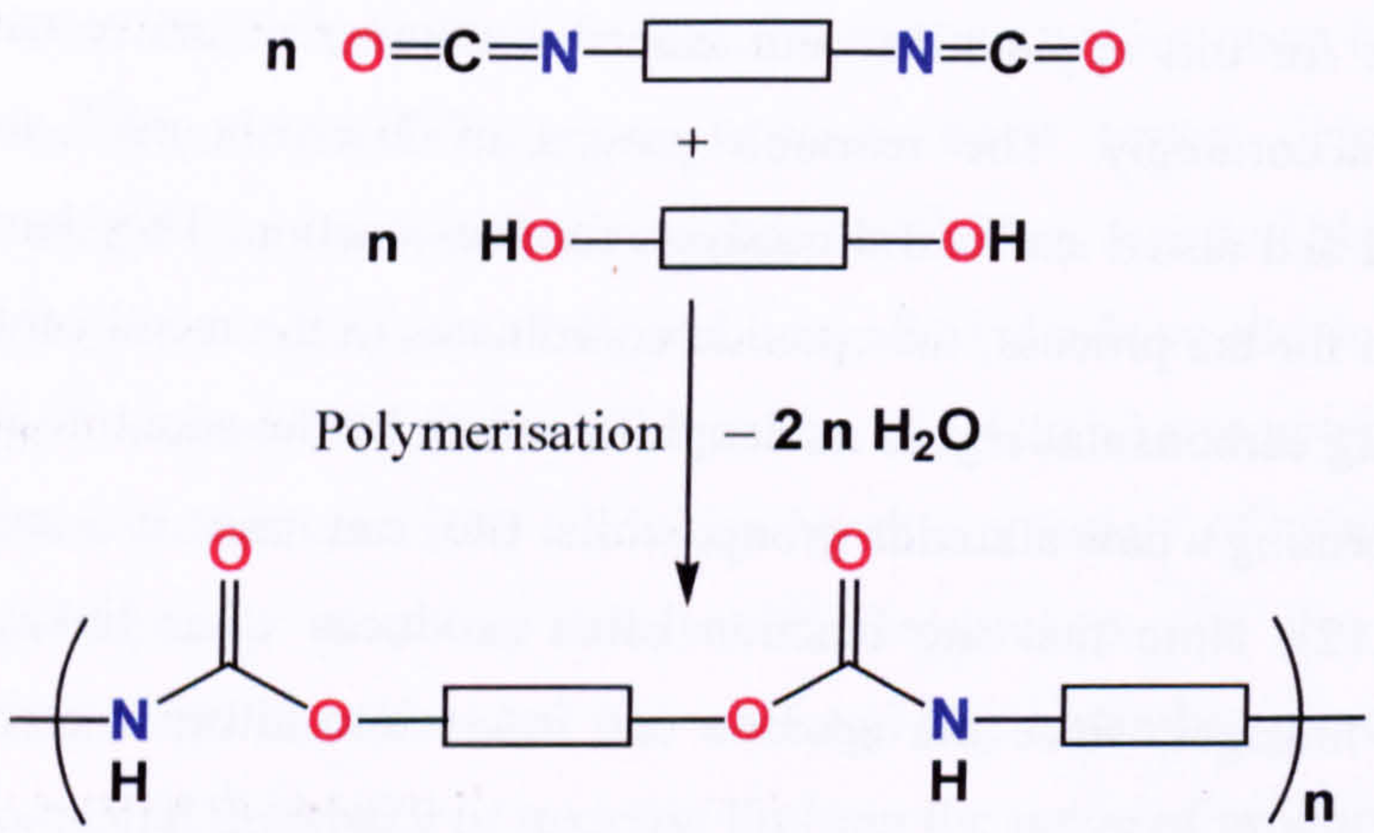

Figure 1.13: Formation of generic polyurethane.

Polyurethanes are used in a wide variety of structural applications, including flexible foams for furniture, binders for the production of fibre boards and surfaces for sport tracks, insulation materials and structural plastics. Previous industrial syntheses of polyurethanes often used mercury-based catalysts, which were toxic, but new-generation catalysts based on titanium are emerging that give equally good performance under comparable conditions without the risk of toxic metal being incorporated into the end product.

1.2.4 e Liver alcohol dehydrogenase (metal alkoxides in nature)

The enzyme liver alcohol dehydrogenase (LADH) catalyses the conversion of ethanol to ethanal (Figure 1.14). Structural and mechanistic information show that a zinc alkoxide species is involved in the catalytic cycle.[38] The active site incorporates a

zinc ion, which is bound to two cysteine sulfur atoms and one histidine nitrogen atom, with a proximal serine residue. It has been proposed that the sulfur atoms of cysteine play a vital role in stabilising the binding of the alcohol substrate relative to water molecules.

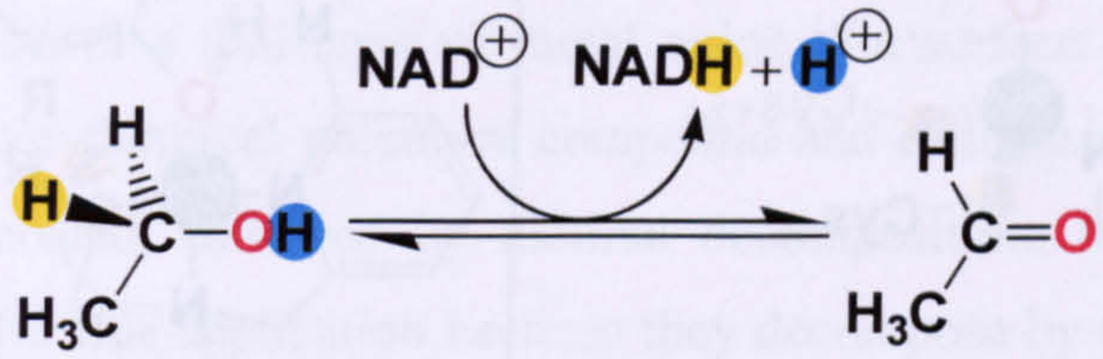

Figure 1.14: Conversion of ethanol to ethanal, catalysed by LADH.

The bound alcohol is deprotonated with assistance from the proximal serine residue, which forms a hydrogen bond to the alkoxide ligand. Binding of the coenzyme, NAD^+, places the C4 atom of the nicotinamide ring and a hydrogen from the ethoxide methylene group in such an orientation that dynamic fluctuations in the enzyme structure can bring the two atoms close enough to allow β-hydride abstraction to occur *via* a hydrogen-tunnelling mechanism (Figure 1.15).

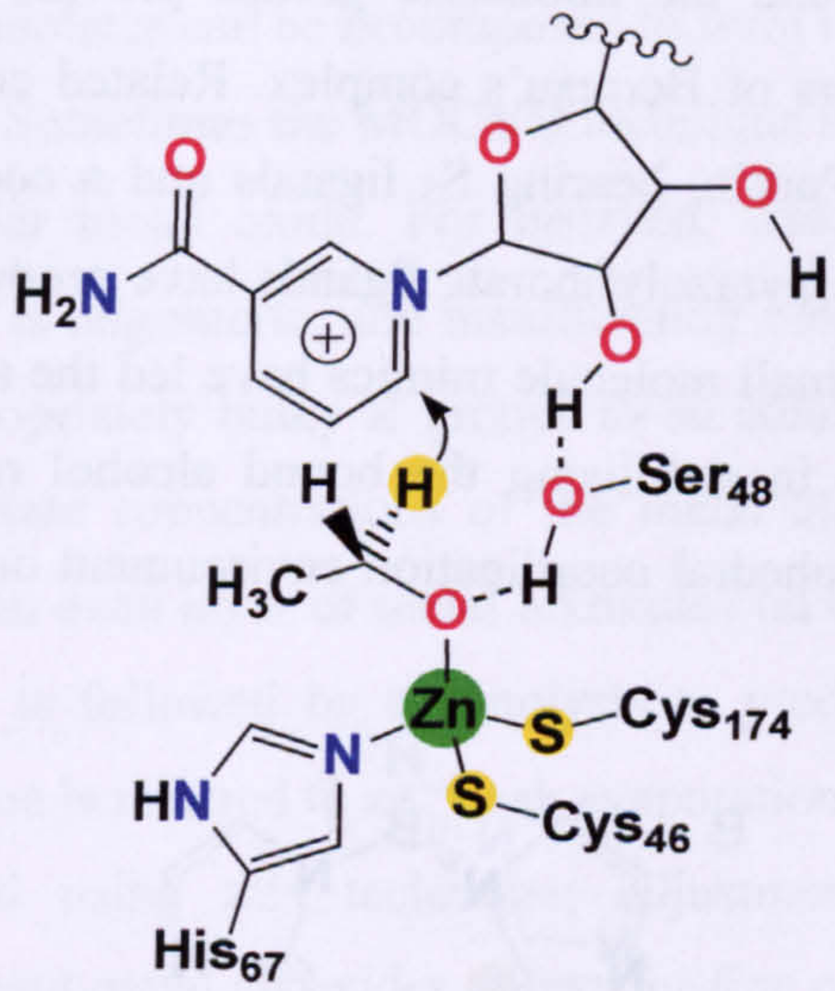

Remainder of NAD molecule is bound to enzyme by hydrogen-bonding interactions

Proximity of nicotinamide ring to β-hydride promotes transfer

Figure 1.15: Active site of LADH, showing the preorganisation of NAD^+ for hydride abstraction from ethoxide ligand.

Several effective structural mimics have been synthesised. The research group of Berreau have synthesised a cationic zinc aryloxide bearing a mixed N_2S_2 ligand.[40] The aryloxide is involved in hydrogen bonding thus mimicking one of the active intermediates in the liver alcohol dehydrogenase catalytic cycle (Figure 1.16). The

limitations of this mimic are that the sulfur atoms are thioethers as opposed to thiolate groups (as in LADH), and the coordination of an additional nitrogen atom.

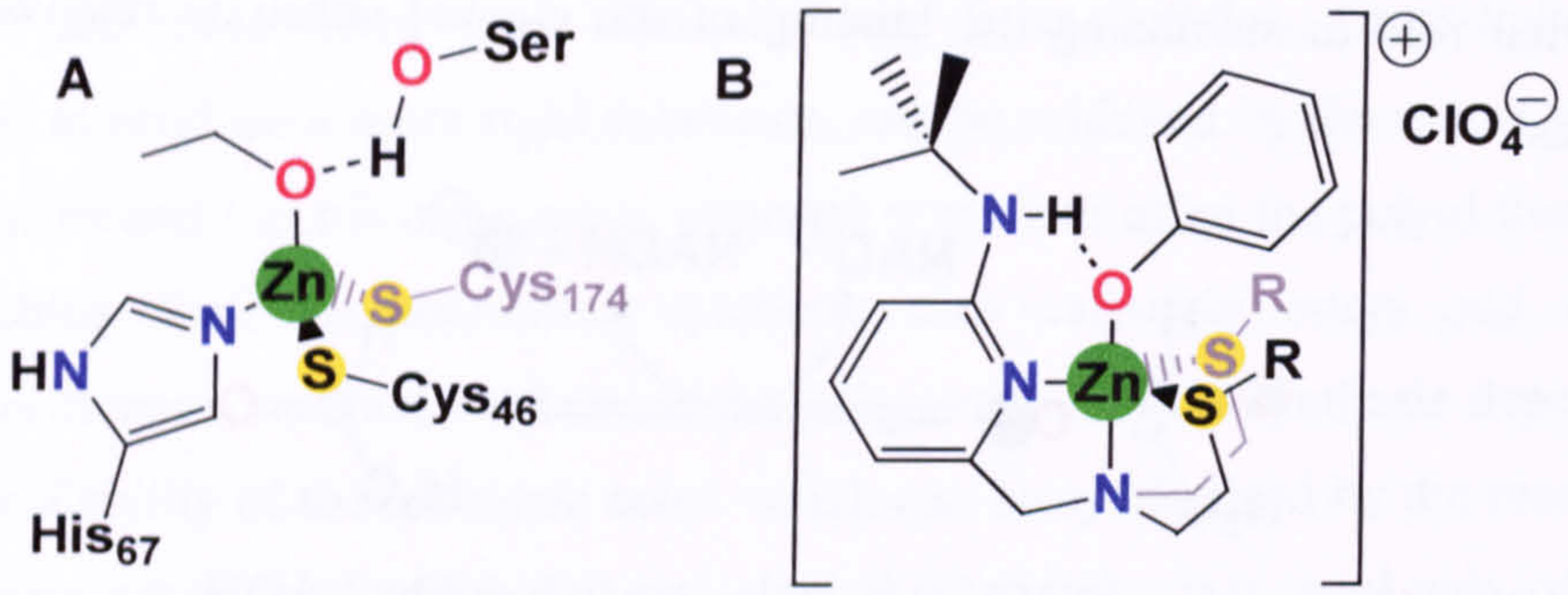

Figure 1.16: Coordination sphere of Zn at the active site of LADH **A**, and a structural model by Berreau *et al.* **B**.

Vahrenkamp *et al.* have synthesised a number of close structural mimics, perhaps the best being a Zn complex bearing a pyrazolyl-*bis*(thioimidazolyl)borate ligand and a coordinated ethanol molecule, which forms a hydrogen bond to an additional ethanol in the solid state (Figure 1.17).[41] The complex recreates the NS_2 coordination sphere at the zinc centre, and the thioamide groups provide a closer analogy to thiol groups than the thioethers of Berreau's complex. Related complexes have been synthesised by the group of Parkin, bearing S_3 ligands and a coordinated methanol.[42] Several mimics based on *tris*(pyrazolyl)borate ligands have produced zinc alkoxide species.[43] The studies of these small molecule mimics have led the authors to suggest that sulfur ligands are essential in stabilising the bound alcohol relative to bound water, and also in enforcing a tetrahedral coordination environment on the zinc centre.

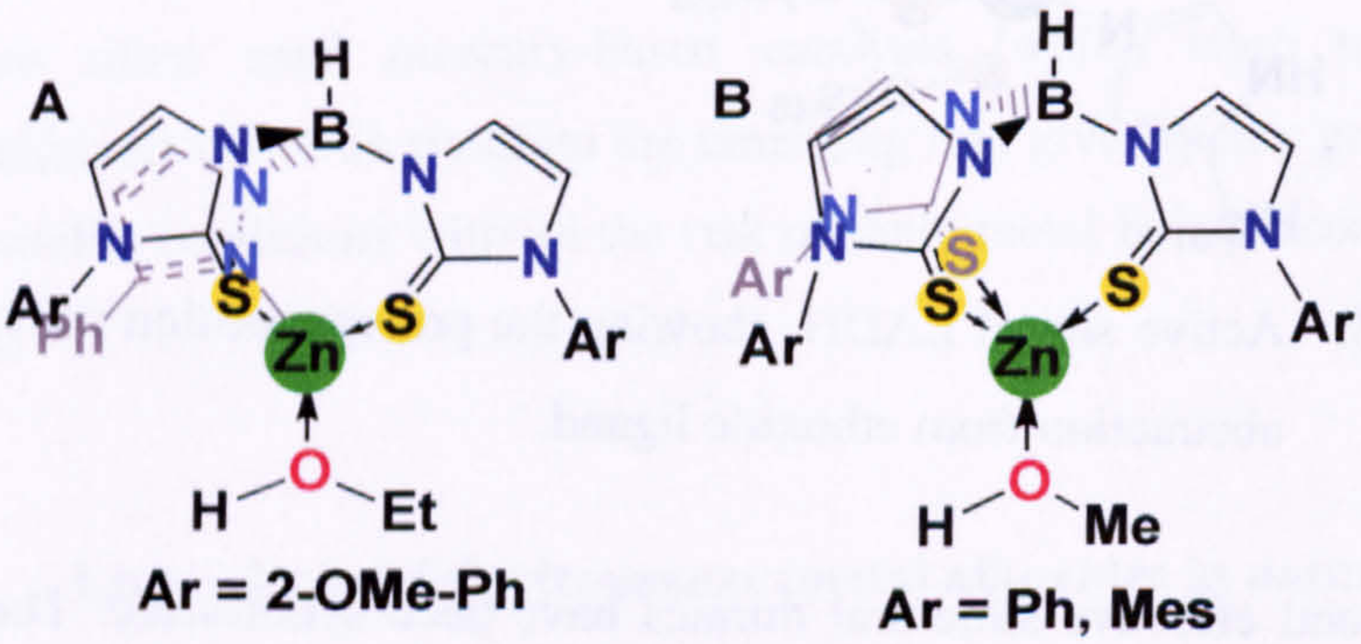

Figure 1.17: Structural mimics of LADH by Parkin (**A**) and Vahrenkamp (**B**).

1.2.4 f Metal oxide films

Metal alkoxides have been used for many years in the preparation of thin films of metal oxides through chemical vapour deposition, for use as semi-conductor devices.[44] Application of a thin layer of metal oxide to a surface can be achieved by vapourising a suitable chemical precursor compound and condensing this vapour onto the surface to be coated, followed by thermal decomposition. Metal alkoxides are suitable precursors for this application because they decompose by thermolysis to yield pure metal oxides; they can also be prepared in high purity, and can be handled with relative ease. The species to be used must be relatively volatile and stable as a vapour under low pressure. For example, titanium tetra-alkoxides can be used to provide a thin film of titanium dioxide on a glass surface, giving superior scratch resistance and improved hydrophilicity; the glass is much more easily cleaned. Fluorinated alkoxides are often used because of their increased volatility. More complex alkoxides of other metals have been synthesised for this purpose. This process can be extended to other materials; metal amides are also synthesised for use as metal nitride precursors, and metal thiolates can be decomposed to form metal sulfides.

Sometimes the MOCVD technique is not a viable option for the preparation of a particular metal oxide. For instance, where the only corresponding metal alkoxide species is oligomeric, and insufficiently volatile, the compound can be modified by use of appropriately bulky R groups to be soluble in volatile organic solvents. The use of appropriate concentrations of the metal alkoxide species and controlled evaporation leaves an even layer of metal alkoxides on the surface to be coated. Evaporation of the solvent is followed by thermolysis to produce the metal oxide as a thin layer. This technique is referred to as “flash evaporation”. Multicomponent metal oxides are readily prepared using this technique; adjustment of the relative concentrations of the component metal alkoxides allows for fine control over the stoichiometry of the product metal oxide, and also ensures homogeneity.

1.2.4 g Sol-gel preparation of ceramics and glasses

Preparation of speciality glasses and ceramics based on metal oxides has traditionally relied on the “grind and bake” method, where particles of metal oxides are ground together in the desired compositions and subjected to high temperatures,

resulting in fusing of the particles and a limited diffusion of the individual compounds. This process has the disadvantages of requiring high temperatures to fuse effectively together the particles of metal oxides, as the reaction of surfaces is relatively slow, and the homogeneity of the end product is, therefore, not guaranteed. The use of metal alkoxides as precursors for this process has attracted interest because it offers a low temperature mechanism for the production of metal oxides.[45] By dissolving the appropriate metal alkoxides in a water miscible organic solvent and hydrolysing them under controlled conditions, extremely fine particles of mixed metal oxides can be formed; these are then compacted and heated together as for the traditional method, but the smaller particle size and the improved mixing enables the use of lower temperatures, and provides a more homogeneous compound.

1.3 Esterification processes and the use of metal alkoxides

Esterification processes can be divided into several classes; the direct esterification reaction, transesterification, interesterification and polyesterification. All of these reactions are used in industrial processes in one capacity or another. There have been a number of reports in the literature of metal alkoxides catalysing esterification reactions.

1.3.1 Transesterification

Transesterification[46] (Figure 1.18) involves the conversion of a starting ester into a new ester by exchange of the alkoxy group; the new alkoxy group derives from an alcohol. This reaction is sometimes referred to as acylation of the alcohol.[47]

Figure 1.18: General transesterification reaction.

Trans-esterification finds use in the synthetic laboratory for the preparation of target esters from commercially available starting materials. For synthetic applications, the equilibrium is forced to the right-hand side by use of excess alcohol (R^2OH) and / or removal of the product alcohol by distillation. Another well-established method for

forcing complete conversion is to start with a vinylic ester, such as isopropenyl acetate.[48] The liberated vinylic alcohol tautomerises to the aldehyde or ketone, and is easily removed from the reaction mixture (Figure 1.19).

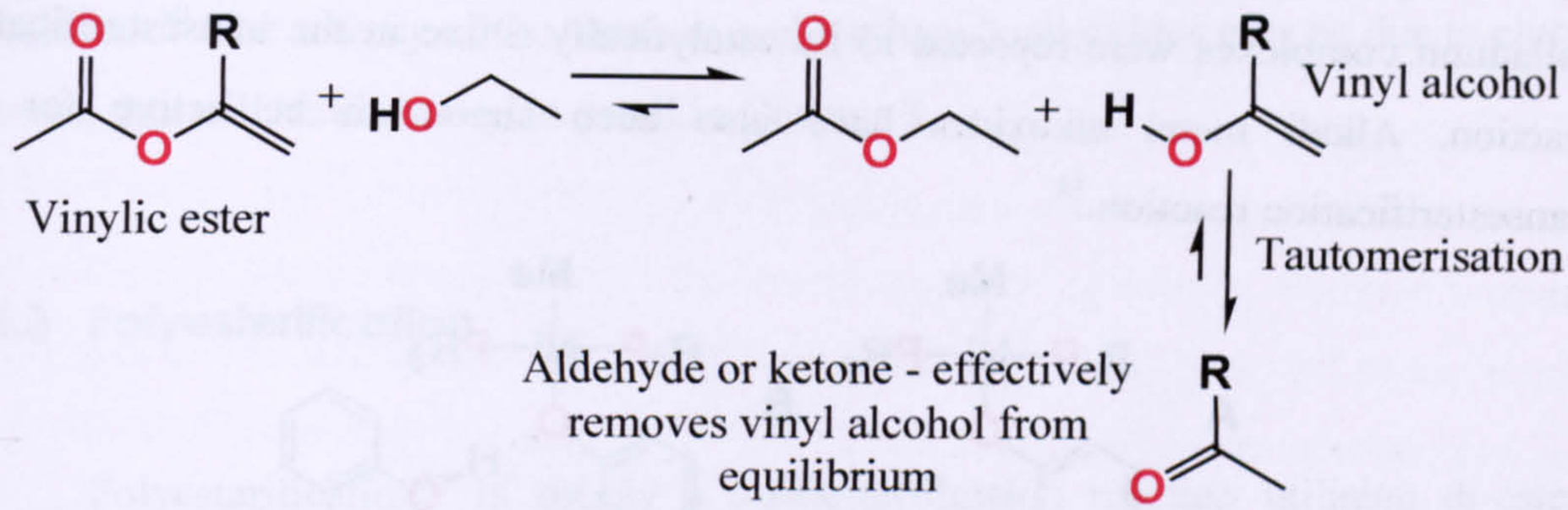

Figure 1.19: Transesterification reaction driven by tautomerisation of liberated vinyl alcohol.

An example of a large scale commercial use of transesterification is the preparation of *bis*(hydroxyethyl)terephtalate monomers for the production of poly(ethylene terephthalate) from dimethyl terephthalate and ethylene glycol (Figure 1.20), although industrial preparations are making increased use of the direct esterification of terephthalic acid with ethylene glycol. Methyl methacrylate is often transesterified to provide new methacrylates for commodity uses. Speciality uses of transesterification include the production of perfumes and insect pheromones.

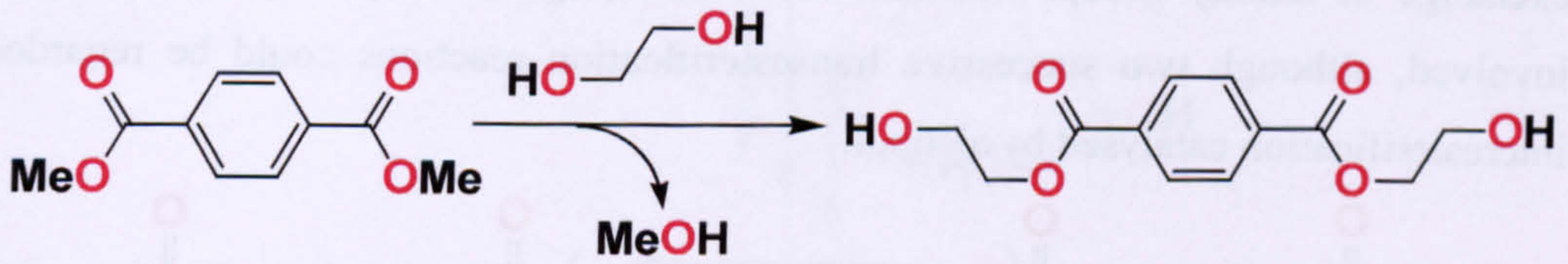

Figure 1.20: Transesterification of dimethyl terephthalate with ethylene glycol.

Aluminium alkoxides were shown to undergo transesterification reactions by Baker in 1938;[49] this reaction was originally used simply to synthesise new aluminium alkoxide derivatives. Divalent metal cations have long been known to catalyse transesterification at temperatures of 150—200°C, and their catalytic activity was ascribed to Lewis acid behaviour.[50] Seebach *et al.* reported the activity of titanium tetra-alkoxides for the transesterification[51] reaction, although the titanium alkoxides were present in high concentrations (10 mol% relative to ester); their study focussed on the range of substrates rather than activity values. Yamamoto *et al.* have reported examples of copper complexes that are catalytically active in the transesterification reaction.[52] Complexes of the type $Cu(PPh_3)_n(OR)$ where n = 1 or 2 were prepared. Yamamoto's

group have also prepared nickel (II) and palladium (II) alkoxides bearing phosphine ligands (Figure 1.21). They found that these complexes readily coordinated one equivalent of phenol by hydrogen bonding to the aryloxide ligand.[53] Both the nickel and palladium complexes were reported to be catalytically active in the transesterification reaction. Alkali metal alkoxides have also been shown to be active for the transesterification reaction.[54]

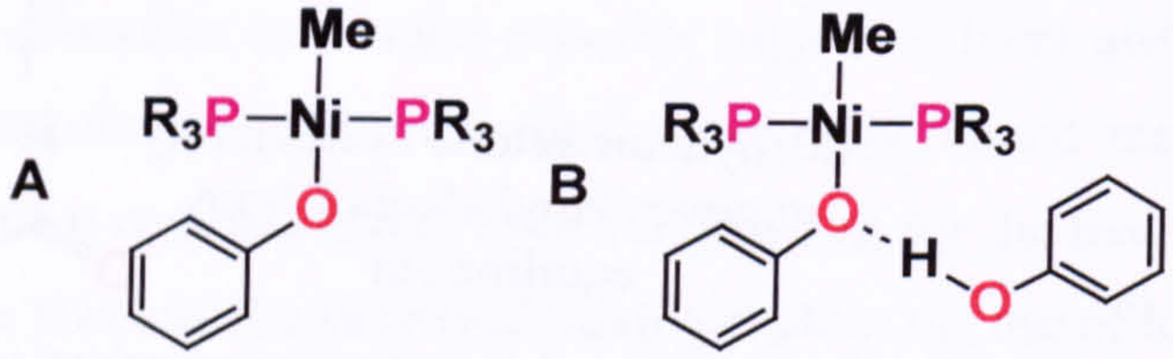

Figure 1.21: Nickel aryloxide complexes, one including hydrogen-bonded phenol (B).

Mechanisms for transesterification proposed in the literature will be discussed in Chapter 3 along with the mechanism proposed from the work in this thesis.

1.3.2 Interesterification

Interesterification, also referred to as the ester interchange reaction, involves the exchange of alkoxy groups between two esters (Figure 1.22), with no free alcohol involved, although two successive transesterification reactions could be regarded as interesterification catalysed by alcohol.

Figure 1.22: General interesterification reaction.

Inter-esterification can be used to produce mixed polymers, for example polyesters and polycarbonates can be mixed[55] to produce polymers of intermediate properties.[56] Fats can be interesterified in order to modify their physical properties and nutritional value (Section 1.6). Gagné *et al.* have reported that alkali metal alkoxides have extremely high activity for the interesterification reaction, with the heavier alkali metals giving the highest activity.[57] They also presented the view that catalysis was due to tetrameric and hexameric species.[58] During their work on transesterification, Seebach *et al.* noted that methyl esters could not be produced by use of methanol, due to the insolubility of titanium tetramethoxide. With methyl propiolate as the source of the

methoxy group the interesterification[59] reaction proceeded, although Seebach referred to it as transesterification. Homoleptic lanthanide alkoxides have been shown to have good activity for the interesterification reaction, even at low temperature, under dry conditions.[60] The activity of the titanium and lanthanide alkoxides may be due to cluster species; this will be discussed in detail in Chapter 3.

1.3.3 Polyesterification

Polyesterification[61] is simply a transesterification reaction utilising di-esters, with the alkoxy groups derived from diols. The transesterification produces a diol and two linked diester units; continued reaction, assisted by removal of liberated diol, results in chain growth (Figure 1.23).

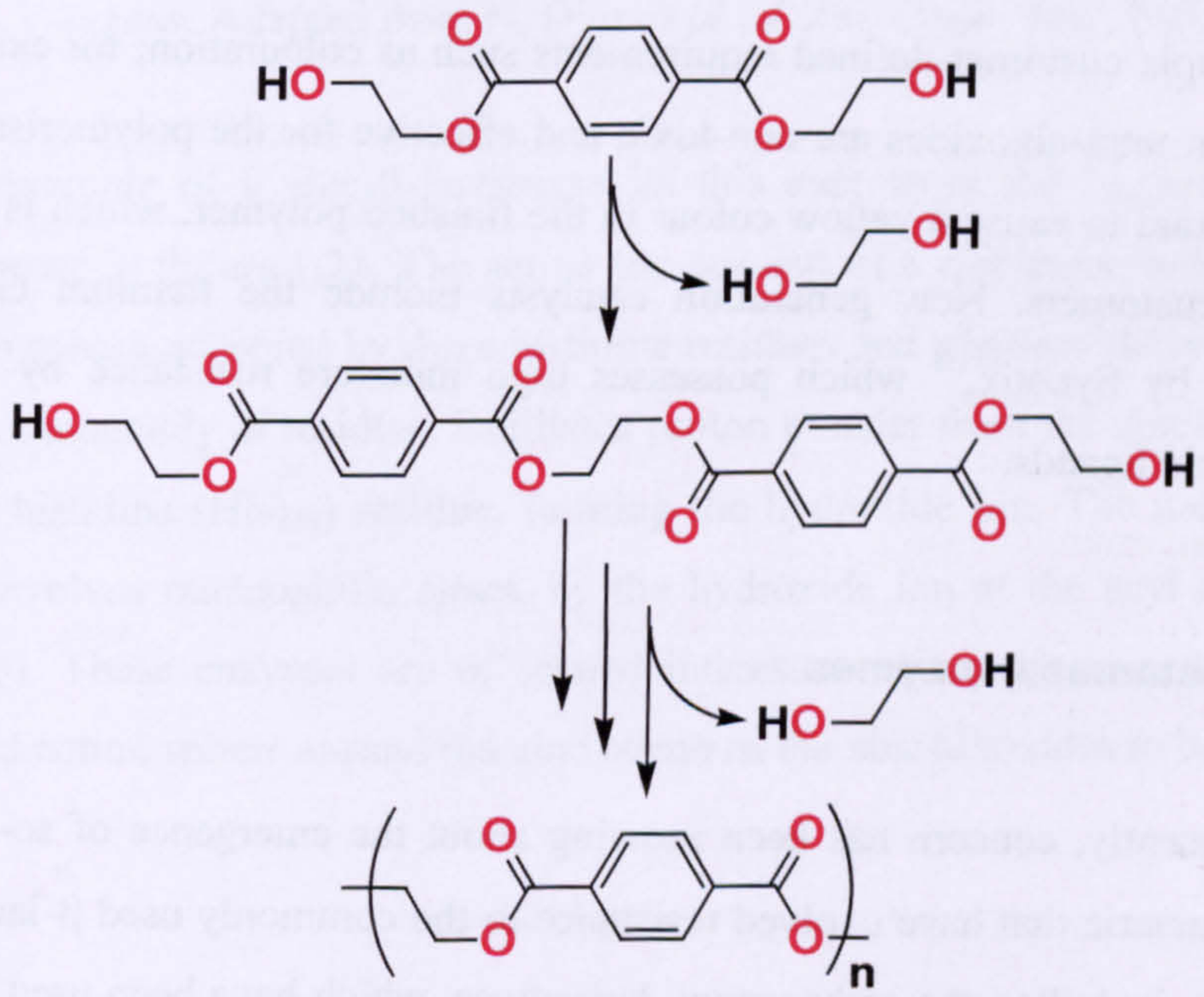

Figure 1.23: Formation of poly(ethylene terephthalate).

Perhaps the largest scale production of polyester is the synthesis of poly(ethylene)terephthalate (PET), which is used widely in packaging materials and in production of artificial fibres for clothing.[62] PET is composed of terephthalate and ethylene diolate groups; the monomer units typically used are bis(hydroxyethyl)terephthalate. The reaction must be run under low pressure and high temperature to ensure continuous removal of ethylene glycol from the reaction mixture.

There are a wide variety of known catalysts for the polyesterification reaction. Simple acid and base catalysts are known to effect the reaction. A number of metal

compounds are known to catalyse the reaction, including: tin, antimony (as Sb_2O_3), titanium (as $Ti(OR)_4$). Many industrial plants currently utilise Sb_2O_3 as the catalyst for PET synthesis due to its reliability in catalysing the polyesterification reaction without causing the formation of side products such as acetaldehyde and dehydration products of ethylene glycol. It is tolerant of the presence of carboxylic acid groups, but is sensitive to hydroxyl groups, necessitating fast removal of ethylene glycol from the reaction mixture. Antimony oxide is also believed to catalyse mass transfer by the formation of fine particles. However, the incorporation of these small grains of Sb_2O_3 in the end products causes problems when polyesters are being spun into fibres for use in clothing; these grains cause the fibres to weaken and break. Replacements are emerging which do not have the disadvantages of the antimony catalyst, including the inherent toxicity of antimony (particularly important when the product is to be used for food packaging). Additional considerations to be taken into account when choosing a catalyst include simple customer-defined requirements such as colouration; for example, whilst the titanium tetra-alkoxides are non-toxic and effective for the polymerisation of PET, they are found to cause a yellow colour in the finished polymer, which is unacceptable to many customers. New generation catalysts include the titanium citrate catalyst developed by Synetix,[63] which possesses high moisture resistance by virtue of the hydroxy acid ligands.

1.4 Lactamase enzymes

Recently, concern has been growing about the emergence of so-called "super-bugs" – bacteria that have evolved resistance to the commonly used β-lactam family of antibiotics, including the carbapenem derivatives, which have been used extensively as broad-spectrum antibiotics. The serine β-lactamase enzymes,[64] which were evolved by bacteria to hydrolyse lactam antibiotics, have been countered in the past by the development of effective inhibitors, but a new class of enzymes, known as zinc-β-lactamases,[65] has been identified; these enzymes not only hydrolyse a broader range of lactam derivatives, but they are also capable of hydrolysing the inhibitors which were developed to counter the serine β-lactamases.[66]

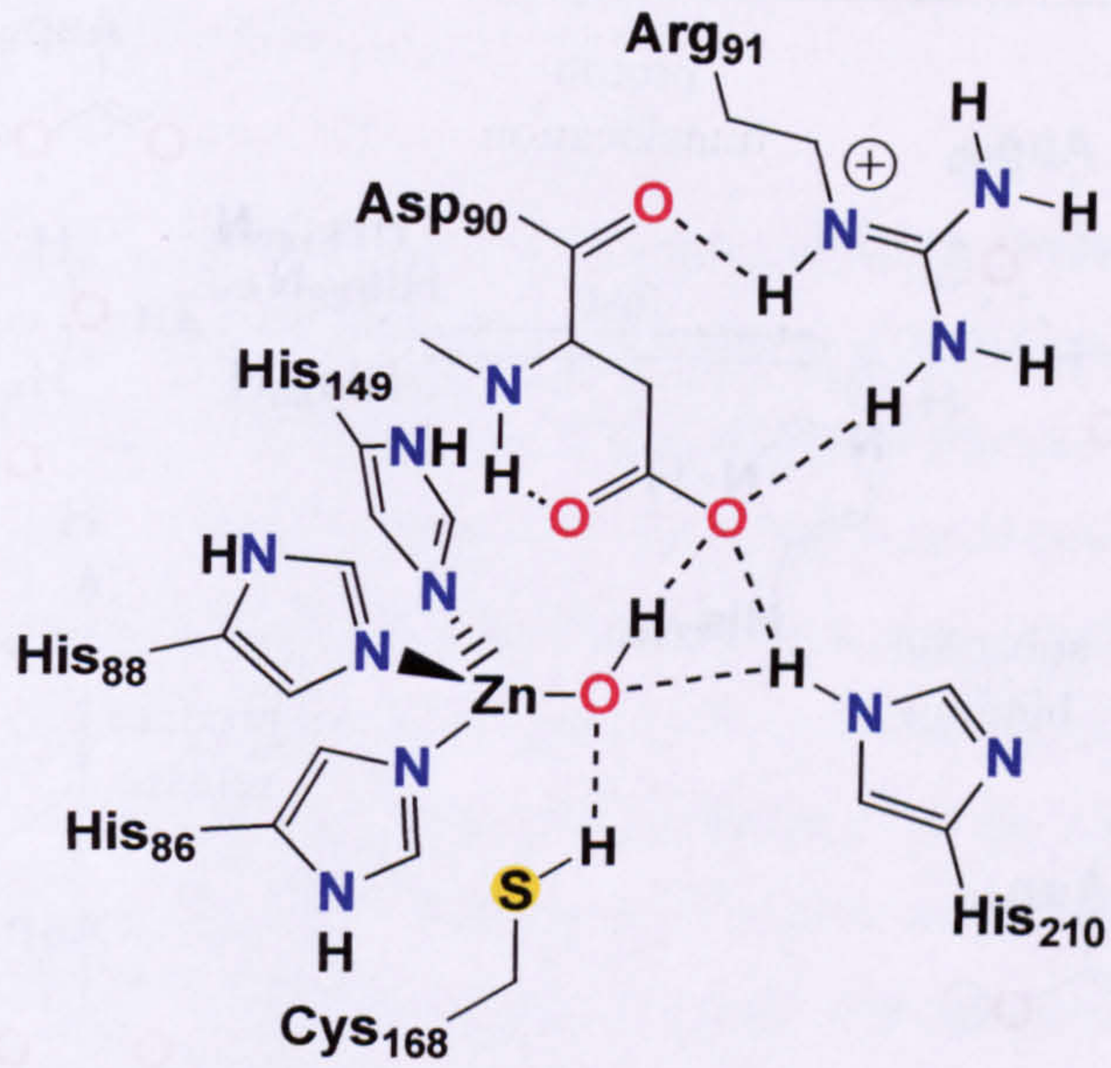

Figure 1.24: Schematic diagram of the active site of zinc-β-lactamase from *Bacillus cereus*. Adapted from N. Diaz *et al.*, *J. Am. Chem. Soc.*, 2001, **123**, 9867.

An example of a zinc-β-lactamase, in this case from the bacterium *Bacillus cereus*, is shown in Figure 1.24. The active site consists of a zinc atom, with its primary coordination sphere occupied by three histidine residues and a hydroxide group or water molecule. An assembly of residues facilitates proton transfer from the zinc-bound water to a nearby histidine (His_{210}) residue, forming the hydroxide ion. The mechanism for hydrolysis involves nucleophilic attack by the hydroxide ion at the acyl carbon atom (Figure 1.25). These enzymes are of related interest to this project as they utilize a similar coordination sphere around the zinc centre as the zinc alkoxides to be discussed.

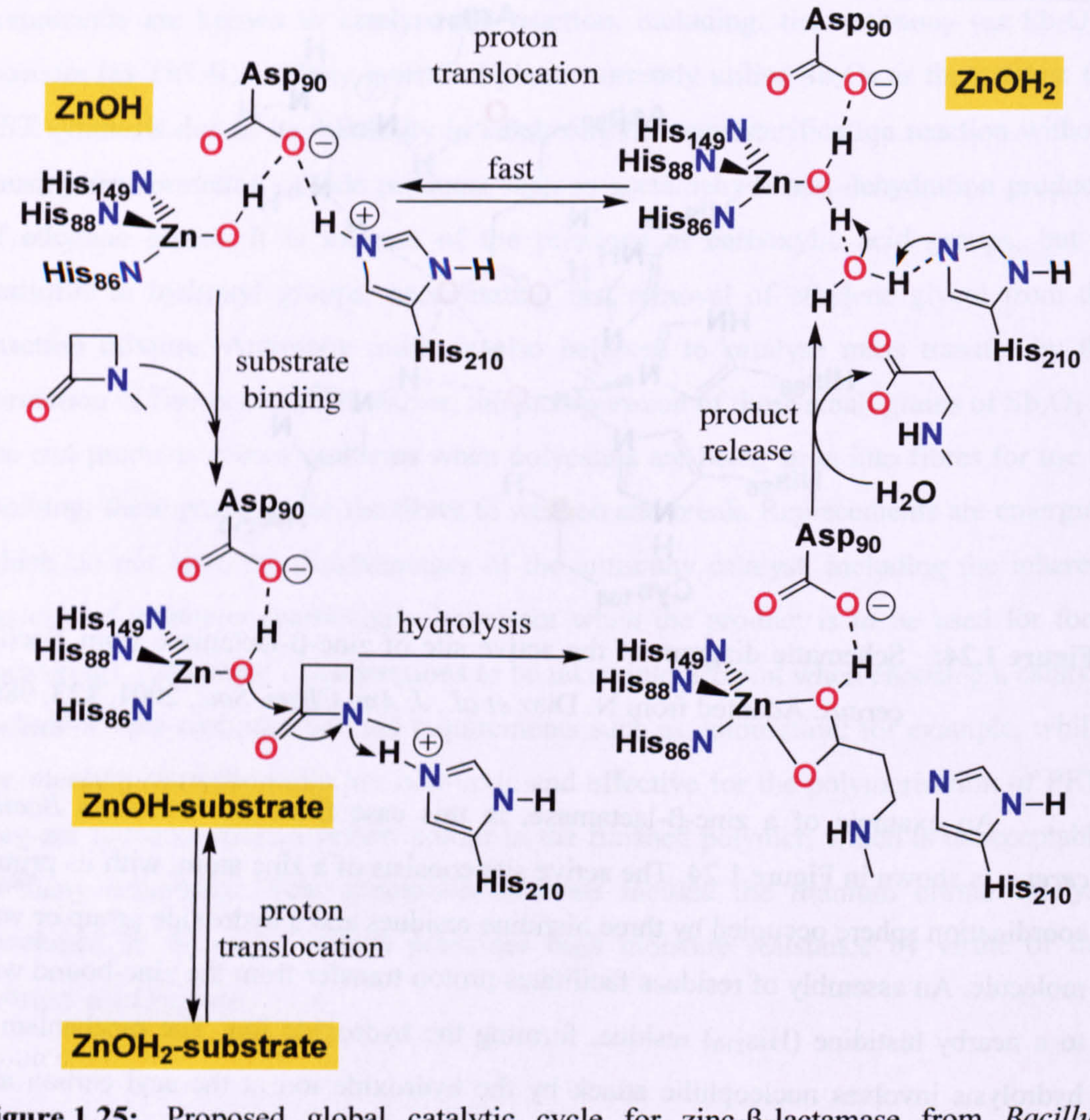

Figure 1.25: Proposed global catalytic cycle for zinc-β-lactamase from *Bacillus cereus*. Adapted from N. Diaz *et al.*, *J. Am. Chem. Soc.*, 2001, **123**, 9867.

1.5 Fats and lipids

Since fats are often referred to as lipids, a definition of lipids and a summary of the various types are included here. Biological molecules that are soluble in organic solvents, and not water, are classified as lipids.[67] There are several major classes of lipids, each having a particular role to play within the body. This section focuses on fatty acids and triglycerides, as they have relevance to the original aims of this project, with other classes given a brief mention to distinguish them from fatty acids and triglycerides. See Appendix 2 (Supplementary Data) for a complete set of diagrams.

1.5.1 Fatty acids

Fatty acids are long-chain carboxylic acids, typically containing between 12 and 20 carbon atoms. They may be completely saturated (purely alkyl) or unsaturated, containing one or more double bonds. Fatty acids are components of triglycerides, phospholipids and sphingolipids. Two fatty acids are considered to be essential fatty acids: linoleic and α-linolenic, often referred to as omega-3 fatty acids, because the body is incapable of introducing unsaturation beyond carbon atom 9 in fatty acids. Other fatty acids can be interconverted within the body by the addition or removal of two carbon atoms, and removal or addition of double bonds, if sufficient energy is available to do so, although highly unsaturated fatty acids (particularly arachidonic) in the diet are considered beneficial to health.

The physical properties of fatty acids, and the triglycerides derived from them, are dependent on the length and saturation of the hydrocarbon chain. A number of common fatty acids are shown in Appendix 1. Most naturally occurring unsaturated fatty acids have the *cis* configuration at the double bond; the majority of *trans* fatty acids found in the diet occur as a side product of hydrogenation processes used in industry, where the double bond becomes isomerised at the metal centre of the hydrogenation catalyst without being hydrogenated. The melting point of a fatty acid increases with the number of carbon atoms in the chain, and decreases with the number of double bonds.

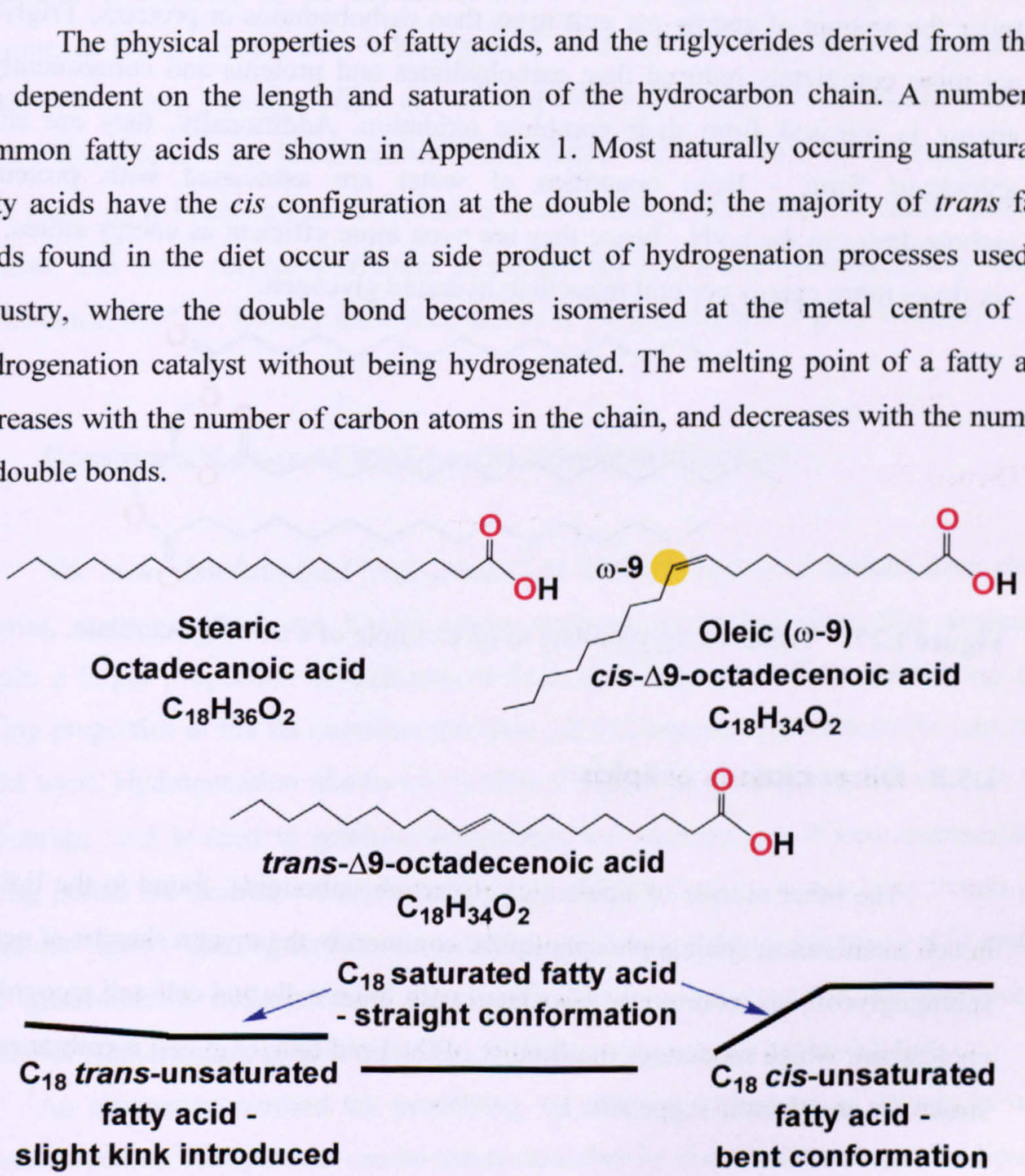

Figure 1.26: Saturated / unsaturated fatty acids, *cis* vs. *trans* conformation.

Note that this is due to the *geometry* of the double bond; the *cis* configuration introduces a "kink" in the molecule, so that the compound packs less efficiently in the solid state, and the melting point decreases relative to the saturated compound. The *trans* fatty acids have melting points comparable to the equivalent saturated fatty acids, as they adopt more linear conformations (Figure 1.26).

1.5.2 Triglycerides

Triglycerides, more commonly known as fats, or oils if liquid, are tri-esters formed between glycerol and three equivalents of fatty acid (Figure 1.27). Triglycerides are used by living creatures as a long-term energy store because they yield more than twice the amount of energy per unit mass than carbohydrates or proteins. Triglycerides are more completely reduced than carbohydrates and proteins and consequently more energy is released from their complete oxidation. Additionally, they are stored in anhydrous form - large quantities of water are associated with proteins and carbohydrates in the body - hence they are even more efficient as energy stores, storing six times more energy per unit mass than hydrated glycogen.

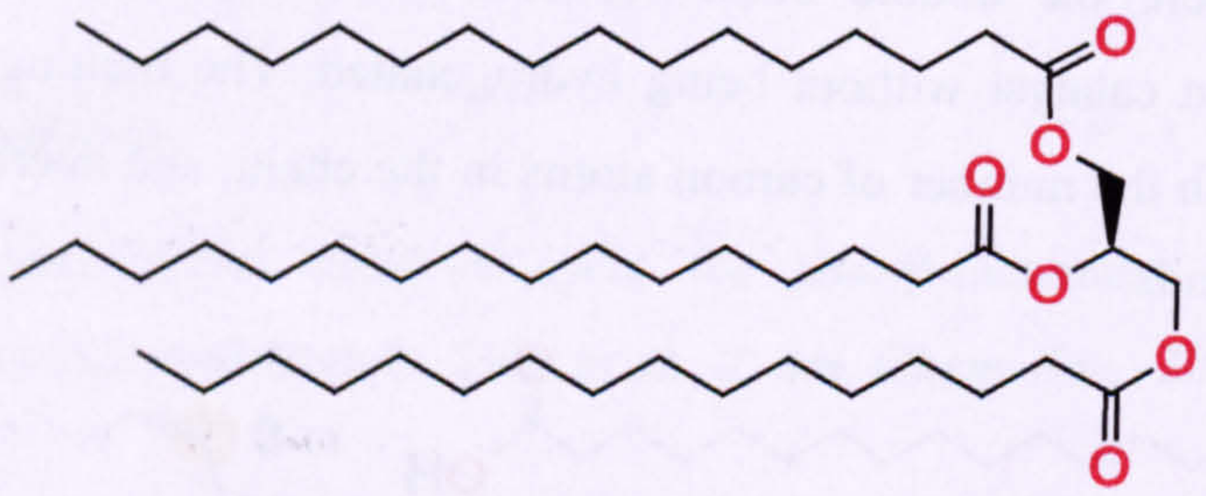

Figure 1.27: Tripalmitylglycerolate as an example of a triacylglycerolate.

1.5.3 Other classes of lipids

The other classes of lipids are: glycerophospholipids, found in the lipid bilayer in cell membranes; sphingophospholipids, common in the myelin sheaths of nerve cells; sphingoglycolipids, commonly associated with brain cells and cell-cell recognition; and cholesterol, which moderates the fluidity of the lipid bilayer in cell membranes. Sample structures are given in Appendix 1.

1.5.4 Fats and human health

Fats, as with all other nutrients, have an optimal level in the diet. Too little, and growth suffers; too much and the body's metabolism is hindered or even poisoned. Storage of excessive body fat leads to the condition of obesity, increasingly common in the more affluent areas of the world, where an excessive calorific intake is common. The precise nature of the fatty acids present in the diet is known to be of importance in health. Certain fatty acids are particularly important for the growth and maintenance of body tissue in humans and other mammals. These include linoleic, linolenic and arachidonic, although as noted above, only linoleic and α-linolenic need be supplied in the diet. The proportion of completely saturated fatty acids in the diet is of concern with regards to circulation, as an excessive intake of saturated fat is implicated in the clogging of blood vessels over a long period of time. *trans*-Fatty acids are generally considered to have a similar effect to saturated fatty acids, and there is currently debate about adding these to the list of nutritional information given with foods. Omega-3 fatty acids (such as α-linolenic) are believed to have a role in prevention of cardiovascular diseases, and some current nutritional guidelines include a recommended daily intake (for instance, the U.S. Dietary Reference Intake is 1.6 g for men, 1.1 g for women).

1.6 Commercial uses of triglyceride interesterification

The most abundant (and least costly) fats available are those derived from plant material, most of which are liquids under ambient conditions since they typically contain a larger proportion of unsaturated fatty acids than animal fat. Modifying the melting properties of the fat increases the range of commercial applications for which it can be used. Hydrogenation allows for modification of the melting properties of the fat (hardening), and is used to produce margarines and shortenings. Where intermediate melting points are desired – for improved "spreadability" and / or taste (i.e.: "melt-in-the-mouth" feel) – the degree of hydrogenation can be modulated. However, it is under these [incomplete] hydrogenation conditions that *trans*-fatty acids are produced, because of isomerisation of the double bonds at the metal centres of the catalyst.

An alternative method for modifying the melting properties of fats is to use interesterification. This process can be catalysed either by chemical species, or by lipase enzymes. Chemical interesterification is exploited on a large scale to produce fats for a

variety of end uses. Commercial interesterification involves heating appropriate proportions of the feedstock triglycerides to 373 K in the presence of sodium methoxide for one hour. The resulting product is a mixture of triglycerides resulting from random exchange of fatty acids (Figure 1.28), along with sodium carboxylates and methyl esters of fatty acids.

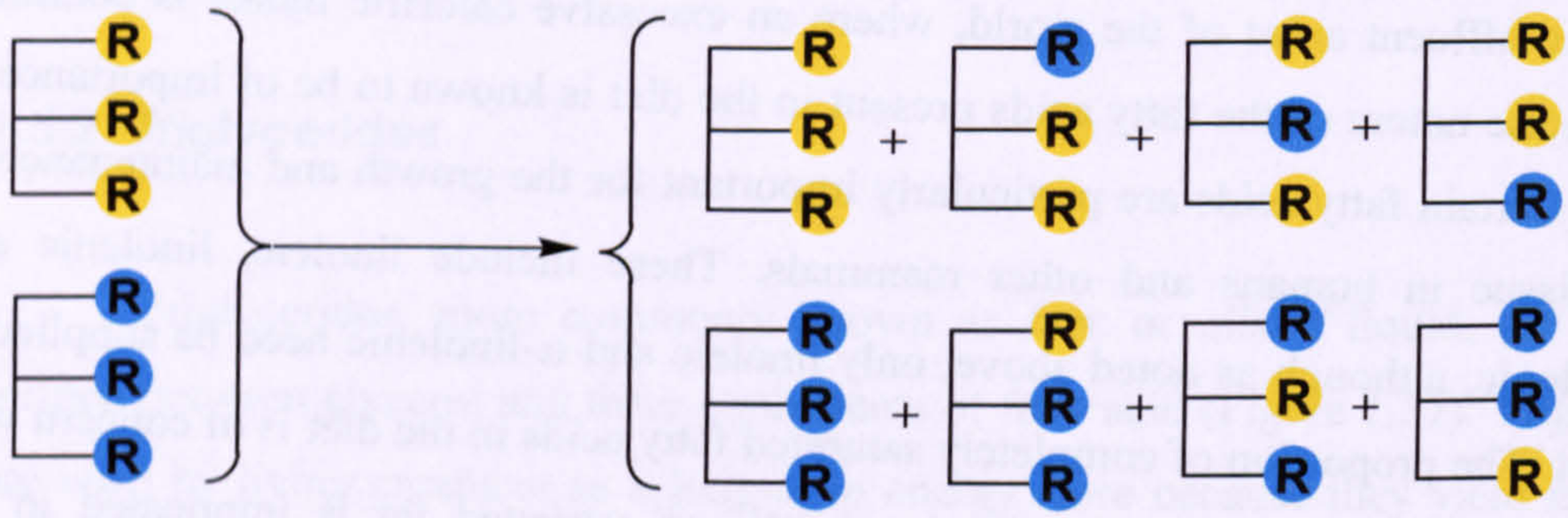

Figure 1.28: Resulting mixture of triglycerides from random interesterification.

The sodium carboxylates and methyl esters must be removed by extensive washing procedures before the product is suitable for human consumption. Fractionation of the resulting blend yields a product with the desired melting point range. A number of companies now exploit lipases to accomplish this process, since it is possible to achieve 1,3-selectivity, thus exerting more control over the melting properties (see also Section 1.5). The lipase enzymes are expensive, although certain lipases can, if handled correctly, be immobilised onto a solid support, allowing them to be re-used a number of times.

An example of a specific application for interesterification is in the production of cocoa butter equivalents. Cocoa butter is primarily composed of triglycerides with oleic acid in the 2-position and stearic or palmitic acids in the 1- and 3-positions (abbreviated to SOS and SOP). Using a base triglyceride containing mainly oleic acids (OOO), or oleic acid with palmitic acids (POP) and interesterifying with glycerol tristearate (SSS) or stearic acid, the desired triglycerides can be produced from non-cocoa sources.[68] Currently, lipase enzmes enzymes appear to be used exclusively for this process because of the need for 1,3-selectivity in producing the correct triglycerides. Unichema use a packed-bed reactor containing lipase from *Rhizomucor miehei* to transesterify sunflower oil (with high oleic acid content) with stearic acid.[69]

Chemical interesterification is used to produce so-called highly digestive triglycerides, which contain one long chain fatty acid and two shorter fatty acids; the shorter chains are preferentially hydrolysed by pancreatic lipase. The resulting

monoglycerides are absorbed readily in the lower intestine. Enzymatic interesterification can be used for this process, but is usually competitive only when the specificity of the enzyme is required, or when highly unsaturated fatty acids (which would undergo side reactions) are being used.[69] Because these triglycerides are readily digested, they are often used in infant food supplements.

1.7 Lipase enzymes

Enzymes that break down triglycerides into glycerol and fatty acids are generally referred to as lipases, and are classified as serine hydrolases.[70] The active site of these enzymes varies slightly depending on the organism, but almost invariably contains a catalytic triad consisting of serine, histidine and either aspartate or glutamate residues.[71] This active site is located within a hydrophobic cavity of the enzyme, which is covered by a "lid" that opens (Figure 1.29) to expose the active site when the enzyme encounters a lipid micelle – the enzymes show little or no activity in aqueous solution.[72]

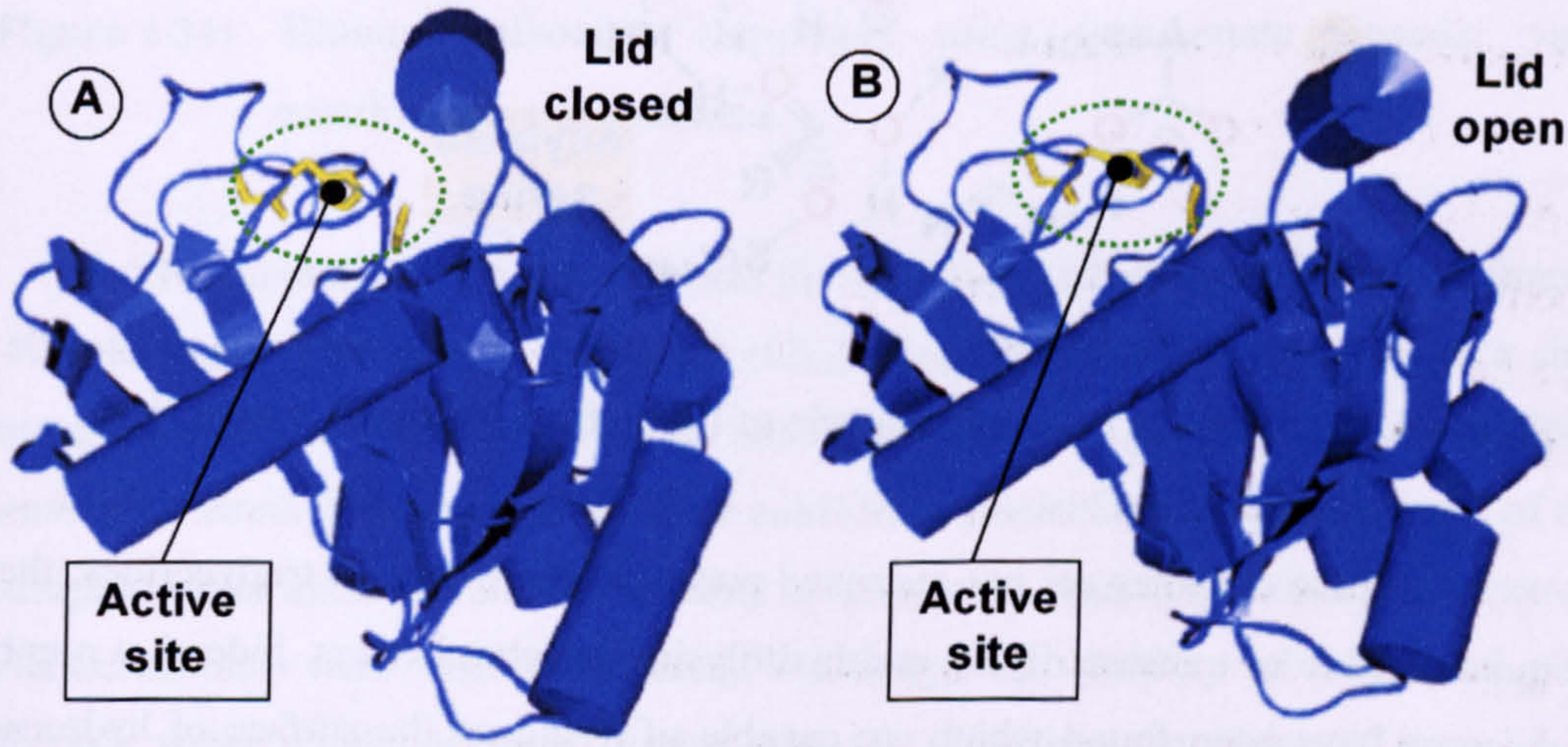

Figure 1.29: Schematic views of lipase enzyme from *Mucor miehei*, showing lid closed (A) and open (B). Adapted from original.[72]

Lipases generally do not show activity for the hydrolysis of related substrates that are targeted by other serine hydrolases (such as peptide and phospholipid cleavage). One exception to this is guinea pig (phospho)lipase, which does not have a lid domain, and is equally capable of hydrolysing both triglycerides and phosphoglycerides.[73] Although all lipases contain effectively the same catalytic triad, the three residues are oriented differently from one enzyme to another; the enzyme (and associated catalytic

cycle) illustrated in Figure 1.30 is the lipase found in the organism *Rhizopus oryzae*.[74] The serine residue is activated by a hydrogen bond relay with histidine and aspartate; the activated serine acts as a nucleophile, attacking the acyl carbon atom of a triglyceride. The tetrahedral intermediate is stabilised by hydrogen bonding between the oxy-anion and nearby amine and hydroxyl side-chains. This reaction sequence forms an acylated enzyme; the catalytic cycle is completed by hydrolysis to release the fatty acid and regenerate the serine residue in the enzyme.

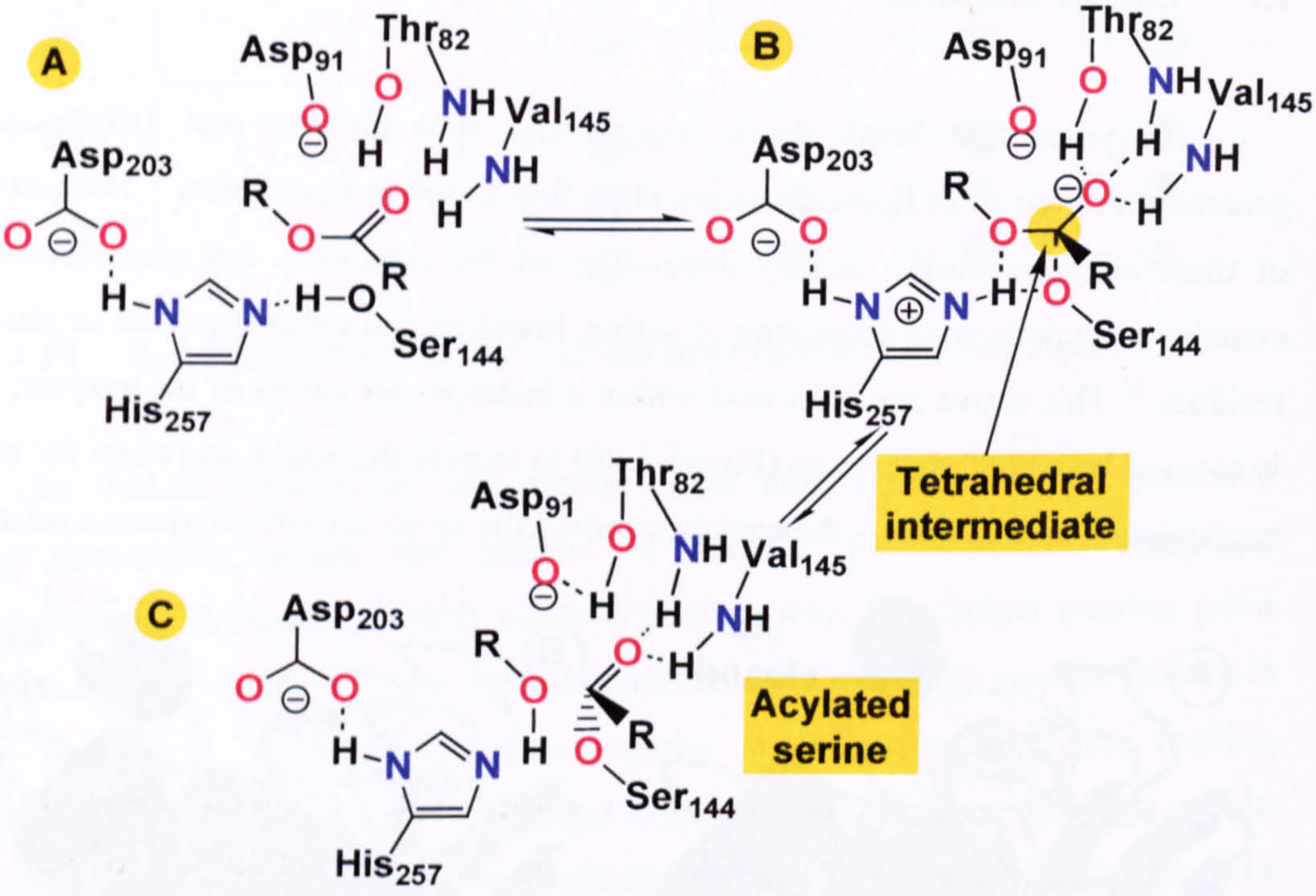

Figure 1.30: Steps in the catalytic cycle of lipase from *Rhizopus oryzae*.[74]

Lipase enzymes are not restricted purely to reaction with triglycerides; they are quite capable of transesterifying and hydrolysing unnatural esters. Indeed, a number of bacteria have been found which are capable of living on the surface of hydrocarbons and can metabolise the hydrocarbon, and their enzymes have developed a measure of tolerance for these conditions. Site-directed mutagenesis has been investigated as a route to engineering enzymes with high chemo- or stereoselctivity for a particular reaction, and can be extremely successful, giving high enantioselectivities after several rounds of mutation, although the product must be of sufficient value to justify such time-consuming research.

1.8 Approach

Two distinct lines of research were pursued during the course of this project. The first was the synthesis and catalytic testing of cationic cobalt (II) and zinc (II) alkoxides. These complexes used a face-capping chelating ligand with an associated cavity to stabilise the terminal alkoxide ligand. Previous research projects have established the synthetic procedures for complexes of this type, and explored the remarkable range of chemistry that is made possible by the controlled environment within the coordination sphere of the metal centre.[76,77] It was suggested that, if the complexes proved to be catalytically competent, the ligand could be modified to provide (or enhance) 1,3-selectivity in the interesterification of triglycerides.

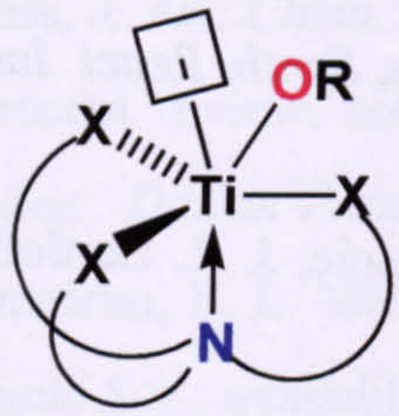

Titanium alkoxide species with tetradentate, trianionic ligand. Vacant coordination site shown (□). **X = O, NR**

Figure 1.31: Titanium alkoxide complexes using tetradentate ligands; vacant coordination site indicated.

The second area of research was the synthesis and catalytic testing of titanium (IV) alkoxides. Tetradentate, trianionic (LX_3) ligands were utilised to produce a single site catalyst with a vacant coordination site (Figure 1.31). A number of potential ligands were considered. Triphenolamines were considered particularly suitable because of their straightforward synthesis and the stability of titanium – phenolate bonds.[78] Isoelectronic triamidoamines were also considered,[79] although the stability of such complexes towards water would be much lower than the phenolate complexes. These ligands would allow the formation of a five-coordinate titanium complex with a labile alkoxide ligand and a vacant coordination site, allowing temporary binding of the ester substrate and nucleophilic attack by the alkoxide ligand. It was envisaged that the chelating ligands would impart a degree of moisture stability upon the complexes, preventing hydrolysis to titanium dioxide. The triphenolamines also have potential, through substituent variation on the aromatic ring, to be tuned for enhanced activity. Ligand modification also has the potential to provide a supported catalyst.[80]

Initial work began with the catalytic testing of titanium tetra-alkoxides, following the work of Seebach *et al.*, to gain experience in the procedures necessary for

successful handling of these materials and develop appropriate methods for catalytic testing.

1.9 References

1 S. Bloomer, P. Adlercreutz and B. Mattiasson, *J. Am. Oil Chem. Soc.*, 1990, **67**, 519.

2 (a) D. C. Bradley, R. C. Mehrotra, I. P. Rothwell and A. Singh, *Alkoxo and Aryloxo Derivatives of Metals*, Academic Press, 2001; (b) N. N. Greenwood, A. Earnshaw, *Chemistry of the Elements*, Pergamon Press.

3 R. A. Bartlett, J. J. Ellison, P. P. Power and S. C. Shoner, *Inorg. Chem.*, 1991, **30**, 2888.

4 J. Fisher, W. G. Vandersluys, J. C. Huffman and J. Sears, *Synth. React. Inorg. Met.-Org. Chem.*, 1993, **23**, 479.

5 P. D. Moran, G. A. Bowmaker, R. P. Cooney, K. S. Finnie, J. R. Bartlett and J. L. Woolfrey, *Inorg. Chem.* 1998, **37**, 2741.

6 D. C. Bradley, R. C. Mehrotra, J. D. Swanwick and W. Wardlaw, *J. Chem. Soc.*, 1953, 2025.

7 H. Meerwein and T. Bersin, *Ann.*, 1924, **475**, 113.

8 A. Singh and R. C. Mehrotra, *Coord. Chem. Rev.*, 2004, **248**, 101.

9 R. H. Cayton, M. H. Chisholm, D. L. Clark and C. E. Hammond, *J. Am. Chem. Soc.*, 1989, **111**, 2751.

10 L. D. Durfee, S. L. Latesky, I. P. Rothwell, J. C. Huffman and K. Folting, *Inorg. Chem.*, 1985, **24**, 4569.

11 M. R. Russo, N. Kaltsoyannis and A. Sella, *Chem. Commun.*, 2002, 2458.

12 Y. T. Wu, Y. C. Ho, C. C. Lin and H. M. Gau, *Inorg. Chem.*, 1996, **35**, 5948.

13 B. Szilard, *Z. Electrochem.*, 1906, **12**, 393.

14 K. G. Caulton and L. G. Hubert-Pfalzgraf, *Chem. Rev.*, 1990, **90**, 969.

15 V. Ugrinova, G. A. Ellis and S. N. Brown, *Chem. Commun.*, 2004, 460.

16 J. Otera, Ed. *Modern Carbonyl Chemistry*; Wiley-VCH: Weinheim, 2000.

17 (a) M. H. Chisholm, *Acc. Chem. Res.*, 1990, **23**, 419. (b) M. Akiyama, M. H. Chisholm, F. A. Cotton, M. W. Extine, D. A. Haitako, D. Little and P. E. Fanwick, *Inorg. Chem.*, 1979, **18**, 225.

18 M. H. Chisholm, *J. Chem. Soc.-Dalton Trans.*, 1996, 1781.

19 M. H. Chisholm, D. M. Hoffman and J. C. Huffman, *Organometallics*, 1985, **4**, 986.

20 T. A. Budzichowski, M. H. Chisholm, D. B. Tiedtke, J. C. Huffman and W. E. Streib, *Organometallics*, 1995, **14**, 2318.

21 M. H. Chisholm, J. C. Huffman, E. A. Lucas, A. Sousa and W. E. Streib, *J. Am. Chem. Soc.*, 1992, **114**, 2710.

22 M. H. Chisholm and J. A. Klang, *J. Am. Chem. Soc.*, 1989, **111**, 2324.

23 T. Katsuki and K. B. Sharpless, *J. Am. Chem. Soc.*, 1980, **102**, 5974.

24 R. M. Hanson and K. B. Sharpless, *J. Org. Chem.*, 1986, **51**, 1922.

25 S. S. Woodard, M. G. Finn, and K. B. Sharpless, *J. Am. Chem. Soc.*, 1991, **113**, 106.

26 M. G. Finn and K. B. Sharpless, *J. Am. Chem. Soc.*, 1991, **113**, 113.

27 V. S. Martin, S. S. Woodard, T. Katsuki, Y. Yamada, M. Ikeda, and K. B. Sharpless, *J. Am. Chem. Soc.*, 1981, **103**, 6237.

28 For a recent review, see: B. J. O'Keefe, M. A. Hillmyer and W. B. Tolman, *J. Chem. Soc., Dalton Trans.*, 2001, 2215.

29 P. Hormnirun, E. L. Marshall, V. C. Gibson, A. J. P. White and D. J. Williams, *J. Am. Chem. Soc.*, available as ASAP article on the web, 2004.

30 (a) M. H. Chisholm, N. W. Eilerts, J. C. Huffman, S. S. Iyer, M. Pacold and K. Phomphrai, *J. Am. Chem. Soc.*, 2000, **122**, 11845. (b) M. H. Chisholm and E. E. Delbridge, *Chem. Commun.*, 2001, 1308.

31 M. H. Chisholm and N. W. Eilerts, *Chem. Commun.*, 1996, 853.

32 Y. Kim, G. K. Jnaneshwara and J. G. Verkade, *Inorg. Chem.*, 2003, **42**, 1437.

33 B. J. O'Keefe, L. E. Breyfogle, M. A. Hillmyer and W. B. Tolman, *J. Am. Chem. Soc.*, 2002, **124**, 4384.

34 S. Inoue, H. Koinuma and T. Tsuruta, *J. Polym. Sci., Part B*, 1969, **7**, 287.

35 K. Soga, E. Imai and I. Hattori, *Polym. J.*, 1981, **13**, 407.

36 D. J. Darensbourg, M. J. Adams, J. C. Yarbrough and A. L. Phelps, *Inorg. Chem.*, 2003, **42**, 7809.

37 D. J. Darensbourg, M. W. Holtcamp, G. E. Struck, M. S. Zimmer, S. A. Niezgoda, P. Rainey, J. B. Robertson, J. D. Draper and J. H. Riebenspies, *J. Am. Chem. Soc.*, 1999, **121**, 107.

38 M. C. Cheng, E. B. Lobkovsky and G. W. Coates, *J. Am. Chem. Soc.*, 1998, **120**, 11018.

39 S. Ramaswamy, H. Eklund and B. V. Plapp, *Biochemistry*, 1994, **33**, 5230.

40 (a) M. M. Makowska-Grzyska, P. C. Jeppson, R. A. Allred, A. M. Arif and L. M. Berreau, *Inorg.Chem.*, 2002, **41**, 4872. (b) D. W. Garner, R. A. Allred, K. J. Tubbs,

A. M. Arif and L. M. Berreau, *Inorg. Chem.*, 2002, **41**, 3533. (c) L. M. Berreau, M. M. Makowska-Grzyska and A. M. Arif, *Inorg. Chem.*, 2001, **40**, 2212.

41 J. Seebacher, M. H. Shu, H. Vahrenkamp, *Chem. Commun.*, 2001, 1026.

42 (a) C. Kimblin, B. M. Bridgewater, D. G.Churchill, G. Parkin, *Chem. Commun.*, 1999, 2301; (b) M. Tesmer, M. H. Shu, H. Vahrenkamp, *Inorg. Chem.*, 2001, **40**, 4022.

43 (a) C. Bergquist and G. Parkin, *Inorg. Chem.*, 1999, **38**, 422. (b) R. Walz, K. Weis, M. Ruf and H. Vahrenkamp, *Chem. Ber.-Recl.*, 1997, **130**, 975.

44 D. C. Bradley, *Chem. Rev.*, 1989, **89**, 1317.

45 L. G. Hubert-Pfalzgraf, *New J. Chem.*, 1987, **11**, 663.

46 J. Otera, *Chem. Rev.*, 1993, **93**, 1447.

47 G. A. Grasa, T. Guveli, R. Singh and S. P. Nolan, *J. Org. Chem.*, 2003, **68**, 2812.

48 H. J. Hagemeyer and D. C. Hull, *Ind. Eng. Chem.*, 1949, **41**, 2920.

49 R. H. Baker, *J. Am. Chem. Soc.*, 1938, **60**, 2673.

50 K.-H. Wolf, B. Kuster, H. Herlinger, C.-J. Tschang and E. Schrollmeyer, *Angew. Makromol. Chem.*, 1978, **68**, 23.

51 D. Seebach, E. Hungerbühler, R. Naef, P. Schnurrenberger, B. Weidmann and M. F. Züger, *Synthesis*, 1982, **2**, 138.

52 (a) M. Kubota and A. Yamamoto, *Bull. Chem. Soc. Jpn.*, 1978, **51**, 2909. (b) M. Kubota, T. Yamamoto and A. Yamamoto, *Bull. Chem. Soc. Jpn.*, 1979, **52**, 146.

53 Y. J. Kim, K. Osakada, A. Takenaka and A. Yamamoto, *J. Am. Chem. Soc.*, 1990, **112**, 1096.

54 O. Meth-Cohn, *J. Chem. Soc., Chem. Commun.*, 1986, 695.

55 A. N. Wilkinson, D. Cole and S. B. Tattum, *Polym. Bull.*, 1995, **35**, 751.

56 M. J. Fernandezberridi, J. J. Iruin and I. Maiza, *Polymer*, 1995, **36**, 1357.

57 (a) M. G. Stanton and M. R. Gagne, *J. Org. Chem.*, 1997, **62**, 8240. (b) M. G. Stanton and M. R. Gagne, *J. Am. Chem. Soc.*, 1997, **119**, 5075.

58 M. G. Stanton, C. B. Allen, R. M. Kissling, A. L. Lincoln and M. R. Gagné, *J. Am. Chem. Soc.*, 1998, **120**, 5981.

59 P. Schnurrenberger, M. F. Züger and D. Seebach, *Helv. Chim. Acta*, 1982, **65**, 1197.

60 T. Okano, Y. Hayashizaki and J. Kiji, *Bull. Chem. Soc. Jpn.*, 1993, **66**, 1863.

61 G. W. Parshall and S. D. Ittel, *Homogeneous Catalysis (2nd Ed.)*, Ch. 11, John Wiley & Sons, Inc., 1992.

62 H. Ludewig *Polyester Fibres*; Wiley-Interscience: New York, 1971.

63 M. G. Davidson and M. G. Partridge, *Chem. Br.*, 2002, **38** (7), 26.

64 N. Diaz, D. Suarez, T. L. Sordo and K. M. Merz, *J. Phys. Chem. B*, 2001, **105**, 11302.

65 N. Diaz, D. Suarez and K. M. Merz, *J. Am. Chem. Soc.*, 2001, **123**, 9867.

66 C. Prosperi-Meys, G. Llabres, D. de Seny, R. P. Soto, M. H. Valladares, N. Laraki, J. M. Frere and M. Galleni, *FEBS Lett.*, 1999, **443**, 109.

67 L. Stryer, *Biochemistry (4th Ed.)*.

68 A. R. Macrae, *J. Am. Oil Chem. Soc.*, 1983, **60**, 291.

69 M. H. Coleman and A. R. Macrae (Unilever N. V.),DE-B 2705608, 1977 [*Chem. Abstr.*, 1977, **87**, 166366].

70 G. G. Haraldsson, B. Ö. Gudmundsson and Ö. Almarsson, *Tetrahedron Lett.*, 1993, **34**, 5791.

71 R. D. Schmid and R. Verger, *Angew. Chem.-Int. Edit.*, 1998, **37**, 1609.

72 G. G. Dodson, D. M. Lawson and F. K. Winkler, *Faraday Discuss.*, 1992, **93**, 95.

73 A. M. Brzozowski, U. Derewenda, Z. S. Derewenda, G. G. Dodson, D. M. Lawson, J. P. Turkenburg, F. Bjorkling, B. Huge-Jensen, S. A. Patkar and L. Thim, *Nature*, 1991, **351**, 491.

74 A. Hjorthe, F. Carrière, C, Cudrey, H. Wöldike, E. Boel, D. M. Lawson, F. Ferrato, C. Cambillau, G. G. Dodson, R. Thim and R. Verger, *Biochemistry*, 1993, **32**, 4702.

75 L. Brady, A. M. Brzozowski, Z. S. Derewenda, E. Dodson, G. Dodson, S. Tolley, J. P. Turkenburg, L. Christiansen, B. Hugejensen, L. Norskov, L. Thim, U. Menge, *Nature*, 1990, **343**, 767.

76 B. Greener and P. H. Walton, *J. Chem. Soc., Dalton Trans.*, 1997, 3773.

77 S, J. Archibald, S. P. Foxon, J. D. Freeman, J. E. Hobson, R. N. Perutz and P. H. Walton, *J. Chem. Soc., Dalton Trans.*, 2002, 2797.

78 L. Michalczyk, S. de Gala and J. W. Bruno, *Organometallics*, 2001, **20**, 5547.

79 (a) A. A. Naiini, W. M. P. B. Menge and J. G. Verkade, *Inorg. Chem.*, 1991, **30**, 5009. (b) Z. Duan, and J. Verkade, *Inorg. Chem.*, 1995, **34**, 4311. (c) G. E. Greco and R. R. Schrock, *Inorg. Chem.*, 2001, **40**, 3850; (d) L. H. Gade, *Chem. Commun.*, 2000, 173.

80 For a review of polymer-supported catalysts, see: N. E. Leadbeater, M. Marco, *Chem. Rev.*, 2002, **102**, 3217.

Chapter 2: Synthesis and characterisation of metal complexes

This chapter presents the techniques used to synthesise the complexes prepared for testing as catalysts in transesterification reactions, and their associated ligands. Some of the complexes have been described previously in the literature, although their use as transesterification catalysts has not—to the best of our knowledge—been investigated before.

The section on the synthesis and characterisation of cobalt complexes also includes the assignment of their paramagnetically shifted ^{1}H NMR spectra. Despite the common perception that paramagnetic complexes are unsuitable for study by NMR spectroscopy, there is a large body of information regarding the principles required for successfully collecting and interpreting such spectra; Bertini and Luchinat have been particularly active in this area.[1] Appendix 3 (Supplementary Data) gives a summary of the important principles for the collection and assignment of spectra of complexes containing a paramagnetic centre. Freeman's assignment of paramagnetically shifted NMR spectra for his cobalt alkoxide complexes[2] has formed the basis for all of the assignments in this thesis. The assignments will be discussed individually for each complex.

2.1 Ligand preparation

This section details the methods used to synthesise the ligands and their precursors for the synthesis of the metal catalyst species described in Sections 2.2, 2.3 and 2.4. Full experimental details are presented in Chapter 6.

2.1.1 Amino-*tris*-phenol ligands

Three amino-*tris*-phenol compounds were prepared for use as ligands: *tris*(2-hydroxyphenyl)amine (TPA-H_3), *tris*(2-hydroxy-3,5-dimethylbenzyl)amine (TDMA-H_3) and *tris*(2-hydroxy-3,5-di-*tert*-butylbenzyl)amine (TDBA-H_3). The ligand precursor for TPA-H_3, *tris*(2-methoxyphenyl)amine, was also prepared in the laboratory. These ligands were prepared according to published procedures—as noted in the descriptions—and were used as chelating ligands for titanium. Note the distinction

between the protonated (free ligand) and deprotonated (coordinated) forms in the abbreviations.

2.1.1 a *Tris*(2-methoxyphenyl)amine

This ligand precursor was synthesised using a copper-promoted coupling reaction[3] between (1-amino-2-methoxy)benzene and 2 equivalents of (1-methoxy-2-iodo)benzene (Figure 2.1). The method followed Bushby *et al.*,[4] although it was found that the product was more easily purified by recrystallisation from acetone and hexane, rather than hexane-ethanol. The light brown product gave ^{1}H NMR and mass spectra in accordance with those described for the authentic compound.

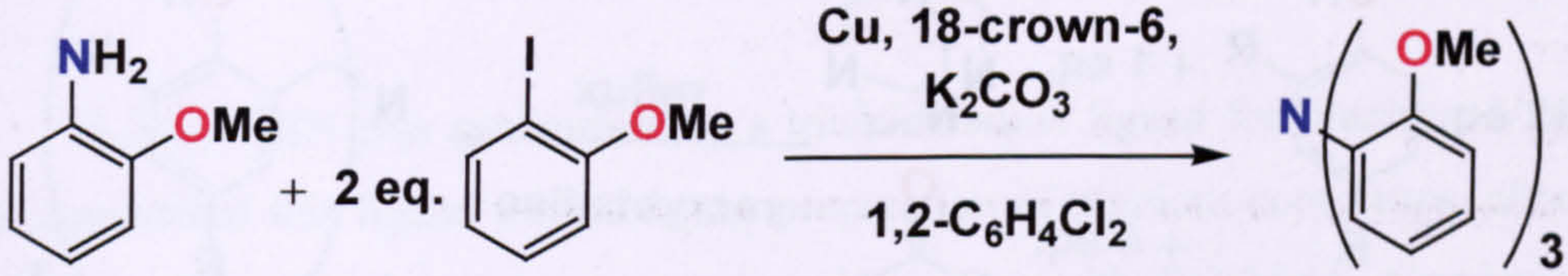

Figure 2.1: Synthesis of *tris*(2-methoxyphenyl)amine.

2.1.1 b *Tris*(2-hydroxyphenyl)amine (TPA-H_3)

Reaction of *tris*(2-methoxyphenyl)amine with boron tribromide and water results in conversion of the methoxy groups to hydroxy groups to give the *tris*-hydroxy compound (Figure 2.2), following the method described by Bushby *et al.* Recrystallisation from acetone and hexane gives the pure compound as a white solid. The ligand was characterised by ^{1}H and ^{13}C NMR spectroscopy, and mass spectrometry, all of which match the data for the authentic compound. The ligand was dessicated thoroughly before complexation to titanium (Section 2.2.1).

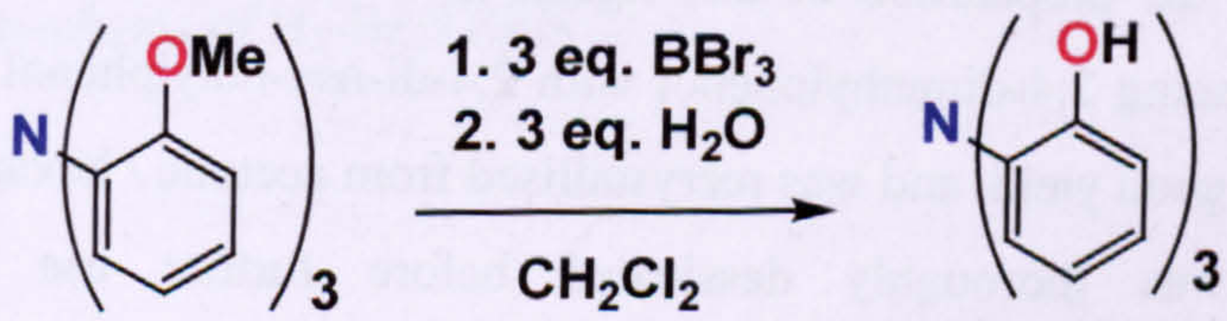

Figure 2.2: Synthesis of *tris*(2-hydroxyphenyl)amine (TPA-H_3).

2.1.1 c *Tris*{(2-hydroxy-3,5-dimethyl)benzyl}amine (TDMA-H_3)

Two different research groups have previously described the preparation of this ligand. Holmes *et al.*[5] described the synthesis of the compound using a Mannich reaction between hexamethylene tetra-amine (HMTA) and 2,4-dimethylphenol, catalysed by *para*-toluene-sulphonic acid. The method of Dargaville *et al.*[6] was found to be more convenient to use and gave a purer product. This preparation varied in the addition of formaldehyde to the Mannich reaction, and the lack of acid (Figure 2.3). The pure compound was isolated as a white solid by recrystallisation from acetone and hexane, and was dessicated thoroughly before reaction with titanium tetra-alkoxides (Section 2.2.2) in order to exclude any traces of water.

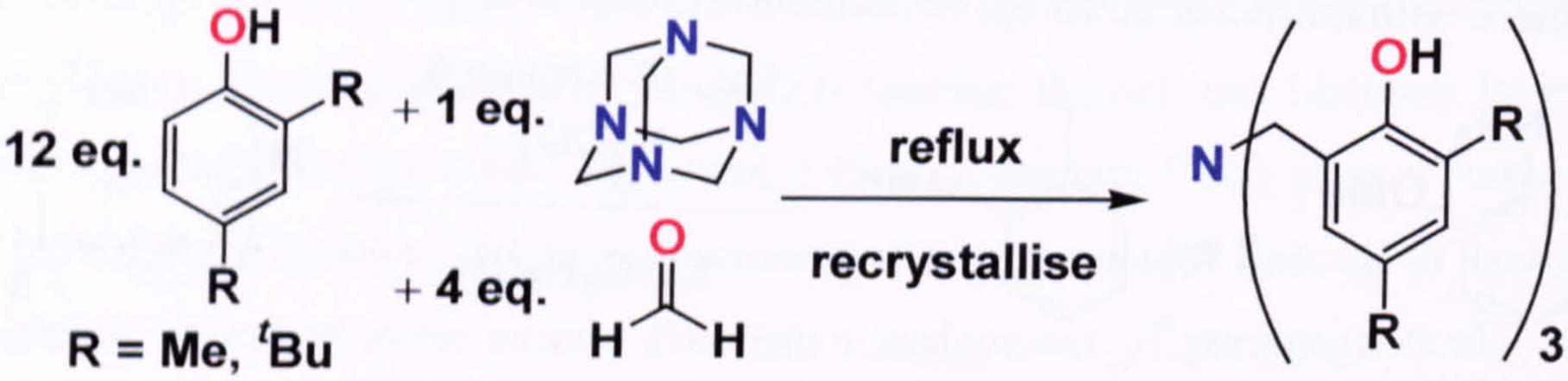

Figure 2.3: Synthesis of *tris*{(2-hydroxy-3,5-dialkyl)benzyl}amine [alkyl = Me (TDMA-H_3), ^{t}Bu (TDBA-H_3)].

The compound was characterised by ^{1}H & ^{13}C NMR spectroscopy and mass spectrometry, giving data that matched the authentic compound.

2.1.1 d *Tris*{(2-hydroxy-3,5-di-*tert*-butyl)benzyl}amine (TDBA-H_3)

TDBA was prepared for use as a chelating ligand for titanium. The substitution of methyl groups with *tert*-butyl groups gives a ligand that provides a more sterically hindered environment around the titanium centre, preventing dimerisation. Kol *et al.* gave details for the preparation of this ligand as a modification of the synthesis of TDMA-H_3, replacing 2,4-dimethylphenol with 2,4-di-*tert*-butylphenol.[7] The compound was obtained in good yield, and was recrystallised from acetone / hexane to give a white solid, which was thoroughly dessicated before further use (Section 2.2.3). Characterisation by ^{1}H & ^{13}C NMR spectroscopy and mass spectrometry gave data consistent with the authentic compound.

2.1.2 Synthesis of alternative ligands for titanium complexes

In addition to the amino-*tris*-phenol ligands, two other ligand types were considered: triamido-amines and amino-*tris*-thiols. The triamido amines have been used extensively in early transition metal chemistry[8] and reviews of the range of chemistry and potential applications have been published.[9] There do not appear to be any reports of amino-*tris*-thiols being used in the literature, but trimercapto-*phosphine* ligands have been used as ligands for early transition metals,[10] although much less frequently than triamido-amines.

2.1.2 a Synthesis of *tris*{(2-benzylamino)ethylene}amine (H_3-Bz_3TREN)

H_3-Bz_3TREN was synthesised as a triamidoamine ligand for titanium. Verkade *et al.* considered this ligand for use in the preparation of titanium complexes, although they reported that the ligand decomposed upon reaction with $Ti(NMe_2)_4$. Condensation reaction between three equivalents of benzaldehyde and TREN produced *tris*(2-benzylideneamino-ethylene)amine *in situ*, which was reduced to the triamino-amine with sodium borohydride (Figure 2.4).[11] The product was obtained as a pale yellow oil, which was degassed and then stored in a dessicator under argon. The product was characterised by ^{1}H NMR spectroscopy and mass spectrometry.

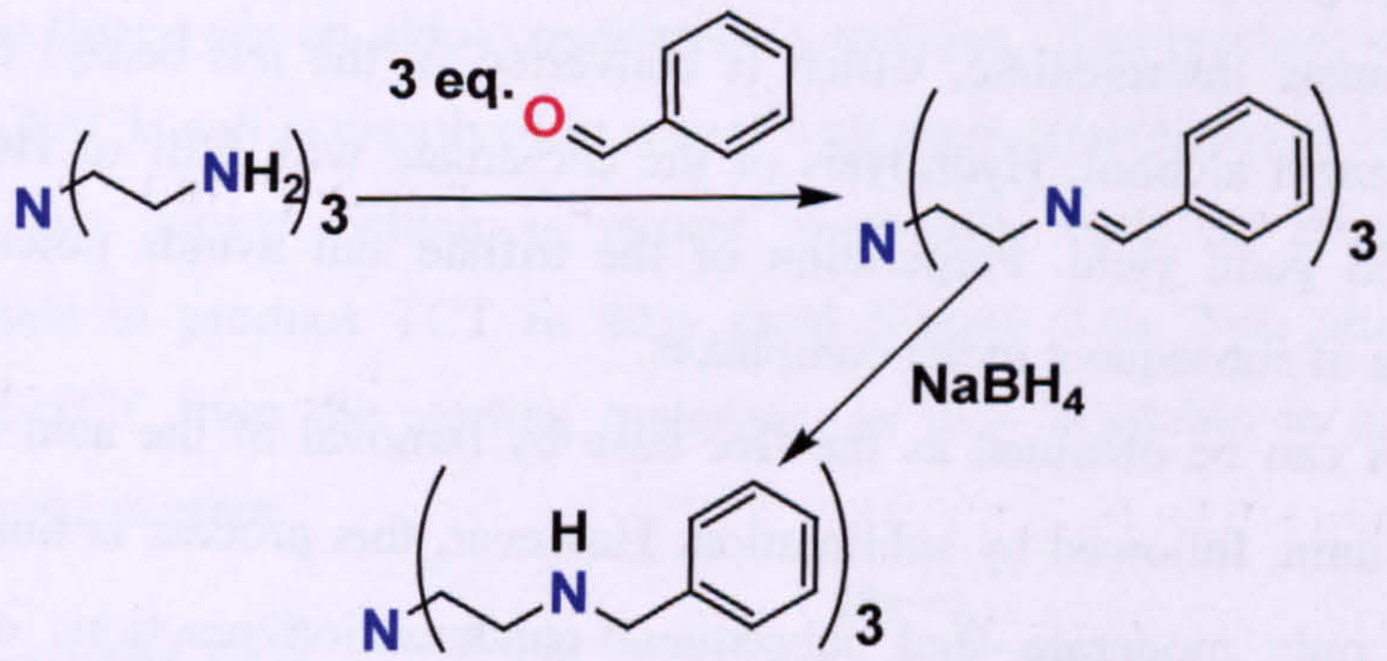

Figure 2.4: Synthesis of H_3-Bz_3TREN.

2.1.3 Ligands utilising cis,cis-1,3,5-triaminocyclohexane (TACH) as a backbone

1,3,5-triaminocyclohexane (TACH) was first synthesised by Hassel and Lunde in 1950, by reduction of 1,3,5-cyclohexane-trione-trioxime with sodium in liquid ammonia and alcohol.[12] The issue of isomeric purity was addressed by Wentworth, who noted a procedure for isolating the free ligand in an isomerically pure form,[13] and shortly afterwards by Turner, who published a more efficient procedure for separation and isolation of *cis* and *trans* isomers.[14] *cis*-TACH has been shown to coordinate to most first-row transition metals, and functionalised TACH derivatives have been used as triamido ligands for zirconium.[15] The compound can also be functionalised by condensation with aldehydes to give *tris*-imine ligands; this method of functionalisation was first reported in 1957,[16] with the aldehyde incorporating additional donor functions to produce hexadentate complexes of iron and cobalt. Condensation with hydrophobic aldehydes produces ligands that can potentially bind transition metal ions in a hydrophobic pocket. Hydrolysis of the imine bond can occur if the side chains have too much bulk directly around the metal centre.[17]

TACH is prepared as its HBr or triflic acid salt from the starting material *cis,cis*-1,3,5-cyclohexane tricarboxylic acid (available commercially) in a three-step synthesis (Figure 2.5). Addition of diphenyl phosphoryl azide results in nucleophilic substitution of the hydroxyl group with azide. The subsequent Curtius rearrangement reaction yields the *tris*-isocyanate intermediate, which is converted to the *tris*-benzyl carbamate by addition of benzyl alcohol. Hydrolysis of the carbamate with HBr or HOTf provides TACH.3HX in good yield. Preparation of the triflate salt avoids potential bromide contamination of subsequent metal complexes.

TACH can be obtained as the free base by removal of the acid using an ion-exchange column, followed by sublimation. However, this process is time-consuming, the yield is only moderate, and subsequent condensation reactions of the TACH produced display far lower yields than when the free base is produced *in situ*. Comparable exclusion of halide ions can be achieved by use of TACH.3HOTf as the intermediate, or by simply extracting (with water) any residual HBr from samples of the TCT ligand (Section 2.1.3 a).

Cis,cis-1,3,5-triaminocyclohexane was characterised by ^{1}H NMR spectroscopy and mass spectrometry.

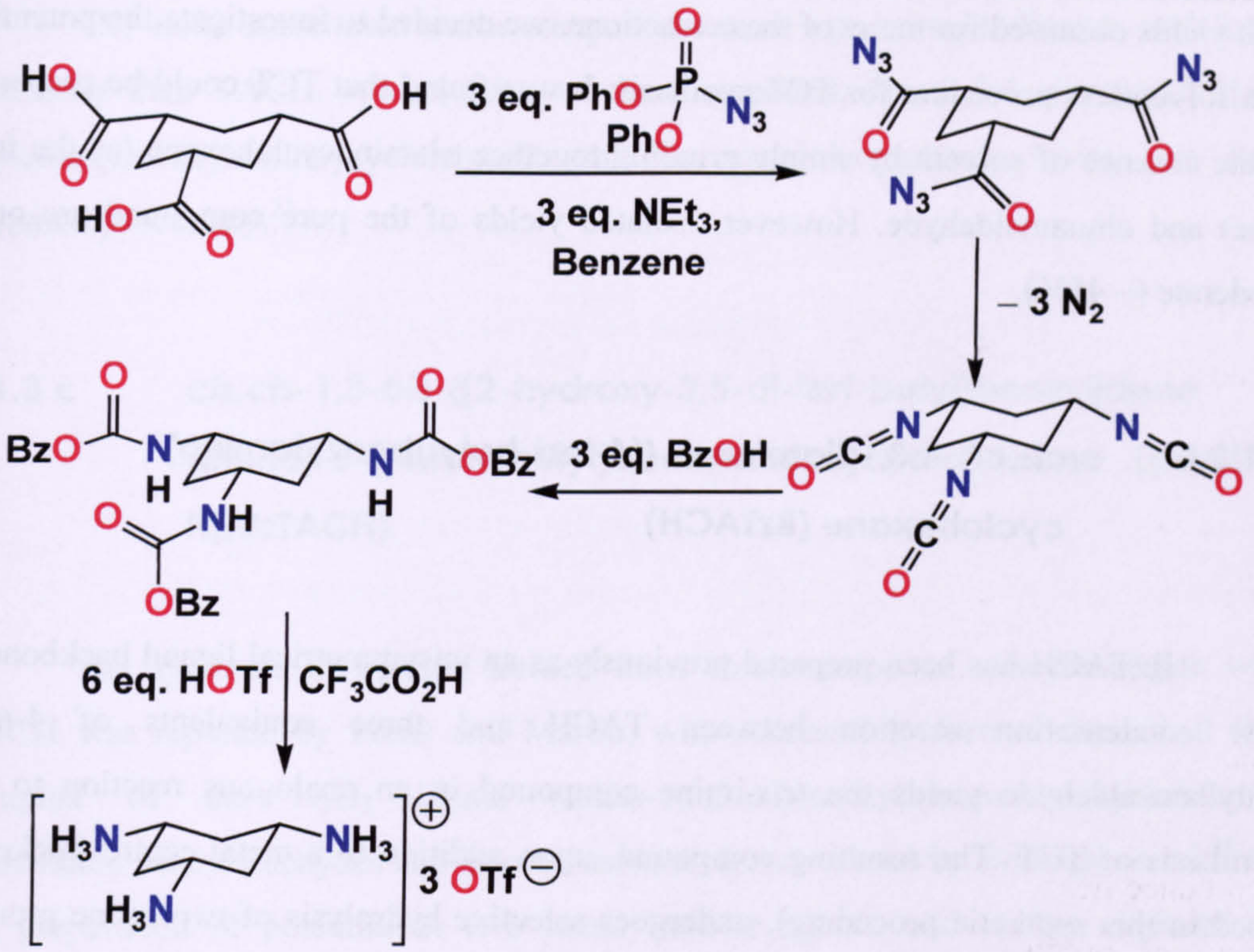

Figure 2.5: Synthesis of TACH.3HOTf.

2.1.3 a *cis,cis*-1,3,5-*tris*(cinnamylideneamino)cyclohexane (TCT)

Reaction of TACH.3HOTf with three equivalents of cinnamaldehyde produces the *tris*-imine ligand via an aldol condensation reaction.[2] The reaction uses a biphasic reaction: the TACH salt is dissolved in water, with three equivalents of NaOH added to liberate the free amine, which is stirred vigorously with an ether solution of cinnamaldehyde to produce TCT in 80% yield (Figure 2.6). This allows for facile separation of TCT from the starting materials, as it is insoluble in water and only sparingly soluble in ether.

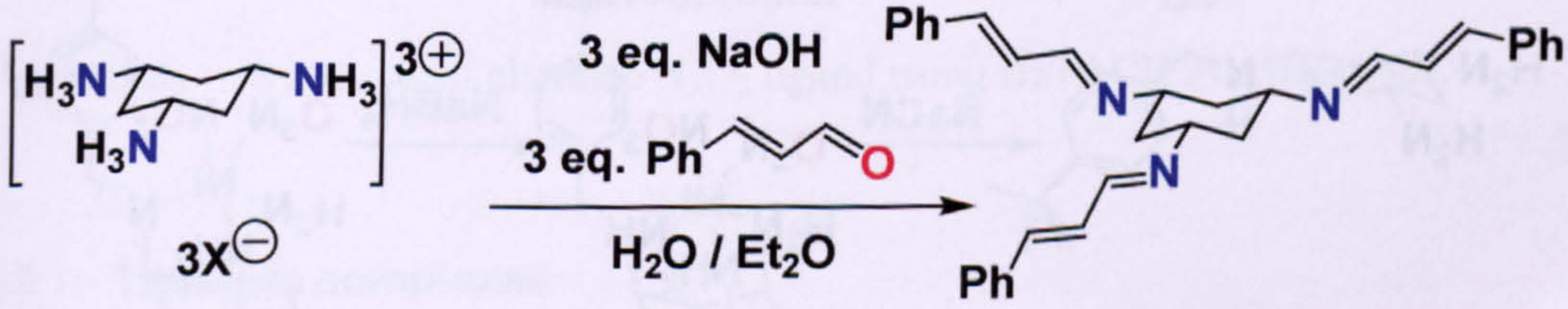

Figure 2.6: Synthesis of TCT.

Recently, a review of solventless reactions described the frequent success of aldol condensation reactions using mechanochemical techniques.[18] Encouraged by the

high yields observed for many of these reactions, we decided to investigate the potential of a solventless procedure for TCT synthesis. It was found that TCT could be prepared in the absence of solvent by simply grinding together triaminocyclohexane (as the free base) and cinnamaldehyde. However, isolated yields of the pure compound are only moderate (~ 45%).

2.1.3 b *cis,cis*-1,3,-diamino-5-{(4-*tert*-butyl)benzylamino} cyclohexane (BzTACH)

BzTACH has been prepared previously as an unsymmetrical ligand backbone.[19] The condensation reaction between TACH and three equivalents of 4-*tert*-butylbenzaldehyde yields the *tris*-imine compound in an analogous reaction to the synthesis of TCT. The resulting compound, upon addition to a metal centre (nickel is used in this synthetic procedure), undergoes selective hydrolysis of two imine groups; the *tris*-imine ligand is too bulky to bind to the nickel centre. This reaction yields a nickel complex bearing the ligand *cis,cis*-1,3,-diamino-5-{(4-*tert*-butyl)benzylideneamino} cyclohexane.[20] Reduction of the benzyl-imine to benzyl-amine, followed by demetallation with cyanide affords the target compound, isolated as a sticky, colourless oil (Figure 2.7).

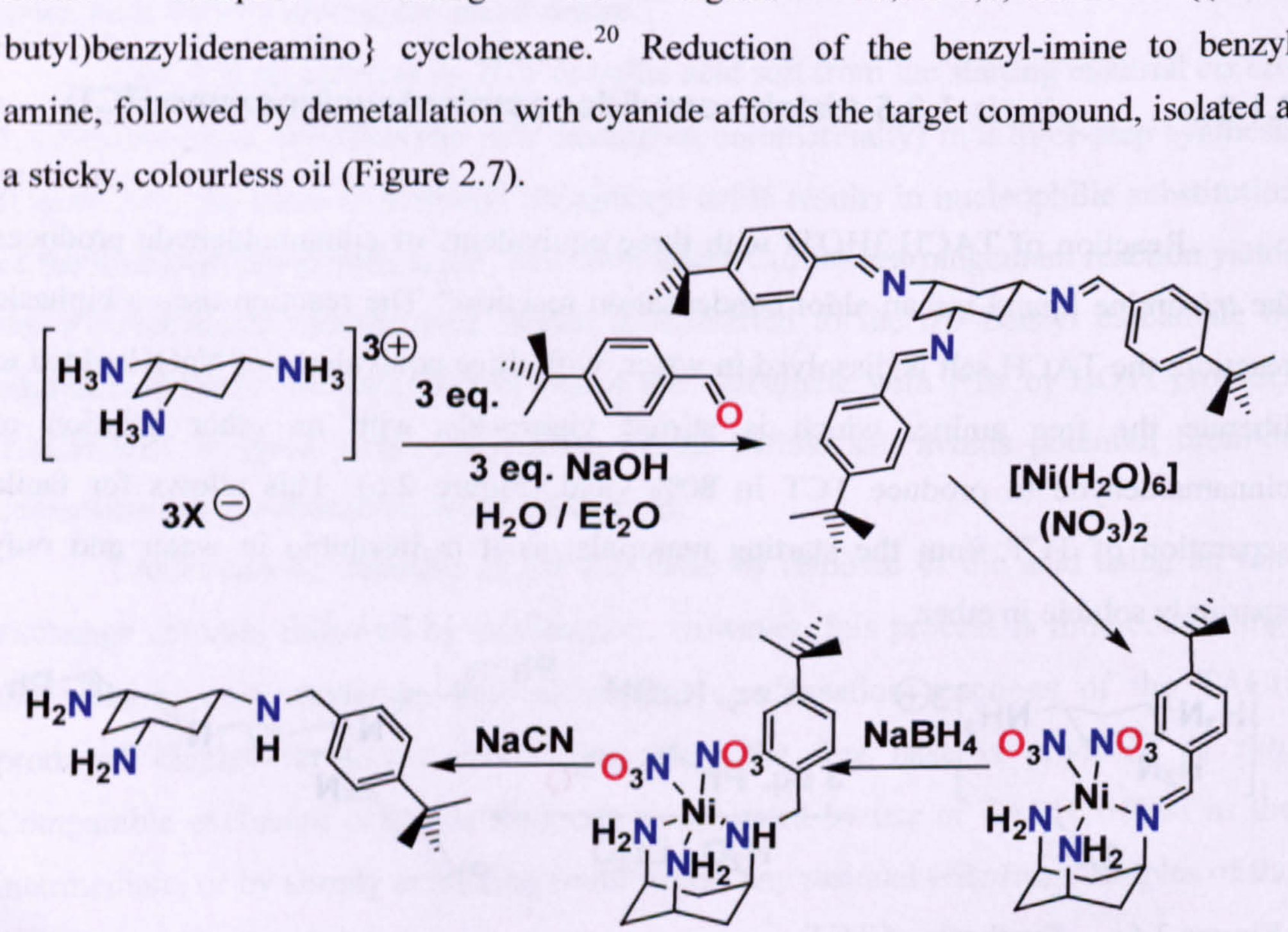

Figure 2.7: Synthesis of BzTACH.

The mono-substituted amine compound acts as a precursor to ligands with lower symmetry than TACH. A derivative of this compound, *cis,cis*-1,3,-diamino-5-{(3,5-dimethoxy)benzylamino}cyclohexane, and its metal complexes, have also been prepared previously.[21]

2.1.3 c *cis,cis*-1,3-*bis*-{(2-hydroxy-3,5-di-*tert*-butyl)benzylidene amino}-5-{(4-*tert*-butyl)benzylamino}cyclohexane ({^{t}Bu$_2$Sal-H}$_2$BzTACH)

The synthesis of ligands formed from condensation of salicylaldehyde with TACH was reported by Lions and Martin, who successfully formed the cobalt (III) complex of the N_3O_3 ligand *cis,cis*-1,3,5-*tris*(salicylideneamino)cyclohexane. Substituted salicylaldehydes can also be used, as demonstrated by Bollinger *et al.*[22] for the preparation of potential *in vivo* metal transfer agents, and further explored by Walton *et al.* in the preparation of mimics of superoxide dismutase[23] and galactose oxidase[24] enzymes. Condensation of BzTACH with two equivalents of 3,5-di-*tert*-butylsalicylaldehyde yields the N_3O_2 ligand (Figure 2.8);[22] Nairn *et al.* described the preparation of the related ligand based on (3,5-dimethoxy)benzylTACH.[20] This ligand was used to prepare a cobalt complex (Section 2.3.6), and also a cationic titanium complex (Section 2.2.4).

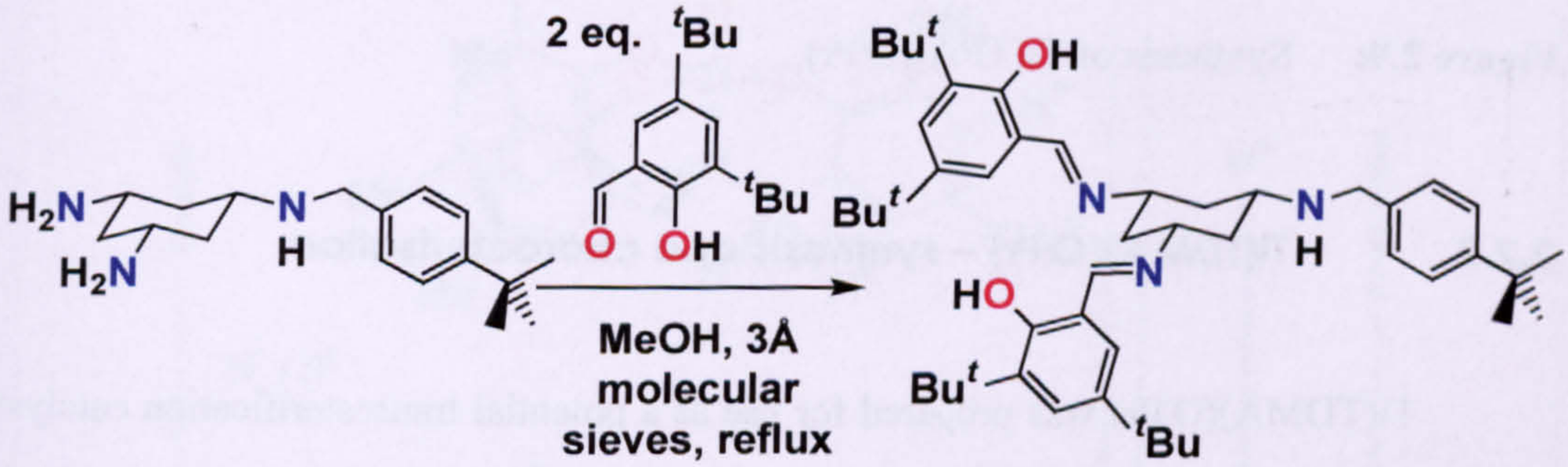

Figure 2.8: Synthesis of alternate N_3O_2 ligand using BzTACH as a backbone.

2.2 Titanium complexes

The titanium complexes described below have been described previously in the literature. They were chosen as single site, Lewis acid complexes with a basic alkoxide ligand, making them suitable candidates for transesterification catalysts. They also have

the potential to be modified by the addition of substituents onto the aromatic ring, allowing for tuning of catalytic activity or, by adding polymerisable groups such as vinyl, cross-linking to a solid support to give a reusable catalyst.

2.2.1 Ti(TPA)(O^{i}Pr) – synthesis and characterisation

Verkade *et al.* made reference to the preparation of this complex in a recent publication,[25] although full experimental details were not given (reference was made to a French patent from 1968)[26]. Adding one equivalent of titanium tetra-*iso*-propoxide to a dichloromethane / *iso*-propanol solution of *tris*(2-hydroxyphenyl)amine results in the substitution of three *iso*-propoxide ligands with the phenolate groups of the chelating ligand (Figure 2.9). This reaction proceeds rapidly at ambient temperature, and is presumably driven by both the formation of strong titanium-phenolate bonds and the chelate effect. Removal of solvent yields the desired complex, although it invariably contains several equivalents of *iso*-propanol, even after recrystallisation and extended periods of evacuation. The complex has been characterised by ^{1}H NMR spectroscopy.

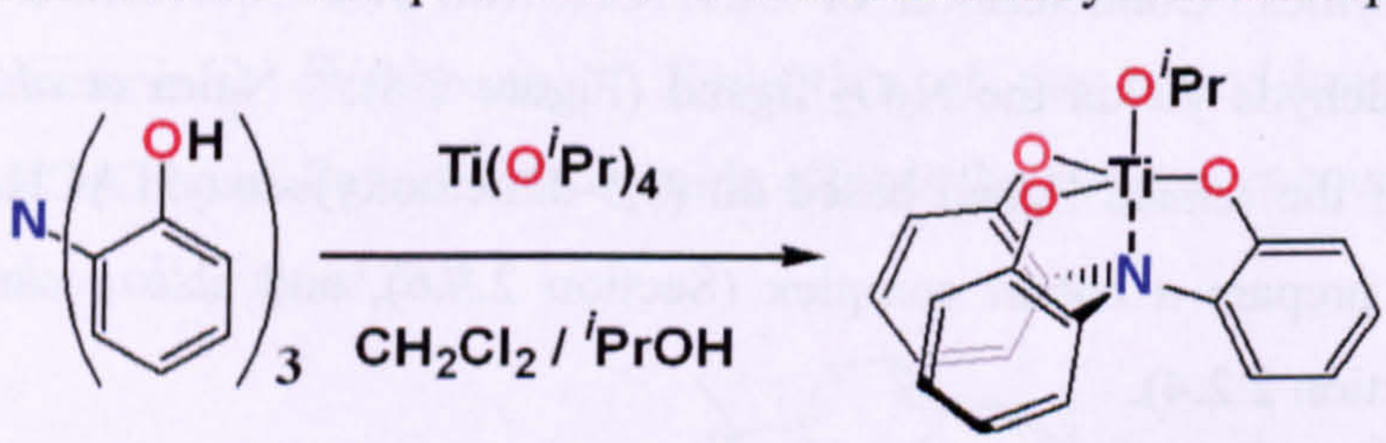

Figure 2.9: Synthesis of Ti(TPA)(O^{i}Pr).

2.2.2 Ti(TDMA)(O^{i}Pr) – synthesis and characterisation

Ti(TDMA)(O^{i}Pr) was prepared for use as a potential transesterification catalyst. The complex has a single terminal alkoxide ligand, suggesting that it may act as a single site catalyst. The presence of the amino-*tris*-phenolate ligand should also provide some degree of moisture stability relative to the parent titanium compound, Ti(O^{i}Pr)$_4$.

Ti(TDMA)(O^{i}Pr) was prepared in the manner described by Kol *et al.*[7] (Figure 2.10), who also reported that the complex can decompose by hydrolysis to form what was assigned as the oxo-bridged dimer [Ti(TDMA)]$_2$(μ-O). Davidson *et al.* have determined the crystal structure of the monomeric complex.[27] They reported a Ti – O – C bond angle of 179.7° and a Ti – O bond length of 1.774(2) Å for the *iso*-propoxide

ligand. The bridgehead nitrogen of the amino-*tris*-phenolate ligand is weakly bound, with a Ti – N bond length of 2.305(2) Å. The essentially linear Ti – O – C bond suggests that the *iso*-propoxide ligand is donating additional electron density to the titanium centre through two π-donor interactions (Section 1.2.1). This suggests that the titanium centre is extremely electron-deficient.

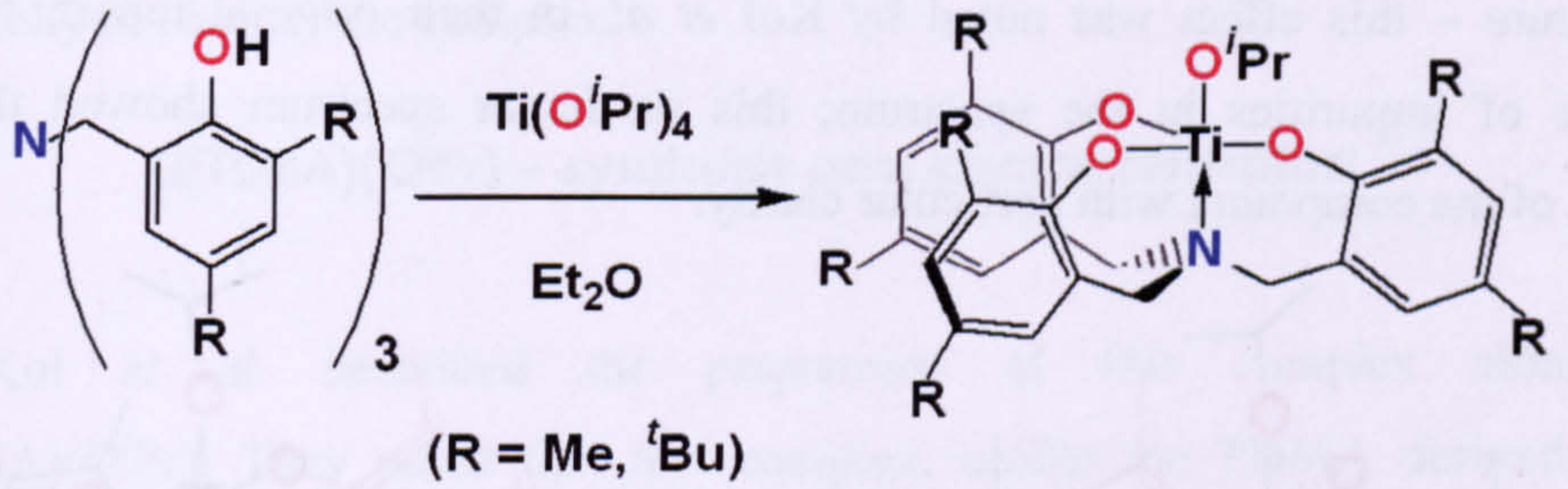

Figure 2.10: Synthesis of Ti(TDMA)(O^{i}Pr) [R = Me] and Ti(TDBA)(O^{i}Pr) [R = ^{t}Bu].

Tris(2-hydroxy-3,5-dimethylbenzyl)amine readily displaces three *iso*-propoxide ligands from the titanium tetra-alkoxide in the same manner as TPA-H_3. A yellow complex is afforded in 94% yield by removal of the solvent; purification can be achieved by recrystallisation from cold ether.

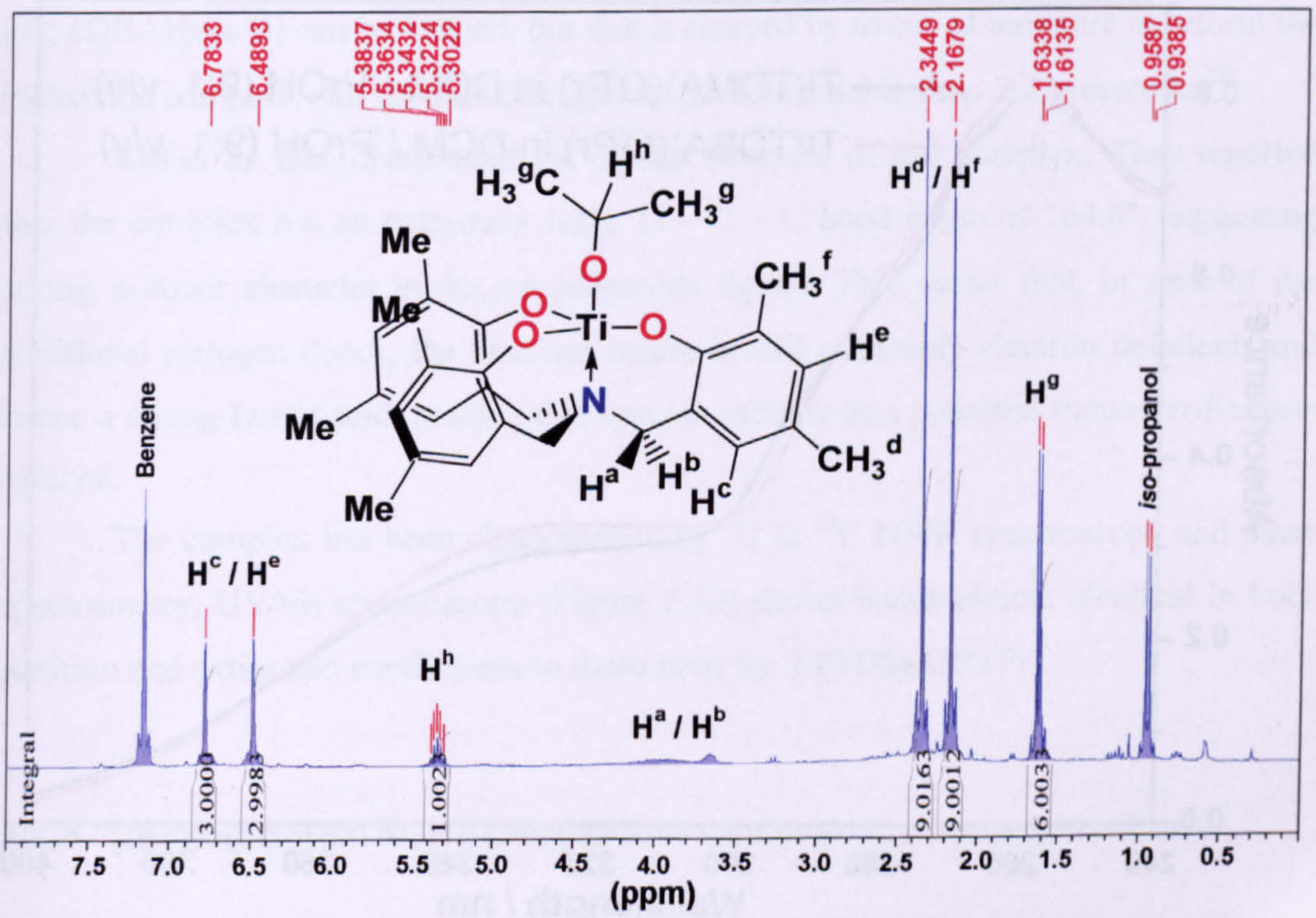

Figure 2.11: ^{1}H NMR spectrum of Ti(TDMA)(O^{i}Pr) in C_6D_6 (300 MHz, 298 K).

The complex has been characterised by ^{1}H (Figure 2.11) and ^{13}C NMR spectroscopy. The complex shows the peaks described in the literature characterisation;[7] note that the complex is fluxional on the NMR timescale (Figure 2.12), with the bridgehead nitrogen donor temporarily dissociating, allowing the phenolate "arms" to change conformation, hence the methylene protons give very broad resonances at room temperature – this effect was noted by Kol *et al.* in their original report. Note the presence of impurities in the spectrum; this particular spectrum showed the main features of the compound with particular clarity.

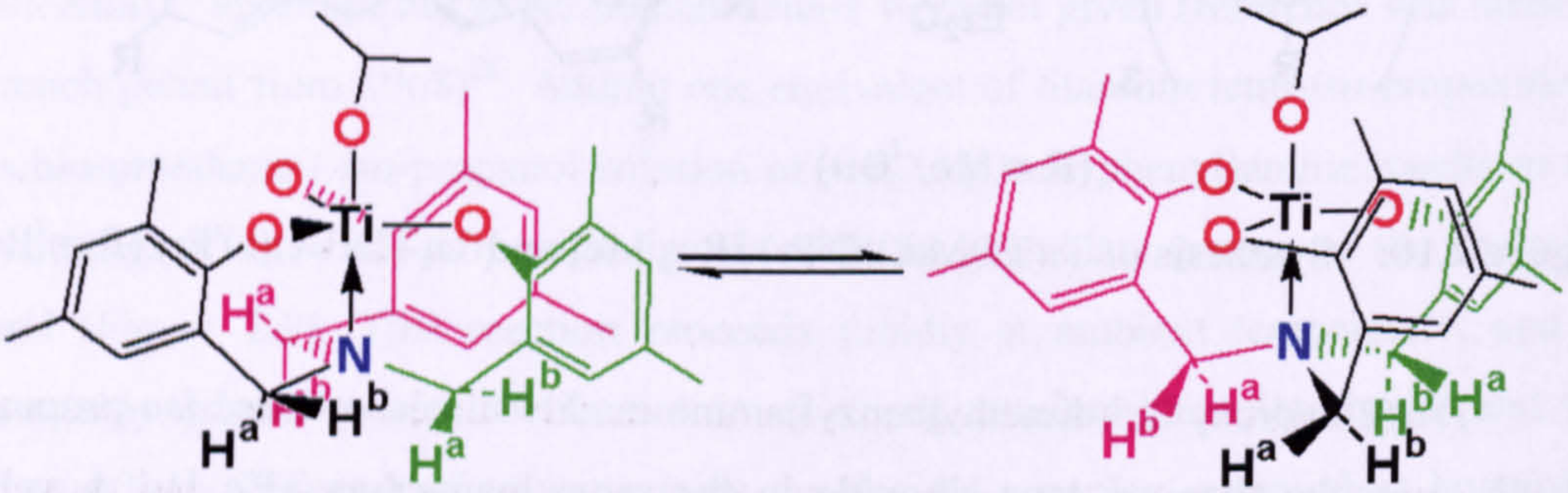

Figure 2.12: Fluxional behaviour of Ti(TDMA)(O^{i}Pr) on the NMR timescale.

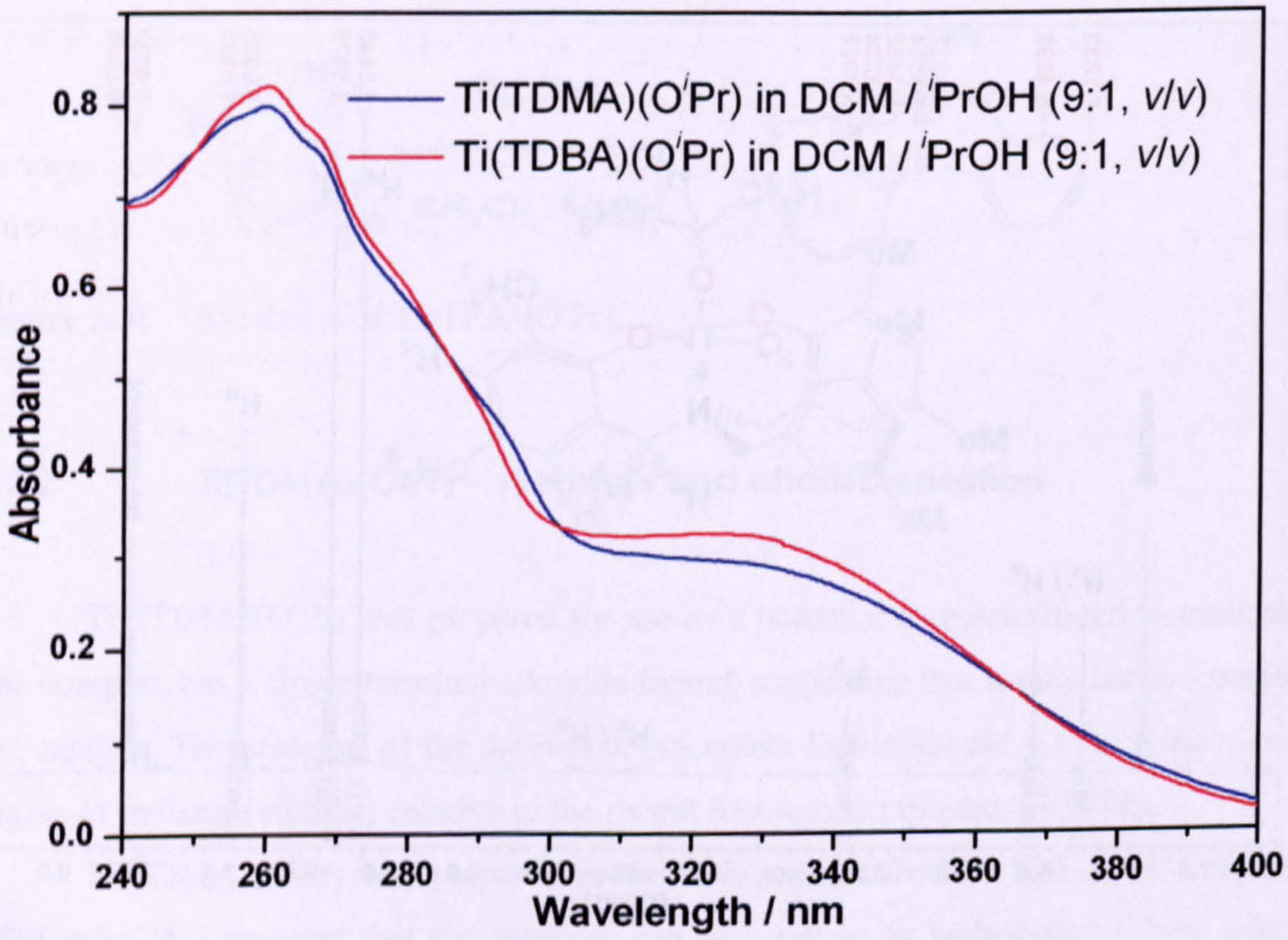

Figure 2.13: UV/vis spectra of Ti(TDMA)(O^{i}Pr) and Ti(TDBA)(O^{i}Pr) in CH_2Cl_2 / ^{i}PrOH (9:1, *v*/*v*).

UV/vis spectroscopy (Figure 2.13) shows a band at 260 nm, with a shoulder at ~270 nm, and a broad band centred at ~326 nm; the tail of this absorption band extends into the blue region, giving the complex its yellow colour. The large extinction coefficients (> 10^4 dm^3 mol^{-1} cm^{-1}) suggest that these are ligand-to-metal charge transfer (LMCT) bands. Electrospray mass spectrometry has also been used successfully to identify the complex.

2.2.3 Ti(TDBA)(O^{i}Pr) – synthesis and characterisation

Kol *et al.* described the preparation of this complex along with Ti(TDMA)(O^{i}Pr). They noted that this complex, unlike the TDMA derivative, was stable to moisture, suggesting that the complex would be a much more robust catalyst. The complex was prepared in the manner described by Kol *et al*. The *tert*-butyl substituted triphenolamine chelates to titanium in the same manner as the methyl substituted derivative, although the resulting complex is stable to air and moisture. Recent work using this ligand has shown that it is possible to form the (stable) hydroxide species Ti(TDBA)(OH) by an indirect route, and that the μ-oxo dimer $[Ti(TDBA)]_2(\mu\text{-}O)$ can be formed, but this is cleaved by traces of moisture to reform the hydroxide complex, and the alkoxide species are more stable than the hydroxide.[28]

Kol *et al.* also determined the crystal structure of this complex. They reported that the complex has an extremely large Ti – O – C bond angle of 164.6°, suggesting strong π-donor character in the *iso*-propoxide ligand. This shows that, in spite of the additional nitrogen donor, the titanium centre is still extremely electron deficient, and hence a strong Lewis acid, making this species suitable as a potential transesterification catalyst.

The complex has been characterised by ^1H & ^{13}C NMR spectroscopy and mass spectrometry. UV/vis spectroscopy (Figure 2.13) shows bands almost identical in both position and extinction coefficients to those seen for Ti(TDMA)(O^{i}Pr).

2.2.4 [Ti({^{t}Bu$_2$Sal}$_2$BzTACH)(O^{i}Pr)]BPh$_4$ – synthesis & characterisation

Encouraged by the success of the cationic cobalt complexes (Section 2.3), we decided to investigate the possibility of forming a cationic titanium alkoxide complex. However, it should be noted that the target complex would not coordinatively

unsaturated. Addition of a solution of $Ti(O^iPr)_3Cl$ in CH_2Cl_2 to one equivalent of $\{^tBu_2Sal\text{-}H\}_2BzTACH$, followed by one equivalent of $NaBPh_4$ (Figure 2.14), gave a yellow solution, which was filtered and evacuated to give an orange solid. ^1H NMR and mass spectrometry suggested that the desired product had been formed.

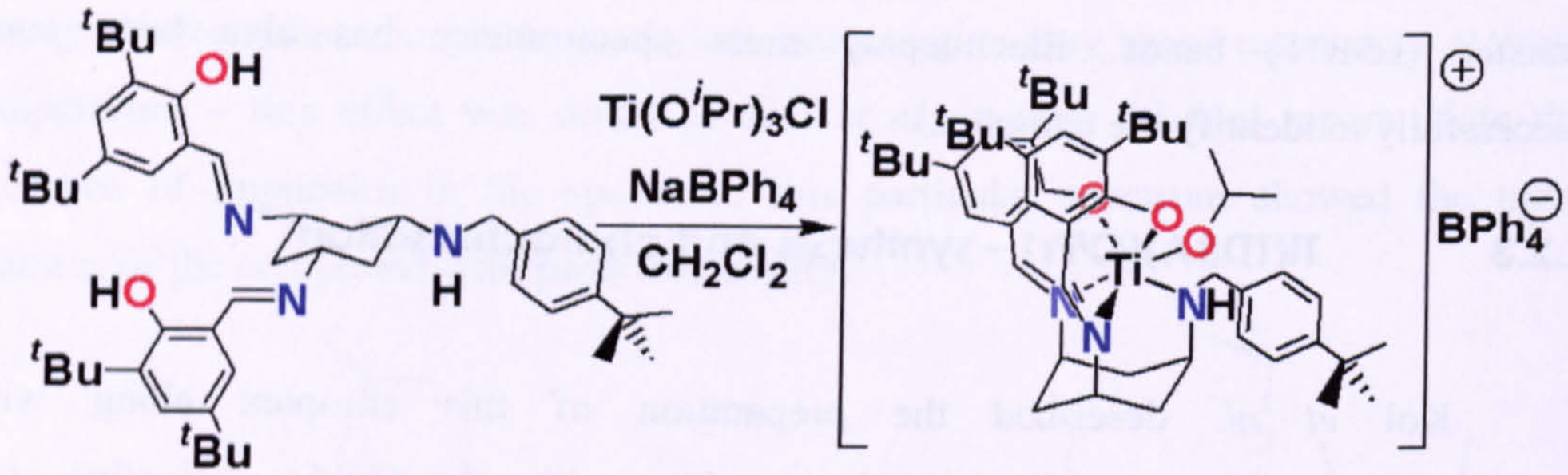

Figure 2.14: Synthesis of $[Ti(Sal_2BzTACH)(O^iPr)]BPh_4$.

2.2.5 Ti(Bz$_3$TREN)(O^{n}Bu) – synthesis & characterisation

The synthesis of triamidoamine titanium alkoxide complexes was attempted to complement the work on the iso-electronic amine *tris*-phenolate complexes. Several problems were envisaged, firstly that the complexes might not have sufficient moisture stability, and secondly that the high oxophilicity of titanium might hamper the formation of stable mononuclear complexes, *via* the formation of Ti – O – Ti moieties. In order to assist in the synthesis of this complex, reaction was attempted from the triclorotitanium alkoxide precursor, using addition of base to remove the HCl produced in the reaction. ^1H NMR suggested that the desired product had been formed, but signals were broad and the complex was prone to decomposition by hydrolysis.

2.3 Cobalt complexes

There have been relatively few reports of cobalt alkoxides, although the preparation of some homoleptic cobalt alkoxides has been reported; $[Co(OMe)_2]$[29] was reported to be a polymeric compound based on infinite CoO_6 octahedra, whilst the use of the bulky *tris*(cyclohexyl)methoxide ligand has allowed the isolation of the dimeric species $[Co_2(\mu_2\text{-}OCCy_3)_2(OCCy_3)_2]$, (Cy = cyclohexyl, *c*-$C_6H_{11}$) and a mononuclear species, $Co(OCPh_3)_2(THF)_2$, has been isolated by the addition of THF ligands.[30] Electrochemical synthesis has allowed the preparation of $[Co(OR)_2]_x$ where R = Me, Et,

decompose by β-hydride elimination.[33] Berreau *et al.* have very recently reported the preparation and characterisation of two mononuclear nitrogen-sulfur ligated cobalt (II) methoxide complexes.[34] They have used paramagnetic ^{1}H NMR spectroscopy as part of their characterisation methods, and have been able to make assignments for all of the protons in the compounds.

Walton *et al.* have utilised the TCT ligand, and a number of related ligand systems, to produce small molecule mimics of a number of enzymes. Complexation of the TCT ligand to a metal centre induces a conformational rearrangement of the cinnamyl arms, from all-equatorial to all-axial arrangement (Figure 2.15).

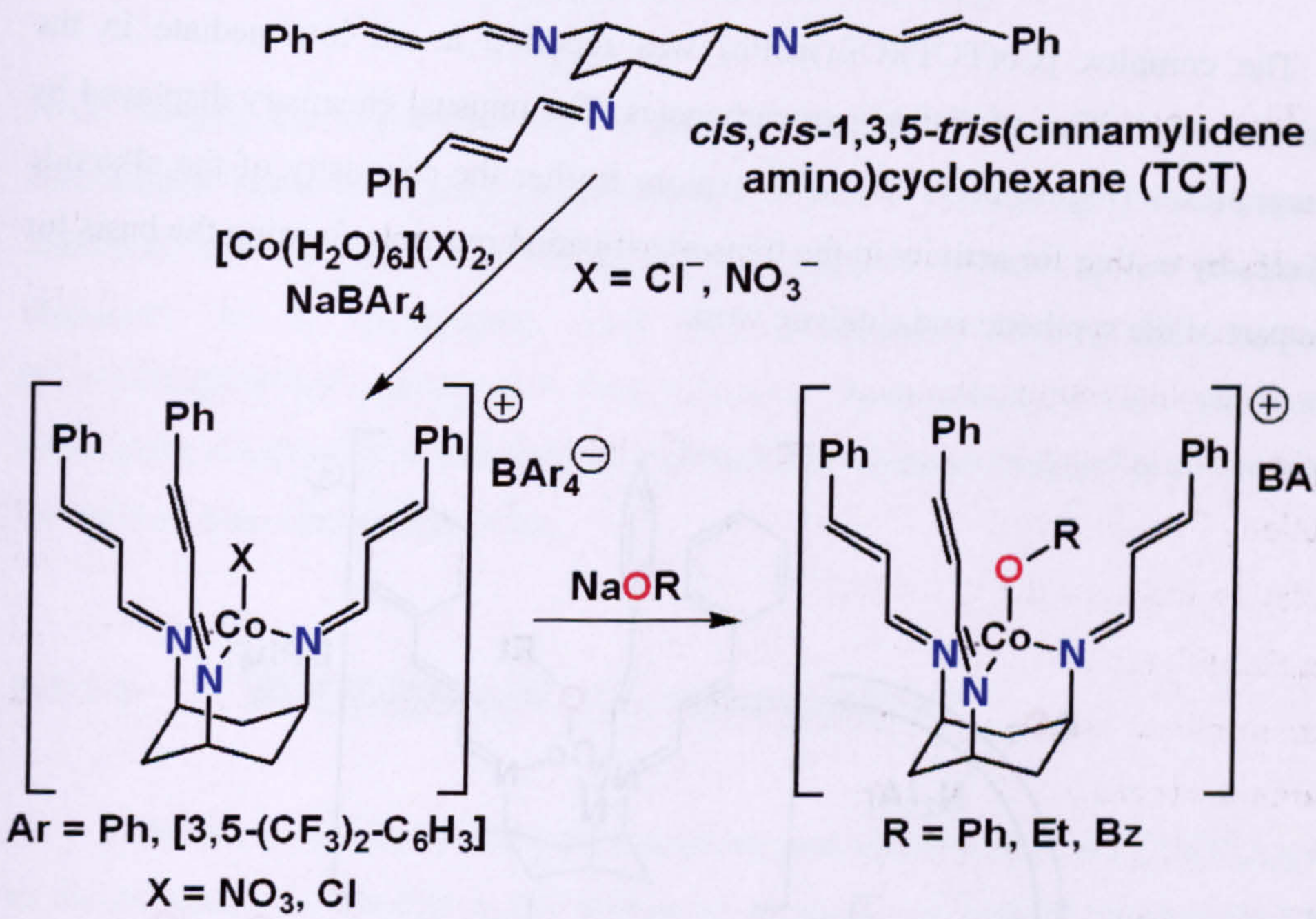

Figure 2.15: Synthesis of cobalt-TCT complexes.

The hydrophobic cavity created by related complexes has allowed the isolation of metal complexes containing chains of hydrogen-bonded solvent molecules.[35] It is this hydrophobic cavity that enables steric control over the environment around the cobalt centre. Complexing TCT to zinc and cobalt has yielded model complexes for HCA II.[36] Freeman has produced a number of alkoxide and aryloxide derivatives as part of an investigation into the reactivity of these complexes with CO_2 (Figure 2.16; see Chapter 4 for discussion).

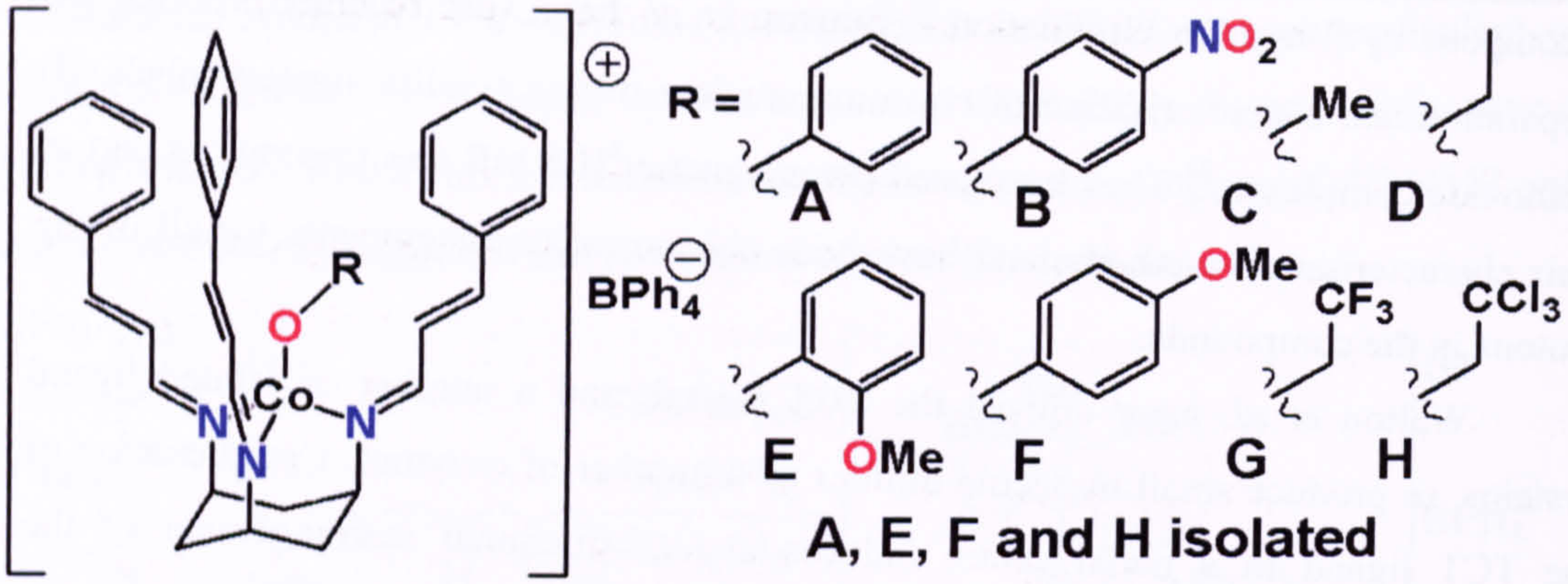

Figure 2.16: Cobalt-TCT-alkoxide complexes, as prepared by Freeman.

The complex $[Co(TCT)(OEt)]BPh_4$ was reported as an intermediate in the catalytic decomposition of dialkyl pyrocarbonates. The unusual chemistry displayed by these complexes (Figure 2.17) led us to explore further the chemistry of the alkoxide complexes by testing for activity in the transesterification reaction, forming the basis for a large part of the synthetic and catalytic work.

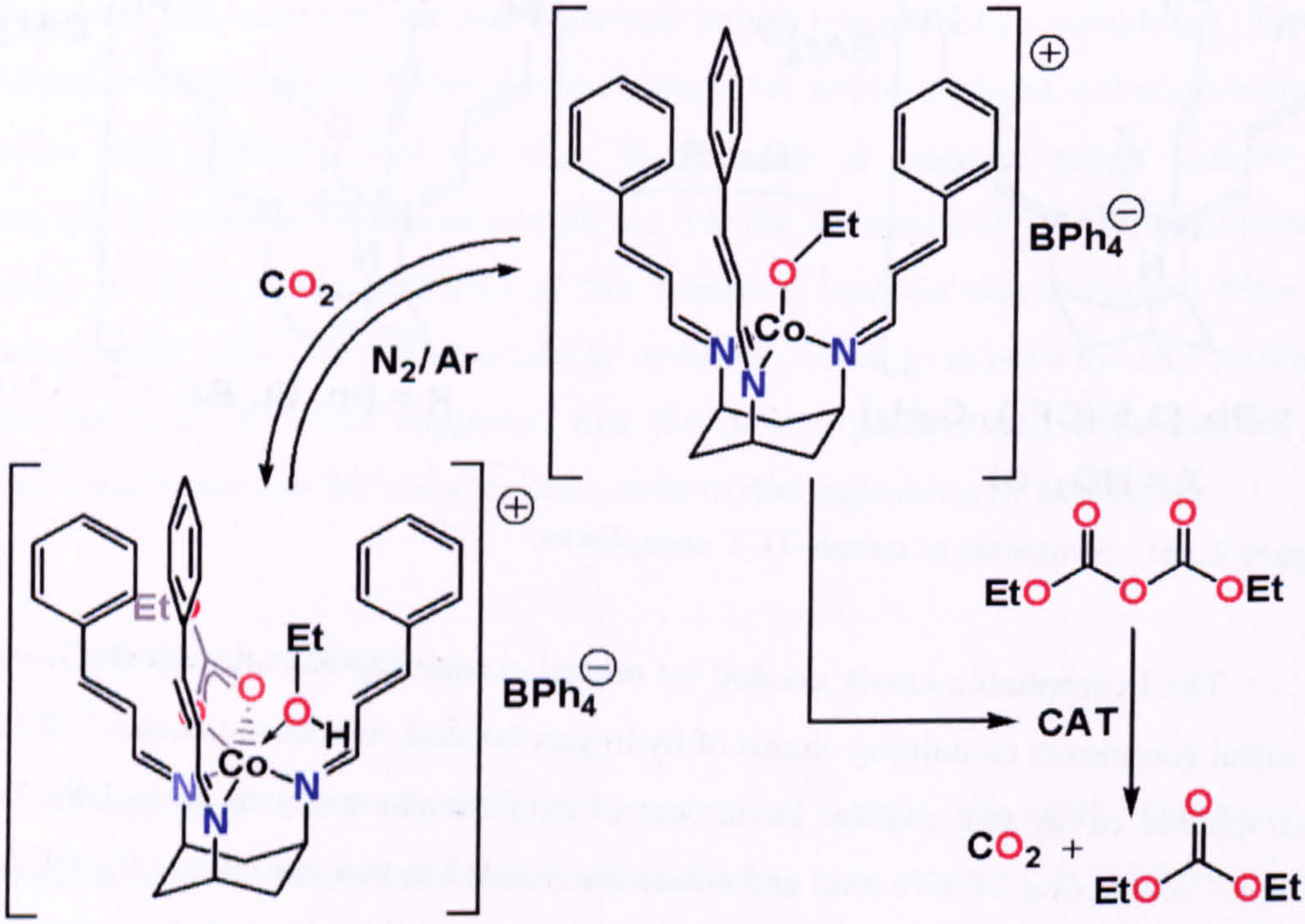

Figure 2.17: Reactivity displayed by $[Co(TCT)(OEt)]BPh_4$.

2.3.1 a [Co(TCT)(NO$_3$)]BAr$_4$ – synthesis and characterisation

Nitrato complexes were prepared as precursors to [Co(TCT)(OEt)]BAr$_4$. [Co(TCT)(NO$_3$)]BPh$_4$ was prepared following the methods described by Greener[37] and Freeman,[38] and [Co(TCT)(NO$_3$)]BAr$^F_4$ was prepared by simply exchanging NaBPh$_4$ with NaBAr$^F_4$. Both of the complexes can be prepared in good yield (~ 80%). As with the chloride complex described below, the UV/vis spectra for the two salts are identical (the nitrate compounds both have a broad absorption centred at 547 nm) despite apparent differences in the solid state. Electro-spray ionisation mass spectrometry shows a peak at *m/z* = 592 corresponding to [Co(TCT)(NO$_3$)]$^+$.

Note: during the course of this project, the BAr$^F_4^-$ species has been found to contaminate subsequent mass spectrometry samples. It is probable that the species is absorbed into the polymeric linings of the injection system due to its lipophilic character. As a consequence, only two compounds bearing this counter-ion ([Co(TCT)(X)]BAr$^F_4$, where X = NO$_3$, Cl) were characterised by mass spectrometry; subsequent compounds relied upon a combination of other techniques to compensate for the lack of mass spectrometry data.

2.3.1 b [Co(TCT)(NO$_3$)]BAr$^F_4$ – crystallography

Diffusion of cyclohexane into a concentrated solution of [Co(TCT)(NO$_3$)]BAr$^F_4$ in dichloromethane resulted in the formation of purple crystals of the complex; these were of suitable quality for X-ray diffraction. The complex forms monoclinic crystals, of $P2_1/_n$ space group. The asymmetric unit consists of the complex, along with 1½ molecules of cyclohexane and a disordered dichloromethane. The cobalt centre adopts a distorted trigonal bipyramidal geometry, with O(1) and N(3) atoms forming the apices (Figure 2.18, also see Table 2.1). There is a noticeable interaction between the cations: pairs of cation units face one another, with the cinnamyl "arms" actually positioned such that there are π-stacking interactions between phenyl rings (referred to as "interdigitation"). Note that previous crystal structures of metal-TCT-nitrate species were grown from coordinating solvents and were octahedrally coordinated, so it is not possible to make meaningful comparisons between their structures and that of [Co(TCT)(NO$_3$)]BAr$^F_4$.

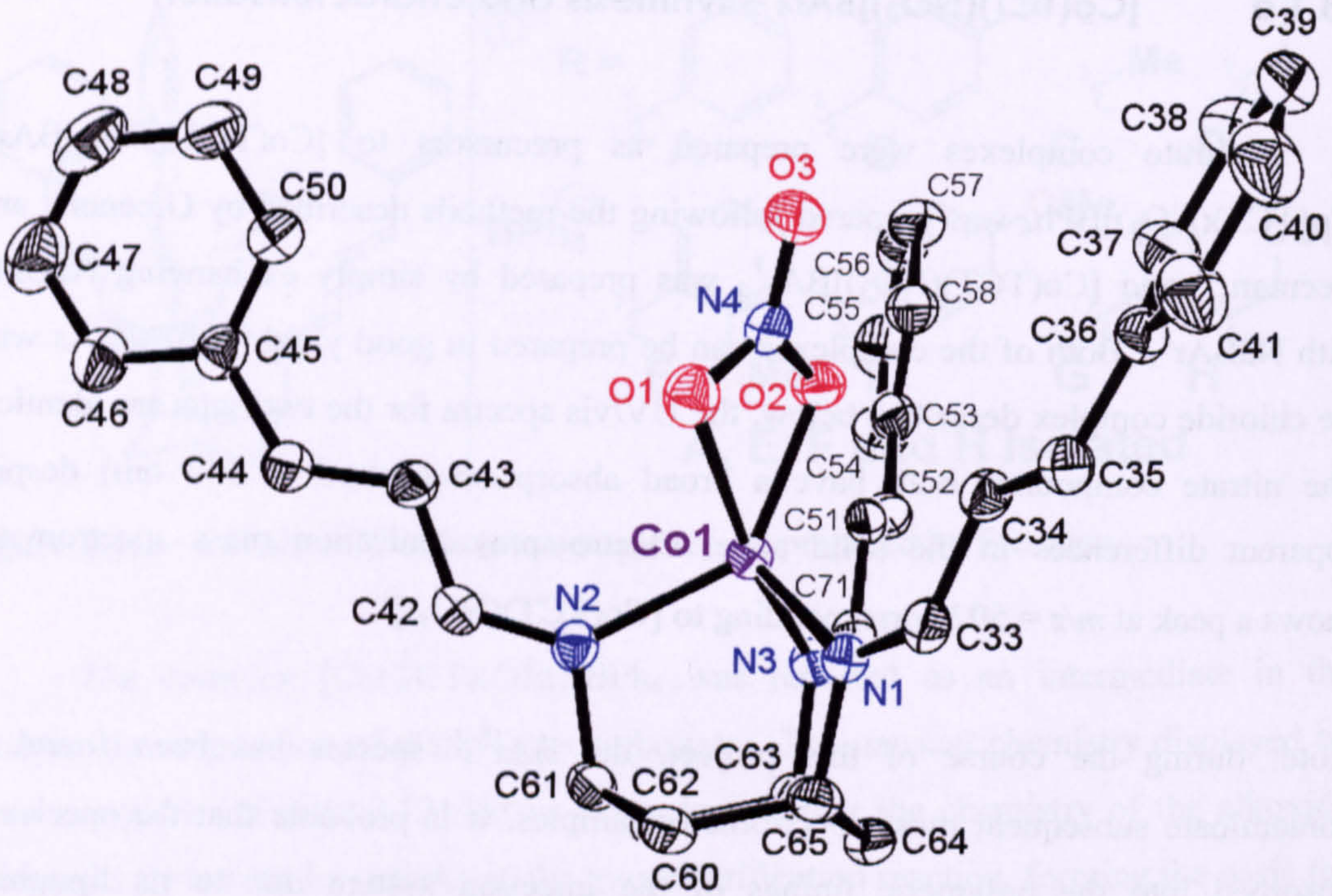

Figure 2.18: An ORTEP[39] representation (30% probability ellipsoids) of $[Co(TCT)(NO_3)]BAr^F{}_4 \cdot 1\frac{1}{2}C_6H_{12} \cdot CH_2Cl_2$, cation only, H atoms omitted for clarity.

Co(1)–N(1)	2.035(3)	**O(1)–N(4)–O(2)**	115.7(3)
Co(1)–N(2)	2.040(3)	**O(3)–N(4)–O(2)**	120.6(3)
Co(1)–N(3)	2.043(3)	**O(3)–N(4)–O(1)**	123.6(3)
mean Co–N	2.039(3)	**N(4)–O(1)–Co(1)**	85.48(17)
N(4)–O(1)	1.252(3)	**N(4)–O(2)–Co(1)**	99.73(18)
N(4)–O(2)	1.288(3)	**O(2)–Co(1)–N(1)**	112.12(10)
N(4)–O(3)	1.223(4)	**O(2)–Co(1)–N(2)**	138.69(10)
Co(1)–O(1)	2.000(2)	**O(2)–Co(1)–N(3)**	109.72(10)
Co(1)–O(2)	2.328(2)	**N(1)–Co(1)–N(2)**	98.61(10)
N(1)–Co(1)–O(1)	91.88(9)	**N(2)–Co(1)–N(3)**	94.12(10)
N(2)–Co(1)–O(1)	94.35(9)	**N(1)–Co(1)–N(3)**	94.33(10)
N(3)–Co(1)–O(1)	168.63(9)	**O(2)–Co(1)–O(1)**	59.02(9)

Table 2.1: Selected bond lengths (/ Å) and angles (/ °) for $[Co(TCT)(NO_3)]^+$ in $[Co(TCT)(NO_3)]BAr^F{}_4 \cdot 1\frac{1}{2}C_6H_{12} \cdot CH_2Cl_2$.

2.3.2 a [Co(TCT)Cl]BAr_4 – synthesis and characterisation

[Co(TCT)Cl]BPh_4 was prepared according to the methods described by Greener and Freeman, and [Co(TCT)Cl]BAr^F_4 was prepared by exchanging $NaBPh_4$ with $NaBAr^F_4$. These complexes were prepared solely for use as precursors to [Co(TCT)(OPh)]BAr_4.

Reaction of $[Co(H_2O)_6]Cl_2$, TCT and $NaBAr_4$ gives the target complexes in good yield (~ 80%). Although the BAr^F_4 derivative is apparently deeper in colour than its tetraphenylborate analogue, the UV/vis spectrum of the compound in dichloromethane shows an identical absorption band (centred at 593 nm). The complexes have also been characterised by electro-spray mass spectrometry, showing the expected peaks at m/z = 565 and 567 (^{35}Cl / ^{37}Cl, 3 : 1 relative intensity).

2.3.2 b [Co(TCT)Cl]BAr^F_4 – crystallography

Crystals of [Co(TCT)Cl]BAr^F_4 suitable for X-ray diffraction were obtained by allowing cyclohexane to diffuse into a concentrated solution of the complex in dichloromethane. The complex forms triclinic crystals, $P\bar{1}$ space group.

Bond length / angle	[Co(TCT)Cl]BAr^F_4	[Co(TCT)Cl]BPh_4
Cl(1)–Co(1)	2.2208(8)	2.203(2)
Co(1)–N(1)	2.000(2)	1.998(4)
Co(1)–N(2)	2.018(2)	2.001(4)
Co(1)–N(3)	2.010(2)	2.014(4)
N(1)–Co(1)–N(2)	97.95(9)	99.7(2)
N(3)–Co(1)–N(2)	93.66(9)	95.3(2)
N(1)–Co(1)–N(3)	97.41(9)	93.2(2)
N(1)–Co(1)–Cl(1)	119.93(7)	119.63(13)
N(2)–Co(1)–Cl(1)	120.67(6)	121.09(12)
N(3)–Co(1)–Cl(1)	121.31(7)	121.77(13)

Table 2.2: Selected bond lengths (/ Å) and angles (/ °) for $[Co(TCT)Cl]^+$ species.

The asymmetric unit consists solely of the complex, with no solvent molecules present. The cobalt centre adopts distorted tetrahedral geometry (Figure 2.19) with wide Cl – Co – N angles (~120°) and compressed N – Co – N angles (94° – 98°) (Table 2.2). The crystal packing shows cation units facing one another but without the cinnamyl arms interdigitating.

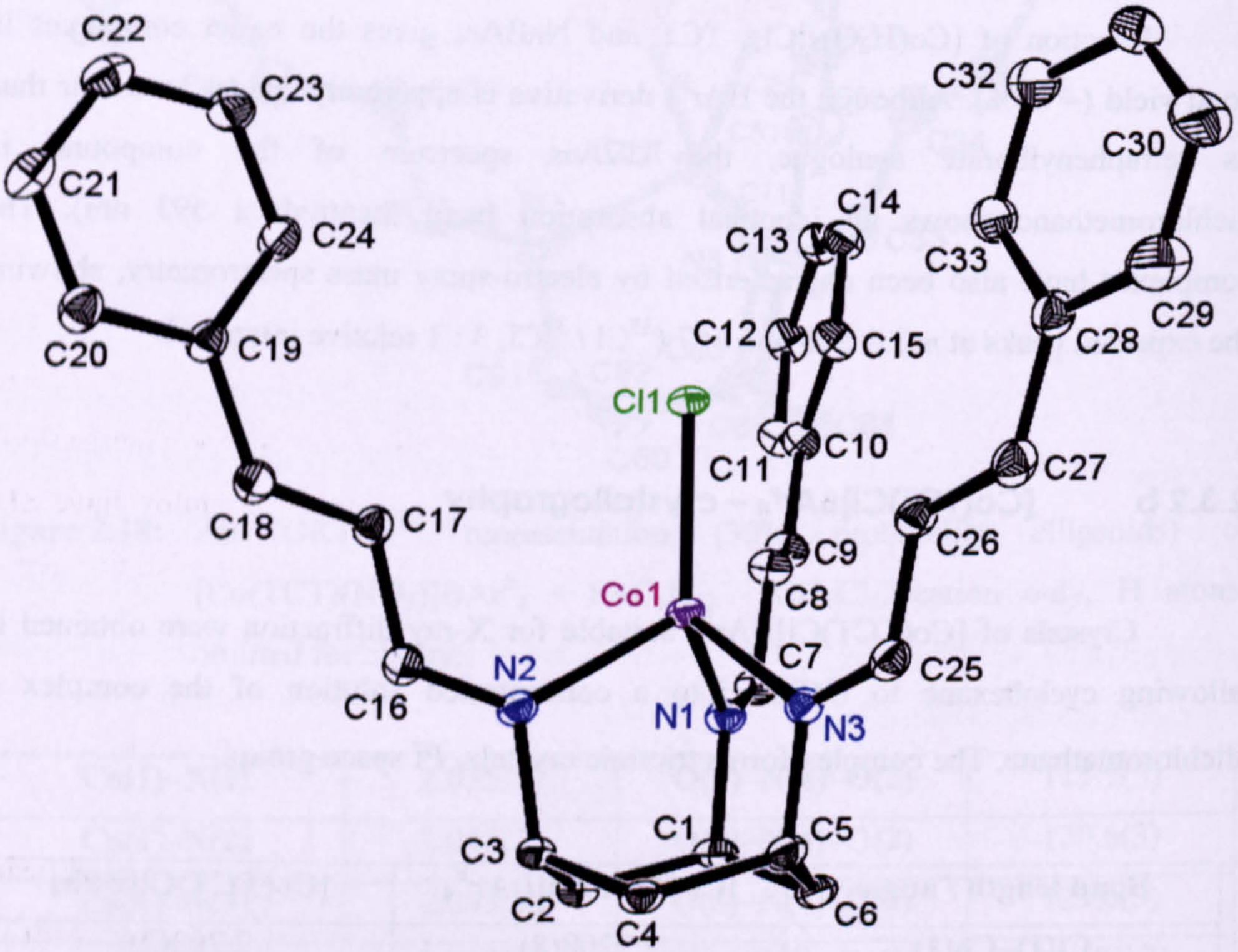

Figure 2.19: An ORTEP representation (30% probability ellipsoids) of $[Co(TCT)Cl]BAr^{F}_{4}$, cation only, H atoms omitted for clarity.

2.3.3 a [Co(TCT)(OEt)]BAr_4 – synthesis and characterisation

$[Co(TCT)(OEt)]BPh_4$ was first reported by Greener and Walton as an intermediate in the catalytic decomposition of dialkyl pyrocarbonates,[40] and was isolated by Freeman. The complex has also been shown to react reversibly with CO_2.[41] The unusual reactivity of this complex provided the motivation to test its potential as a transesterification catalyst (Chapter 3); in addition, further studies of its reactivity towards CO_2 were undertaken (Chapter 4). The synthesis has been refined to give a more reliable and convenient reaction. Previous syntheses used the displacement of a

nitrate ligand with hydroxide, followed by reaction with ethanol. Direct substitution of a nitrate ligand with ethoxide can be achieved by addition of a slight excess of sodium ethoxide, as a concentrated solution in ethanol, to a solution of the nitrate precursor in dichloromethane under an argon atmosphere. This method was found to be more reliable, and avoided the formation of the hydroxide complex and associated decomposition products. Attempts to synthesise the complex from the chloride precursor invariably resulted in either failure or heavy contamination (>10%) with starting compound. Note that the complex is stable to air once isolated as a dry solid.

It was envisaged that substituting the tetraphenyl-borate counter-ion with the more bulky and less coordinating *tetrakis*(*bis*-3,5-trifluoromethyl-phenyl)borate would give a more active catalyst due to less interference from the counter-ion.[42] The preparation of this anion was first reported by Kobayashi *et al.*,[43] and its potential as a non-coordinating counter-ion has been exploited most notably by Brookhart *et al.*, who have used it in the preparation of extremely active catalysts for olefin polymerisation[44] and carbon monoxide / olefin copolymerisation.[45] Schrock and Yandulov have also recently used this counter-ion to great effect in the catalytic reduction of dinitrogen to ammonia at a molybdenum center,[46] where its bulk and lack of coordination are key to the catalytic action of the metal complex. Synthesis of $[Co(TCT)(OEt)]BAr^F{}_4$ was achieved using the method described for the synthesis of $[Co(TCT)(OEt)]BPh_4$, replacing $NaBPh_4$ with $NaBAr^F{}_4$.

Both complexes have been characterised by UV/vis spectroscopy, showing identical absorption bands for the $[Co(TCT)(OEt)]^+$ unit, in good agreement with the values reported by Freeman. The absorption bands are very close in energy to those of $[Co(TCT)(OBz)]BPh_4$ (Section 2.3.5), whilst showing noticeable differences to the spectrum of $[Co(TCT)(OPh)]BAr_4$ (Figure 2.20). Electro-spray ionisation mass spectrometry showed a peak at m/z = 575, consistent with the mass expected for the cation.

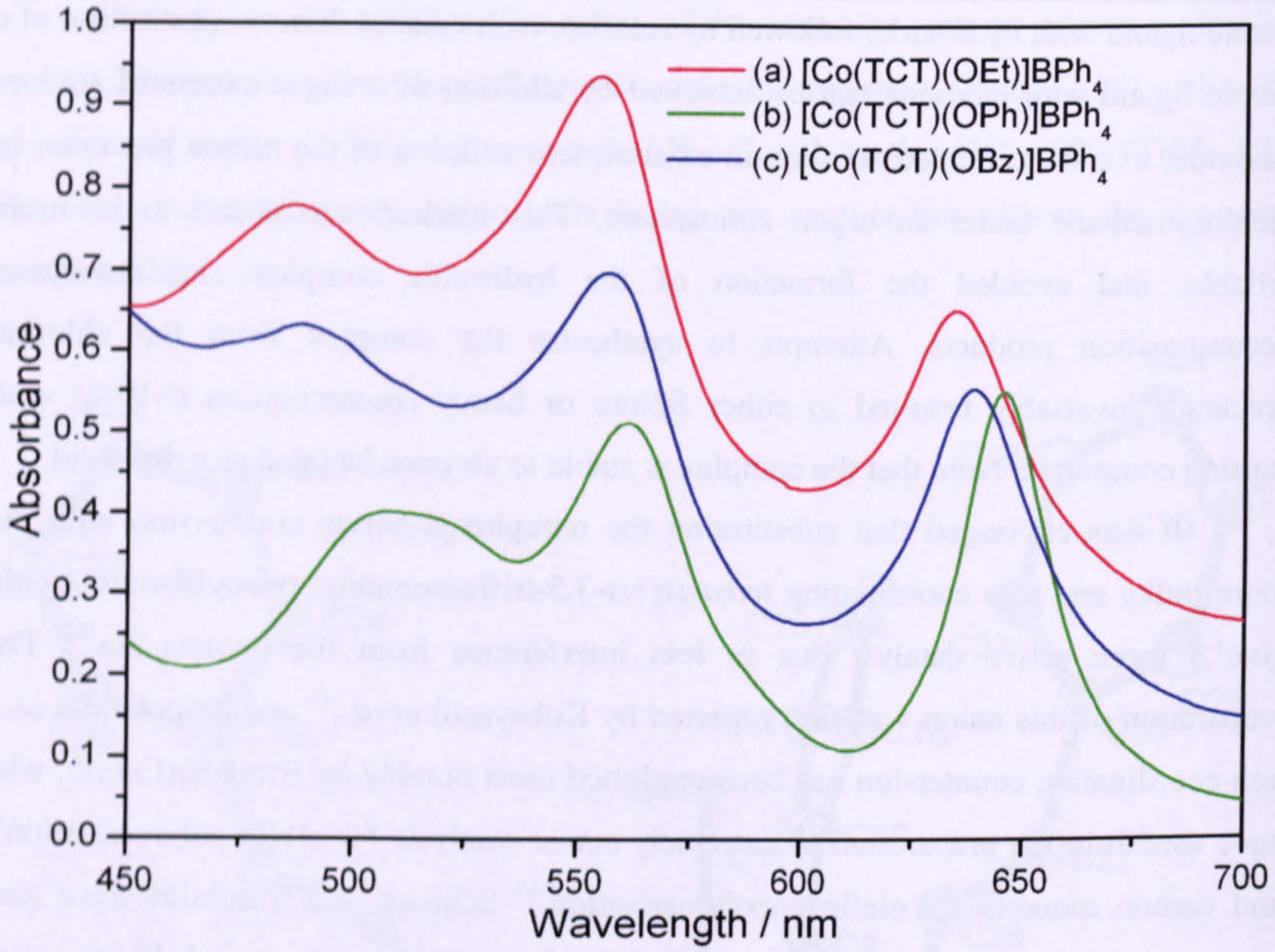

Figure 2.20: UV/vis spectra of the complexes $[Co(TCT)(OR)]BPh_4$. (a) R = Et, solvent = CH_2Cl_2 / EtOH (9:1, *v*/*v*). (b) R = Ph, solvent = CH_2Cl_2. (c) R = Bz, solvent = CH_2Cl_2 / BzOH (9:1, *v*/*v*).

The paramagnetically shifted ^1H NMR spectra of these complexes showed similar resonances for the TCT ligand, but assignment of the ethoxide protons has not been possible, due to the extreme shifts and broadening. Exchanging the counter-ion gave rise to slight changes in the chemical shifts (Table 2.3, Figures 2.21 – 2.23).

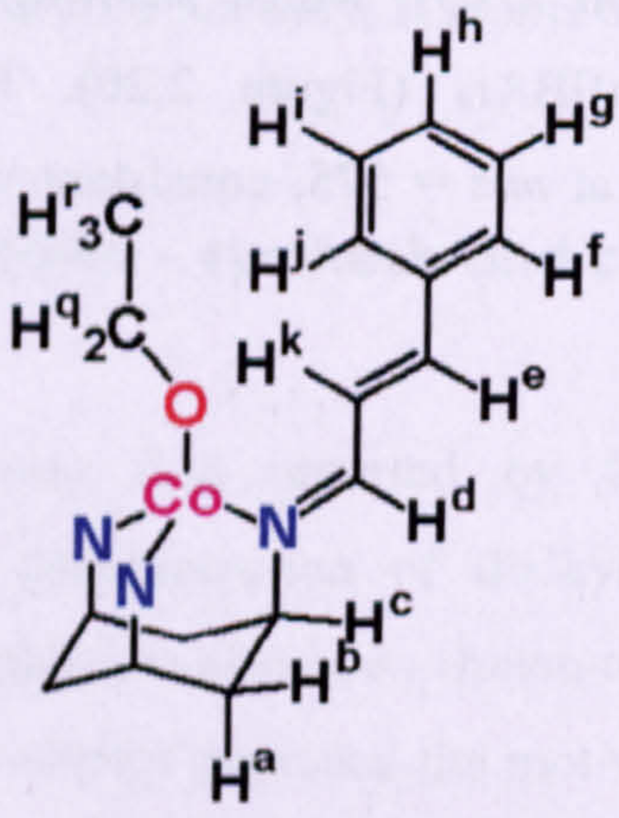

$[Co(TCT)(OEt)]^+$

Figure 2.21: Proton labels for $[Co(TCT)(OEt)]^+$ (BPh_4 & $BAr^F{}_4$ analogues).

Proton	δ / ppm [Co(TCT)(OEt)]BPh_4	δ / ppm [Co(TCT)(OEt)]$BAr^F{}_4$
a	~ –18	~ –20
b	1.80	1.79
c	430 / 374	423 / 371
d	374 / 430	371 / 423
e	16.14	15.85
f / j	9.72	9.77
g / i	7.32	7.15
h	9.41	9.38
k	~ –9	~ –4

Table 2.3: Assignment of peaks for $[Co(TCT)(OEt)]^+$.

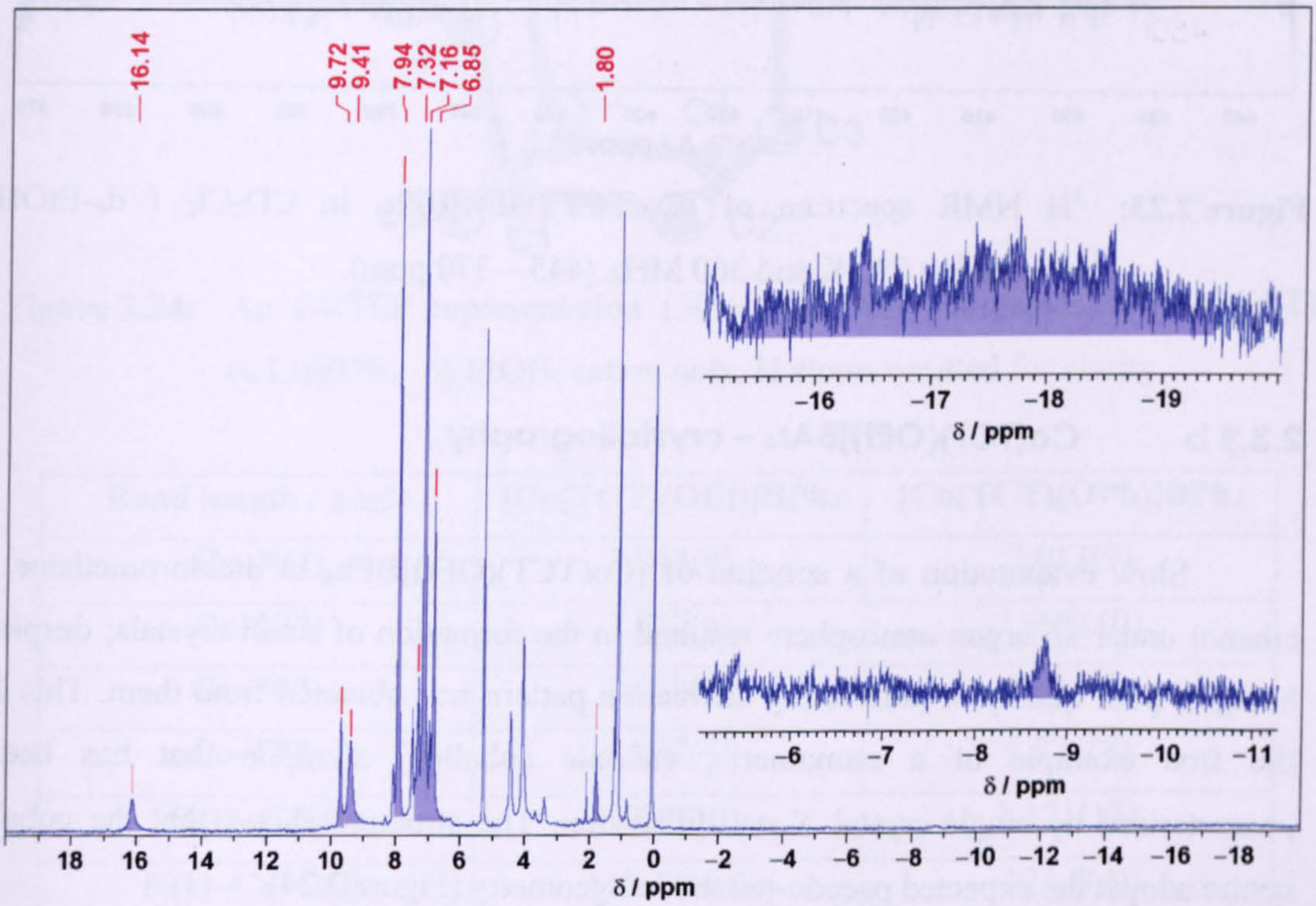

Figure 2.22: ^1H NMR spectrum of $[Co(TCT)(OEt)]BPh_4$ in CD_2Cl_2 / d_6-EtOH recorded at 295 K and 300 MHz (20 – –20 ppm).

The protons closest to the cobalt centre ($H^{c/d}$) undergo the most extreme shifts, with the effect reduced with increasing distance and number of bonds from the paramagnetic centre. Note that H^a and H^k (hardly observable due to broadening) undergo *negative* shifts, because they are separated from the cobalt centre by an *even*

number of bonds. Further, H_q and H_r are not observable at all because d^6-EtOH has been added to the sample, which exchanges with the ethoxide ligand.

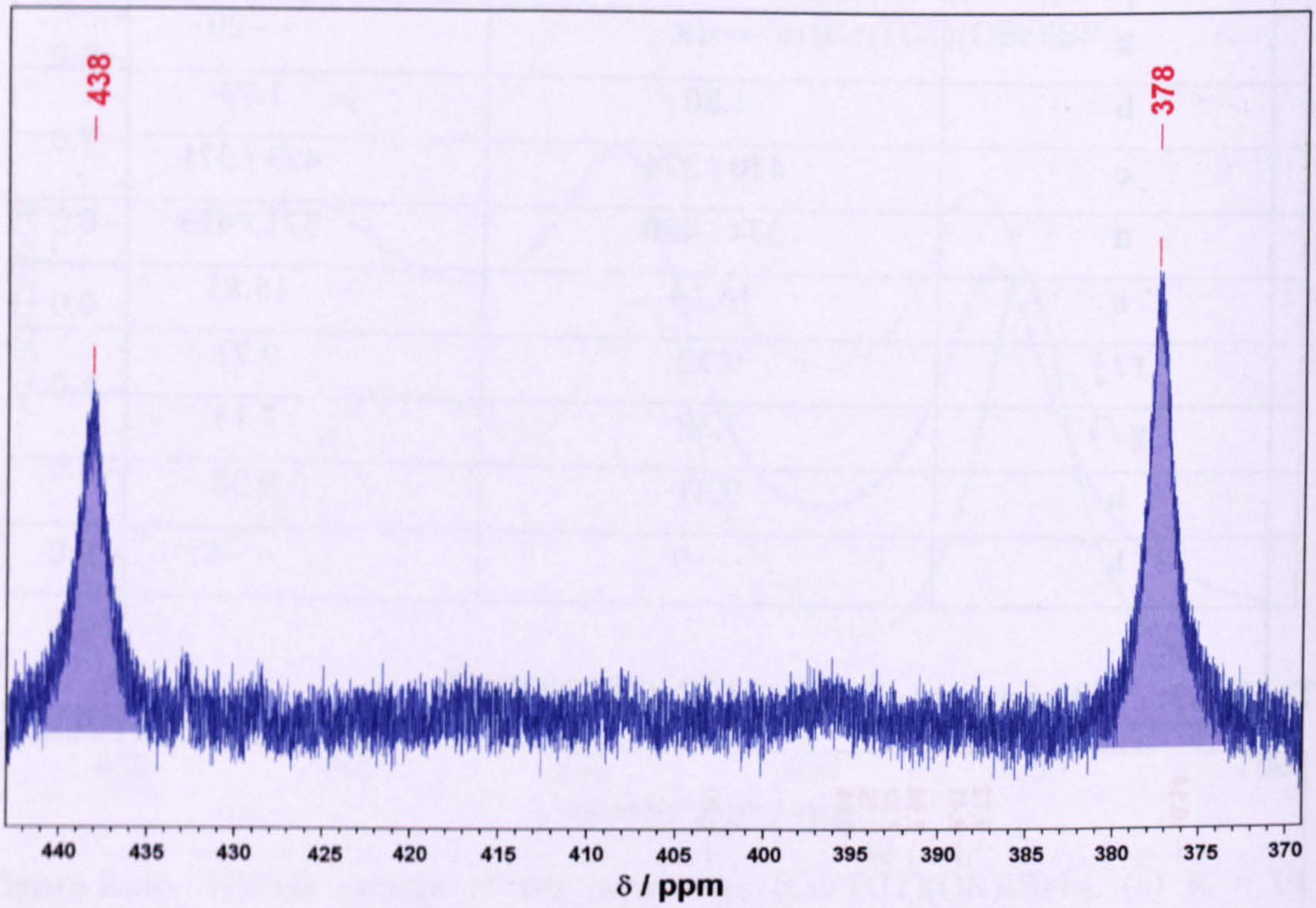

Figure 2.23: ^{1}H NMR spectrum of $[Co(TCT)(OEt)]BPh_4$ in CD_2Cl_2 / d_6-EtOH recorded at 295 K and 300 MHz (445 – 370 ppm).

2.3.3 b Co(TCT)(OEt)]BAr$_4$ – crystallography

Slow evaporation of a solution of $[Co(TCT)(OEt)]BPh_4$ in dichloromethane / ethanol under an argon atmosphere resulted in the formation of small crystals; despite being of poor quality, a satisfactory diffraction pattern was obtained from them. This is the first example of a monomeric, cationic cobalt(II) alkoxide that has been characterised by single-crystal X-ray diffraction. The structure shows that the cobalt centre adopts the expected pseudo-tetrahedral geometry (Figure 2.24).

The structural parameters (Table 2.4) show that the complex has a slightly shorter Co – O bond than $[Co(TCT)(OPh)]BPh_4$ (1.22 Å versus 1.31 Å) and a significantly larger Co – O – C angle (137° versus 129°). The increased bond angle suggests that the ethoxide ligand is acting as a π-donor ligand, donating additional electron density through a lone pair of electrons on the oxygen atom. This interaction helps to stabilise the complex.

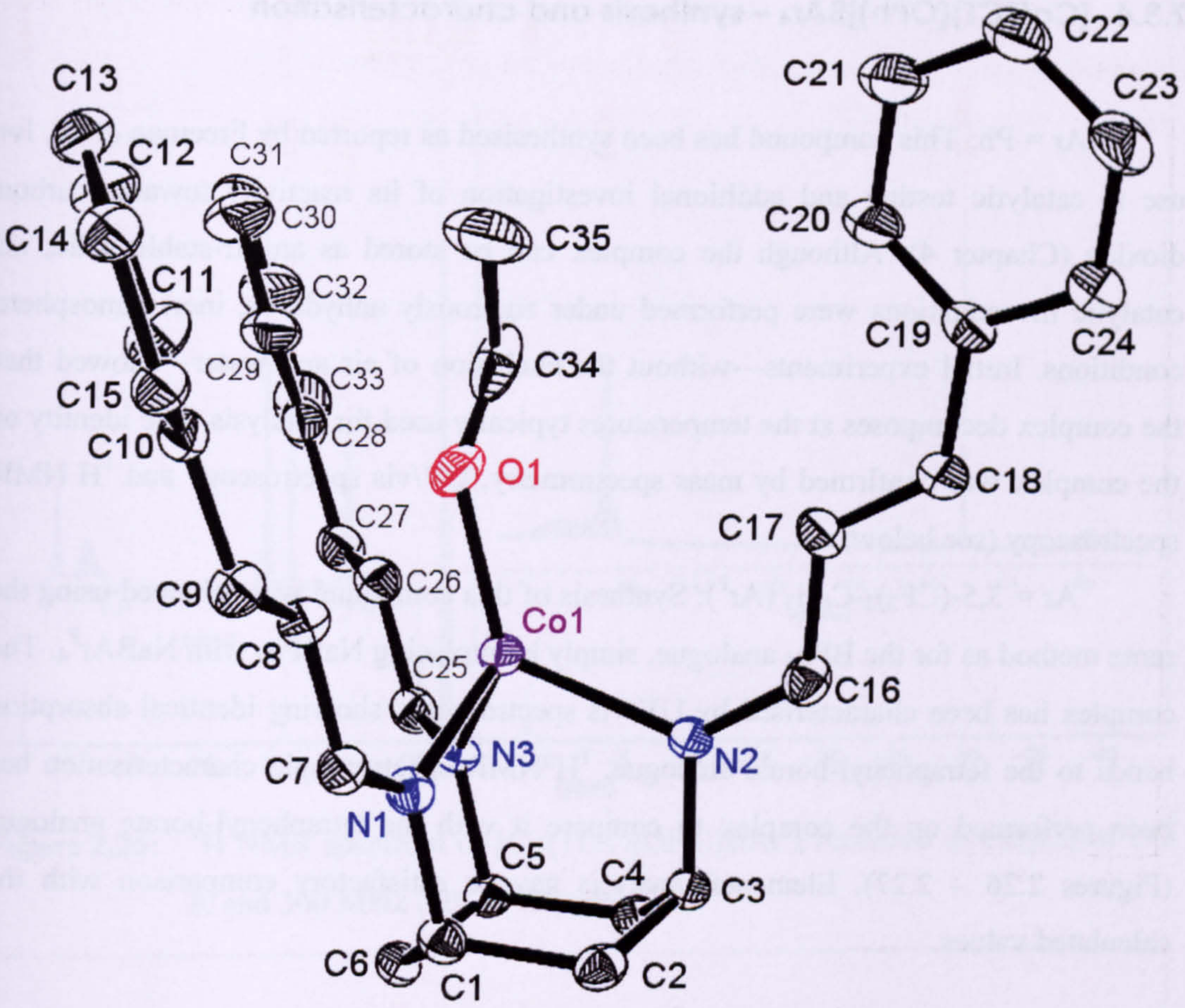

Figure 2.24: An ORTEP representation (30% probability ellipsoids) of [Co(TCT)(OEt)]BPh_4 · ½ EtOH, cation only, H atoms omitted for clarity.

Bond length / angle	[Co(TCT)(OEt)]BPh_4	[Co(TCT)(OPh)]BPh_4
Co–N(1)	2.014(4)	2.013(9)
Co–N(2)	2.027(4)	1.998(10)
Co–N(3)	2.019(4)	2.011(9)
Co–O(1)	1.867(4)	1.871(8)
O(1)–C(34)	1.224(10)	1.321(13)
N(1)–Co–O(1)	115.11(19)	124.8(4)
N(2)–Co–O(1)	125.82(19)	114.8(4)
N(3)–Co–O(1)	122.96(18)	122.4(4)
Co–O(1)–C(34)	136.8(5)	128.7(7)

Table 2.4: Selected bond lengths (/ Å) and angles (/ °) for [Co(TCT)(OEt)]BPh_4; values for [Co(TCT)(OPh)]BPh_4 are included for comparison.

2.3.4 [Co(TCT)(OPh)]BAr_4 – synthesis and characterisation

Ar = Ph: This compound has been synthesised as reported by Freeman *et al.*, for use in catalytic testing and additional investigation of its reactivity towards carbon dioxide (Chapter 4). Although the complex can be stored as an air-stable solid, all catalytic investigations were performed under rigorously anhydrous, inert atmosphere conditions. Initial experiments—without the exclusion of air and water—showed that the complex decomposes at the temperatures typically used for catalysis. The identity of the complex was confirmed by mass spectrometry, UV/vis spectroscopy and ^{1}H NMR spectroscopy (see below).

Ar = 3,5-$(CF_3)_2$-C_6H_3 (Ar^F): Synthesis of this compound was achieved using the same method as for the BPh_4 analogue, simply by replacing $NaBPh_4$ with $NaBAr^F{}_4$. The complex has been characterised by UV/vis spectroscopy, showing identical absorption bands to the tetraphenyl-borate analogue. ^{1}H NMR spectroscopic characterisation has been performed on the complex to compare it with the tetraphenyl-borate analogue (Figures 2.26 – 2.27). Elemental analysis gave a satisfactory comparison with the calculated values.

^{1}H NMR characterisation:

Systematic labelling was used for the cobalt complex, as shown below:

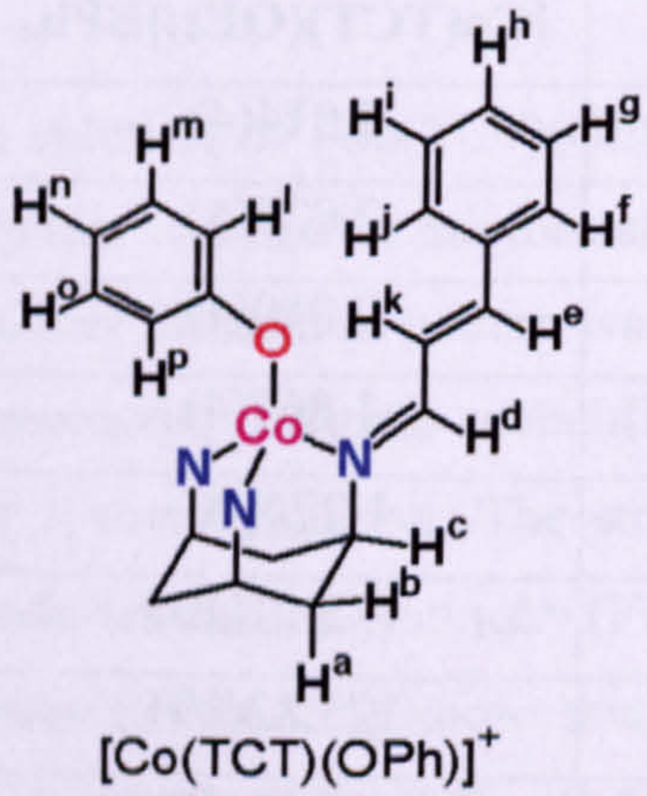

$[Co(TCT)(OPh)]^+$

Figure2.25: Proton labels for $[Co(TCT)(OPh)]^+$ (BPh_4 & $BAr^F{}_4$ analogues).

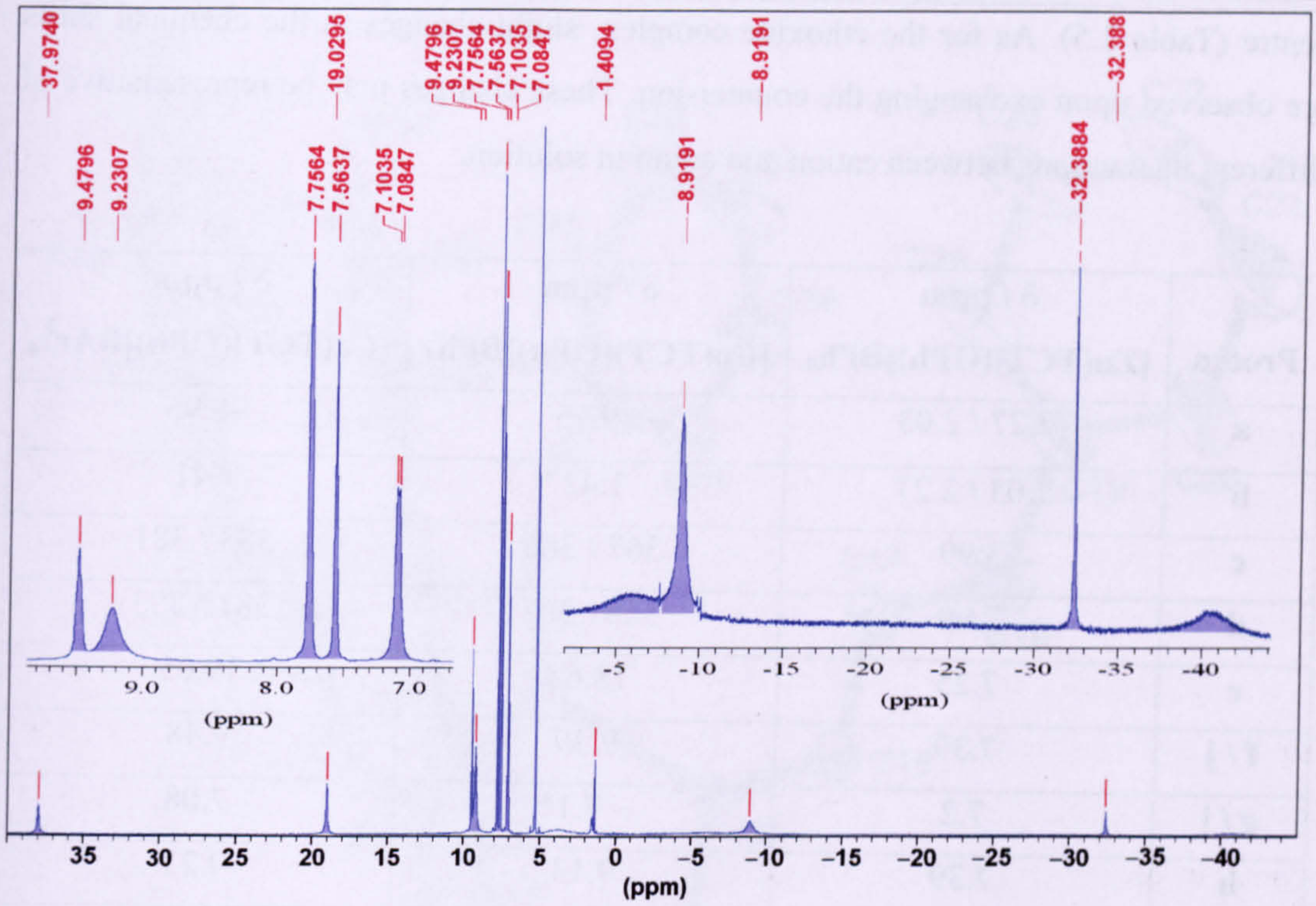

Figure 2.26: ^{1}H NMR spectrum of $[Co(TCT)(OPh)]BAr^{F}_{4}$ recorded in CD_2Cl_2 at 295 K and 300 MHz (40 – –45 ppm).

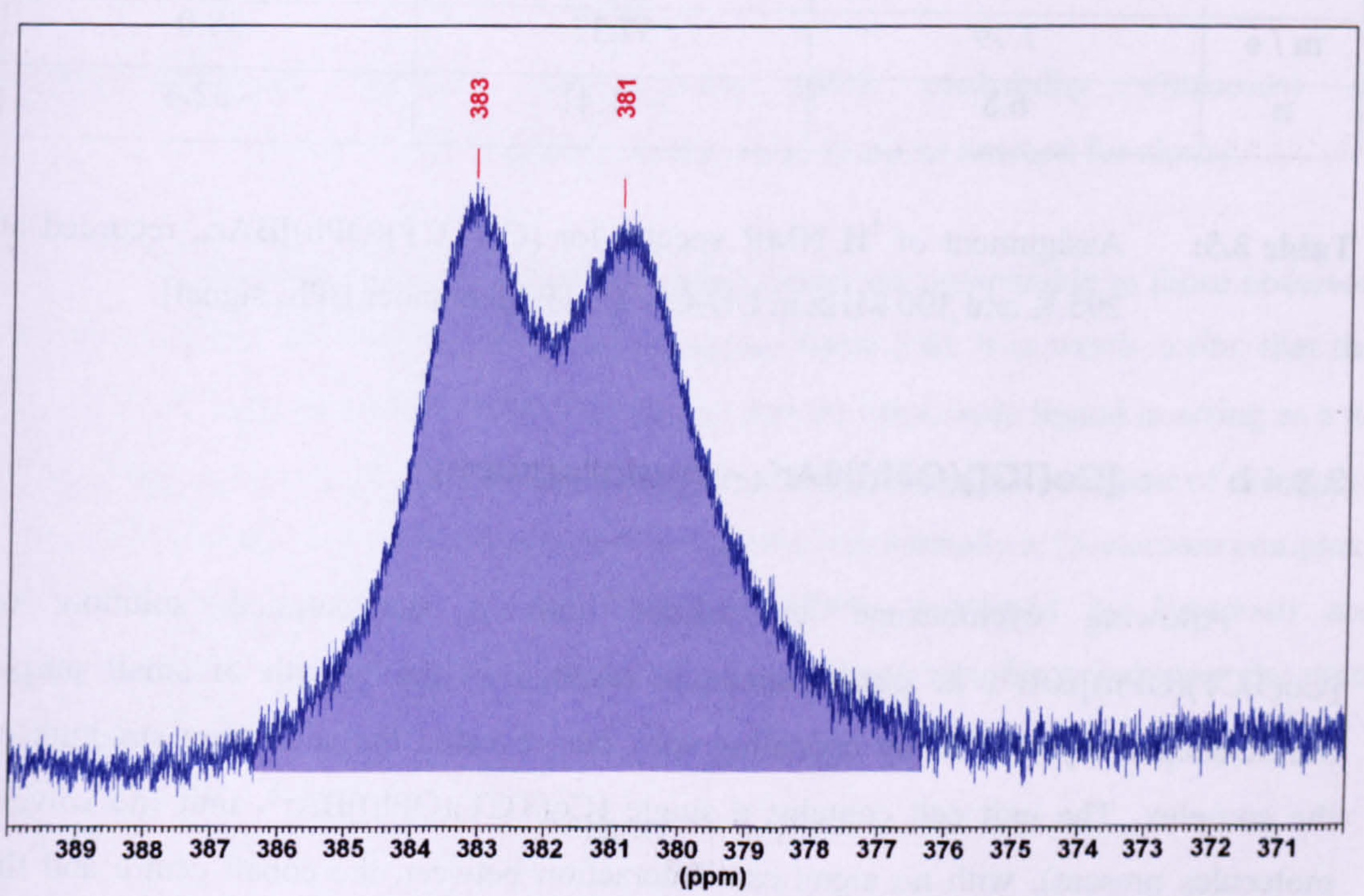

Figure 2.27: ^{1}H NMR spectrum of $[Co(TCT)(OPh)]BAr^{F}_{4}$ recorded in CD_2Cl_2 at 295 K and 300 MHz (390 – 370 ppm).

These chemical shifts can be compared to the equivalent peaks in the corresponding zinc complexes (section 2.4) in order to evaluate the effect of the cobalt

centre (Table 2.5). As for the ethoxide complex, slight changes in the chemical shifts are observed upon exchanging the counter-ion. These changes may be representative of different interactions between cation and anion in solution.

Proton	δ / ppm [Zn(TCT)(OPh)]BPh_4	δ / ppm [Co(TCT)(OPh)]BPh_4	δ / ppm [Co(TCT)(OPh)]BAr^F_4
a	2.27 / 2.03	–9.75	–8.95
b	2.03 / 2.27	1.42	1.41
c	3.99	367 / 366	383 / 381
d	7.99	366 / 367	381 / 383
e	7.25	18.65	19.05
f / j	7.39	9.39	9.48
g / i	7.2	~ 7.1*	7.08
h	7.39	9.13	9.23
k	7.44	~ –6 (br)	~ –6 (br)
l / p	6.87	–39.5	~ –40.5 (br)
m / o	7.39	37.35	38.0
n	6.8	–31.41	–32.4

Table 2.5: Assignment of ^{1}H NMR spectra for [Co(TCT)(OPh)]BAr_4, recorded at 295 K and 300 MHz in CD_2Cl_2. [*: Hidden under BPh_4 signal]

2.3.4 b [Co(TCT)(OPh)]BAr^F_4 – crystallography

Allowing cyclohexane to diffuse into a concentrated solution of [Co(TCT)(OPh)]BAr^F_4 in dichloromethane resulted in the growth of small purple needle-shaped crystals. X-ray crystallography has revealed the solid-state structure of the complex. The unit cell contains a single [Co(TCT)(OPh)]BAr^F_4 unit (no solvent molecules present), with no significant interaction between the cobalt centre and the anion, although there are several close contacts between the ligand and the fluorine atoms of the anion. Inspection of the structure (Figure 2.28) clearly shows the expected pseudo-tetrahedral coordination environment of the cobalt centre.

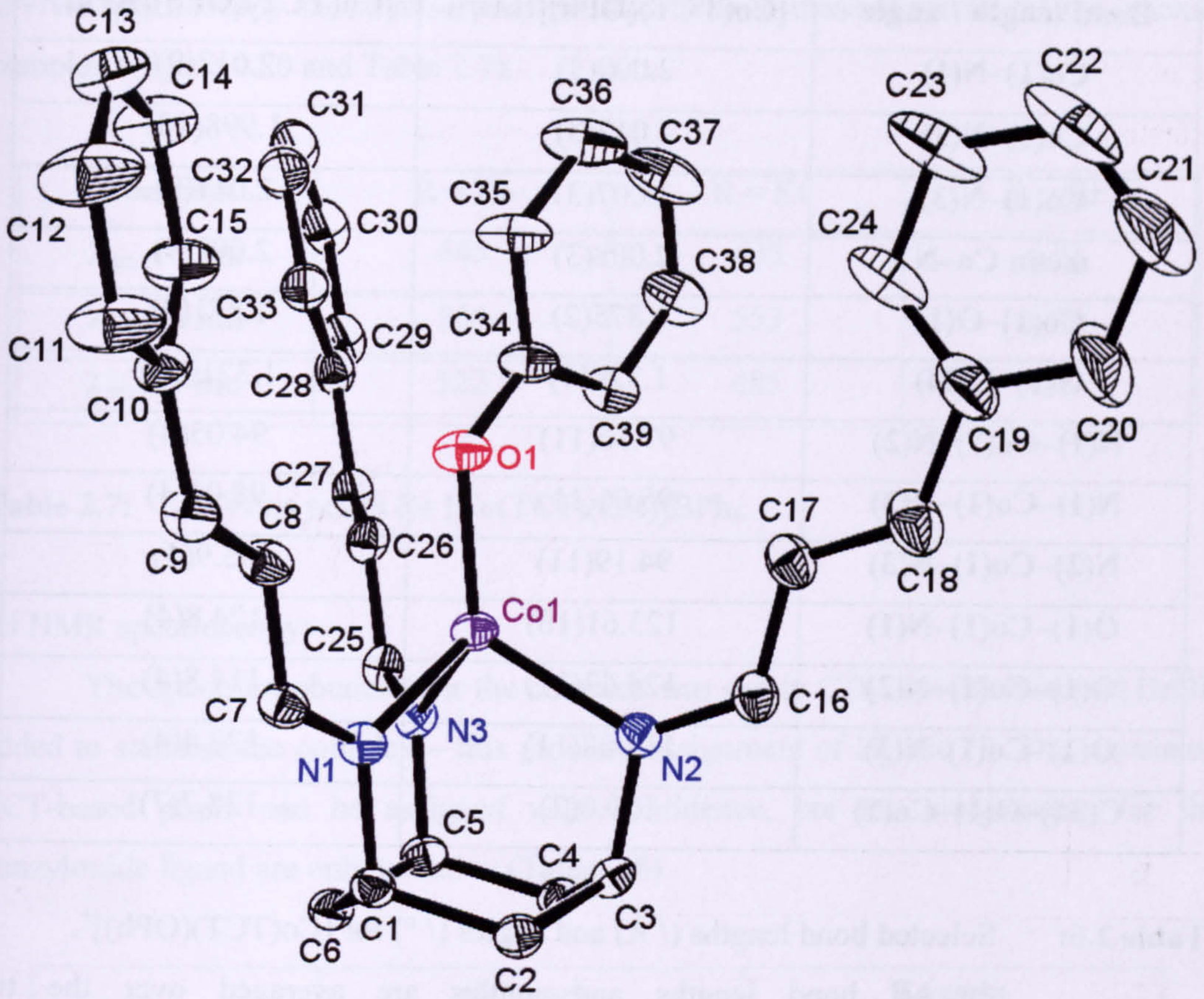

Figure 2.28: An ORTEP representation (30% probability ellipsoids) of $[Co(TCT)(OPh)]BAr^{F}_{4}$, cation only, H atoms omitted for clarity.

The structural parameters for the cobalt centre are comparable to those observed by Freeman for the tetraphenyl-borate analogue (Table 2.6). It is worth noting that the Co – O – C angle of 129.0° (Table 2.6) shows that the phenoxide ligand is acting as a π-donor ligand, i.e.: donating electrons to the metal centre through a lone pair of electrons. This interaction helps to stabilise the complex, which is formally a 15-electron complex. The structural parameters for $[Co(TCT)(OPh)]BPh_4$ (obtained by Freeman) are presented here for comparison; there are only minor variations between the two structures.

Bond length / angle	[Co(TCT)(OPh)]BAr^F_4	[Co(TCT)(OPh)]BPh_4 *
Co(1)–N(1)	2.000(3)	2.013(9)
Co(1)–N(2)	2.017(3)	1.998(10)
Co(1)–N(3)	2.007(3)	2.011(9)
mean Co–N	2.008(3)	2.007(9)
Co(1)-O(1)	1.875(2)	1.871(8)
O(1)-C(34)	1.329(4)	1.321(13)
N(1)-Co(1)-N(2)	97.56(11)	94.05(4)
N(1)-Co(1)-N(3)	95.06(11)	98.05(4)
N(2)-Co(1)-N(3)	94.19(11)	95.9(4)
O(1)-Co(1)-N(1)	123.61(10)	124.8(4)
O(1)-Co(1)-N(2)	124.43(11)	114.8(4)
O(1)-Co(1)-N(3)	114.88(11)	122.4(4)
C(34)-O(1)-Co(1)	129.0(2)	128.7(7)

Table 2.6: Selected bond lengths (/ Å) and angles (/ °) for $[Co(TCT)(OPh)]^+$.

*: All bond lengths and angles are averaged over the two $[Co(TCT)(OPh)]^+$ units.

2.3.5 [Co(TCT)(OBz)]BPh_4 – synthesis and characterisation

Thus far, it has not been possible to assign the ethoxide protons for [Co(TCT)(OEt)]BPh_4 because of their proximity to the paramagnetic cobalt centre. It was anticipated that the complex would allow for more convenient characterisation of a cobalt alkoxide complex by ^1H NMR spectroscopy; the aromatic protons of the benzyloxide ligand might be observable in a ^1H NMR experiment. Synthesis of this complex was also undertaken in order to investigate the possible exchange mechanisms taking place in the catalytic reactions; it seemed probable that alcohol / alkoxide exchange mechanisms were taking place during catalysis, and isolation of the benzyloxide complex would provide support for its existence in the catalytic cycle.

Addition of a solution of sodium benzyloxide in benzyl alcohol to a solution of [Co(TCT)(NO_3)]BPh_4 in CH_2Cl_2 followed by filtration, removal of solvent and washing with toluene, gave the desired product as a purple microcrystalline solid in 87% yield.

UV/vis spectroscopy shows absorption bands similar to those observed for the ethoxide complex (Figure 2.20 and Table 2.7).

Complex	R = Ph	R = Et	R = Bz
$\lambda_{max}1$ / nm	645	633	639
$\lambda_{max}2$ / nm	564	553	556
$\lambda_{max}3$ / nm	522	485	488

Table 2.7: UV/vis peaks for $[Co(TCT)(OR)]BPh_4$.

^1H NMR spectroscopy:

The spectrum obtained for the complex was run in CD_2Cl_2 with minimal BzOH added to stabilise the complex – this prevents assignment of H_g and H_i. The remaining TCT-based peaks can be assigned with confidence, but the assignments for the benzyloxide ligand are only tentative (Table 2.8).

Proton	δ / ppm $[Co(TCT)(OBz)]BPh_4$	δ / ppm $[Co(TCT)(OPh)]BPh_4$
a	–8.8	–8.95
b	2.33	1.41
c	375 / 363	383 / 381
d	363 / 375	381 / 383
e	20.3	19.05
f / j	10.05	9.48
g / i	Hidden under BzOH	7.08
h	8.68	9.23
k	–4	~ –6
l / p	[14.53]	~ –40.5
m / o	[–9.5]	38.0
n	[13.46]	–32.4
q	Not observed	-

Table 2.8: Assignment of peaks for $[Co(TCT)(OBz)]^+$; assignments for $[Co(TCT)(OPh)]^+$ included for comparison.

2.3.6 [Co({^{t}Bu$_2$Sal}$_2$BzTACH)]

This complex was synthesised in order to explore the possibility of using different ligands for cobalt. Addition of cobalt nitrate to a solution of the ligand produced a dark green / brown compound, which was purified by flash alumina chromatography. Mass spectrometry evidence indicates that the desired compound was formed. Attempts to crystallise the compound for X-ray analysis have been unsuccessful.

2.4 Zinc complexes

The synthesis of zinc alkoxide complexes was attempted in order to test their potential as transesterification catalysts. It was hoped that the Lewis acid character of the zinc centre would give increased activity relative to the cobalt derivatives, as is observed for the hexa-aqua salts,[47] and the lower toxicity of zinc would be a distinct advantage for commercial use. A number of zinc complexes have been reported which have activity for the hydrolysis of carboxy[48] and phospho-esters.[49] Parkin and Vahrenkamp have produced zinc alkoxide complexes as small molecule mimics of liver alcohol dehydrogenase.[50] Chisholm *et al.* have reported high activity in the polymerisation of lactides for the complex TpZn(OEt),[51] which suggests that the Zn-TCT complexes are potential lactide polymerisation catalysts.

2.4.1 a [Zn(TCT)(NO$_3$)]BAr$_4$ – synthesis and characterisation

A method for the synthesis and characterisation of [Zn(TCT)(NO$_3$)]BPh$_4$ was reported by Greener in his DPhil thesis, but yields were too low (21%) for practical use; the synthesis has been refined to give a higher yield by adapting the method reported by Lusby for preparation of [Zn(4-styrene-proTACH)(NO$_3$)]BPh$_4$,[52] replacing (4-styrene-proTACH) with TCT. Addition of NaBPh$_4$ in MeOH to a solution of [Zn(H$_2$O)$_6$](NO$_3$)$_2$ and TCT in MeOH / CH_2Cl_2, followed by filtration and removal of solvent gave the target complex in 80% yield. The identity of the complex was confirmed by ^{1}H NMR spectroscopy and mass spectrometry.

Reaction of $[Zn(H_2O)_6](NO_3)_2$, TCT and $NaBAr^F{}_4$ in dichloromethane / methanol gives $[Zn(TCT)(NO_3)]BAr^F{}_4$ in 60% yield after recrystallisation from dichloromethane / cyclohexane. The complex has been characterised by ^1H NMR spectroscopy. No mass spectrum – see section 2.5.1.

2.4.1 b [Zn(TCT)(NO$_3$)]BAr$_4$ - crystallography

Crystals of $[Zn(TCT)(NO_3)BAr^F{}_4$ suitable for X-ray crystallography were obtained by allowing cyclohexane to diffuse into a concentrated solution of the complex in dichloromethane. The zinc centre displays approximately trigonal bipyramidal symmetry, with O(1) and N(3) atoms forming the apices (Figure 2.29). The structural parameters (Table 2.9) are comparable to those observed for $[Co(TCT)(NO_3)]BAr^F{}_4 \cdot 1\frac{1}{2}\ C_6H_{12} \cdot CH_2Cl_2$ (Section 2.3.1 b), with bond lengths and angles differing slightly.

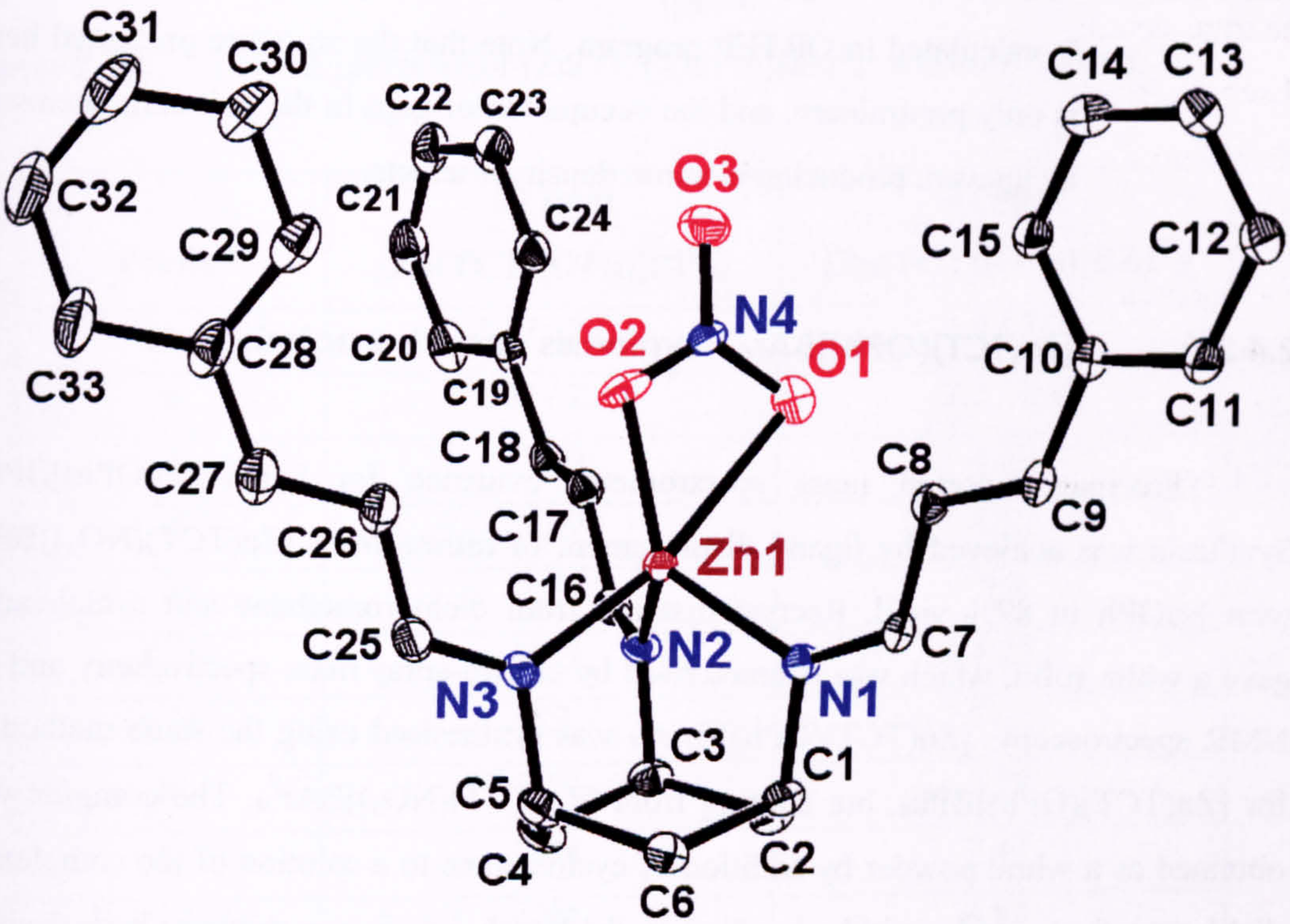

Figure 2.29: ORTEP representation (30% probability ellipsoids) of $[Zn(TCT)(NO_3)]BAr^F{}_4 \cdot CH_2Cl_2$, cation only, H atoms omitted for clarity.

Zn(1)–N(1)	1.995(5)	**O(1)–N(4)–O(2)**	119.0(5)
Zn(1)–N(2)	2.022(5)	**O(3)–N(4)–O(2)**	121.9(6)
Zn(1)–N(3)	2.035(5)	**O(3)–N(4)–O(1)**	118.8(7)
mean Zn–N	2.017(5)	**N(4)–O(1)–Zn(1)**	78.65*
N(4)–O(1)	1.285(8)	**N(4)–O(2)–Zn(1)**	106.9(4)
N(4)–O(2)	1.202(9)	**O(2)–Zn(1)–N(1)**	129.8(2)
N(4)–O(3)	1.241(8)	**O(2)–Zn(1)–N(2)**	119.6(2)
Zn(1)–O(1)	2.520*	**O(2)–Zn(1)–N(3)**	111.8(2)
Zn(1)–O(2)	1.974(5)	**N(1)–Zn(1)–N(2)**	100.5(2)
N(1)–Zn(1)–O(1)	96.10*	**N(2)–Zn(1)–N(3)**	91.8(2)
N(2)–Zn(1)–O(1)	93.63*	**N(1)–Zn(1)–N(3)**	94.5(2)
N(3)–Zn(1)–O(1)	167.04*	**O(2)–Zn(1)–O(1)**	55.37*

Table 2.9: Selected bond lengths (/ Å) and angles (/ °) for $[Zn(TCT)(NO_3)]BAr^F{}_4$. *: calculated in ORTEP program. Note that the structure presented here is only preliminary, and the occupation of gaps in the unit cells seems to be uneven, producing electron density artefacts.

2.4.2 a [Zn(TCT)(OPh)]BAr_4 – synthesis and characterisation

Freeman reported mass spectrometry evidence for $[Zn(TCT)(OPh)]BPh_4$. Synthesis was achieved by ligand displacement of nitrate from $[Zn(TCT)(NO_3)]BPh_4$ with NaOPh in 89% yield. Recrystallisation from dichloromethane and cyclohexane gave a white solid, which was characterised by electro-spray mass spectrometry and ^1H NMR spectroscopy. $[Zn(TCT)(OPh)]BAr^F{}_4$ was synthesised using the same method as for $[Zn(TCT)(OPh)]BPh_4$, but starting from $[Zn(TCT)(NO_3)]BAr^F{}_4$. The complex was obtained as a white powder by addition of cyclohexane to a solution of the complex in dichloromethane, and could be handled on the bench, i.e.: it was stable to hydrolysis in the solid state. Characterisation was achieved by ^1H NMR spectroscopy (Figure 2.30, Table 2.10). Assignments were based on those of similar complexes characterised by Greener, and by using proton-proton couplings for confirmation of connectivity. ^{13}C NMR spectroscopy has been performed, although assignment of peaks is incomplete (Chapter 6).

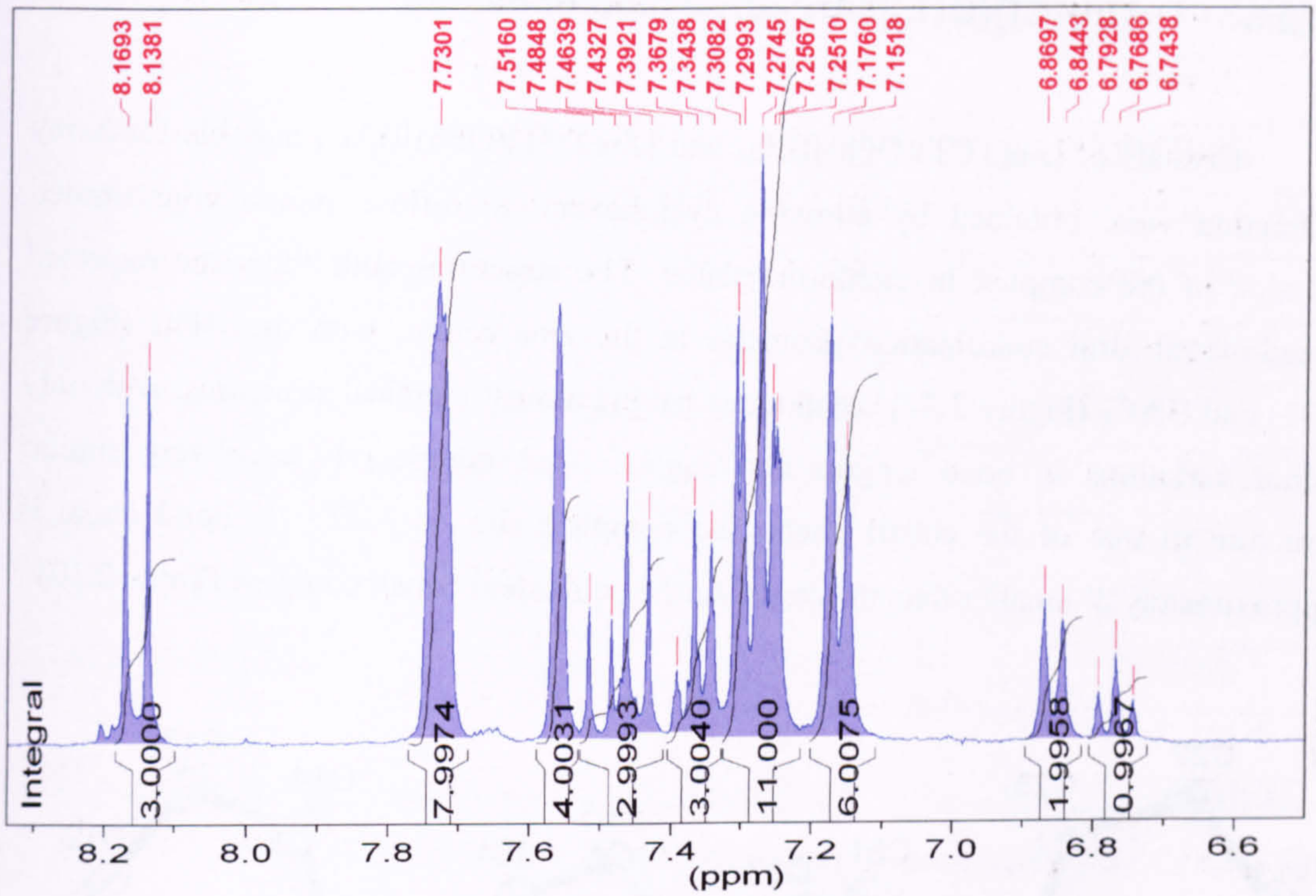

Figure 2.30: ^{1}H NMR spectrum of [Zn(TCT)(OPh)]BAr^{F}_{4} (aromatic region).

Proton	δ / ppm [Zn(TCT)(OPh)]BPh_4	δ / ppm [Zn(TCT)(OPh)]BAr^{F}_{4}
a	2.27 / 2.03	2.4 / 2.2
b	2.03 / 2.27	2.2 / 2.4
c	3.99	4.17
d	7.99	8.15
e	7.25	7.4
f / j	7.39	7.27
g / i	7.2	7.16
h	7.39	7.28
k	7.44	7.47
l / p	6.87	6.87
m / o	7.4	7.3
n	6.8	6.77

Table 2.10: ^{1}H NMR assignments for [Zn(TCT)(OPh)]BAr_4.

2.4.2 b [Zn(TCT)(OPh)]BAr_4 - crystallography

Crystals of [Zn(TCT)(OPh)]BPh_4 and [Zn(TCT)(OPh)]$BAr^F{}_4$ suitable for X-ray diffraction were obtained by allowing cyclohexane to diffuse into a concentrated solution of the complex in dichloromethane. The structures both show the expected pseudo-tetrahedral coordination geometry at the zinc centre, with the BPh_4 (Figure 2.31) and $BAr^F{}_4$ (Figure 2.32) compounds having almost identical structures, with only minor variations in bond lengths and angles. The compounds have very similar structure to that of the cobalt phenoxide complex; the Zn – O – C bond angle is approximately 2° smaller than the angle for the equivalent cobalt complex (Table 2.10).

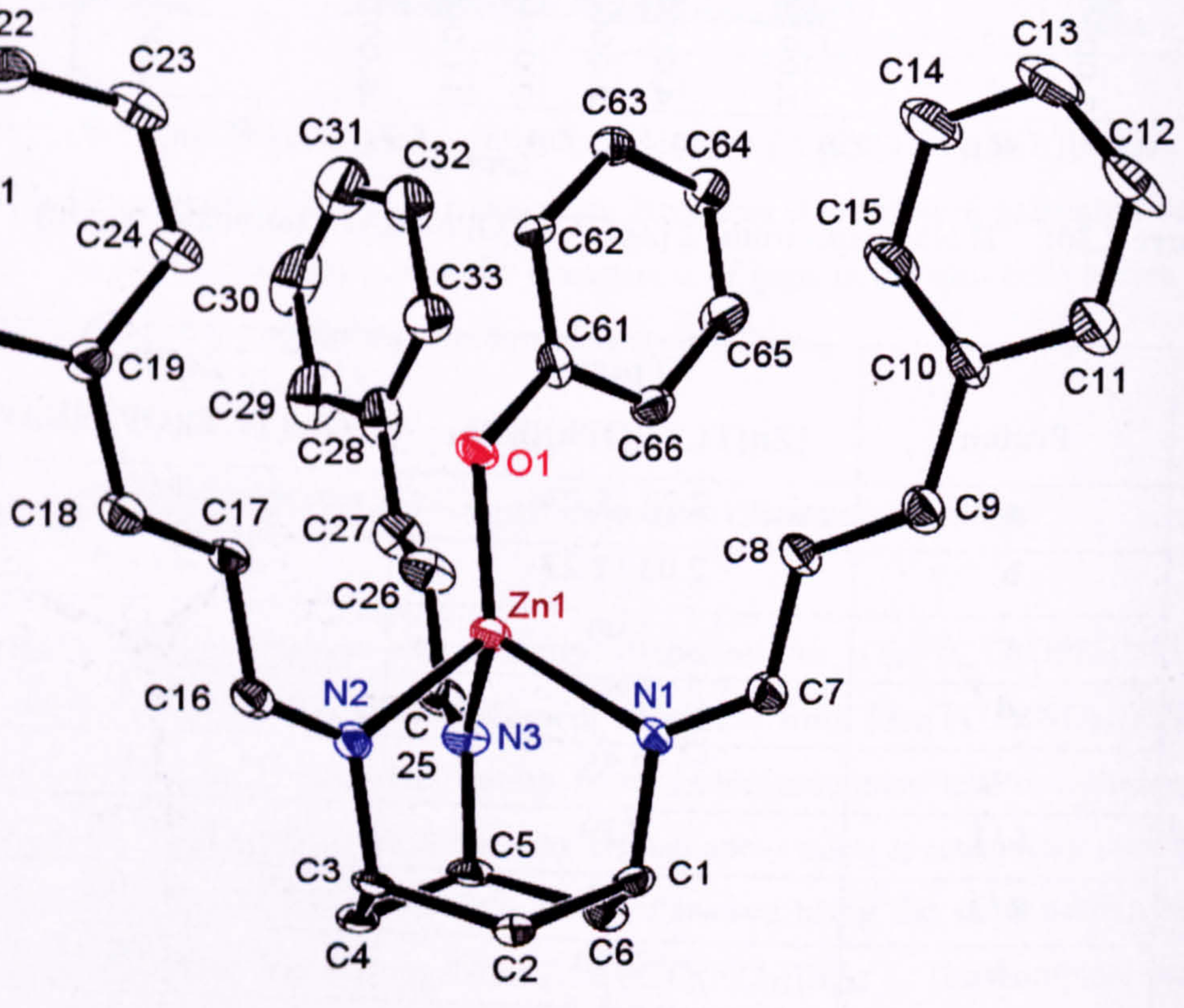

Figure 2.31: An ORTEP representation (30% probability ellipsoids) of [Zn(TCT)(OPh)]$BPh_4 \cdot ½$ c-C_6H_{12}, cation only, H atoms omitted for clarity.

Bond length / angle	[Co(TCT)(OPh)] BPh_4	[Zn(TCT)(OPh)] BPh_4	[Zn(TCT)(OPh)] BAr^F_4
M(1)–O(3)	1.871(8)	1.885(3)	1.8669(15)
O(3)–C(*)	1.321(13)	1.340(5)	1.341
M(1)–N(2)	2.013(9)	2.028(4)	2.0279(18)
M(1)–N(1)	1.998(10)	2.036(4)	2.0417(19)
M(1)–N(3)	2.011(9)	2.037(4)	2.0383(18)
C(*)–O(3)–M(1)	128.7(7)	126.7(3)	127.63(14)
O(3)–M(1)–N(2)	114.8(4)	116.08(15)	126.19(7)
O(3)–M(1)–N(1)	124.8(4)	122.83(14)	124.12(7)
O(3)–M(1)–N(3)	122.4(4)	125.70(16)	115.30(7)

Table 2.11: Selected bond lengths (/ Å) and angles (/ °) for [Zn(TCT)(OPh)]BAr_4, with data for [Co(TCT)(OPh)]BPh_4 presented for comparison. [*: in all cases the carbon atom is the *ipso*-carbon of the phenoxide ligand.]

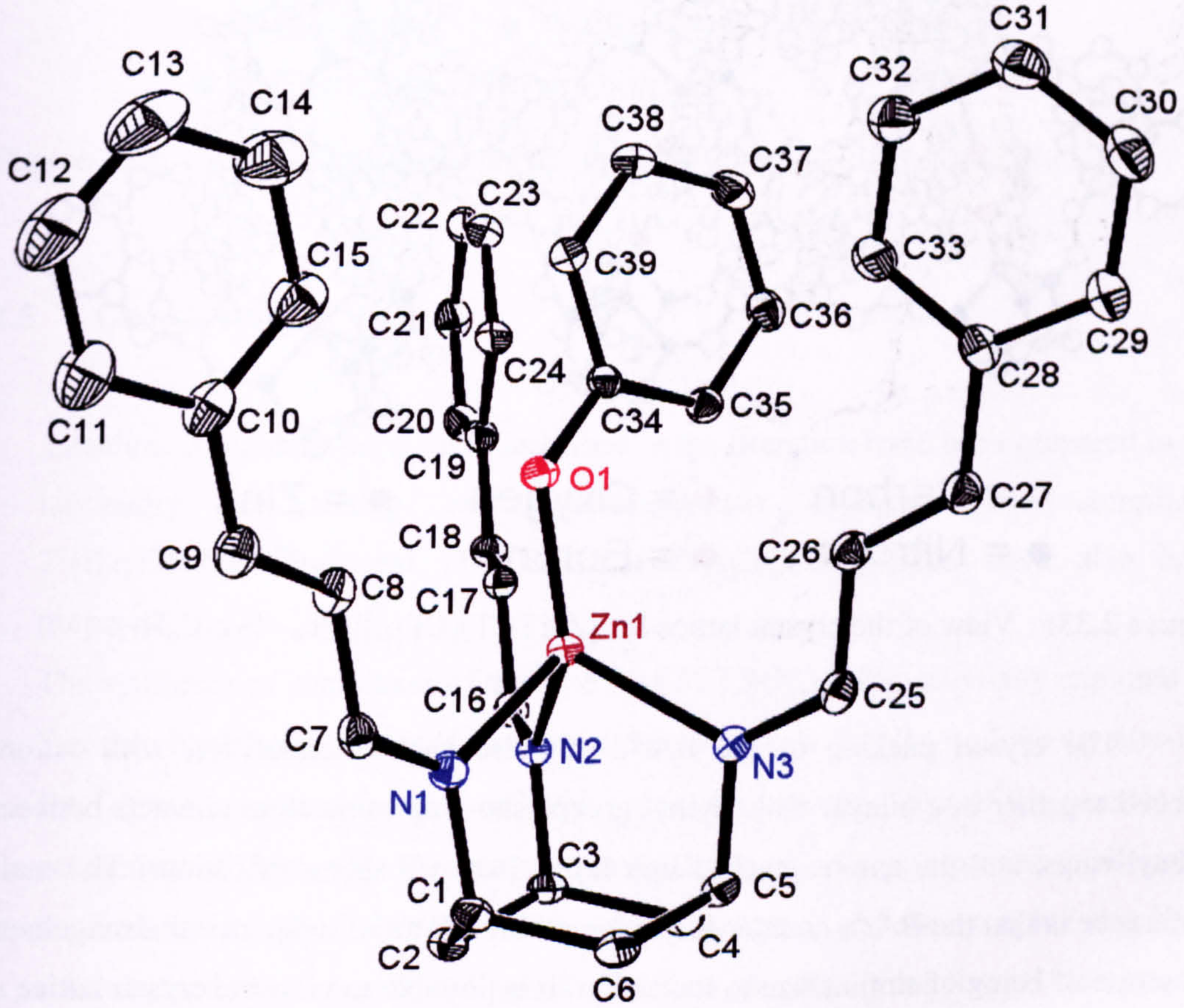

Figure 2.32: An ORTEP representation (30% probability ellipsoids) of [Zn(TCT)(OPh)]$BAr^F_4 \cdot c\text{-}C_6H_{12}$, cation only, H atoms omitted for clarity.

Each asymmetric unit of $[Zn(TCT)(OPh)]BPh_4$ contains half a molecule of cyclohexane, whilst the $BAr^F{}_4$ analogue contains a complete (disordered) cyclohexane molecule in each unit cell. The extended crystal structure reveals a layered packing arrangement, with cations and anions stacked together in alternating layers. The cations pack in a bilayer with alternating up and down orientations, with phenyl rings in close proximity to one another (Figure 2.33).

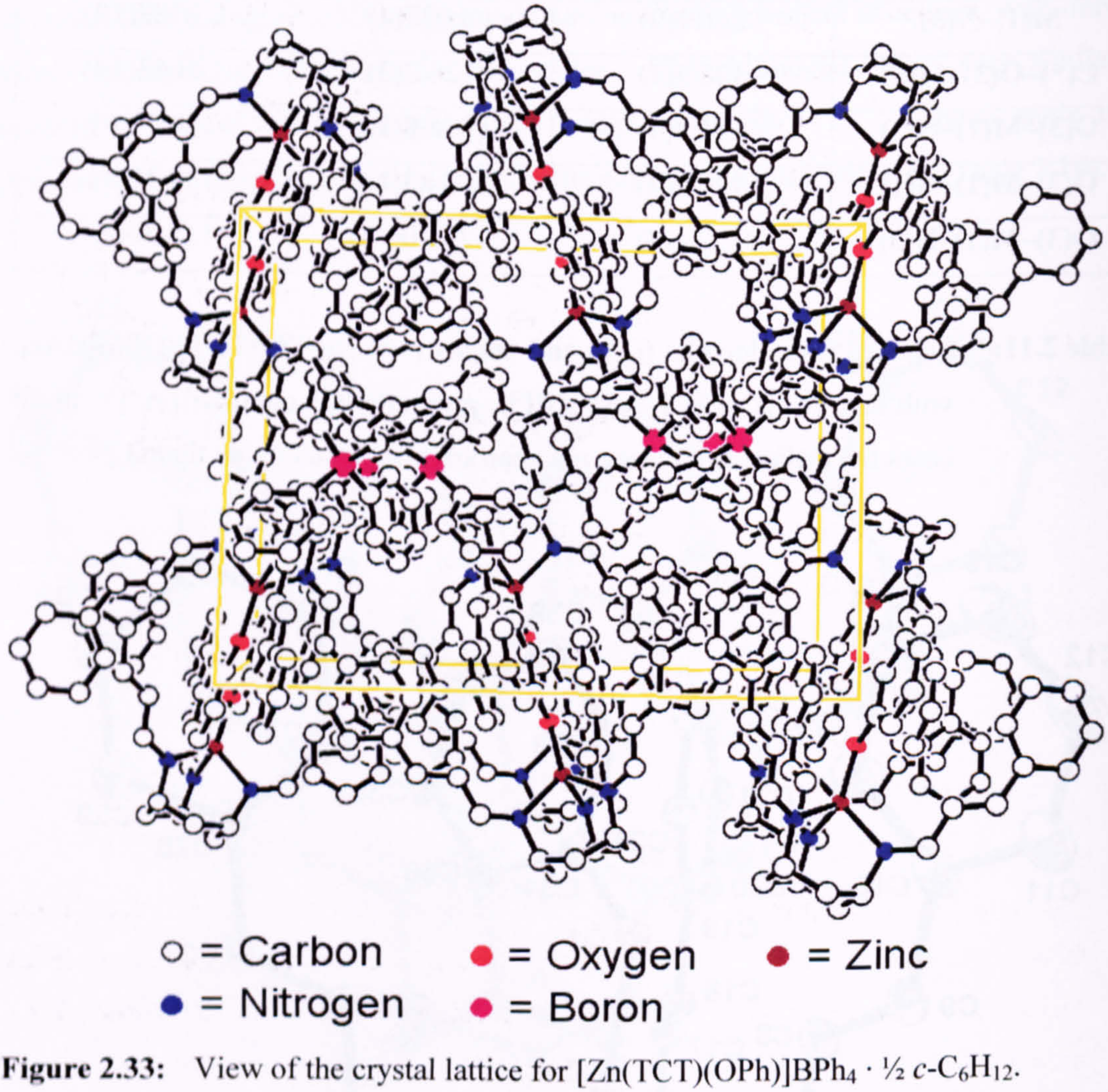

Figure 2.33: View of the crystal lattice for $[Zn(TCT)(OPh)]BPh_4 \cdot \frac{1}{2}\ c\text{-}C_6H_{12}$.

The crystal packing of the $BAr^F{}_4$ salt also shows similarities, with cations stacked together in a bilayer with phenyl groups showing some close contacts between phenyl rings, and the anions stacked into layers between sheets of cations. The main difference is that the $BAr^F{}_4$ counter-ion enforces a much more symmetrical arrangement by virtue of being of similar size to the cation; it is possible to view the crystal lattice at such an angle as to see the anions clearly arranged in rows (Figure 2.34).

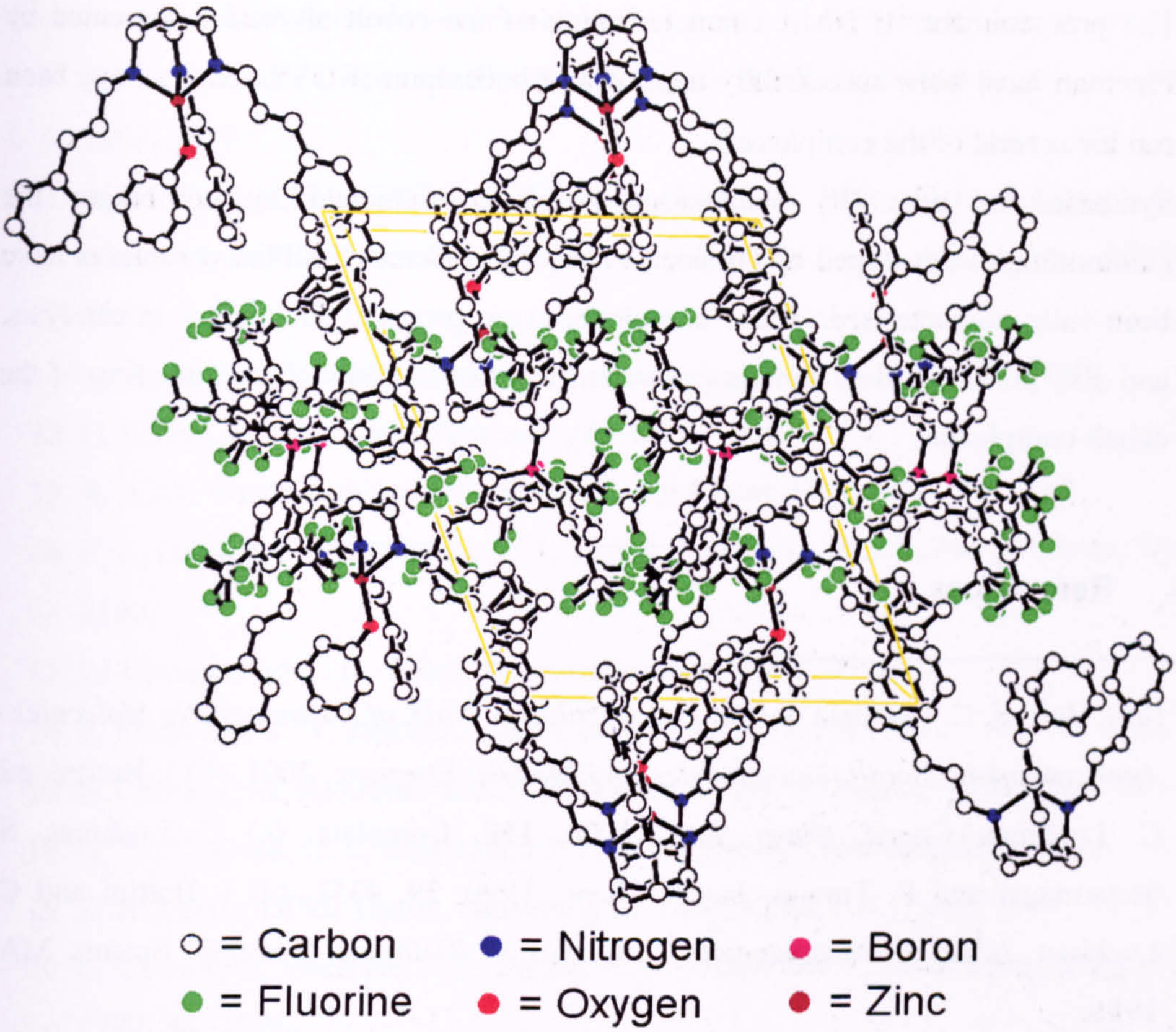

Figure 2.34: View of the crystal lattice of $[Zn(TCT)(OPh)]BAr^{F}_{4} \cdot c\text{-}C_6H_{12}$.

2.5 Conclusions

- Titanium complexes previously described in the literature have been prepared in the laboratory for testing as transesterification catalysts. The complexes $Ti(Bz_3TREN)(O^{n}Bu)$ and $[Ti(\{^{t}Bu_2Sal\}_2BzTACH)(O^{i}Pr)]BPh_4$ have also been prepared.

- The syntheses of complexes of the type $[Co(TCT)(OR)]BPh_4$ originally explored by Freeman have been continued, and expanded to include R = Bz, and the counter-ion $BAr^{F}_{4}{}^{-}$ has been used in place of $BPh_4{}^{-}$, to investigate the effect of the counter-ion on catalysis (Chapter 3). The synthetic methodology has been improved to allow for the isolation of $[Co(TCT)(OEt)]BPh_4$ in a pure form, and the complex has been characterised by X-ray crystallography; this is the first time that a monomeric, cationic cobalt (II) alkoxide has been crystallographically characterised.

- The protocols for ^{1}H NMR characterisation of the cobalt alkoxides presented by Freeman have been successfully applied and built upon (COSY spectra have been run for several of the complexes).
- Syntheses of zinc (II) phenoxides has been achieved by combining the methodologies developed by Greener, Lusby and Freeman, and the complexes have been fully characterised. These complexes were prepared for testing in catalysis, and also provide a diamagnetic equivalent for the ^{1}H NMR characterisation of the cobalt complexes.

2.6 References

1 (a) I. Bertini, C. Luchinat and G. Parigi, *Solution NMR of Paramagnetic Molecules - Applications to Metallobiomolecules and Models*; Elsevier:, 2001. (b) I. Bertini and C. Luchinat, *Coord. Chem. Rev.*, 1996, **150**, Complete. (c) C. Luchinat, S. Steuernagel and P. Turano, *Inorg. Chem.*, 1990, **29**, 4351. (d) I. Bertini and C. Luchinat, *NMR of Paramagnetic Molecules in Biological Systems*; Boston, MA, 1986.

2 J. D. Freeman, DPhil Thesis, University of York, 2001.

3 J. Lindley, *Tetrahedron*, 1984, **40**, 1433.

4 R. J. Bushby, D. R. McGill, K. M. Ng and N. Taylor, *J. Mater. Chem.*, 1997, **7**, 2343.

5 A. Chandrasekeran. R. O. Day and R. R. Holmes, *J. Am. Chem. Soc.*, 2000, **122**, 1066.

6 T. R. Dargaville, P. J. DeBruyn, A. S. C. Lim, M. G. Looney, A. C. Potter, D. H. Solomon and X. Q. Zhang, *J. Polym. Sci. Pol. Chem.*, 1997, **35**, 1389.

7 M. Kol, M. Shamis, I. Goldberg, Z. Goldschmidt, S. Alfi, E. Hayut-Salant, *Inorg. Chem. Commun.*, 2001, **4**, 177.

8 (a) S. Schneider and A. C. Filippou, *Inorg. Chem.*, 2001, **40**, 4674. (b) C. Morton, I. J. Munslow, C. J. Sanders, N. W. Alcock, and P. Scott, *Organometallics*, 1999, **18**, 4608. (c) R. R. Schrock, C. C. Cummins, T. Wilhelm, S. Lin, S. M. Reid, M. Kol, and W. M. Davis, *Organometallics*, 1996, **15**, 1470. (d) Z. B. Duan and J. G. Verkade, *Inorg. Chem.*, 1995, **34**, 4311. (e) M. Schubart, L. Odwyer, L. H. Gade, W. S. Li, and M. McPartlin, *Inorg. Chem.*, 1994, **33**, 3893. (f) C. C. Cummins, R. R. Schrock, and W. M. Davis, *Organometallics*, 1992, **11**, 1452.

9 (a) L. H. Gade, *Chem. Commun.*, 2000, 173. (b) R. R. Schrock, *Acc. Chem. Res.*, 1997, **30**, 9.

10 (a) H.-F. Hsu, W.-C. Chu, C.-H. Hung, and J.-H. Liao, *Inorg. Chem.*, 2003, **42**, 7369. (b) E. Block, G. Oforiokai, and J. Zubieta, *J. Am. Chem. Soc.*, 1989, **111**, 2327.

11 A. A. Naiini, W. Menge and J. G. Verkade, *Inorg. Chem.*, 1991, **30**, 5009.

12 O. Hassel and K. Lunde, *Research (London)*, 1950, **3**, 484.

13 R. A. D. Wentworth and J. J. Felten, *J. Am. Chem. Soc.*, 1968, **90**, 621.

14 F. L. Urbach, J. E. Sarneski, L. J. Turner, and D. H. Busch, *Inorg. Chem.*, 1968, **7**, 2169.

15 L. Turculet and T. D. Tilley, *Organometallics*, 2002, **21**, 3961.

16 F. Lions and K. V. Martin, *J. Am. Chem. Soc.*, 1957, **79**, 1572.

17 B. Greener, M. H. Moore and P. H. Walton, *Chem. Commun.*, 1996, 27.

18 G. W. V. Cave, C. L. Raston and J. L. Scott, *Chem. Commun.*, 2001, 2159.

19 E. A. Lewis, DPhil Thesis, University of York, 2002.

20 L. Cronin, B. Greener, S. P. Foxon, S. L. Heath and P. H. Walton, *Inorg. Chem.*, 1997, **36**, 2594.

21 A. K. Nairn, DPhil Thesis, University of York, 2001.

22 J. E. Bollinger, J. T. Mague, C. J. O'Connor, W. A. Banks, and D. M. Roundhill, *J. Chem. Soc., Dalton Trans.*, 1995, 1677.

23 E. A. Lewis, J. R. L. Smith, P. H. Walton, S. J. Archibald, S. P. Foxon, and G. M. P. Giblin, *J. Chem. Soc., Dalton Trans.*, 2001, 1159.

24 A. K. Nairn, R. Bhalla, S. P. Foxon, X. M. Liu, L. J. Yellowlees, B. C. Gilbert, and P. H. Walton, *J. Chem. Soc, Dalton Trans.*, 2002, 1253.

25 Y. Kim, G. K. Jnaneshwara and J. G. Verkade, *Inorg. Chem.*, 2003, **5**, 1437.

26 C. L. Frye, Fr. Patent 1511256, *Chem. Abstr.*, 1968, **70**, 87303.

27 S. D. Bull, M. G. Davidson, A. L. Johnson, D. Robinson and M. F. Mahon, *Chem. Commun.*, 2003, 1750.

28 V. Ugrinova, G. A. Ellis and S. N. Brown, *Chem. Commun.*, 2004, 460.

29 R. W. Adams, E. Bishop, R. L. Martin and G. Winter, *Aust. J. Chem.*, 1966, **19**, 207.

30 G. A. Sigel, R. A. Bartlett, D. Decker, M. M. Olmstead and P. P. Power, *Inorg. Chem.*, 1987, **26**, 1773.

31 H. Lehmkuhl and W. Eisenbach, *Ann. Chem.*, 1975, 672.

32 N. Y. Turova, E. P. Turevskaya, V. G. Kessler, N. I. Kozlova and A. I. Belokon, *Russ. J. Inorg. Chem.*, 1992, **37**, 26.

33 (a) O. Blum and D. Milstein, *J. Am. Chem. Soc.*, 1995, **117**, 4582. (b) D. M. Hoffman, D. Lappas and D. A. Wierda, *J. Am. Chem. Soc.*, 1989, **111**, 1531. (c) A. S. Goldman and J. Halpern, *J. Am. Chem. Soc.*, 1987, **109**, 7537. (d) H. E. Bryndza, J. C. Calabrese, M. Marsi, D. C. Roe, W. Tam and J. E. Bercaw, *J. Am. Chem. Soc.*, 1986, **108**, 4805.

34 K. J. Tubbs, E. Szajna, B. Bennett, J. A. Halfen, R. W. Watkins, A. M. Arif and L. M. Berreau, *J. Chem. Soc., Dalton Trans.*, 2004, Advance Article.

35 (a) L. Cronin, B. Greener, M. H. Moore and P. H. Walton, *J. Chem. Soc.-Dalton Trans.*, 1996, 3337. (b) C. J. Boxwell and P. H. Walton, *Chem. Commun.*, 1999, 1647.

36 (a) B. Greener, S. P. Foxon and P. H. Walton, *New J. Chem.*, 2000, **24**, 269. (b) L. Cronin and P. H. Walton, *Chem. Commun.*, 2003, 1572.

37 B. Greener, DPhil Thesis, University of York, 1997.

38 J. D. Freeman, DPhil Thesis, University of York, 2001.

39 C. K. Johnson, 1976, ORTEP-11, *A FORTRAN Thermal-Ellipsoid Plot Program*, Report ORNL-5138, Oak Ridge National Laboratory, Oak Ridge, Tennessee.

40 B. Greener and P. H. Walton; *J. Chem. Soc., Dalton. Trans.*, 1997, 3733

41 S. J. Archibald, S. P. Foxon, J. D. Freeman, J. E. Hobson, R. N. Perutz and P. H. Walton, *J. Chem. Soc.-Dalton Trans.*, 2002, 2797.

42 S. H. Strauss, *Chem. Rev.*, 1993, **93**, 927.

43 H. Nishida, N. Takada, M. Yoshimura, T. Sonoda and H. Kobayashi, *Bull. Chem. Soc. Jpn.*, 1984, **57**, 2600.

44 (a) M. Brookhart, B. Grant and A. F. Volpe Jr., *Organometallics*, 1992, **11**, 3920. (b) M. Brookhart and S. Sabo-Etienne, *J. Am. Chem. Soc.*, 1991, **113**, 2777.

45 M. Brookhart, F. C. Rix, J. M. DeSimone and J. C. Barborak, *J. Am. Chem. Soc.*, 1992, **114**, 5894.

46 D. V. Yandulov and R. R. Schrock, *Science*, 2003, **301**, 76.

47 G. W. Parshall and S. D. Ittel, "*Homogeneous Catalysis*"; 2nd Ed.; John Wiley & Sons, Inc., 1992.

48 J. Huang, D. F. Li, S. A. Li, D. X. Yang, W. Y. Sun and W. X. Tang, *J. Inorg. Biochem.*, 2004, **98**, 502.

49 M. M. Ibrahim, K. Ichikawa and M. Shiro, *Inorg. Chim. Acta*, 2003, **353**, 187.

50 R. Walz, K. Weis, M. Ruf and H. Vahrenkamp, *Chem. Ber.-Recl.*, 1997, **130**, 975.

51 M. H. Chisholm, N. W. Eilerts, J. C. Huffman, S. S. Iyer, M. Pacold and K. Phomphrai, *J. Am. Chem. Soc.*, 2000, **122**, 11845.

52 P. J. Lusby, DPhil Thesis, University of York, 2000.

Chapter 3: Catalytic experiments

This chapter discusses the experimental methods used to investigate the catalytic activity of the metal complexes synthesised in this project. Catalytic activities for trans- and interesterification are reported, and the differences in observed activities are considered. A discussion of the possible mechanisms involved in this reaction is presented, along with evidence to support the proposed mechanism for transesterification.

3.1 Transesterification

Transesterification (eq. 3.1) is widely used in research and industry for the preparation of esters from more readily available starting materials.[1]

$$RCO_2R'' + R'OH \rightleftharpoons RCO_2R' + R''OH \quad \text{(eq. 3.1)}$$

A number of metal alkoxide species are known to have activity for the transesterification reaction, as discussed below. An account of the activity of titanium tetra-alkoxides for transesterification was published by Seebach *et al.* in 1982,[2] who also noted that the titanium alkoxides were compatible with a wide variety of functional groups. This was one of the earlier *published* uses of titanium alkoxides for an organic synthesis reaction, coming just two years after the initial report of asymmetric epoxidation by Sharpless.[3] Seebach noted that titanium alkoxides had been known by industrial chemists to be useful reagents for a variety of organic reactions (including transesterification) since the 1960's, but their use had remained hidden amongst patent literature.

Lanthanide alkoxides ($Ln(OR)_3$) were also reported to be active for transesterification by Okano *et al.*,[4] who investigated their use in the synthesis of a variety of different esters and found that they were useful for the synthesis of a wide variety of esters, with only *tert*-butyl esters being difficult to synthesise. They also noted that the activity of the catalysts tested decreased in the order La > Nd > Gd > Yb (relative activities of 27 : 8 : 2 : 1, based on conversions quoted in paper). The larger metal ions give higher reactivity, showing that the nucleophilicity of the alkoxide ligands, as opposed to the Lewis acidity of the metal, is the major influence on the transesterification activity. Alkali metal alkoxides are known to be catalytically active

for transesterification,[5] and they also show a dependency on metal ion size, with caesium alkoxides being the most active. However, this study did not include investigation of lanthanide or alkali metal species.

Tin (IV) alkoxides have been investigated for catalytic activity in transesterification also.[6] Initial studies focussed on a range of different tin-containing species, from which the active tin alkoxides were formed *in situ*. An activity order was observed: $R_2Sn(OAc)_2 > R_2SnO > R_2SnCl_2 > R_2SnS > R_4Sn$, corresponding to the relative difficulty of forming the active tin alkoxide species. The study compared the tin alkoxides with other catalysts, and concluded that tin alkoxides were not as effective as titanium alkoxides. However, this view was changed by the discovery of distannoxane catalysts, prepared from R_2SnO and R_2SnCl_2.[7] These compounds were found to be air-stable and far less toxic than other tin compounds because of their high melting points. Despite the presence of a large metalloxane core, the eight alkyl groups effectively provide an organic "mask", making the compounds soluble in organic solvents. It is the metalloxane core which provides the unique reactivity of the compounds, with the proximity of the tin atoms allowing direct interaction between groups bonded to them, giving high catalytic activity for transesterification (up to 2000 turnovers in 20 h, equivalent to ~ 100 T.O. h^{-1}, at 353 K).[8]

$$R_2SnO + R_2SnX_2 \longrightarrow XR_2SnOSnR_2X \qquad \text{(Eq. 3.2)}$$

$$3\ R_2SnO + R_2SnX_2 + H_2O \longrightarrow 2\ XR_2SnOSnR_2OH \qquad \text{(Eq. 3.3)}$$

(X = OH, NCS)

Initially, the compounds formed are thiocyanates or hydroxides (eq. 3.2 & 3), and these are converted to the alkoxides *in situ*.

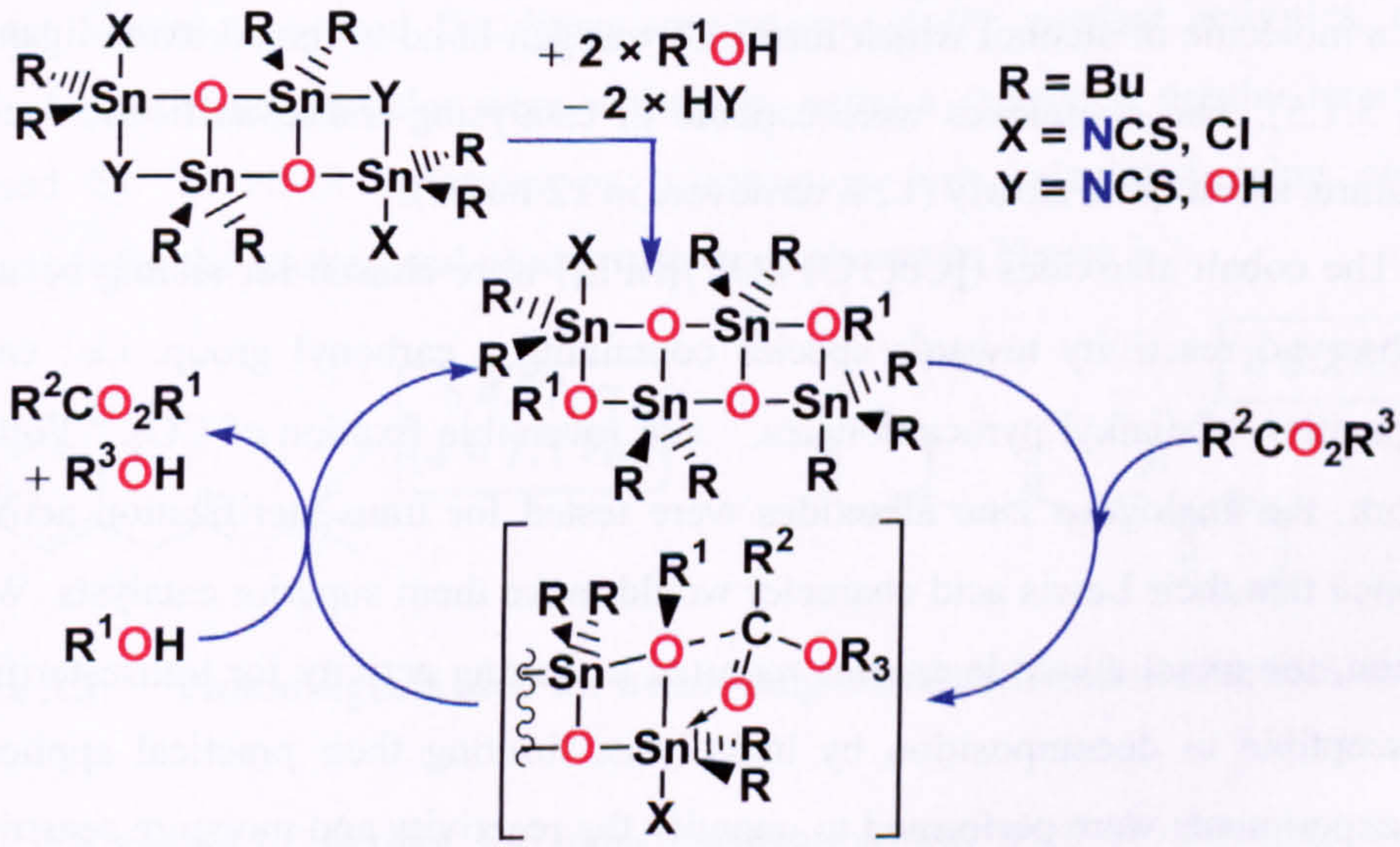

Figure 3.1: Proposed transesterification mechanism for distannoxane catalysts.

The authors of the report proposed that the reaction involved coordination of a molecule of ester to a tin atom as the initial step (with bulky esters failing to react) and alcoholysis then taking place to form the new ester and regenerate the alkoxydistannane (Figure 3.1); it is important to note that the reaction is not slowed by steric bulk in the alcohol component. Although these compounds are relatively low in toxicity for handling, they are homogeneous catalysts and would therefore be hard to exclude from the final product, so their toxicity would still be an issue for certain applications. Otera *et al.* have recently published an account of their research into the use of fluorous distannoxanes as more effective and reusable catalysts for transesterification.[9]

Transesterification catalysed by late transition metals has been reported for a number of systems. Yamamoto *et al.* reported the catalytic activity of alkoxo(triphenylphosphine)copper (I) complexes. These were of the general formula $Cu(OR)(PPh_3)_n$, where $n = 1$ for R = ^{n}Pr, ^{i}Pr, and n = 2 for R = Me, Et, allyl, Bz, Ph. It should be noted that these complexes were not characterised crystallographically. Drawing on the knowledge of metal alkoxide behaviour summarised in Chapter 1, it is likely that these complexes are present in dimeric form, at least in the solid state. The complexes were shown to be catalytically active for transesterification, performing approximately 50 turnovers in 12 h at –5 °C. The fact that the complexes show catalytic activity at such low temperature is remarkable, although the complexes were not stable at elevated temperatures. Later work by Yamamoto *et al.* detailed the synthesis and characterisation of a series of nickel (II) and palladium (II) alkoxides of the general formula $Pd(R)(OR')(HOR')(L)_2$,[10] where R is an alkyl group, OR' is either a fluorinated alkoxide or a *para*-substituted phenol, and L is a tri-alkyl phosphine. The complexes contain a molecule of alcohol which forms a hydrogen-bond to the alkoxide ligand (see Section 3.1.5). The complexes were capable of catalysing transesterification at room temperature, albeit quite slowly (12.6 turnovers in 12 hours).

The cobalt alkoxides ($[Co(TCT)(OR)]BPh_4$) were chosen for testing because of their observed reactivity towards species containing a carbonyl group, i.e.: catalytic decomposition of dialkyl pyrocarbonates,[11] and reversible fixation of CO_2.[12] Following this work, the analogous zinc alkoxides were tested for transesterification activity; it was hoped that their Lewis acid character would make them superior catalysts. Without exception, the metal alkoxide species reported as having activity for transesterification are susceptible to decomposition by hydrolysis, limiting their practical applications. Initial experiments were performed to quantify the reactivity and moisture sensitivity of the titanium species. Coordination catalysts based on titanium alkoxides were then

synthesised and tested to find derivatives that would be more resistant to hydrolysis; this was achieved by using bulky ligands which could prevent inactivation of the catalysts by the formation of oxo-bridged dimers.

3.1.1 Standard test reaction for transesterification

After initial experiments to reproduce the results of Seebach *et al.*, the trans-esterification of 2-phenylacetic acid ethyl ester with benzyl alcohol to produce 2-phenylacetic acid benzyl ester (Figure 3.2) was chosen as the test reaction.

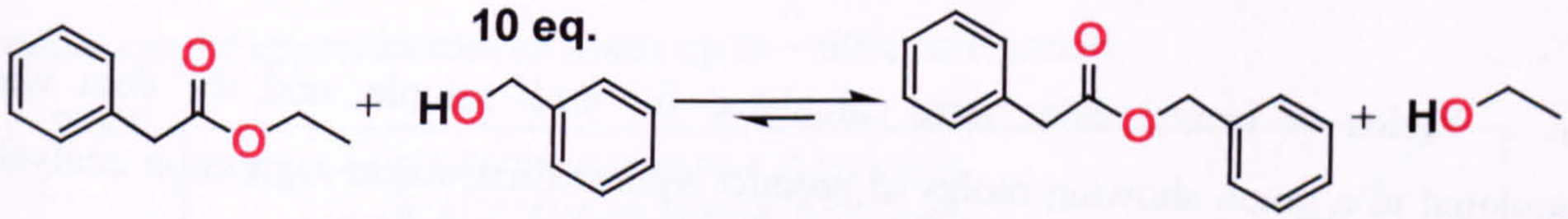

Figure 3.2: Trans-esterification test reaction.

The use of β-keto esters was attempted, but was discontinued due to the formation of stable titanium complexes with these species – the acetoacetate species deprotonates to form a stable ligand. Dried 2-phenylacetic acid ethyl ester, ten equivalents of dried benzyl alcohol (with respect to ester) and the catalyst were mixed together in an argon-filled glove-box. The reaction vessels were sealed and removed from the glove-box, and the mixture was heated to 100 °C under reflux conditions with a continuous flow of argon over the apparatus; identical conditions were used for all catalysts, regardless of the expected stability or instability towards moisture and air. A carousel reactor was used for direct comparison of the catalyst activities, ensuring identical conditions. Samples were withdrawn using a syringe at regular intervals and analysed by ^{1}H NMR spectroscopy. Conversion was calculated using distinctive resonances for the starting and product esters, as shown in Figure 3.3.

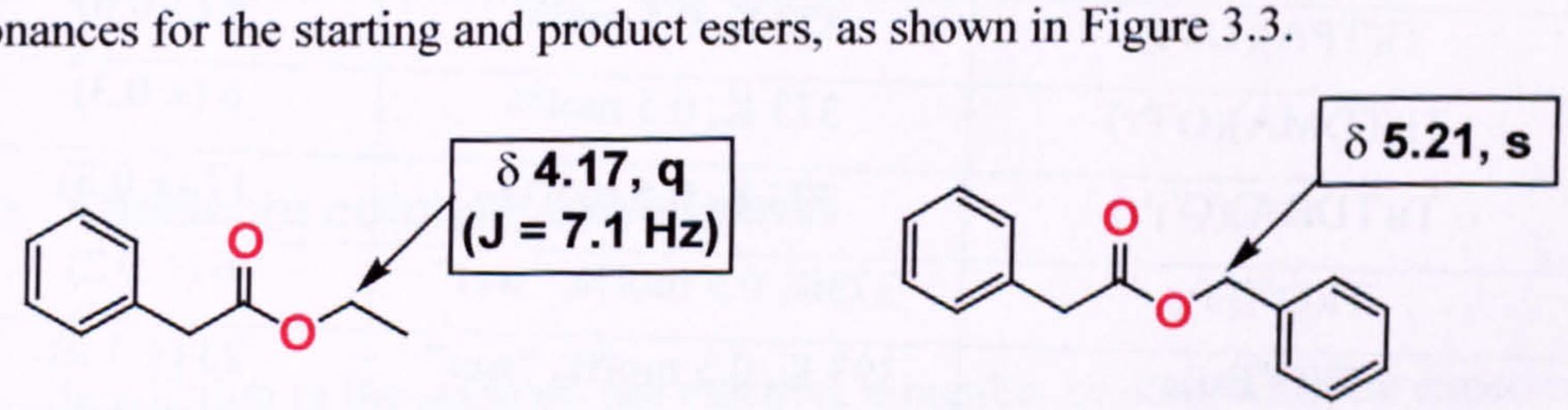

Figure 3.3: Proton signals used for monitoring transesterification reaction.

An excess of alcohol for transesterification was used to encourage complete conversion, and to maintain a relatively constant rate of transesterification (pseudo-first

order conditions), thus facilitating kinetic analysis. The reactions were performed in the absence of any solvent, with the catalysts being sufficiently soluble in the reaction medium. Initial experiments also included isolation of the ester produced to confirm purity and calculate yields, but later experiments used ^{1}H NMR spectroscopy to give *in situ* yields. Control experiments using $[Co(H_2O)_6](NO_3)_2$ and $[Zn(H_2O)_6](NO_3)_2$ were performed, as Co^{II} and Zn^{II} salts are known to catalyse transesterification at high temperatures (>150 °C), but neither compound showed any activity at 373 K.

3.1.2 Activities of catalysts for test reaction

Yields of benzyl ester were calculated for each sample, and the data was converted to a graph showing moles of product against time; linear regression analysis was performed to give a rate of conversion, which was then converted to turnover frequency. The activity values obtained for the different catalysts are listed in Table 3.1, along with the temperature and relative catalyst concentration used. Note that catalyst concentrations are quoted in mol% (relative to ester) and activities (or turnover frequencies, T.O.F.) are given as turnovers per hour, i.e.: the average number of ester molecules converted per hour per molecule of catalyst.

Catalyst species	Conditions	T.O.F. / h^{-1}
$[Co(TCT)(OEt)]BPh_4$	373 K, 0.25 mol%	47 (± 2.7)
$[Co(TCT)(OPh)]BPh_4$	373 K, 0.25 mol%	45 (± 1.8)
$[Co(TCT)(OPh)]BAr^F{}_4$	373 K, 0.25 mol%	65 (± 3.1)
$[Co(\{^tBu_2Sal\}_2BzTACH)]$	373 K, 0.25 mol%	no activity
$[Zn(TCT)(OPh)]BPh_4$	373 K, 0.25 mol%	29 (± 0.6)
$Ti(TPA)(O^iPr)$	373 K, 0.5 mol%	4 (± 0.6)
$Ti(TDMA)(O^iPr)$	373 K, 0.5 mol%	6 (± 0.3)
$Ti(TDBA)(O^iPr)$	373 K, 0.5 mol%	17 (± 0.3)
$Ti(O^nBu)_4$	373K, 0.5 mol%, "wet"	6 (± 0.2)
$Ti(O^nBu)_4$	393 K, 0.5 mol%, "wet"	23 (± 1.0)

Table 3.1: Observed transesterification activities for the standard test reaction.

The cobalt catalysts show the highest activities, especially when the $BAr^F{}_4^-$ counter-ion is used. There is very little difference in activity between $[Co(TCT)(OEt)]BPh_4$ and $[Co(TCT)(OPh)]BPh_4$. The zinc catalyst gives a slightly lower activity than the cobalt alkoxides, but has higher activity than the titanium tetra-alkoxides. The titanium complexes give lower activities, with Ti(TDBA)(O^{i}Pr) being the most effective, and actually having higher activity than the titanium tetra-alkoxides, although the titanium tetra alkoxides quite likely suffered from decomposition. Further experiments were performed to test the moisture stability of the titanium coordination catalysts (Section 3.1.3 c). The catalytic activities were calculated by performing linear regression on the reaction profiles shown in Figure 3.4; the rate of appearance of product can be approximated as linear up to ~ 60% conversion.

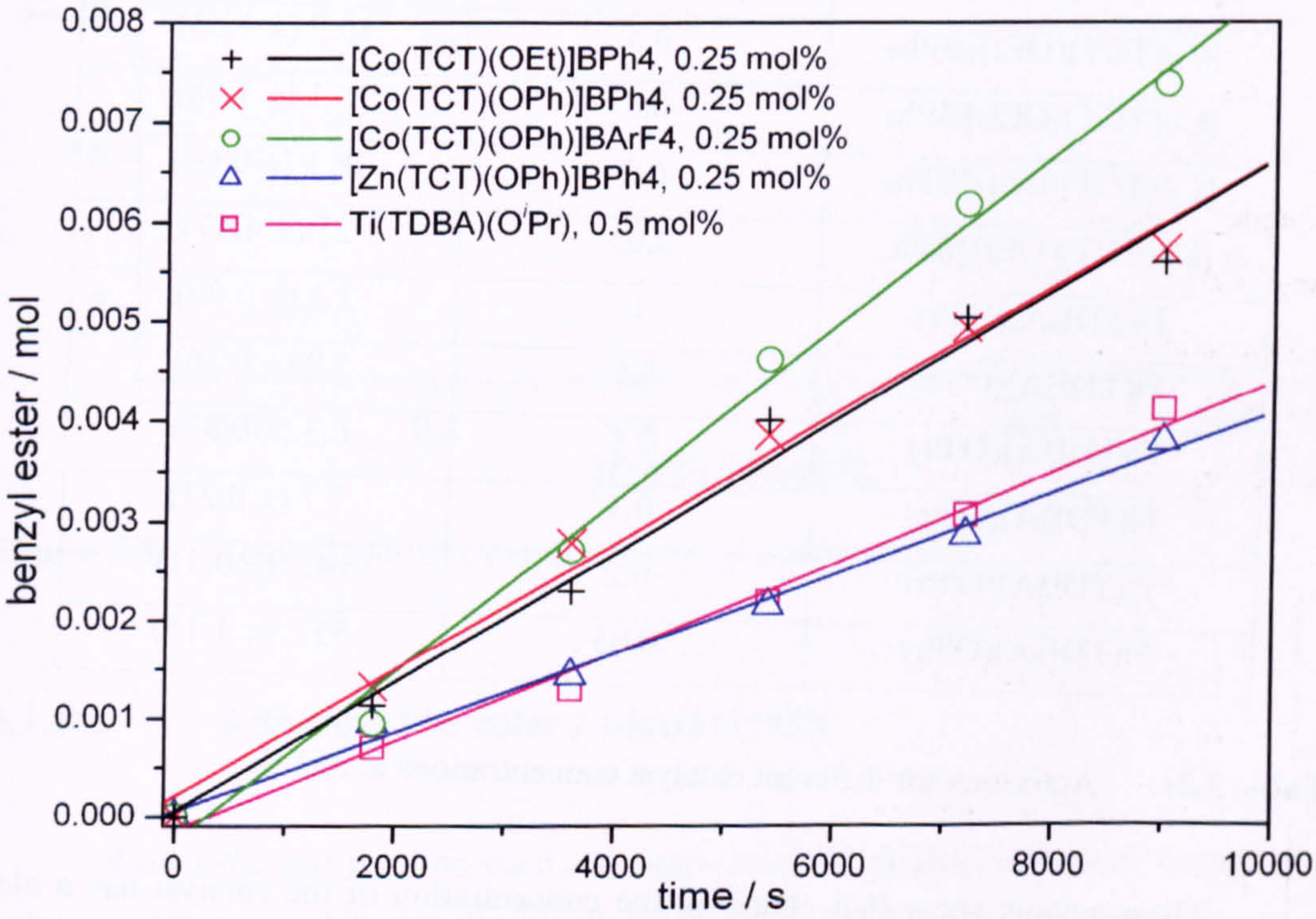

Figure 3.4: Reaction profiles for trans-esterification reaction.

3.1.3 Additional catalytic experiments

In addition to the standard test reaction, a number of other catalytic experiments were run, adjusting the conditions of the experiment to acquire more insight into the catalytic mechanism, and to evaluate further the performance of the catalysts.

3.1.3 a Adjusting catalyst concentration

A set of experiments was performed, under identical conditions, to test the efficiency of the catalysts at different concentrations. $[Co(TCT)(OEt)]BPh_4$ and Ti(TDBA)(O^{i}Pr) were used for these experiments, to give a sample of each of the two types of catalyst. The standard test reaction was used, and conversion of ethyl ester to benzyl ester was measured by ^{1}H NMR spectroscopy. Table 3.2 summarises the results for the two catalysts.

Catalyst	mol% catalyst	T.O.F. / h^{-1}
$[Co(TCT)(OEt)]BPh_4$	1	20.2 (± 2.65)
$[Co(TCT)(OEt)]BPh_4$	0.5	30.7 (± 1.63)
$[Co(TCT)(OEt)]BPh_4$	0.3	25.1 (± 1.08)
$[Co(TCT)(OEt)]BPh_4$	0.2	18.1 (± 0.64)
$[Co(TCT)(OEt)]BPh_4$	0.05	27 (± 4.47)
Ti(TDBA)(O^{i}Pr)	1	3.3 (± 0.09)
Ti(TDBA)(O^{i}Pr)	0.5	5.9 (± 0.26)
Ti(TDBA)(O^{i}Pr)	0.4	6.3 (± 0.33)
Ti(TDBA)(O^{i}Pr)	0.3	7.7 (± 0.21)
Ti(TDBA)(O^{i}Pr)	0.2	14.7 (± 0.51)
Ti(TDBA)(O^{i}Pr)	0.05	55.2 (± 1.15)

Table 3.2: Activities for different catalyst concentrations at 353 K.

These results show that changing the concentration of the catalyst has a clear effect on Ti(TDBA)(O^{i}Pr), with the catalyst becoming more active at lower concentrations (Figure 3.5). The effect upon $[Co(TCT)(OEt)]BPh_4$ is uncertain; the erratic results suggest that varying amounts of decomposition have taken place, perhaps due to differences in the reaction vessel conditions.

Increasing activity with decreasing concentration is a strong indication that a catalyst is being hindered by aggregation at high concentration, perhaps forming dimers in solution. This is supported by the fact that Ti(TDMA)(O^{i}Pr) and (Ti(TPA)(O^{i}Pr) show extremely low activity; Ti(TDBA)(O^{i}Pr) has a large hydrophobic component,

which would assist its dissolution in the substrates, whereas the other two catalysts have their titanium centres more exposed, favouring aggregation.

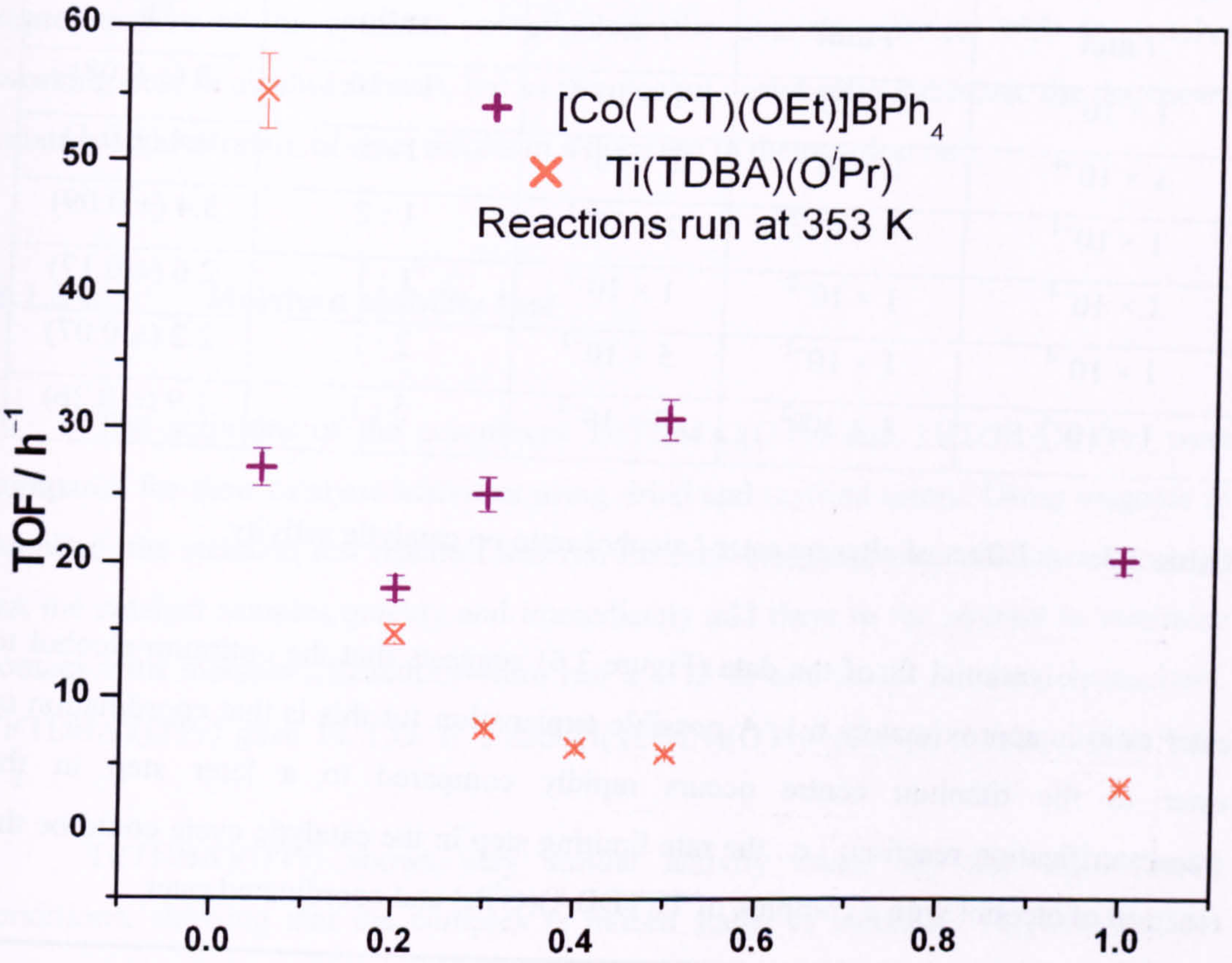

Figure 3.5: Dependence of catalyst activity on concentration.

3.1.3 b Adjusting the ester / alcohol ratio

Whilst the test reaction used ten equivalents of alcohol to impose pseudo-first order conditions, enabling facile kinetic analysis, it is likely that this ratio does not maximise the rate of conversion, since the transesterification reaction will be in competition with the alcohol / alkoxide exchange (Section 3.1.4 b). In order to establish the optimum ester / alcohol ratio for transesterification, a series of catalytic experiments was carried out, using a range of different ester / alcohol ratios, with the catalyst activity evaluated for each experiment. Ti(TDBA)(O^{i}Pr) was used for these experiments due to its robust nature, and reactions were run at 353 K to ensure moderate—and hence easily measured—reaction rates. The activity values (Table 3.3) were calculated by performing linear regression on the conversion data provided by ^{1}H NMR spectroscopy.

Ti(TDBA)(O^iPr) / mol	$PhCH_2CO_2Et$ / mol	BzOH / mol	Ester / alcohol ratio	T.O.F. / h^{-1}
1×10^{-4}	1×10^{-2}	1×10^{-1}	1 : 10	3 (± 0.08)
1×10^{-4}	1×10^{-2}	5×10^{-2}	1 : 5	4.4 (± 0.1)
1×10^{-4}	1×10^{-2}	2×10^{-2}	1 : 2	3.4 (± 0.09)
1×10^{-4}	1×10^{-2}	1×10^{-2}	1 : 1	2.6 (± 0.17)
1×10^{-4}	1×10^{-2}	5×10^{-3}	2 : 1	2.2 (± 0.07)
1×10^{-4}	1×10^{-2}	2×10^{-3}	5 : 1	1.9 (± 0.26)

Table 3.3: Effect of altering ester / alcohol ratio on catalytic activity.

A polynomial fit of the data (Figure 3.6) suggests that the optimum alcohol to ester ratio is approximately 6:1. A possible explanation for this is that coordination of ester to the titanium centre occurs rapidly compared to a later step in the transesterification reaction; i.e.: the rate limiting step in the catalytic cycle could be the reaction of alcohol with a complex of Ti(TDBA)(O^iPr) and coordinated ester.

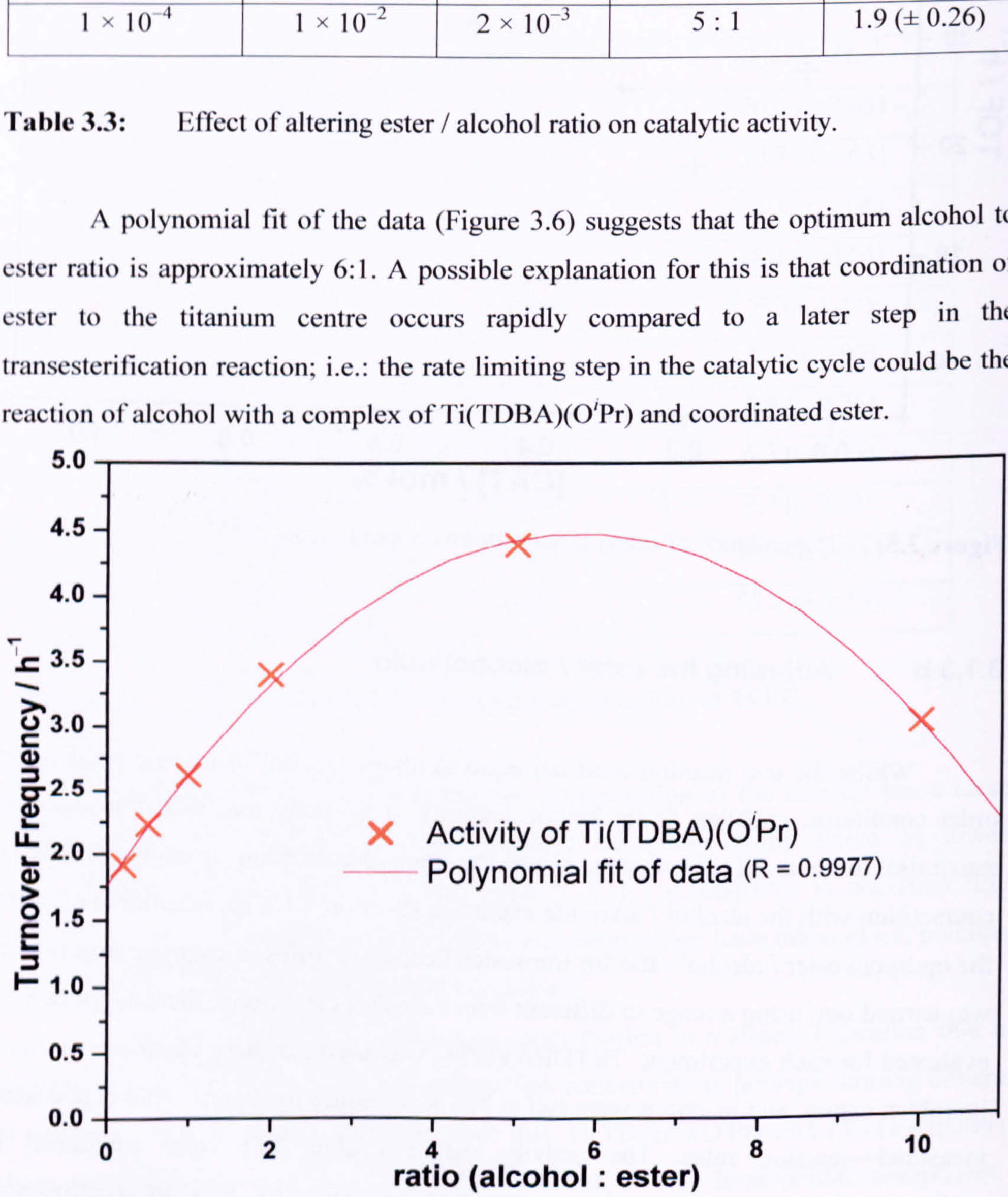

Figure 3.6: Effect of alcohol: ester ratio on catalyst activity.

Increasing the alcohol : ester ratio too far simply increases the rate of the competing alcohol / alkoxide interchange reaction. Alternatively, this could be representative of the optimum solvation for the titanium species, with the catalyst working best in alcohol solvent, but as the alcohol : ester ratio increases, the decreasing relative concentration of ester results in a decrease in the reaction rate.

3.1.3 c Moisture stability test

The activities of the complexes Ti(TDMA)(O^{i}Pr) and Ti(TDBA)(O^{i}Pr) were compared for their catalytic activities using dried and undried esters. Using reagents as supplied, the standard test reaction was run for each complex; care was taken to weigh out the catalyst samples quickly and immediately add them to the alcohol to minimise contact with moisture. Reactions were run at 373 K and under ambient atmosphere. Ti(TDBA)(O^{i}Pr) gave 14 T.O. h^{-1}, and Ti(TDMA)(O^{i}Pr) gave an activity of 10 T.O. h^{-1}.

Ti(TDBA)(O^{i}Pr) shows very similar activity under dry and under moist conditions, showing that the complex is indeed stable to moisture. Ti(TDMA)(O^{i}Pr) seems to show slightly higher activity under moist conditions. The increase in activity may result from some formation of the hydroxide complex, Ti(TDMA)(OH), which may be more active than the alkoxide.

3.1.4 Mechanistic investigations

3.1.4 a Interaction between metal centre and carbonyl group

Interaction between carbonyl groups and Lewis acid centres has been extensively documented,[13] and Lappert showed (as early as 1961) that the carbonyl function of esters can bind to a metal centre.[14] There are several possible modes of interaction between a metal centre and a carbonyl group, or between a bimetallic centre and a carbonyl group (Figure 3.7). Metals which act as simple Lewis acids favour a σ-interaction with the carbonyl oxygen (modes A – C), whether this constitutes simple electrostatic attraction, or donation of electron density to the metal centre (occasionally, steric bulk may dictate the orientation of the carbonyl group), whereas transition metals favour the π-interaction with the electrons of the C = O bond (modes D, E);[15] the C = O bond donates electrons to the metal, and can also act as a π-acceptor ligand. Examples of the binuclear complexes have been isolated. [16]

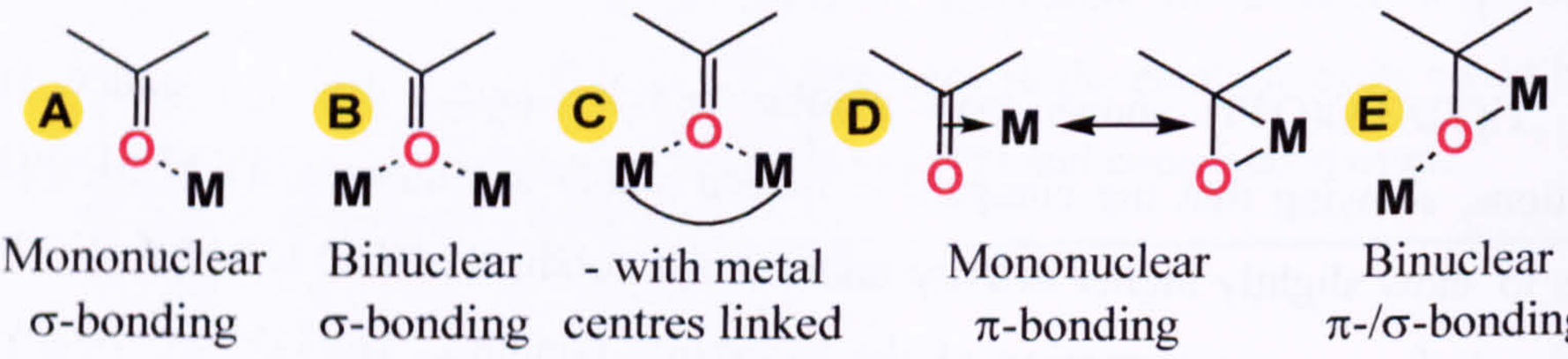

A	B	C	D	E
Mononuclear σ-bonding	Binuclear σ-bonding	- with metal centres linked	Mononuclear π-bonding	Binuclear π-/σ-bonding

Figure 3.7: Possible coordination modes between metal centres and carbonyl functions (including bimetallic interactions).

Infra-red spectroscopy studies of the titanium and cobalt species showed no detectable changes in the spectra of the ester or metal alkoxide species in solution, at concentrations where meaningful spectra could be recorded. This result was interpreted to mean that there is no *equilibrium* interaction between metal centre and carbonyl group at room temperature in *dilute* solution. NMR studies of the titanium species in the presence of esters in dilute solution showed no measurable changes in the proton chemical shifts of either the metal alkoxides or the esters. These NMR studies provide additional evidence for a lack of equilibrium interaction between metal centre and carbonyl group in dilute solution. However, it does not rule out the presence of transient interactions.

Figures 3.8 – 3.10 show the UV/vis spectra taken from 3 experiments designed to test for interaction between the cobalt centre and carbonyl functions.

Figures 3.8 – 3.10 show the UV/vis spectra taken from 3 experiments designed to test for interaction between the cobalt centre and carbonyl functions.

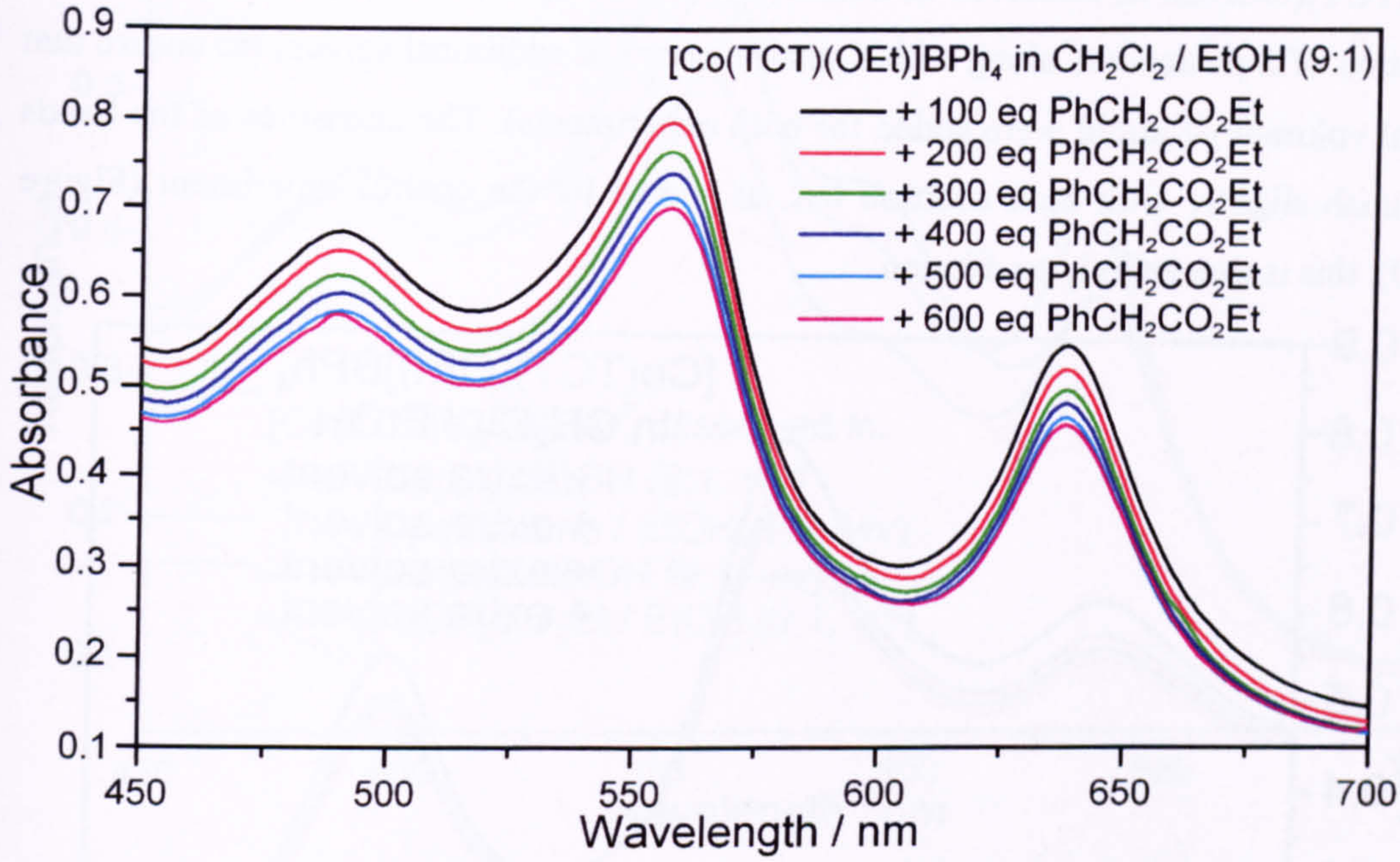

Figure 3.8: Overlaid UV/vis spectra showing the addition of 2-phenylacetic acid ethyl ester to a solution of $[Co(TCT)(OEt)]BPh_4$ in CH_2Cl_2 / EtOH (9:1, *v*/*v*).

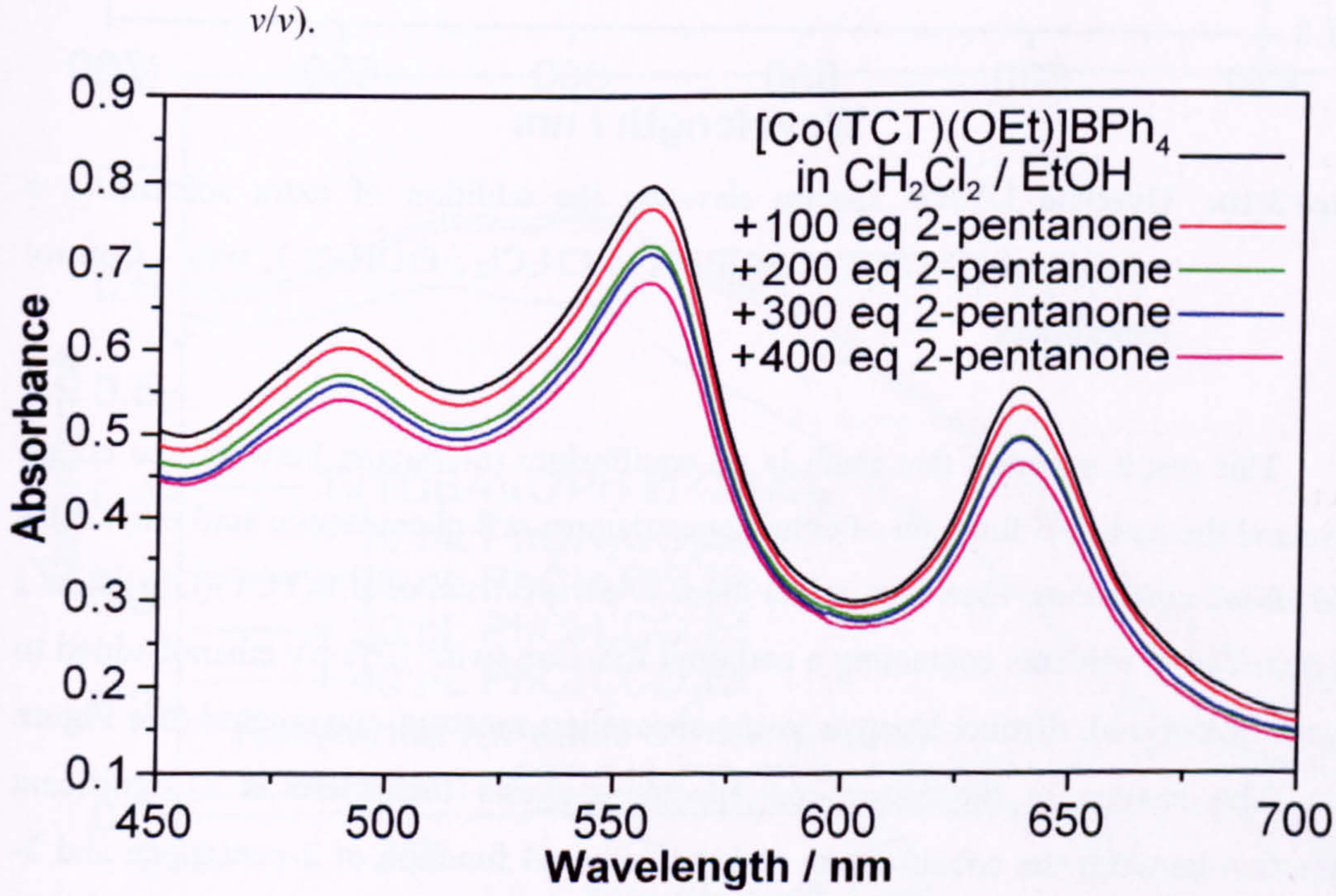

Figure 3.9: Overlaid UV/vis spectra showing the addition of 2-pentanone to a solution of $[Co(TCT)(OEt)]BPh_4$ in CH_2Cl_2 / EtOH (9:1, *v*/*v*).

Figure 3.8 shows the addition of 2-phenylacetic acid ethyl ester to a solution of [Co(TCT)(OEt)]BPh_4 dissolved in CH_2Cl_2 / EtOH (9:1, *v/v*), and Figure 3.9 shows the addition of 2-pentanone, along with a small amount of additional solvent (to ensure that equal volumes of liquid were added for both experiments). The intensities of the bands diminish slightly with each addition but, as shown by the control experiment (Figure 3.10), this is due entirely to dilution.

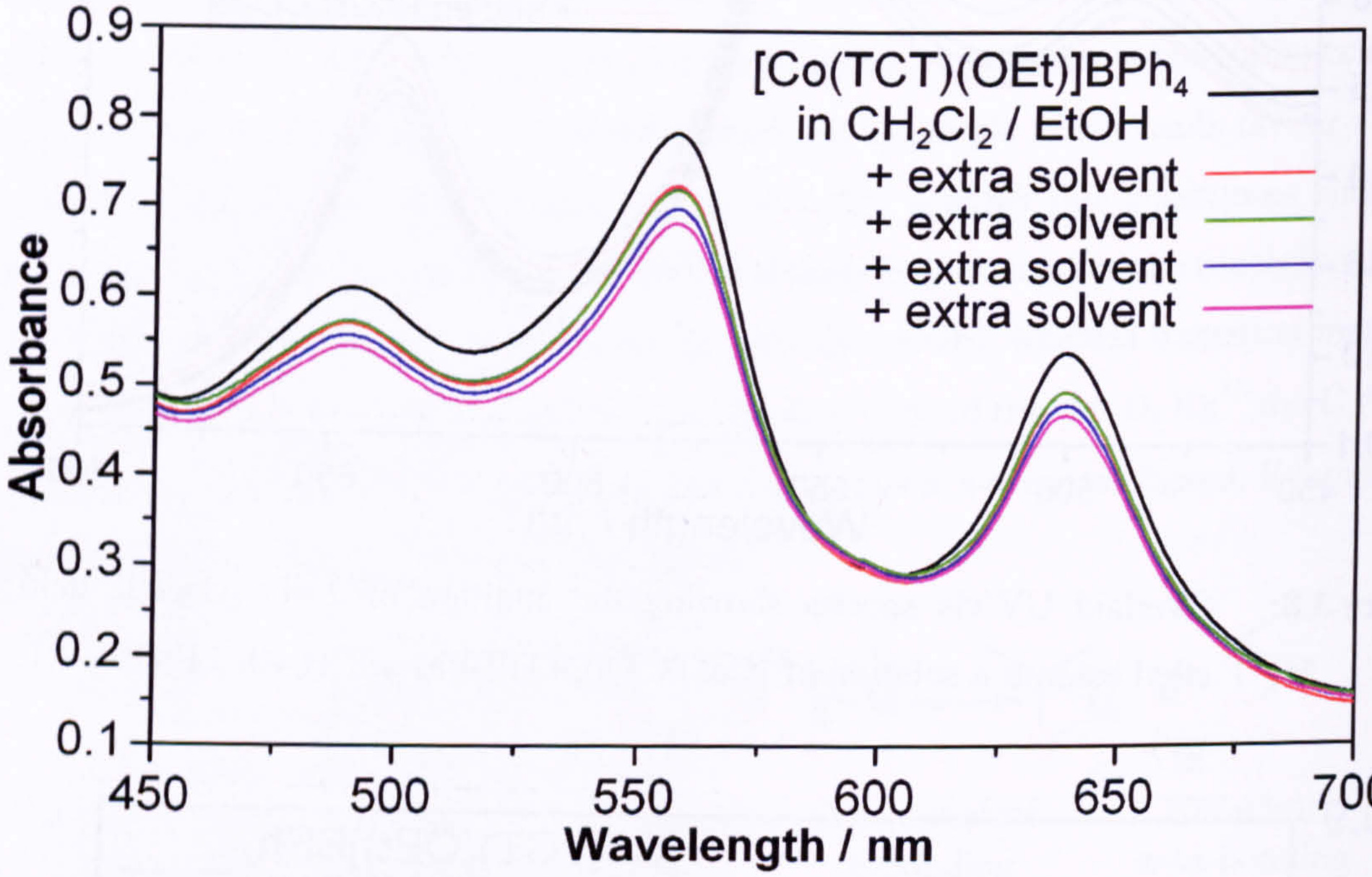

Figure 3.10: Overlaid UV/vis spectra showing the addition of extra solvent to a solution of [Co(TCT)(OEt)]BPh_4 in CH_2Cl_2 / EtOH (9:1, *v/v*) – Control experiment.

This result suggests that there is no equilibrium interaction between the cobalt centre and the carbonyl function of either 2-pentanone or 2-phenylacetic acid ethyl ester *under dilute conditions*. However, when the UV/vis spectrum of [Co(TCT)(OEt)]$BAr^F{}_4$ was recorded in solvents containing a carbonyl function (with 10% *v/v* ethanol added to prevent hydrolysis), distinct changes in the absorption spectrum were noted (see Figure 3.11). The change in the absorption spectra suggests that there is a significant interaction between the cobalt centre and the carbonyl function of 2-pentanone and 2-phenyl acetic acid ethyl ester under these conditions. The spectrum of [Co(TCT)(OEt)]$BAr^F{}_4$ in acetone/ethanol (9:1, *v/v*) and in CH_2Cl_2 / ethanol do not show any significant differences, suggesting no equilibrium interaction between acetone and the cobalt centre. It seems possible that the interaction is strongest when the carbonyl species contains a significant hydrophobic component.

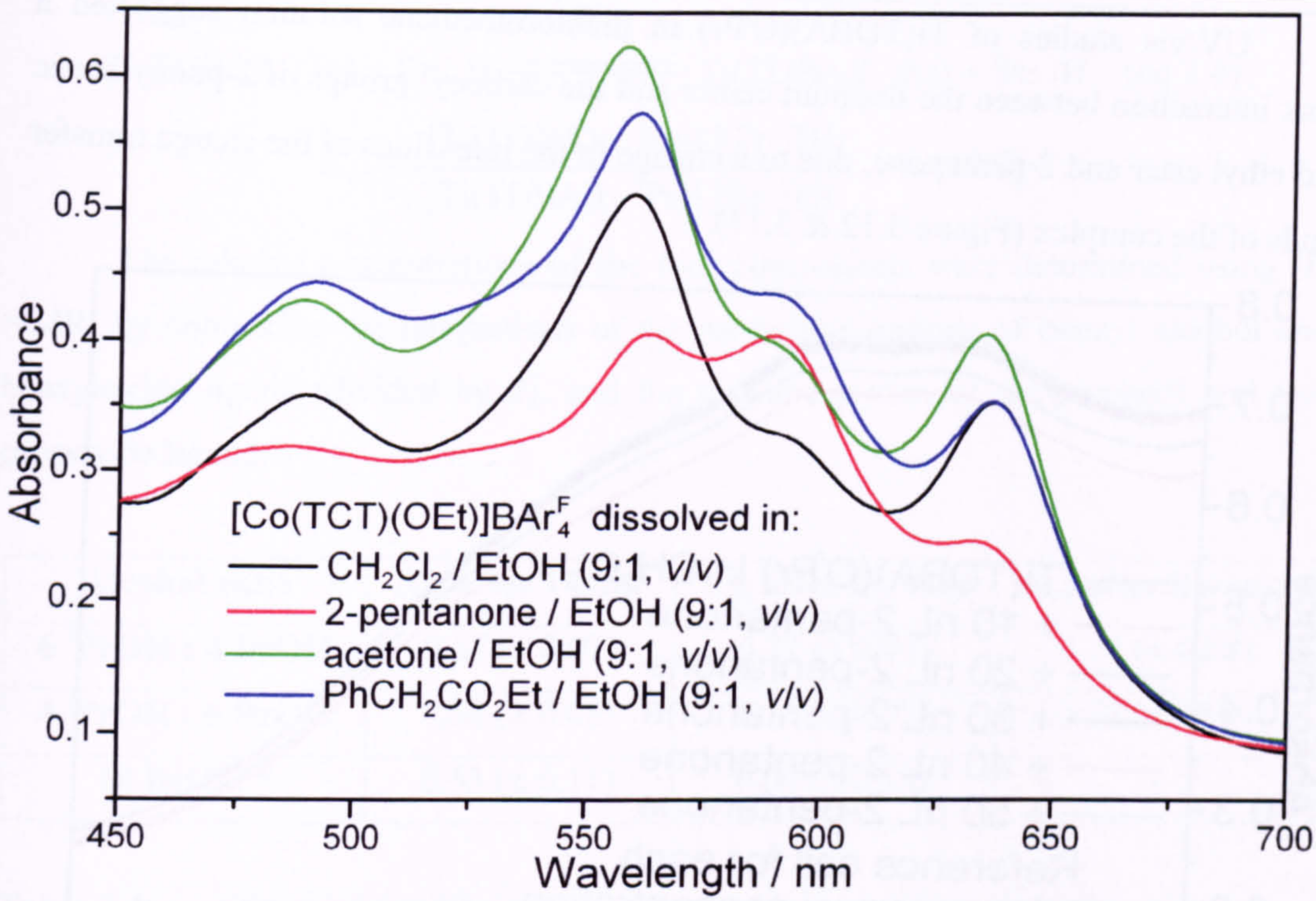

Figure 3.11: Overlaid UV/vis spectra of [Co(TCT)(OEt)]BAr$^F_4$ dissolved in 9:1, *v/v* mixtures of carbonyl species and ethanol.

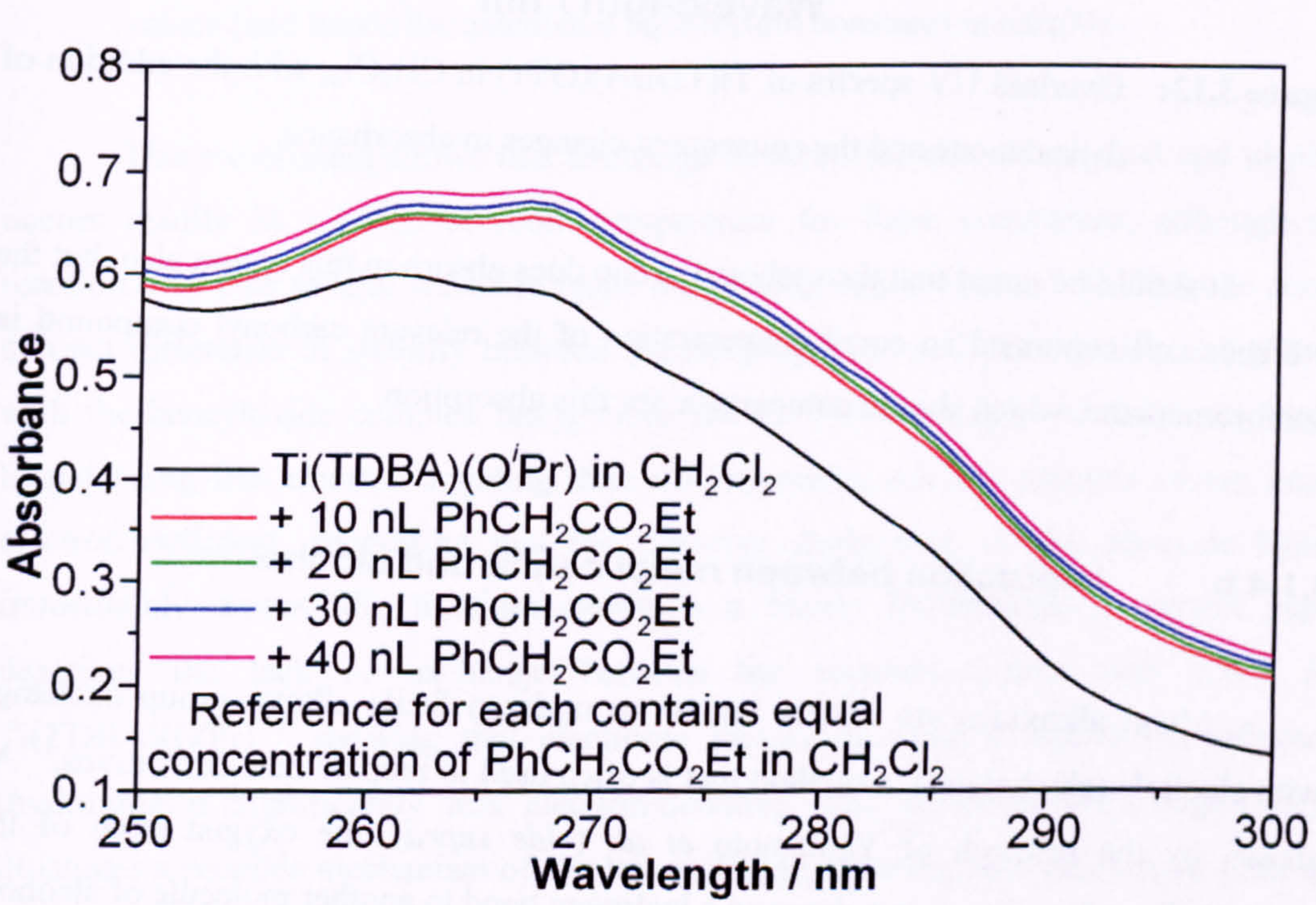

Figure 3.12: Overlaid UV spectra of Ti(TDBA)(O^{i}Pr) in CH_2Cl_2, with the addition of 2-phenylacetic acid ethyl ester and the consequent changes in absorption.

UV/vis studies of Ti(TDBA)(O^{i}Pr) in dichloromethane solution suggested a weak interaction between the titanium centre and the carbonyl groups of 2-phenylacetic acid ethyl ester and 2-pentanone, due to a change in the intensities of the charge transfer bands of the complex (Figure 3.12 & 3.13).

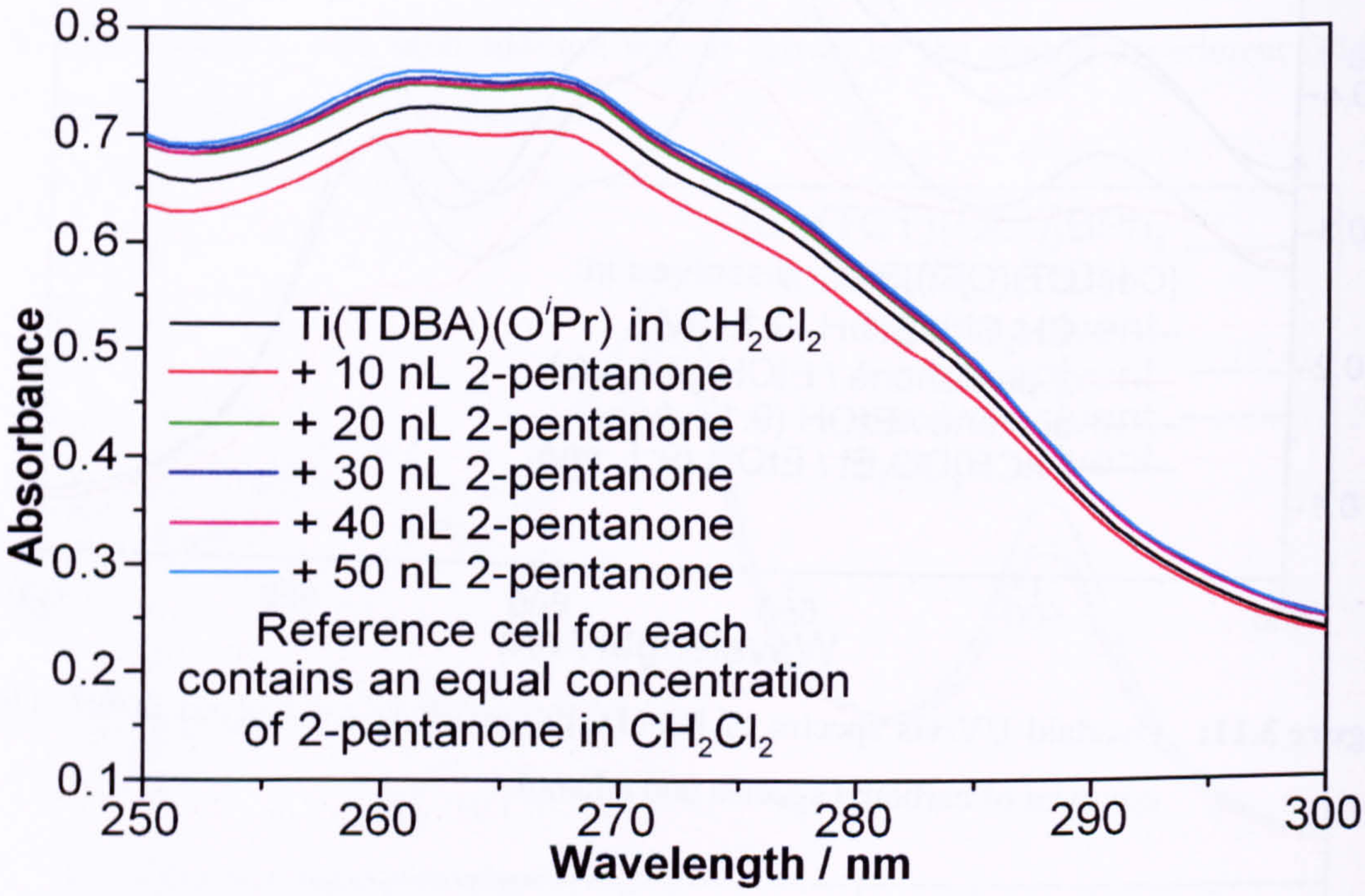

Figure 3.13: Overlaid UV spectra of Ti(TDBA)(O^{i}Pr) in CH_2Cl_2, with the addition of 2-pentanone and the consequent changes in absorbance.

It should be noted that the carbonyl group does absorb in this region also, but the reference cell contained an equal concentration of the relevant carbonyl compound in dichloromethane, which should compensate for this absorption.

3.1.4 b Interaction between metal centre and alcohol

Metal alkoxides are widely known to undergo facile alkoxo group exchange with alcohols (alcoholysis), a method that is often used to prepare new derivatives.[17] As shown by the research of Yamamoto *et al.* (*vide supra*), the oxygen atom of the alkoxide ligand can serve as a donor in a hydrogen bond to another molecule of alcohol.

Dissolving Ti(TDBA)(O^{i}Pr) in d_8-toluene along with a mixture of *iso*-propanol and benzyl alcohol allowed the determination of the equilibrium constant for the exchange reaction between *iso*-propoxide / benzyl acohol and benzyloxide / *iso*-propanol as shown in equations 3.4 & 3.5:

$$\text{Ti(TDBA)(O}^{i}\text{Pr)} + \text{BzOH} \underset{}{\overset{\mathbf{K_{eq}}}{\rightleftharpoons}} \text{Ti(TDBA)(OBz)} + {}^{i}\text{PrOH} \quad \text{(eq 3.4)}$$

$$\mathbf{K_{eq}} = \frac{[\text{Ti(TDBA)(OBz)}].[{}^{i}\text{PrOH}]}{[\text{Ti(TDBA)(O}^{i}\text{Pr)}].[\text{BzOH}]} \quad \text{(eq. 3.5)}$$

The relative concentrations of the four components were determined using ^{1}H NMR, by comparing the integrations of the methylene protons of benzyl alcohol and benzyloxide ligand (divided by 2), and the methine proton of *iso*-propanol and *iso*-propoxide ligand.

Alcohol ratio	K_{eq} after 1 hour	K_{eq} after 2 weeks	K_{eq} after 8 weeks
6 ^{i}PrOH : 4 BzOH	0.67 (± 0.07)	0.72 (± 0.07)	0.75 (± 0.08)
4 ^{i}PrOH : 6 BzOH	0.58 (± 0.06)	0.71 (± 0.07)	0.72 (± 0.07)
10 BzOH *	0.53 (± 0.11)	0.64 (± 0.13)	-

Table 3.4: Observed equilibrium constants for alcohol / alkoxide exchange.

*: At this concentration ratio, the *iso*-propoxide and *iso*-propanol signals become swamped by those of benzyloxide and benzyl alcohol, making the integration values (and hence the calculated equilibrium constant) unreliable.

This experiment shows that exchange between the alkoxide ligand and alcohol occurs readily in solution at room temperature for these complexes, although the reaction may take several weeks to reach a true equilibrium (Table 3.4). There is also a distinct difference in stability between the *iso*-propoxide and benzyloxide complexes, with the benzyloxide complex being more stable. This is in spite of the benzyloxide ligand being less electron-donating than *iso*-propoxide, and the titanium centre being electron deficient, suggesting that the effective steric bulk of the alkoxide ligand immediately around the titanium centre is a factor. Interestingly, a recent paper describes the lack of exchange between the alkoxide ligand and water for Ti(TDBA)(O^{i}Pr),[18] showing that electronic factors do have a significant influence (hydroxide is significantly less electron-donating than *iso*-propoxide). Figure 3.14 illustrates a possible mechanism of alcohol exchange, showing how the H-bond with the incoming alcohol can facilitate the process (see below). Nickel (II) and palladium (II) complexes containing a molecule of alcohol coordinated by H-bonding to an alkoxide ligand have been isolated by Yamamoto *et al.*[19]

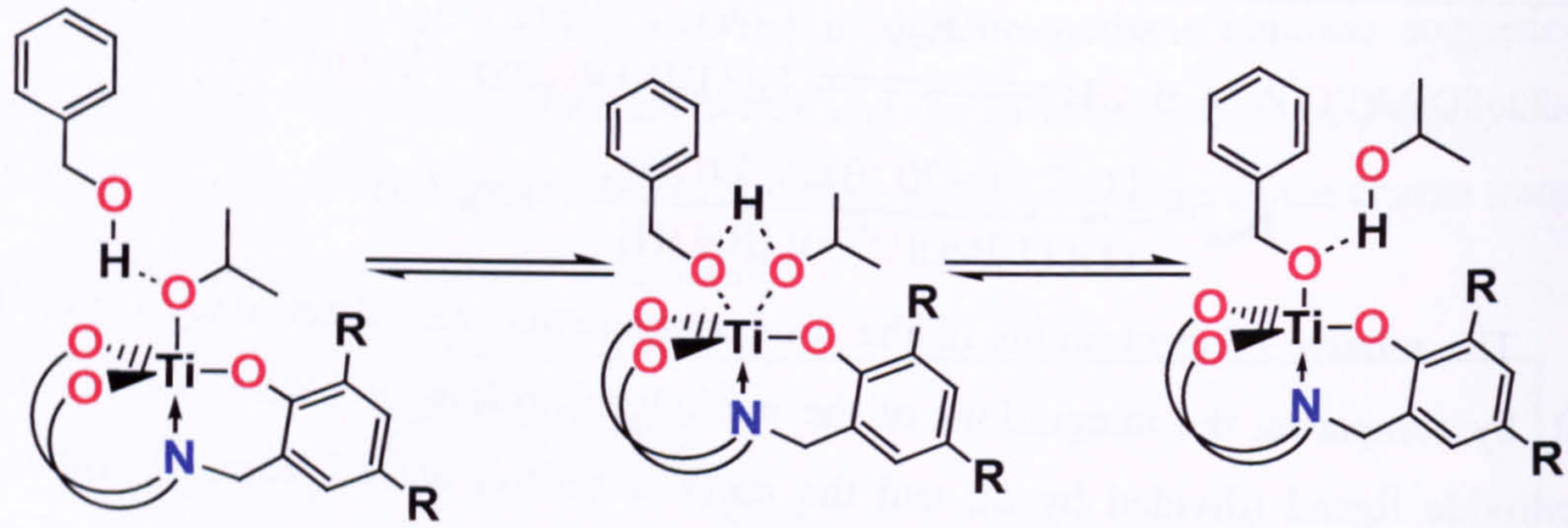

Figure 3.14: Alkoxide / alcohol exchange for Ti complexes (two phenolate "arms" abbreviated for simplicity).

3.1.5 Proposed mechanism

Several groups have proposed possible mechanisms for transesterification reactions. The most plausible mechanism involves reaction between one molecule of ester and one molecule of alcohol, taking place within the coordination sphere of the metal. Both species interact with the metal alkoxide in such a way as to activate them towards reaction. Coordination of the ester through the oxygen atom of the carbonyl function (the ester acting as a σ-donor ligand) results in electron density being drawn away from the acyl carbon atom. This interaction activates the acyl carbon atom towards nucleophilic attack by the alcohol. Note that, in the case of cobalt complexes, the carbonyl group could donate electron density through a π-interaction, although the end result would be the same, namely an activation of the acyl carbon atom towards nucleophilic attack. The complete range of possible interactions between a metal centre and a carbonyl function is summarised in Figure 3.7 (*vide supra*).

The hydrogen bonding between the alcohol and the alkoxide facilitates the nucleophilic attack by the alcohol, because the alkoxide can readily accept the proton, thus being converted to the corresponding alcohol (Figure 3.15).

Coordination to metal centre pulls electron density away from carbon atom, thus activating it towards attack

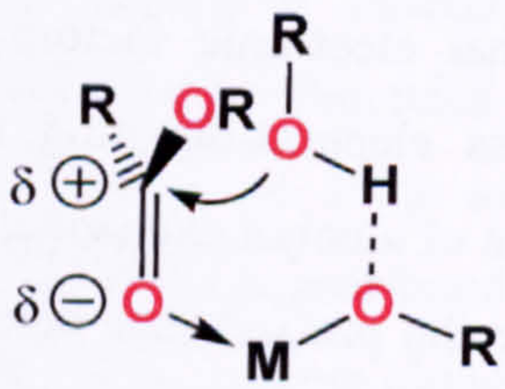

Hydrogen-bond to alkoxide increases nucleophilicity of alcohol

Figure 3.15: Proposed intermediate for transesterification reaction as catalysed by metal alkoxide complexes.

The nucleophilic attack yields a transient alkoxide ligand, where the carbon atom (originally of the carbonyl function) is now tetrahedral, with two alkoxy groups and one alkyl group attached. A complete catalytic cycle for transesterification is shown in Figure 3.16.

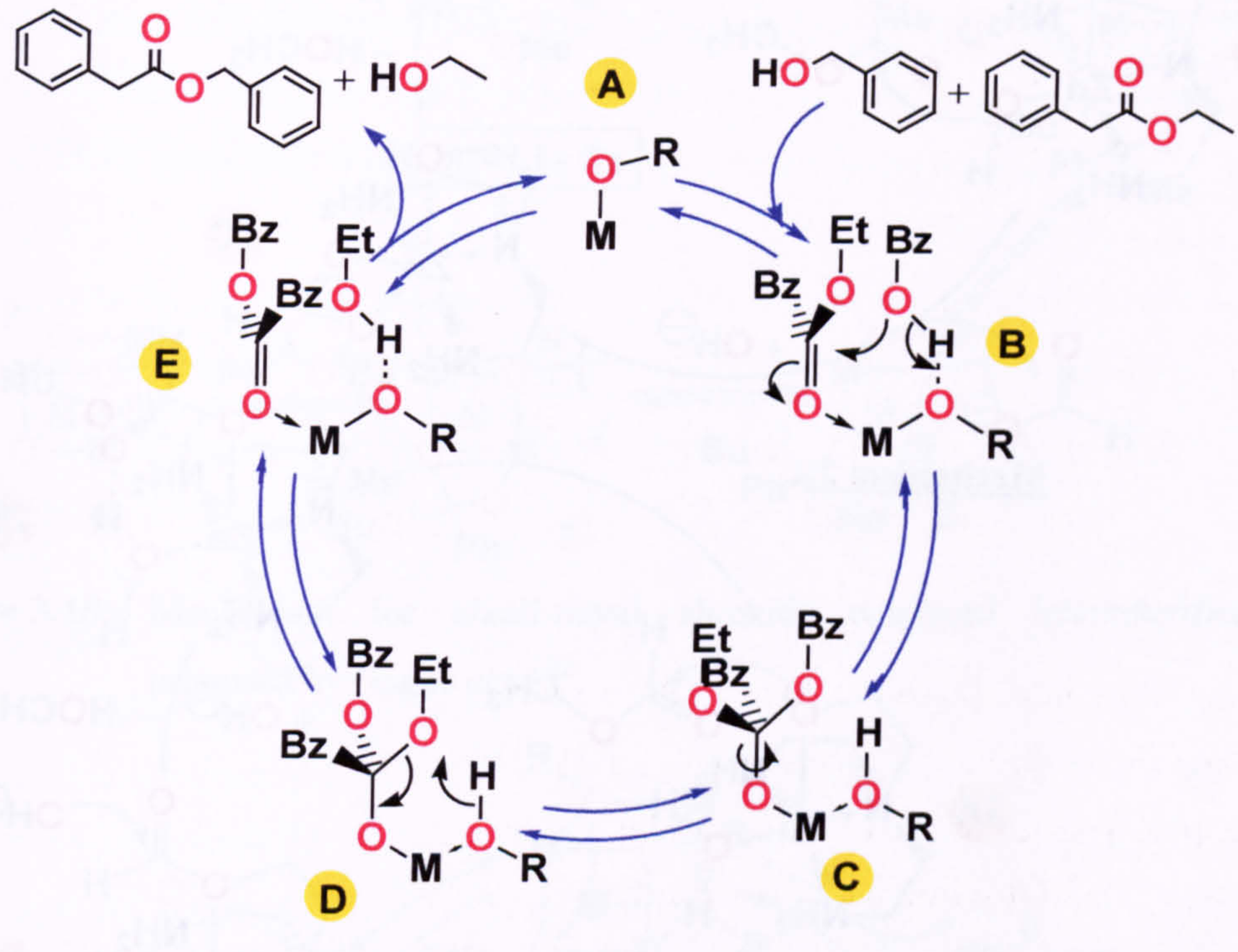

Figure 3.16: Proposed catalytic cycle for transesterification reaction as catalysed by metal alkoxide complexes.

Proton transfer from the coordinated alcohol to one of the alkoxy groups regenerates the original alkoxide ligand along with ester and alcohol; note that the intermediate can react to reform the original complex, resulting in no overall reaction. Hydrogen-bonded solvent chains have been observed within the hydrophobic cavity of a ligand similar to TCT, although the complex did not include an alkoxide ligand.[20]

The transesterification reaction is likely to compete with alkoxide / alcohol exchange when alcohol is present in excess, as this process is known to occur readily in solution for the titanium alkoxide species even at room temperature.

Recent work on zinc complexes containing polydentate amine-alcohol / alkoxide ligands has shown that such complexes can catalyse the hydrolysis of carboxylic esters.[21] Two possible mechanisms were proposed, which are summarised in Figure 3.17.

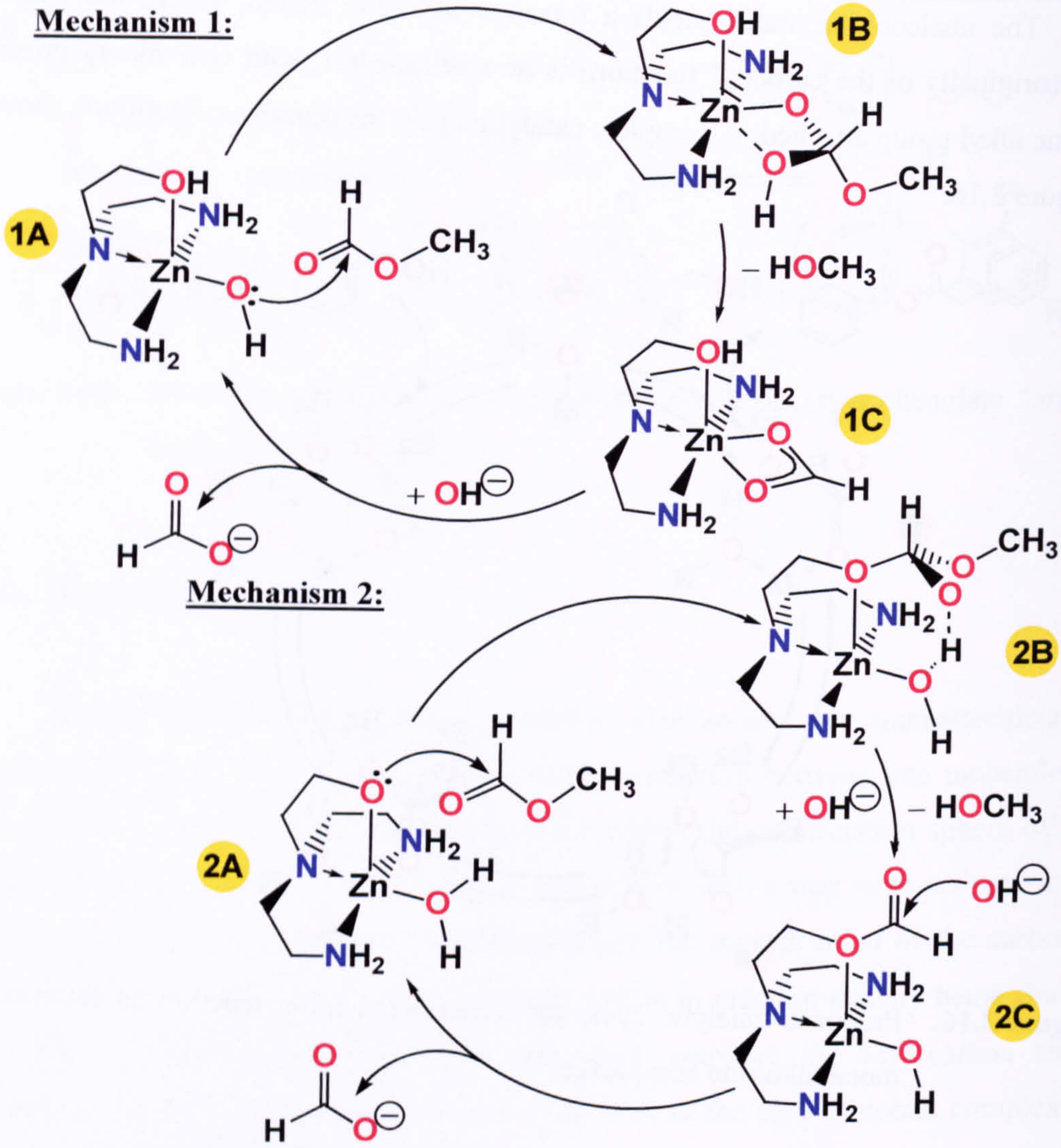

Figure 3.17: Possible mechanisms proposed for ester hydrolysis by Zn complex. Attack by hydroxide (Mechanism 1) and by alkoxide (Mechanism 2)

3.2 Interesterification

Several reports of direct interesterification (equation 3.6) catalysed by metal alkoxide species have appeared in the literature.

$$R^1CO_2R' + R^2CO_2R'' \rightleftharpoons R^1CO_2R'' + R^2CO_2R' \quad \text{(eq. 3.6)}$$

Gagné *et al.* reported extremely high turnover frequencies for alkali metal alkoxides, particularly Ru and Cs, which were believed to exhibit activity as tetramers and / or hexamers.[22] They proposed a mechanism based on the tetrameric form, with the ester initially coordinating through a σ-interaction (Figure 3.18).

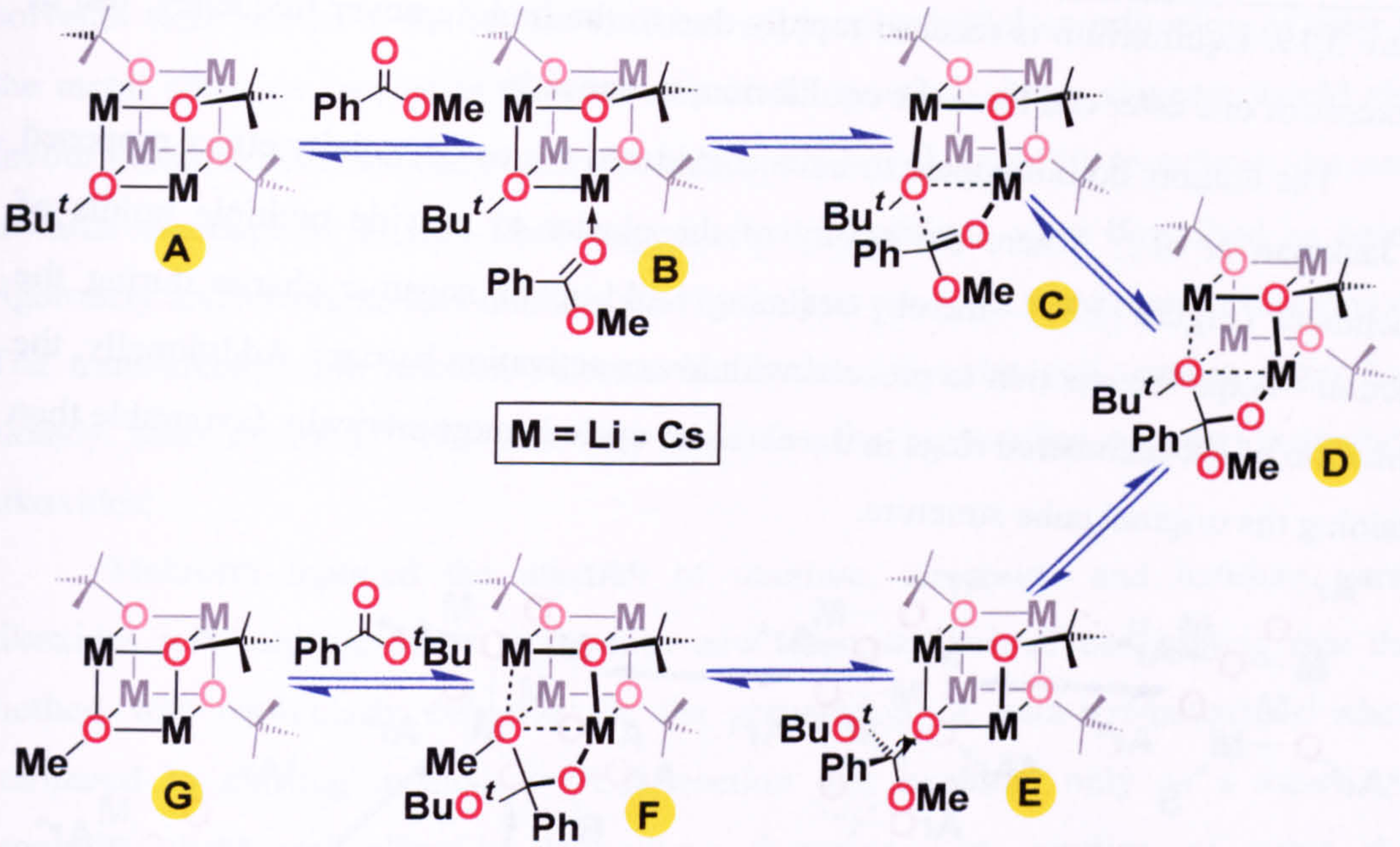

Figure 3.18: Mechanism for alkali-metal alkoxide catalysed interesterification, proposed by Gagné *et al.*[22]

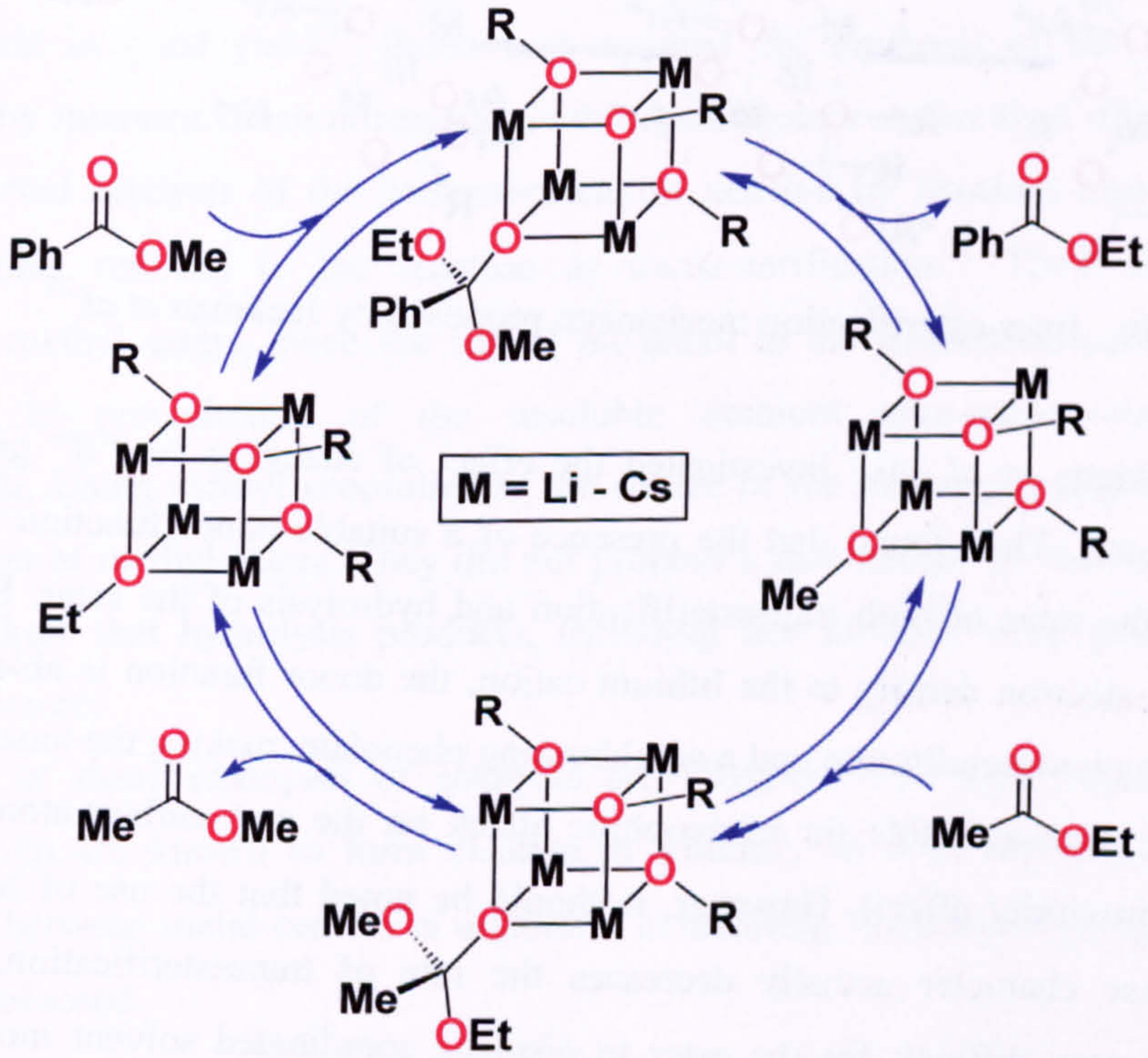

Figure 3.19: Catalytic cycle for interesterification, intermediates not shown.[22]

The acyl carbon atom then undergoes nucleophilic attack from the alkoxide ligand, and temporarily assumes a tetrahedral geometry; the intermediate then decays to release either the product ester or the starting ester. The full catalytic cycle is shown in

Figure 3.19. Equilibrium is reached rapidly due to the high turnover frequency; use of an excess of one ester can force the equilibrium to one side.

The authors do not appear to have considered the co-operativity effect proposed by Jackman *et al.*,[23] where the ability of the cluster to provide multiple points of attachment (Figure 3.20)—thereby reducing build-up of negative charge during the reaction—helps the reaction to proceed with lower activation barriers. Additionally, the formation of six-membered rings in the catalytic cycle is more sterically favourable than retaining the original cube structure.

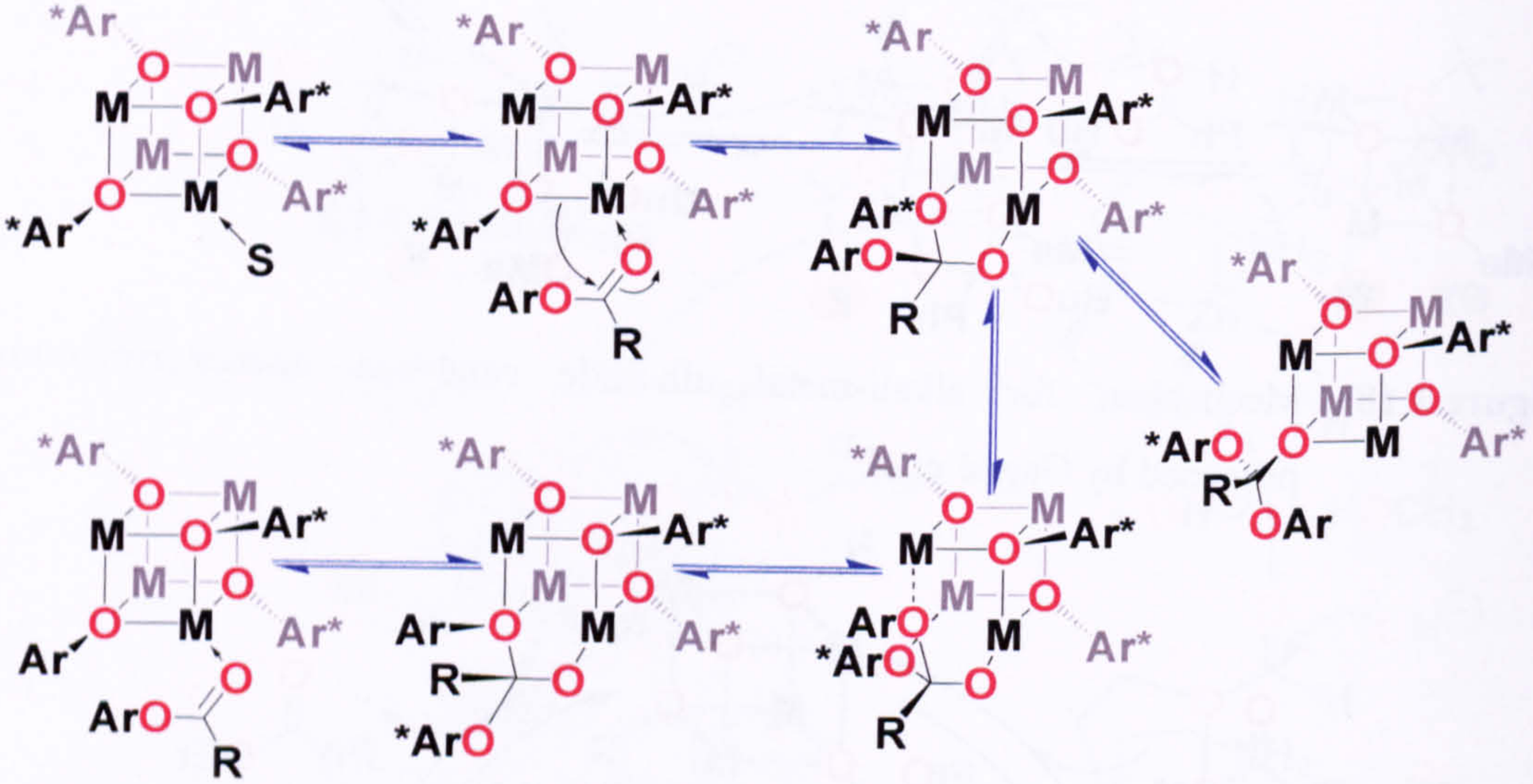

Figure 3.20: Inter-esterification mechanism proposed by Jackman *et al.*[23]

Jackman *et al.* also investigated the effect of changing the "R" group of the substrate ester. They found that the presence of a suitable donor function in the ester increases the rates of both transesterification and hydrolysis of the ester. By donating additional electron density to the lithium cation, the donor function is able to weaken the bonding between lithium and a neighbouring phenolate, making the lone pairs of the phenolate more available for nucleophilic attack on the acyl carbon atom (complex-induced proximity effect). However, it should be noted that the use of solvents with Lewis base character actually decreases the rate of transesterification, because it becomes more difficult for the ester to displace coordinated solvent molecules. The authors used anhydrous conditions to avoid hydrolysis of the catalysts.

Okano *et al.* reported the catalytic activity of lanthanide tri-alkoxide species for the interesterification reaction.[24] Although the authors did not propose a mechanism for the reaction, it is well known that lanthanoid alkoxides form aggregates,[25] and the authors proposed that aggregates might play a role in the reaction. Polar (donor)

solvents were shown to inhibit the reaction, supporting initial coordination of ester to the metal alkoxide species as the first step in the reaction; donor solvents would also favour monomeric behaviour of the alkoxides, reducing their ability to activate the ester towards nucleophilic attack. Their experimental conditions were described as being rigorously anhydrous, so it is unlikely that hydrolysis products were present in solution. The trans-alkoxylation reaction between lanthanide alkoxides and organic esters had already been reported,[26] but was only used for the preparation of new lanthanide alkoxides.

Mehrotra reported the reaction of titanium, zirconium and hafnium tetra-alkoxides with organic esters to produce new alkoxide derivatives,[27] noting that the method was particularly effective for the preparation of tetra-*tert*-butoxides when compared to existing methods.[28] This reaction was explored only as a means of preparing the metal alkoxide derivatives; there was no mention of using the interesterification reaction for organic synthesis. Mehrotra also reported an analogous reaction between aluminium alkoxides and *tert*-butyl-esters to produce the aluminium *tert*-butoxide in good yield.[29] Baker had reported the synthesis of new aluminium alkoxides by interesterification reaction with organic esters earlier than this.[30] Seebach *et al.* reported catalysis of the interesterification reaction by titanium tetra-alkoxides, although they referred to the reaction as transesterification.[31] Their aim was to synthesise methyl esters, since the use of methanol in the transesterification reaction gave rise to precipitation of the insoluble titanium tetra-methoxide tetramer, $[Ti(OMe)_4]_4$. Using methyl propiolate as the source of the methoxy group allowed for the synthesis of methyl esters. They did not propose a mechanism for the reaction, and it seems likely that hydrolysis products, including free alcohol, were present in the reaction mixture.

All of these examples of catalysts are alkoxides of "hard", electropositive metals, which are known to form clusters in solution, so it is very likely that co-operativity between metal centres is important in allowing the direct interesterification reaction to proceed.

3.2.1 Standard test reaction for interesterification

The chosen test reaction was the interesterification of 2-phenyl acetic acid ethyl ester and benzyl acetate, to produce an equilibrium with ethyl acetate and 2-phenylacetic acid benzyl ester (Figure 3.21).

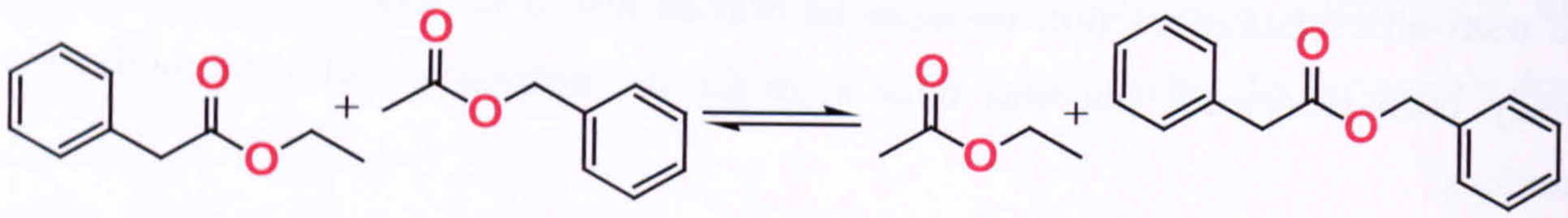

Figure 3.21: Test reaction for interesterification.

After initial experiments to establish the activity of catalysts, kinetic experiments were performed to evaluate the reaction rate. Due to the high activity of the titanium tetra-alkoxides, samples were withdrawn at 30 s intervals and quenched by addition to a solution of dilute hydrochloric acid, to allow the reaction to be monitored accurately. ^{1}H NMR spectroscopy was used to evaluate the conversion, using distinctive peaks for each species, as shown in Figure 3.22.

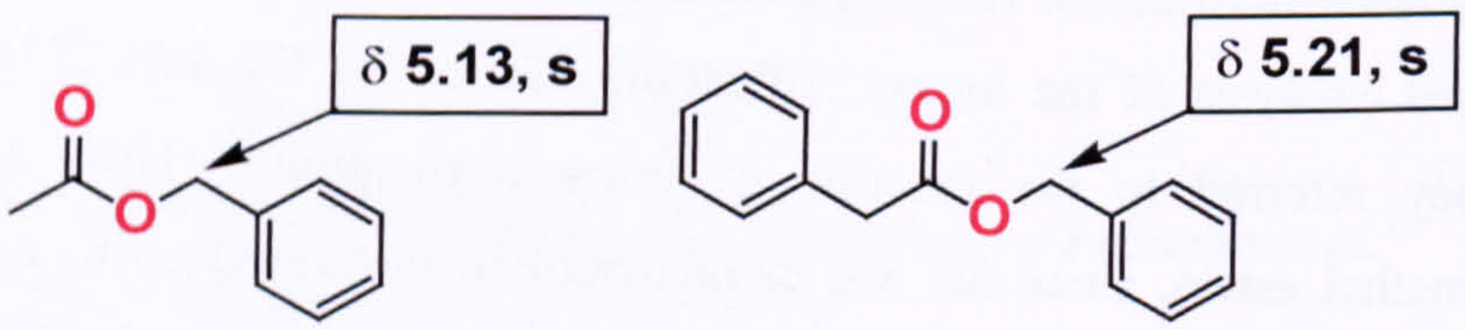

Figure 3.22: Proton signals used for monitoring interesterification reaction.

Table 3.5 summarises the catalytic activity (or lack thereof) for the titanium tetra-alkoxides and three of the coordination catalysts.

Catalyst species	Conditions	Activity / T.O. h^{-1}
$Ti(O^{n}Bu)_4$	373 K, 'wet'	137 (± 9)
$Ti(O^{n}Bu)_4$	383 K, 'wet'	338 (± 20)
$Ti(O^{i}Pr)_4$	353 K, dry	49 (± 5)
$Ti(TDMA)(O^{i}Pr)$	353 K, dry	None
$Ti(TDBA)(O^{i}Pr)$	353 & 373 K, dry	None
$[Co(TCT)(OPh)]BPh_4$	353 K, dry	None

Table 3.5: Catalytic activities for interesterification.

Titanium tetra-*n*-butoxide catalysed this reaction, although significant quantities of free alcohol were certainly present in the reaction due to hydrolysis of the titanate, since the initial experiments were performed using un-dried reagents; a high ratio of titanate : ester was required for the reaction to proceed. An experiment using dried esters and $Ti(O^iPr)_4$ in a glove-box under argon gave a catalytic activity that was lower—although the temperature was lower also—in spite of the dried conditions. This gives further support to the proposal that clusters are involved in the catalytic reaction, since the *iso*-propoxide ligand imposes more steric bulk around the titanium centre, inhibiting cluster formation. If the amount of hydrolysis for $Ti(O^nBu)_4$ could be accounted for, the true activity value for the actual catalytic species would be far higher than that reported above.

None of the catalysts prepared in the laboratory catalysed this reaction without the addition of free alcohol. Attempting the reaction for $[Co(TCT)(OPh)]BPh_4$ with the addition of increasing amounts of alcohol showed a steady increase in the rate of reaction with mol% of added alcohol – there is an approximately linear relationship (Table 3.6, Figure 3.23).

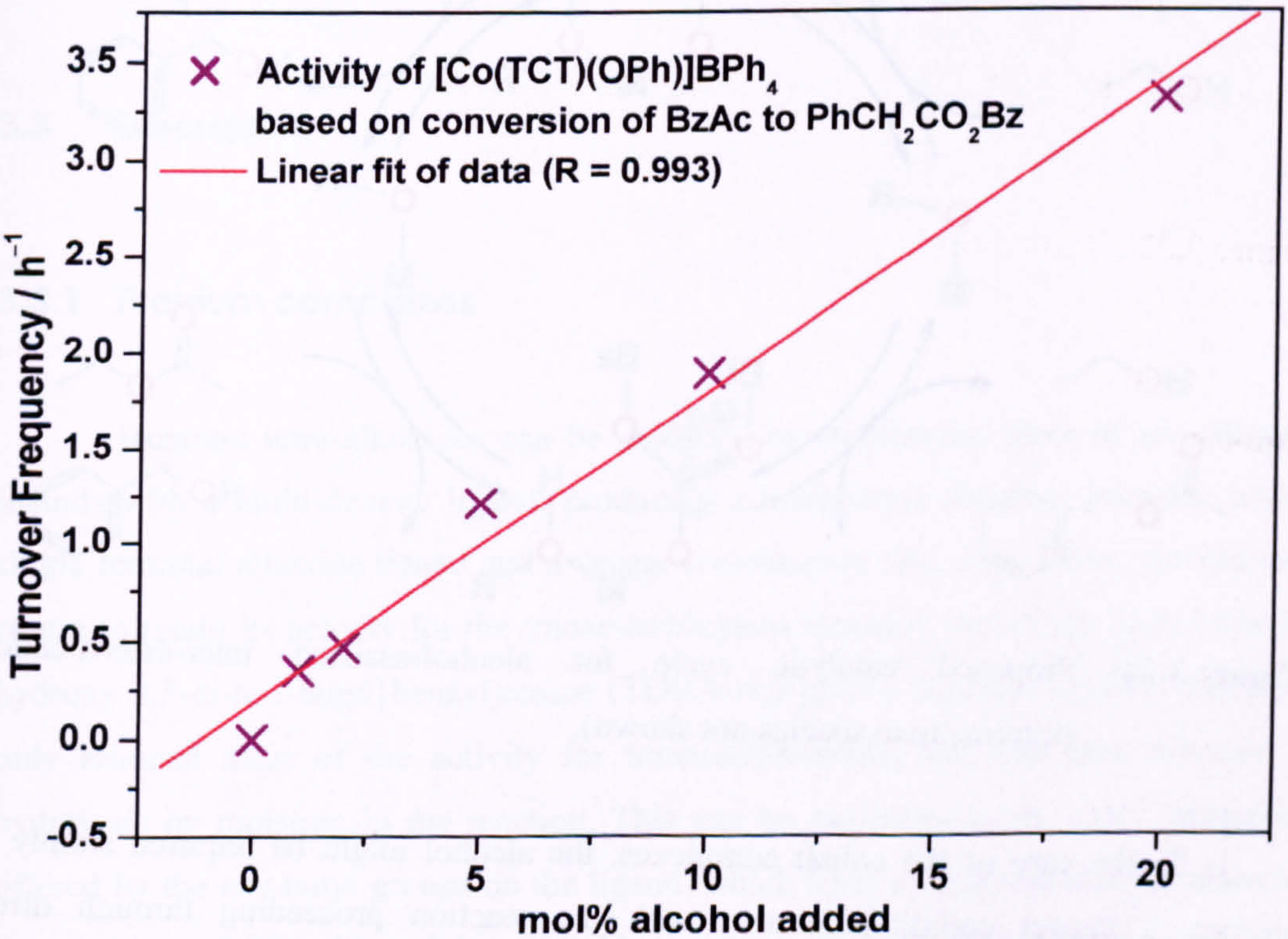

Figure 3.23: Effect of alcohol addition to interesterification reaction.

Catalyst	mol% alcohol added	Activity (T. O. h^{-1})
$[Co(TCT)(OPh)]BPh_4$	0	0
$[Co(TCT)(OPh)]BPh_4$	1	0.35 (± 0.03)*
$[Co(TCT)(OPh)]BPh_4$	2	0.47 (± 0.05)*
$[Co(TCT)(OPh)]BPh_4$	5	1.21 (± 0.12)*
$[Co(TCT)(OPh)]BPh_4$	10	1.89 (± 0.10)
$[Co(TCT)(OPh)]BPh_4$	20	3.3 (± 0.17)

Table 3.6: Effect of addition of alcohol to interesterification reaction.
*: Values are approximate due to extremely low conversion.

This suggests that interesterification, as catalysed by these coordination compounds, proceeds through two successive transesterification reactions, as shown in Figure 3.24.

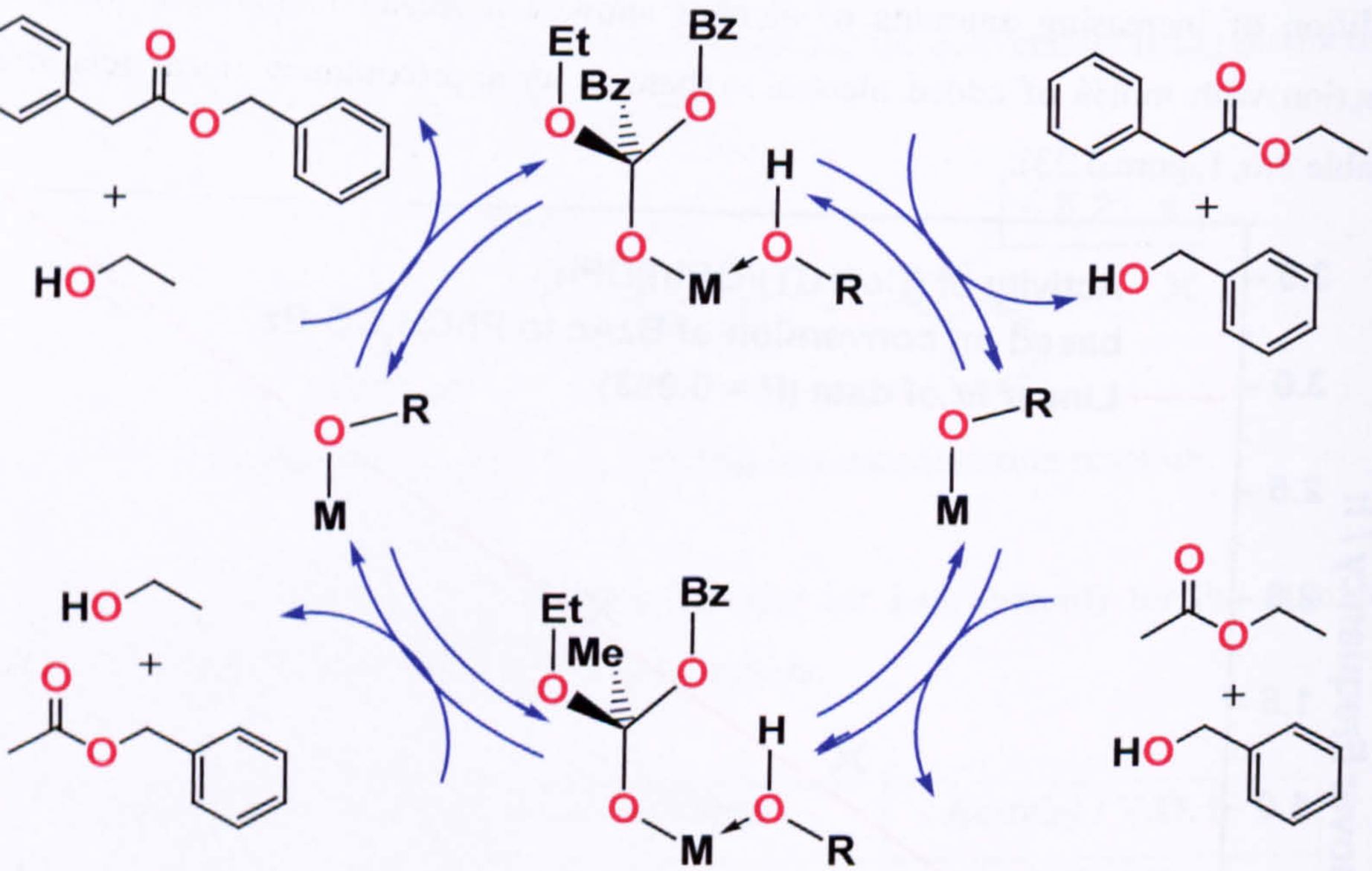

Figure 3.24: Proposed catalytic cycle for alcohol-assisted inter-esterification (intermediate species not shown).

In the case of the cobalt complexes, the alcohol might be required simply to occupy a vacant coordination site, with the reaction proceeding through direct nucleophilic attack at the acyl carbon atom by the alkoxide ligand. If this were true, then simply adding a donor solvent to the reaction might allow the direct interesterification to proceed without the need for free alcohol. However, adding

acetonitrile to the reaction mixture did not allow the catalysis of interesterification, in fact the catalyst decomposed under these conditions, despite the use of rigorously dried reagents. This result gives further support to the proposal that the complexes catalyse the transesterification reaction by a concerted reaction with ester and alcohol.

3.2.2 Additional reactions

In addition to the standard test reaction, the interesterification of ethyl benzoate and 2-phenylacetic acid ethyl ester was attempted (eq. 3.7), in order to expand the range of esters tested.

$$PhCH_2CO_2Et + PhCO_2Bz \rightleftharpoons PhCH_2CO_2Bz + PhCO_2Et \quad \text{(eq. 3.7)}$$

A range of the metal complexes were tested for this reaction: $[Co(TCT)(OEt)]BPh_4$; $[Co(TCT)(OPh)]BPh_4$; $[Zn(TCT)(OPh)]BPh_4$; and $Ti(TDMA)(O^iPr)$. However, none of these complexes showed any activity for this reaction. Initial experiments with phenyl esters were discontinued because the high stability of titanium phenolate compounds inhibited the reaction.

3.3 Discussion

3.3.1 Titanium complexes

Titanium tetra-alkoxides can be modified by exchanging three of the alkoxide ligands with a multi-dentate ligand, producing a monomeric titanium complex with a single terminal alkoxide ligand and a vacant coordination site. This allows the titanium centre to retain its activity for the transesterification reaction; use of the ligand *tris*({2-hydroxy-3,5-di-*tert*-butyl}benzyl)amine (TDBA-H_3) gave a titanium species which not only retained most of the activity for transesterification, but was also resistant to hydrolysis by moisture in the reaction. This can be attributed to the steric protection offered by the *tert*-butyl groups on the ligand, which form a cavity around the alkoxide ligand (Figure 3.25); although it is possible to form both the hydroxide complex and the μ-oxo dimer,[32] their formation is disfavoured because of the extreme steric crowding. For most other titanium alkoxide species, the hydrolysis reactions are energetically and

kinetically favourable. Complexes that are moisture resistant allow for a lower catalyst loading and the use of undried reagents.

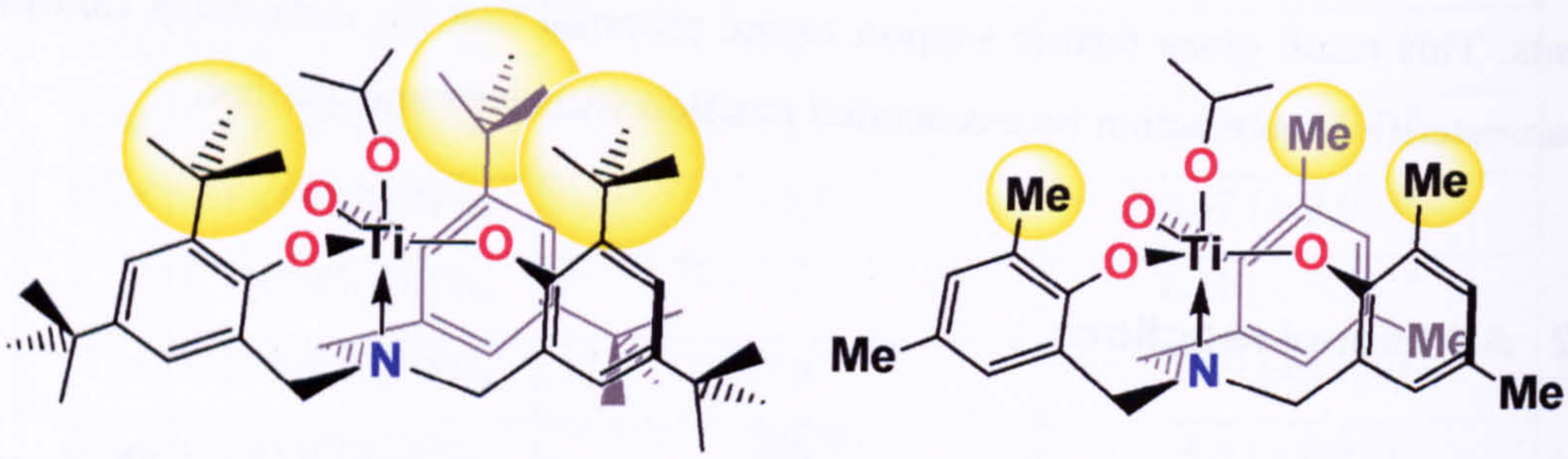

Figure 3.25: Hydrophobic cavities provided by Ti(TDMA)(O^{i}Pr) & Ti(TDBA)(O^{i}Pr).

Despite the increased steric shielding around the titanium centre in Ti(TDBA)(O^{i}Pr) [relative to Ti(TDMA)(O^{i}Pr) and Ti(TPA)(O^{i}Pr)], this is actually the most active catalyst for transesterification under the conditions used. It also shows increased turnover frequency at lower concentrations (although these experiments were not repeated for the other two catalysts). None of the complexes appeared to be insoluble in the reaction medium (no suspended material was observed in any of the reaction vessels), so this result suggests that the complexes form aggregates at higher concentrations. The substrates used all contain hydrophobic groups, with the result that the alkoxide moiety of the catalysts would be relatively unstable in the reaction medium; aggregation would be favoured in order to stabilise the catalysts. This would explain why the more sterically encumbered species, Ti(TDBA)(O^{i}Pr), is the most active catalyst – it would favour the non-aggregated, active form because the *tert*-butyl substituents provide an organic mask (Scheme 3.1).

$$\underset{\text{Active}}{\text{Ti(TDBA)(O}^i\text{Pr)}} \rightleftharpoons \underset{\text{Inactive}}{[\text{Ti(TDBA)(O}^i\text{Pr)}]_2}$$

$$\text{Ti(TDMA)(O}^i\text{Pr)} \rightleftharpoons [\text{Ti(TDMA)(O}^i\text{Pr)}]_2$$

Scheme 3.1: Suggested aggregation behaviour for titanium species.

None of the titanium complexes are active for the direct interesterification reaction; this suggests that poly-nuclear species are responsible for the interesterification catalysis by titanium tetra-alkoxides (Section 5.5).

There is a notable difference in activity between the titanium complexes. Initially, it was expected that the less sterically hindered complexes would give higher activity, but experiments showed that Ti(TDBA)(O^{i}Pr) was the more effective catalyst under the conditions used. The activities of Ti(TPA)(O^{i}Pr) and Ti(TDMA)(O^{i}Pr) may

be inhibited by the formation of dimeric species in solution, or hydrolysis by trace amounts of water in the reagents; Ti(TDBA)(O^{i}Pr) is catalytically robust under ambient atmosphere. To ensure that no dimerisation had occurred prior to the experiment, the samples of Ti(TPA)(O^{i}Pr) and Ti(TDMA)(O^{i}Pr) used for catalysis were analysed by ^{1}H NMR spectroscopy. The samples of the catalysts were both found to be in the active monomeric form. An experiment investigating the effect of catalyst concentration on turnover frequency suggests that Ti(TDBA)(O^{i}Pr) becomes far more active (55 T.O. h^{-1} at 353 K) at lower concentrations, supporting the possibility that catalyst aggregation is taking place at higher concentrations. Another possibility is that the hydrophobic pocket created by the *tert*-butyl groups helps to enhance the reactivity by providing hydrophobic interactions with the substrates (the cobalt and zinc complexes both have a hydrophobic pocket, provided by the cinnamyl arms of the TCT ligand).

3.3.2 Cobalt complexes

Complexes of the type [Co(TCT)(OR)]BAr$_4$ (where R = Ph, Et, Bz, and Ar = Ph or 3,5-(CF$_3$)$_2$-C$_6$H$_2$) are suitable catalyst precursors for the transesterification reaction. The ethoxide and phenoxide complexes show almost identical activities (47 and 45 turnovers per hour at 373 K, respectively, where Ar = Ph), suggesting that both compounds are converted into the same species in the reaction medium by alkoxide / alcohol exchange; successful synthesis of the benzyloxide complex proves that this species is stable both in solution and the solid state. The complexes are both stable to air in the solid state—at room temperature—and the phenoxide complex is also stable in solution, although both complexes decompose at elevated temperatures unless rigorously dried solvents and inert atmospheres are used.

Substituting the tetraphenyl-borate counter-ion for the fluorinated analogue, BAr$^F{}_4^-$, afforded a more active catalyst (65 T.O. h^{-1} for [Co(TCT)(OPh)]BAr$^F{}_4$), which is attributed to the reduced association between the cation and anion, allowing more rapid diffusion of the reactants to, and products from, the catalytic centre. The rate enhancement (approximately 50%) is highly significant, suggesting that the cationic nature of these complexes is a factor in their high activity relative to the neutral titanium complexes. The catalytic activity of the best catalyst is approximately ⅔ that of the distannoxane catalysts reported by Otera *et al.* (~ 100 T.O. h^{-1}).[33] The phenyl rings draw electron density away from the boron centre and also provide steric bulk, whilst

the trifluoromethyl groups act to pull the electron density further away from the centre by means of their inductive effect. Combining these two effects results in an anion where the negative charge is delocalised throughout the entire molecule, thus there is less electrostatic attraction between the cation and any particular atom(s) of the anion, so the anion should be less associated with the cation in solution. As a result, there is less resistance to substrate molecules diffusing to and from the cavity around the catalyst centre, increasing catalytic activity. The $BAr^F{}_4^-$ counter-ion also has the effect of making the complex more soluble in non-polar solvents, and has proved to be extremely useful in other areas of research for the use of highly electrophilic species without hindrance by anion association.[34]

None of the cobalt complexes show any activity for the *direct* interesterification reaction between two esters. However, adding a small amount of alcohol to the reaction mixture allows for an overall interesterification reaction to proceed slowly. This reaction shows an approximately linear dependence between rate and the alcohol concentration, supporting the assumption that interesterification occurs *via* two successive transesterification reactions (Scheme 3.2).

$$\begin{array}{lcl} PhCH_2CO_2Et + BzOH & \rightleftharpoons & PhCH_2CO_2Bz + EtOH \\ AcOBz + EtOH & \rightleftharpoons & AcOEt + BzOH \\ \hline PhCH_2CO_2Et + AcOBz & \rightleftharpoons & PhCH_2CO_2Bz + AcOEt \end{array}$$

Scheme 3.2: Overall interesterification via two successive transesterification reactions.

These complexes do have significant drawbacks in terms of potential industrial applications. Their instability towards high temperature, except under rigorously dry conditions and inert atmospheres, coupled with the expense and synthetic challenge of making the TCT ligand, would limit the catalysts to high value applications. Secondly, cobalt is toxic, which makes the catalysts unsuitable for use in food applications. Successful use as an industrial catalyst would require the use of a polymer-supported version (Section 5.2.2 a), and cobalt leaching would have to be considered.

3.3.3 Zinc complexes

Complexes of the type $[Zn(TCT)(OPh)]BAr_4$ (Ar = Ph, 3,5-$(CF_3)_2$-C_6H_3) were made in an attempt to give catalysts with improved activity relative to the analogous

cobalt complexes. This plan was based on the increased Lewis acidity of zinc (II) relative to cobalt (II), and the observation that, for the free ions in solution, Zn^{II} has a higher transesterification activity than Co^{II}. A number of Zn^{II} complexes incorporating the TCT ligand have already been produced, and Walton *et al.* recently reported a zinc methoxide complex using a related ligand system.[35]

The complexes $[Zn(TCT)(OPh)]BPh_4$ and $[Zn(TCT)(OPh)]BAr^F{}_4$ have been successfully prepared and characterised. Attempts to synthesise the ethoxide derivatives have all been unsuccessful, giving low yields of an unidentifiable product. A possible explanation for the failure of this synthesis is that the zinc ethoxide complex is unstable due to β-hydride abstraction (Figure 3.26),[36] which is perhaps not surprising in view of the mode of action of liver alcohol dehydrogenase. If this is the case, then synthesis of a zinc alkoxide complex without β-hydrogen atoms (such as *tert*-butoxide) might be more successful. $[Zn(TCT)(OPh)]BPh_4$ gave lower activity for the trans-esterification reaction than $[Co(TCT)(OPh)]BPh_4$; it was initially hoped that the zinc centre, with its Lewis acid character, would give higher activity than the cobalt derivatives. Under the standard reaction conditions, $[Zn(TCT)(OPh)]BPh_4$ gave higher activity than Ti(TDBA)(O^{i}Pr), although the activity of the titanium catalyst has been shown to increase substantially at lower concentrations.

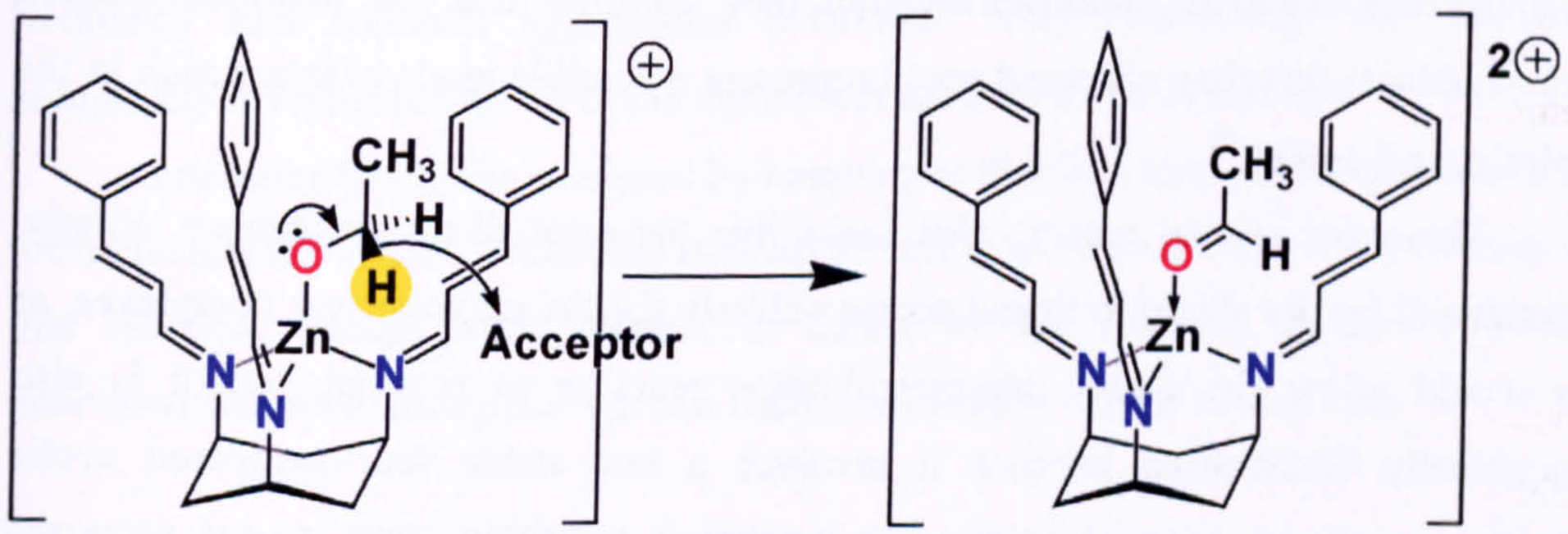

Figure 3.26: Possible route for decomposition of zinc ethoxide complex.

Despite their lower activity, the zinc complexes do have a significant advantage over the cobalt catalysts: they are not inherently toxic, and are therefore suitable for use in food applications. Additionally, their lack of colour would be an advantage for applications where colour of the product is an issue. However, the high cost of the ligand would limit their use, and a modification of the ligand to allow attachment to a solid support would be essential for practical use.

3.3.4 Mechanism

During the course of this project, a certain amount of insight into the catalytic mechanism has been gained. Extensive consultation of the available literature, combined with our own laboratory investigations, has led to some new ideas about the processes taking place. Whilst our results agree with previous studies that the mechanism is first order with respect to ester and alcohol, we propose a different mechanism to that proposed by other groups.[37] Our suggested mechanism involves nucleophilic attack at the acyl carbon by a molecule of alcohol. Both of the substrates are activated by their interaction with the metal alkoxide species. The ester coordinates to the metal, either by a σ-interaction in the case of titanium and zinc, or possibly by a π-interaction in the case of cobalt; in both cases, the result is a decrease in the electron density at the acyl carbon, activating it towards nucleophilic attack (Otton *et al.*[36(a)] do not appear to consider coordination of the carbonyl function to the metal centre). We propose that the alcohol is activated as a nucleophile through hydrogen bonding to the alkoxide ligand. Yamamoto *et al.* did not consider this possibility during their original work on copper-catalysed transesterification,[36(b)] although in their later work on nickel- and palladium-catalysed transesterification they consider that the hydrogen-bonded alcohol adducts that they observed could represent a possible mode of interaction in the catalytic mechanism.[18]

There are several reasons that make this the most likely mechanism. Firstly, direct attack by the alkoxide ligand seems unlikely for the mononuclear complexes, as this would allow the direct interesterification reaction to proceed, and it is also energetically disfavoured because it involves a less stable four-membered cyclic transition state, as opposed to the six-membered transition state in our proposed mechanism. In the case of the titanium tetra-alkoxides, it is possible that double electrophilic activation by bridged titanium centres allows for direct attack by an alkoxide ligand. Secondly, hydrogen bonding between the alcohol and alkoxide ligand would help to make the alcohol more nucleophilic, further lowering the activation barrier – hydrogen-bonded solvent chains have been observed within hydrophobic cavities.[38] The evidence from UV/vis spectroscopy (Section 3.1.4 a) supports the involvement of an interaction between the metal centre and the carbonyl bond. The linear dependence of catalyst activity upon alcohol concentration (Figure 3.23) confirms that the mechanism is first order with respect to alcohol.

The coordination complexes do not show activity for the *direct* interesterification reaction, with the presence of alcohol being essential for catalytic activity. Although initially a disappointment, this result has in itself given a useful insight into the mechanism, and highlighted that research into binuclear complexes is essential for improved interesterification catalysts.

During the course of this research, it has become clear that the design of catalysts for transesterification and interesterification has obvious parallels with the design of catalysts for a number of other important reactions, including lactide polymerisation and CO_2 / epoxide copolymerisation. All of these reactions can be catalysed by a Lewis acid species that is capable of coordinating to the acyl oxygen atom, thus activating the carbonyl function towards nucleophilic attack. It has already been shown that species that have activity for lactide polymerisation[39] also have activity for transesterification. Therefore it is possible that a known catalyst for lactide polymerisation may also give activity for transesterification. The increased understanding of the mechanism will assist in the rational design of future catalysts.

Evidence has been uncovered for aggregation behaviour in the titanium coordination complexes, with the more sterically shielded complex Ti(TDBA)(O^{i}Pr) being the most active complex, and showing a relationship between concentration and turnover frequency that supports aggregation behaviour. This relationship has not been completely investigated for all of the complexes described in this thesis.

Interesterification is catalysed by homoleptic titanium tetra-alkoxides, which can form clusters in solution, whilst the monomeric complexes do not show any activity for this reaction, except when alcohol is added to the reaction mixture, allowing interesterification to take place via two transesterification reactions (eq. 3.8).

$$\begin{array}{ccc} PhCH_2CO_2Et + BzOH & \rightleftharpoons & PhCH_2CO_2Bz + EtOH \\ AcOBz + EtOH & \rightleftharpoons & AcOEt + BzOH \end{array}$$

$$PhCH_2CO_2Et + AcOBz \rightleftharpoons PhCH_2CO_2Bz + AcOEt \quad \text{(eq. 3.8)}$$

The lack of interesterification activity for the monomeric complexes is a strong indication that cooperativity between metal centres is essential for the strong electrophilic activation required for the direct interesterification reaction.

3.4 Conclusions

- Transesterification is catalysed by the metal alkoxide complexes prepared in this project. [Co(TCT)(OPh)]BAr^F_4 is the best catalyst (65 T.O. h^{-1}) under the standard conditions. Complexes of the type [Co(TCT)(OR)]BPh_4 show activities of 47 (R = Et) and 45 T.O. h^{-1} (R = Ph) and [Zn(TCT)(OPh)]BPh_4 shows an activity of 27 T.O. h^{-1}. Ti(TDBA)(O^iPr), Ti(TDMA)(O^iPr) and Ti(TPA)(O^iPr) show activities of 17, 5 and 4 T.O. h^{-1}, respectively.
- Ti(TDBA)(O^iPr) increases its activity to 55 T.O. h^{-1} at 353 K under dilute conditions (0.05 mol%), which is indicative of aggregation behaviour in the titanium catalysts.
- *Direct* interesterification is not catalysed by the mononuclear metal alkoxide complexes, but is catalysed by titanium tetra-alkoxides.
- The available evidence suggests that reaction takes place through a concerted mechanism between ester and alcohol at the metal centre. We propose that this mechanism involves hydrogen-bonding between alcohol and the alkoxide ligand.

3.5 References

1 (a) J. Otera, *Chem. Rev.*, 1993, **93**, 1449. (b) G. W. Parshall and S. D. Ittel *Homogeneous Catalysis*; 2nd ed.; John Wiley & Sons, Inc., 1992.

2 D. Seebach, E. Hungerbühler, R. Naef, P. Schnurrenberger, B. Weidmann and M. F. Züger, *Synthesis*, 1982, **2**, 138.

3 T. Katsuki and K. B. Sharpless, *J. Am. Chem. Soc.*, 1980, **102**, 5974.

4 T. Okano, K. Miyamoto, J. Kiji; *Chem. Lett.*, 1995, **3**, 246.

5 O. Meth-Cohn, *J. Chem. Soc., Chem. Commun.*, 1986, 695.

6 F. Pilati, P. Manaresi, B. Fortunato, A. Murari and V. Passalacqua, *Polymer*, 1981, **22**, 799.

7 (a) R. Okawra and M. Wada, *Adv. Organomet. Chem.*, 1967, **5**, 137. (b) J. Otera and H. Nozaki, *J. Chem. Soc. Jpn.*, 1990, 601.

8 (a) J. Otera, T. Yano, A. Kawabata and H. Nozaki, *Tetrahedron Lett.*, 1986, **27**, 2383. (b) J. Otera, N. Dan-oh and H. Nozaki, *J. Org. Chem.*, 1991, **56**, 5307.

9 J. Otera, Acc. Chem. Res., 2004, 37, 288.

10 Y. J. Kim, K. Osakada, A. Takenaka, and A. Yamamoto, *J. Am. Chem. Soc.*, 1990, **112**, 1096.

11 B. Greener and P.H. Walton; *J. Chem. Soc., Dalton. Trans.*, 1997, 3733

12 (a) J. D. Freeman, DPhil Thesis, University of York, 2001. (b) S. J. Archibald, S. P. Foxon, J. D. Freeman, J. E. Hobson, R. N. Perutz and P. H. Walton, *J. Chem. Soc.-Dalton Trans.*, 2002, 2797.

13 J. Otera, Ed. *Modern Carbonyl Chemistry*; Wiley-VCH: Weinheim, 2000.

14 M. F. Lappert, *J. Chem. Soc.*, 1961, 817.

15 (a) N. Q. Mendez, A. M. Arif and J. A. Gladysz, *Angew. Chem.-Int. Ed. Engl.*, 1990, **29**, 1473. (b) Y. J. Kim, K. Osakada and A. Yamamoto, *Bull. Chem. Soc. Jpn.*, 1989, **62**, 964.

16 (a) M. Tschinkl, A. Schier, J. Riede and F. P. Gabbaï, *Organometallics*, 1999, **18**, 1747. (b) H. Adams, N. A. Bailey, J. T. Gauntlett, and M. J. Winter, *J. Chem. Soc., Chem. Commun.*, 1984, 1360.

17 D. C. Bradley, R. C. Mehrotra, I. P. Rothwell and A. Singh, *Alkoxo and Aryloxo Derivatives of Metals*; Academic Press, 2001.

18 V. Ugrinova, G. A. Ellis and S. N. Brown, *Chem. Commun.*, 2004, 460.

19 Y. J. Kim, K. Osakada, A. Takenaka and A. Yamamoto, *J. Am. Chem. Soc.*, 1990, **112**, 1096.

20 C. J. Boxwell and P. H. Walton, *Chem. Commun.*, 1999, 1647.

21 (a) J. Huang, D. F. Li, S. A. Li, D. X. Yang, W. Y. Sun and W. X. Tang, *J. Inorg. Biochem.*, 2004, **98**, 502. (b) J. Xia, Y. B. Shi, Y. Zhang, Q. Miao and W. X. Tang, *Inorg. Chem.*, 2003, **42**, 70.

22 M. G. Stanton, C. B. Allen, R. M. Kissling, A. L. Lincoln and M. R. Gagné, *J. Am. Chem. Soc.*, 1998, **120**, 5981.

23 L. M. Jackman, M. M. Petrei and B. D. Smith, *J. Am. Chem. Soc.*, 1991, **113**, 3451.

24 T. Okano, Y. Hayashizaki and J. Kiji, *Bull. Chem. Soc. Jpn.*, 1993, **66**, 1863.

25 R. C. Mehrotra, A. Singh, and U. M. Tripathi, *Chem. Rev.*, 1991, **91**, 1287.

26 (a) B. S. Sankhla and R. N. Kapoor, *Aust. J. Chem.*, 1967, **20**, 2013. (b) P. P. Sharma and R. C. Mehrotra, *J. Ind. Chem. Soc.*, 1968, **45**, 736. (c) R. C. Mehrotra and J. M. Batwara, *Inorg. Chem.*, 1970, **9**, 2505.

27 R. C. Mehrotra, *J. Am. Chem. Soc.*, 1954, **76**, 2266.

28 D. C. Bradley and W. Wardlaw, *J. Chem. Soc.*, 1951, 280.

29 R. C. Mehrotra, *J. Ind. Chem. Soc.*, 1953, **30**, 585.

30 R. H. Baker, *J. Am. Chem. Soc.*, 1938, **60**, 2673.

31 P. Schnurrenberger, M. F. Züger and D. Seebach, *Helv. Chim. Acta*, 1982, **65**, 1197.

32 V. Ugrinova, G. A. Ellis and S. N. Brown, *Chem. Commun.*, 2004, 460.

33 (a) J. Otera, T. Yano, A. Kawabata and H. Nozaki, *Tetrahedron Lett.*, 1986, **27**, 2383. (b) J. Otera, N. Dan-oh and H. Nozaki, *J. Org. Chem.*, 1991, **56**, 5307.

34 For a review, see: S. H. Strauss, *Chem. Rev.*, 1993, **93**, 927. (a) D. V. Yandulov and R. R. Schrock, *Science*, 2003, **301**, 76. (b) M. Brookhart, B. Grant and A. F. Volpe Jr., *Organometallics*, 1992, **11**, 3920.

35 L. Cronin and P. H. Walton, *Chem. Commun.*, 2003, 1572.

36 R. Walz and H. Vahrenkamp, *Inorg. Chim. Acta*, 2001, **314**, 58.

37 (a) J. Otton, S. Ratton, V. A. Vasnev, G. D. Markova, K. M. Nametov, V. I. Bakhmutov, L. I. Komarova, S. V. Vinogradova, and V. V. Korshak, *J. Polym. Sci. Part A: Polym. Chem.*, 1988, **26**, 2199. (b) M. Kubota, T. Yamamoto, and A. Yamamoto, *Bull. Chem. Soc. Jpn.*, 1979, **52**, 146

38 C. J. Boxwell and P. H. Walton, *Chem. Commun.*, 1999, 1647.

39 Y. Kim, G. K. Jnaneshwara and J. G. Verkade, *Inorg. Chem.*, 2003, **42**, 1437.

Chapter 4: Reactivity of metal complexes towards CO_2 and CO

4.1 Reactivity of metal alkoxides and related species with CO_2

The insertion of carbon dioxide into the M – O bonds of metal alkoxides (and the M – N bonds of metal amides) has been documented for a wide variety of metal alkoxide and amide species. One of the first examples of CO_2 inserting into the M – O bond of a metal alkoxide ($Cu(OMe)_2$ in pyridine solution) was reported by Tsuda and Saegusa in 1972; this reaction was noted to be reversible, and also required the presence of an auxiliary ligand for reaction with CO_2 to occur.[1] Chisholm *et al.* made the first reports of insertion of CO_2 into the M – N σ-bonds of group 4 and 5 metal amides,[2] producing carbamato complexes, which were formally eight-coordinate (Figure 4.1).

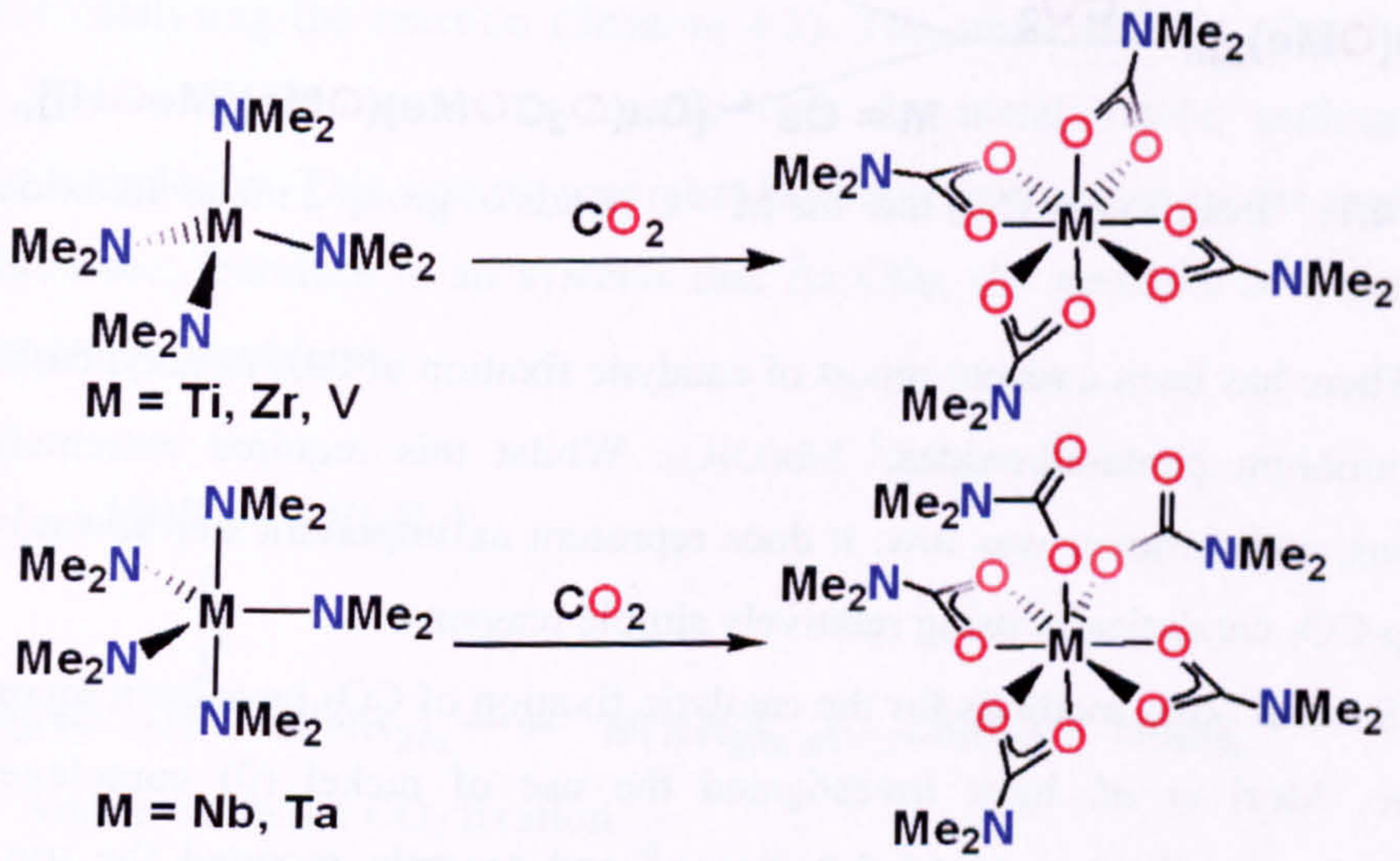

Figure 4.1: Insertion of CO_2 into the M – N bonds of group 4 & 5 metal amides.

They have continued their research to include insertion into the M – N and M – O bonds of ditungsten amides and alkoxides (Figure 4.2).[3] The reactivity of these species is discussed in more detail in Section 1.2.3, but also includes insertion of CO into the M – O bond (Section 4.4).

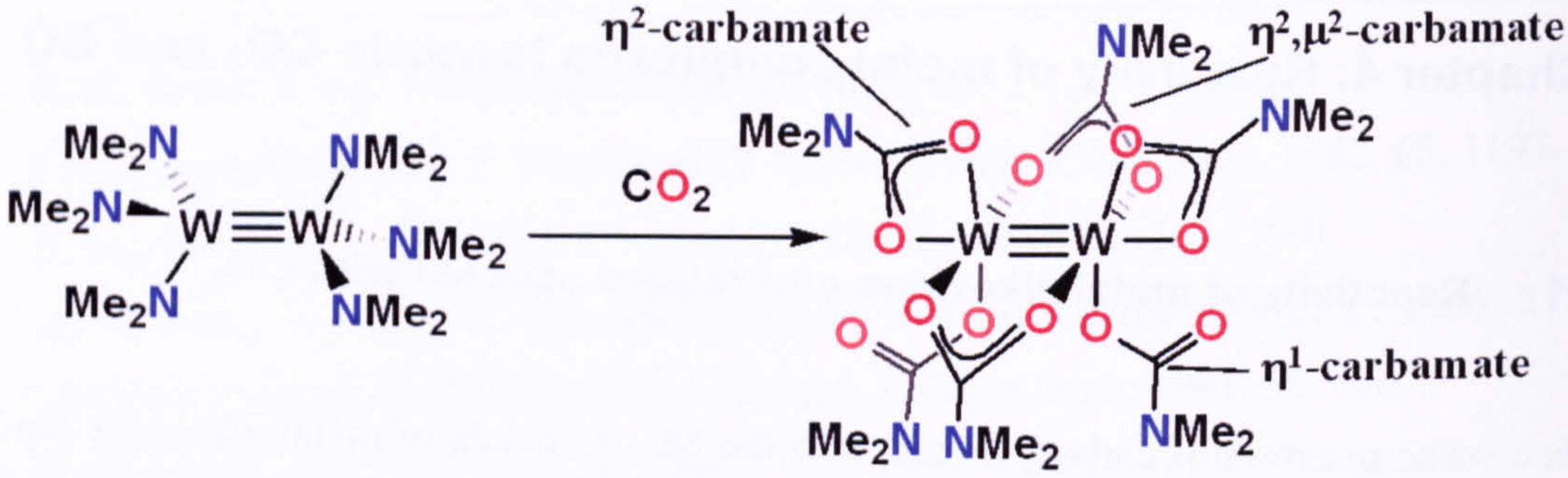

Figure 4.2: Insertion of CO_2 into the M – N bonds of di-tungsten amides.

Insertion reactions of small molecules (such as CO_2, COS, CS_2 and SO_2) with Group 2 metal alkoxides have been investigated by Mingos *et al.*[4] These species can readily insert into the M – O bonds to form a range of insertion products, depending on the reagents and conditions used (Scheme 4.1).

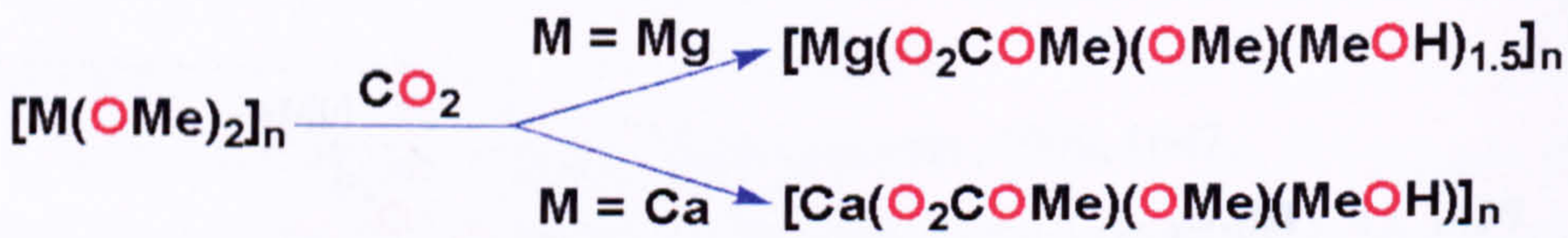

Scheme 4.1: Insertion of CO_2 into the M – O bonds of group 2 metal alkoxides.

There has been a recent report of catalytic fixation of CO_2 as alkyl carbonates by simple niobium penta-alkoxides,[5] $Nb(OR)_5$. Whilst this required extremely forcing conditions, and turnover was low, it does represent an important step towards the goal of fixing CO_2 catalytically using relatively simple reagents.

Several other methods for the catalytic fixation of CO_2 have been reported in the literature. Mori *et al.* have investigated the use of nickel (0) complexes for the carboxylative cyclisation of *bis*-1,3-dienes,[6] and recently reported the use of chiral phosphine ligands to make the process highly enantioselective (Figure 4.3).[7] This reaction is proposed to involve a nickel allyl intermediate; although the initial coordination mode of CO_2 at the nickel centre is unclear, the CO_2 molecule inserts into the Ni – C bond. The research groups of Darensbourg[8] and Coates[9] have made notable advances in the use of transition metal catalysts for the co-polymerisation of carbon dioxide and epoxides to form polycarbonates. These catalysts have largely been based on metal alkoxides, which can insert both CO_2 and epoxides into the M – O bond.

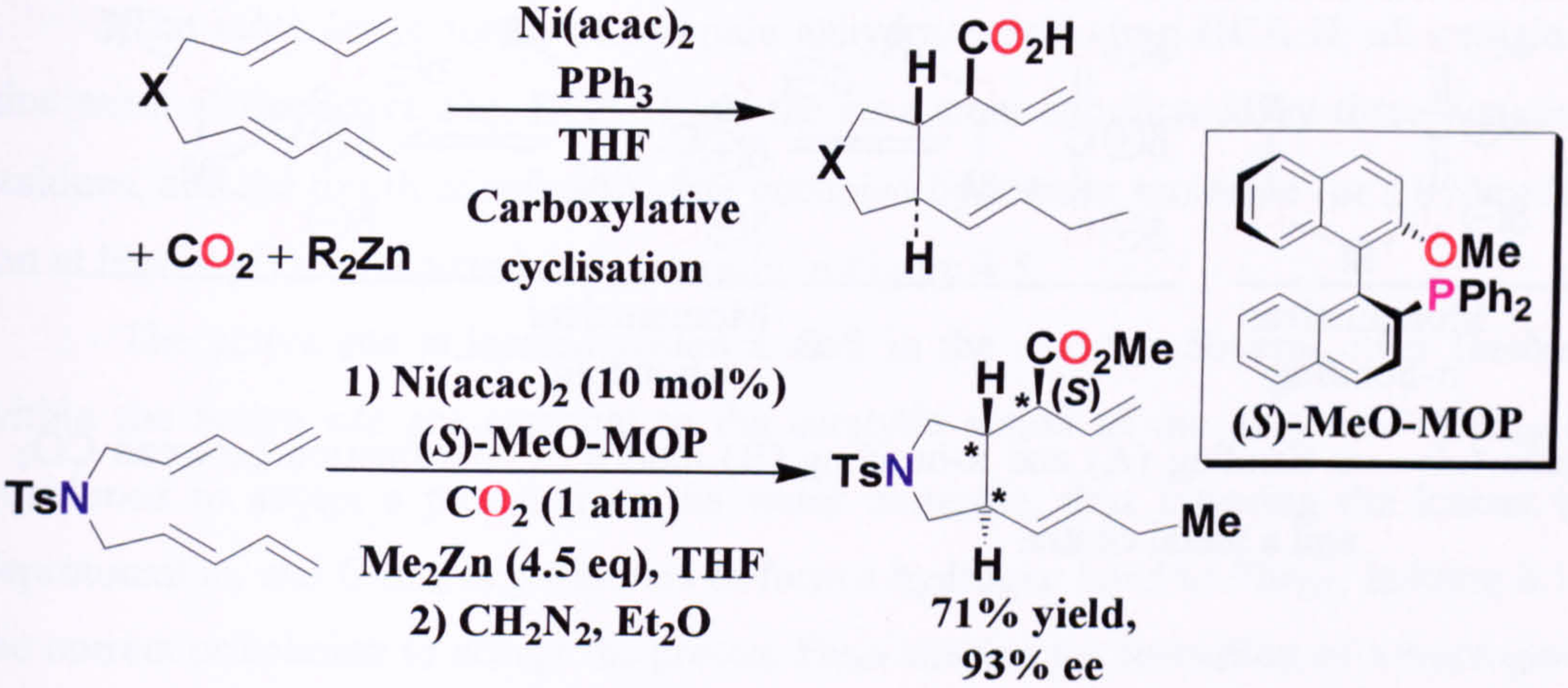

Figure 4.3: Carboxylative cyclisation of dienes, racemic and enantioselective.

The mechanism by which CO_2 inserts into the M – O bond deserves some discussion. During their initial investigation, Chisholm *et al.* found that, for the case of insertion into M – N bonds, the presence of adventitious free amine in the samples was responsible for catalysing the reaction (Scheme 4.2). The small amount of carbamic acid present in the equilibrium reacts rapidly with the metal amide, pulling the equilibrium to completion. This finding may also have some relevance to the reaction with metal alkoxides; therefore in all systems that fix CO_2, the presence of a similar mechanism should be considered.

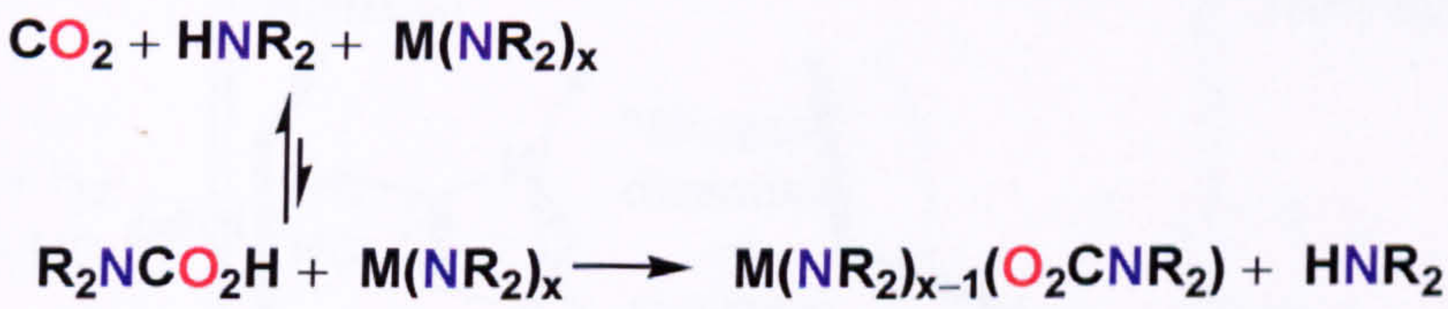

Scheme 4.2: Amine-catalysed CO_2 fixation.

The *direct* insertion of CO_2 into the M – O bond can be proposed to proceed through two possible mechanisms, varying in the initial coordination of CO_2 at the metal centre. CO_2 can be regarded as a carbonyl function, so it can potentially bind through either a σ- or π-interaction in a similar manner to the carbonyl function of an ester (Chapter 3). Early transition metals in high oxidation states tend to act as simple Lewis acids, and would probably favour the σ-bonding mode, but late transition metals may favour a π-bonding mode (Figure 4.4). Both modes of coordination draw electron density away from the carbon atom, activating it towards nucleophilic attack by the alkoxide ligand.

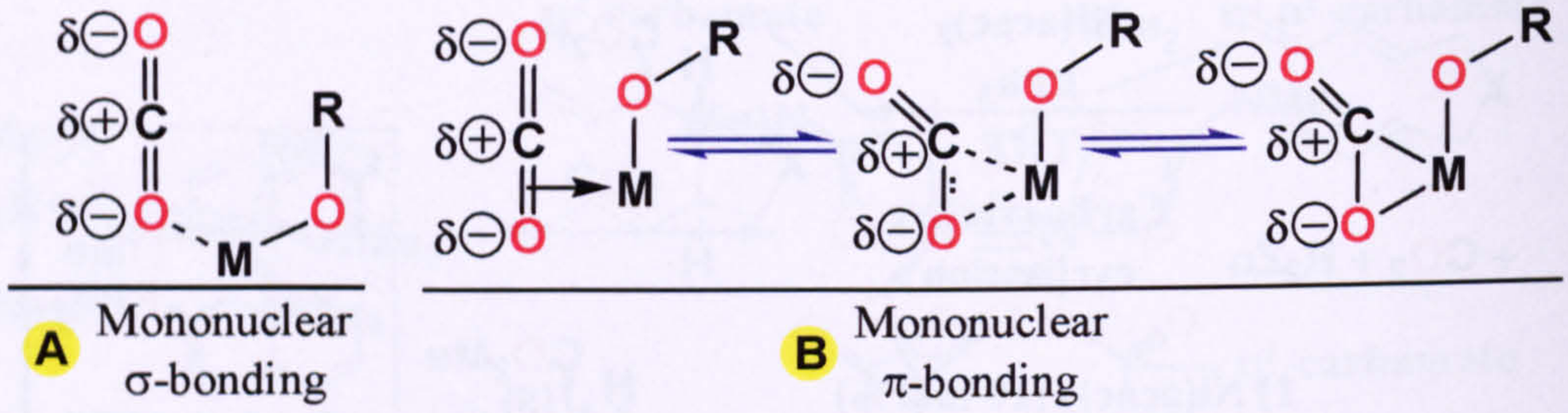

Figure 4.4: σ-bonding (A) and π-bonding (B) modes of coordination between CO_2 and a metal centre.

4.2 Reaction of cobalt alkoxides with CO_2

4.2.1 Background – Human Carbonic Anhydrase

Human Carbonic Anhydrase II (HCA II) is the most active enzyme known for the hydration of CO_2, with a second order rate constant of 1.5×10^8 dm^3 mol^{-1} s^{-1} (approaching the diffusion limit). This has led several groups to synthesise small molecule mimics of this enzyme, both for academic interest in confirming the mechanism of action for this protein,[10] and with a view to the potential commercial benefits of catalytically fixing an abundant C_1 feedstock.

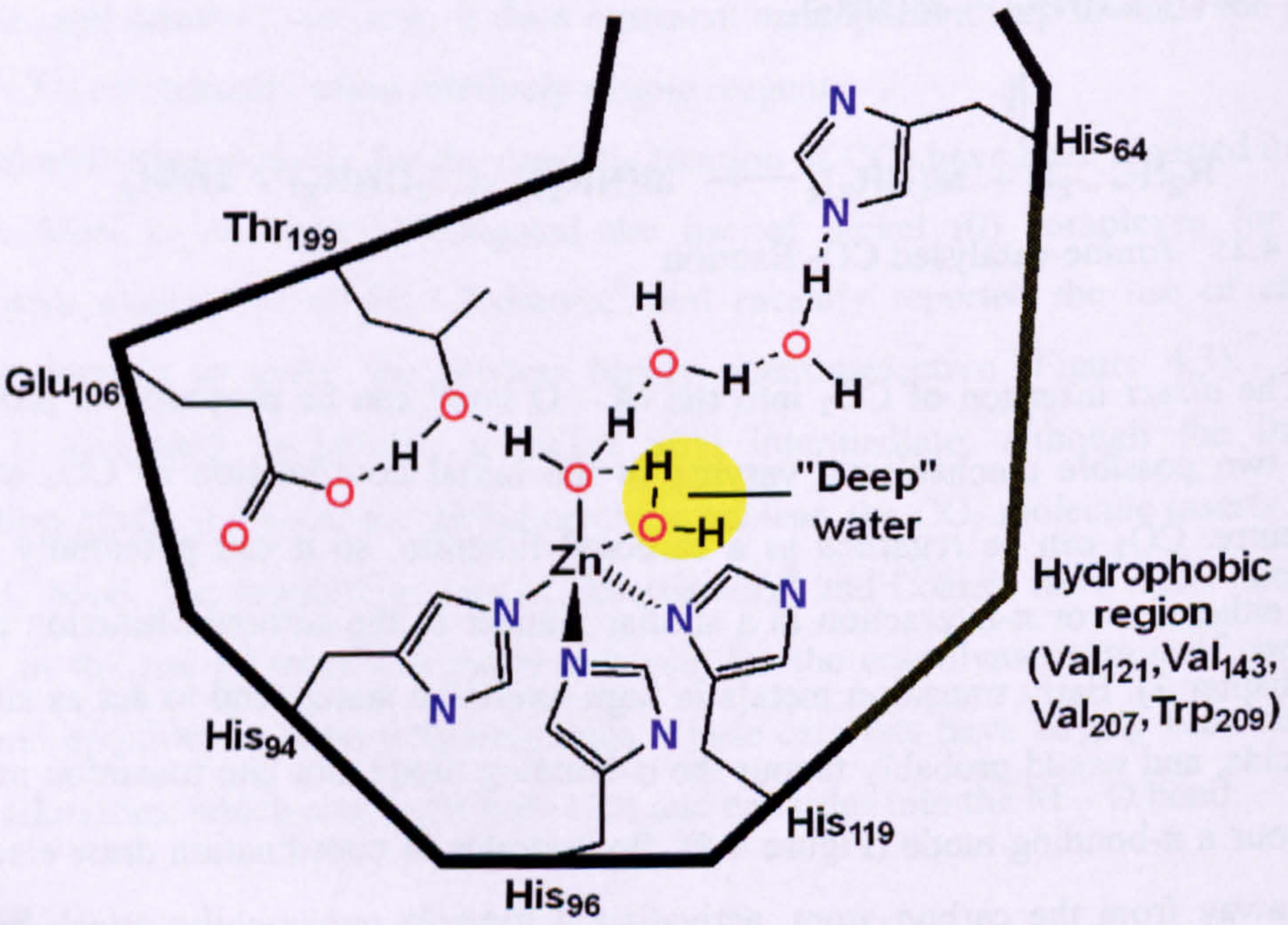

Figure 4.5: A schematic diagram of the active site of HCA II.

The most active forms of carbonic anhydrase, including HCA II, all contain a zinc atom at the active site. HCA II has the zinc atom coordinated by three histidine residues, and the fourth coordination site occupied by a water molecule (or a hydroxide ion at higher pH), as depicted schematically in Figure 4.5.

The active site is located within a cleft in the enzyme. Several other features within the active site are essential to the catalytic action of the enzyme.[11] Thr_{199} is positioned to accept a proton from the water molecule, thus lowering the barrier to deprotonation, and Glu_{166} is positioned to form a hydrogen bond to Thr_{199}, holding it in the correct orientation to accept the proton. His_{64} enables the formation of a hydrogen-bonded water chain, thus increasing the rate of proton transfer to and from the bulk solution to the active site. Additionally, there is a hydrophobic pocket (formed by Val_{121}, Val_{143}, Val_{207} and Trp_{209}), which—it is believed—acts as store for CO_2 molecules. There is also a "deep" water molecule, shown as weakly bound to both the zinc ion and the zinc-bound water molecule; the role of this water molecule is proposed to be in negating the entropic effects of free CO_2 becoming bound to the zinc atom (i.e.: the water and CO_2 molecules exchange places). There is still some debate about the precise mode of action of HCA II, but a reasonable cycle is shown in Figure 4.6.[12]

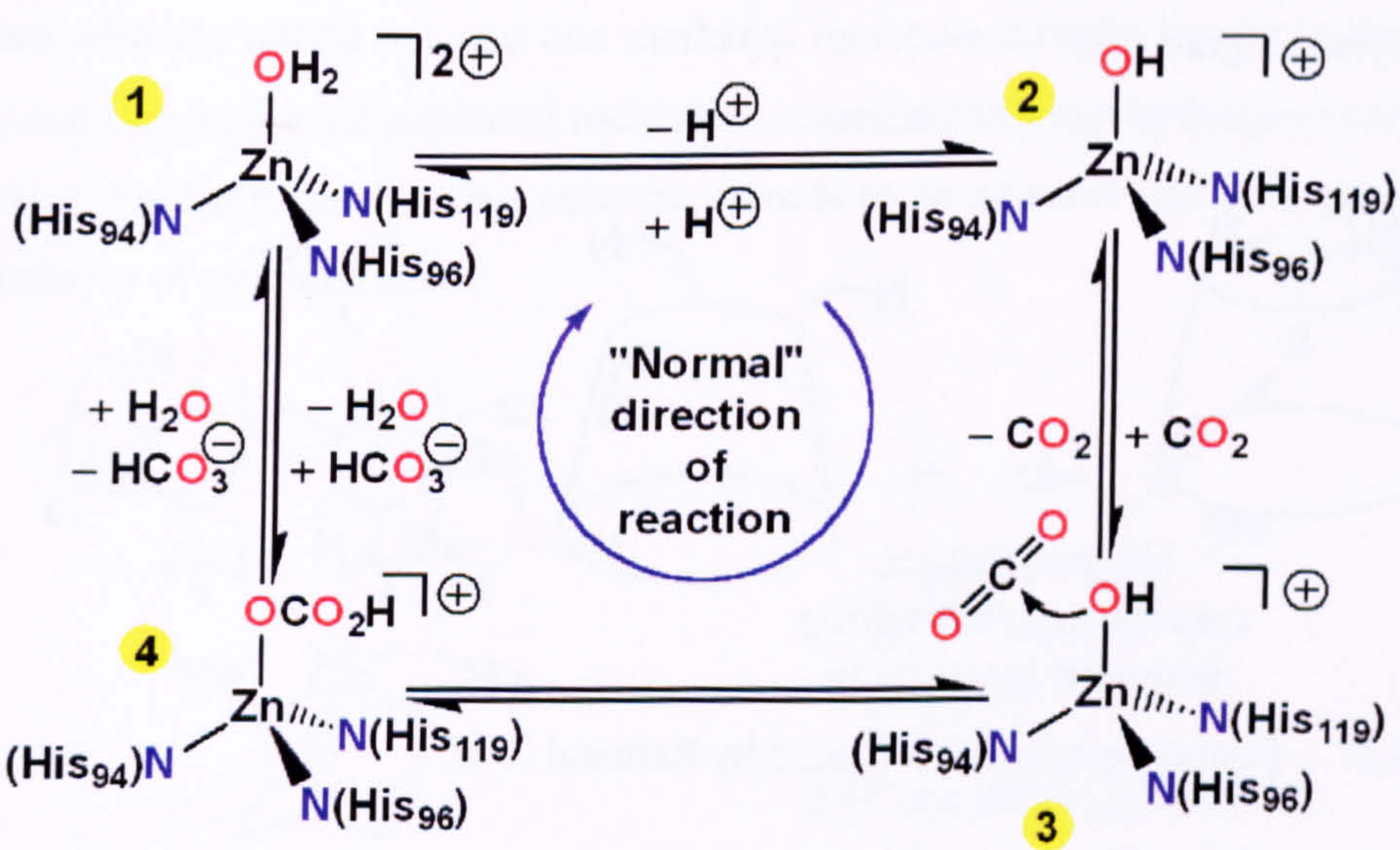

Figure 4.6: Catalytic cycle for the hydration of carbon dioxide by HCA II.[12]

The deprotonation step (1 – 2) is assisted by Thr_{199} and Glu_{106}, as noted above. The next step proceeds by the addition of CO_2, supplied either by diffusion into the cleft, or by transfer from the hydrophobic pocket. Nucleophilic attack on the carbon atom yields the bound bicarbonate ion, which is displaced by water to complete the cycle. Because of the design of the active site, the enzyme is able to catalyse the

hydration of carbon dioxide at close to the diffusion limit, and HCA II is often referred to as a "perfectly evolved" enzyme.[13] It is known that the zinc ion can be replaced by cobalt (II), giving an enzyme with about half the activity, whilst other metal atoms such as cadmium result in a deactivated enzyme. Substituting zinc with cobalt allows the active site to be studied by UV/vis spectroscopy (the zinc form has no electronic spectrum), and could potentially allow for solution state structure determination by ^{1}H NMR spectroscopy.[14]

Several research groups have constructed small molecule mimics of the enzyme, which recreate several features of the enzyme's active site. The research groups of Vahrenkamp[15] and Parkin[16] have produced zinc hydroxide, alkoxide and aryloxide complexes containing *tris*-pyrazolyl borate ligands to simulate the N_3 coordination sphere of the enzyme, and adding large, hydrophobic groups to these ligands allows for simulation of the cavity of the enzyme. Use of functionalised calixarene ligands has allowed Kersting *et al.* to produce metal complexes effectively buried within a hydrophobic pocket,[17] whilst Reinaud *et al.* have further built upon these frameworks by adding imidazole groups, producing Co^{II}, Ni^{II},[18] Cu^{I} & Cu^{II},[19] and Zn^{II}-containing complexes[20] which reproduce both the coordination sphere and the hydrophobic pocket of the enzyme (Figure 4.7).

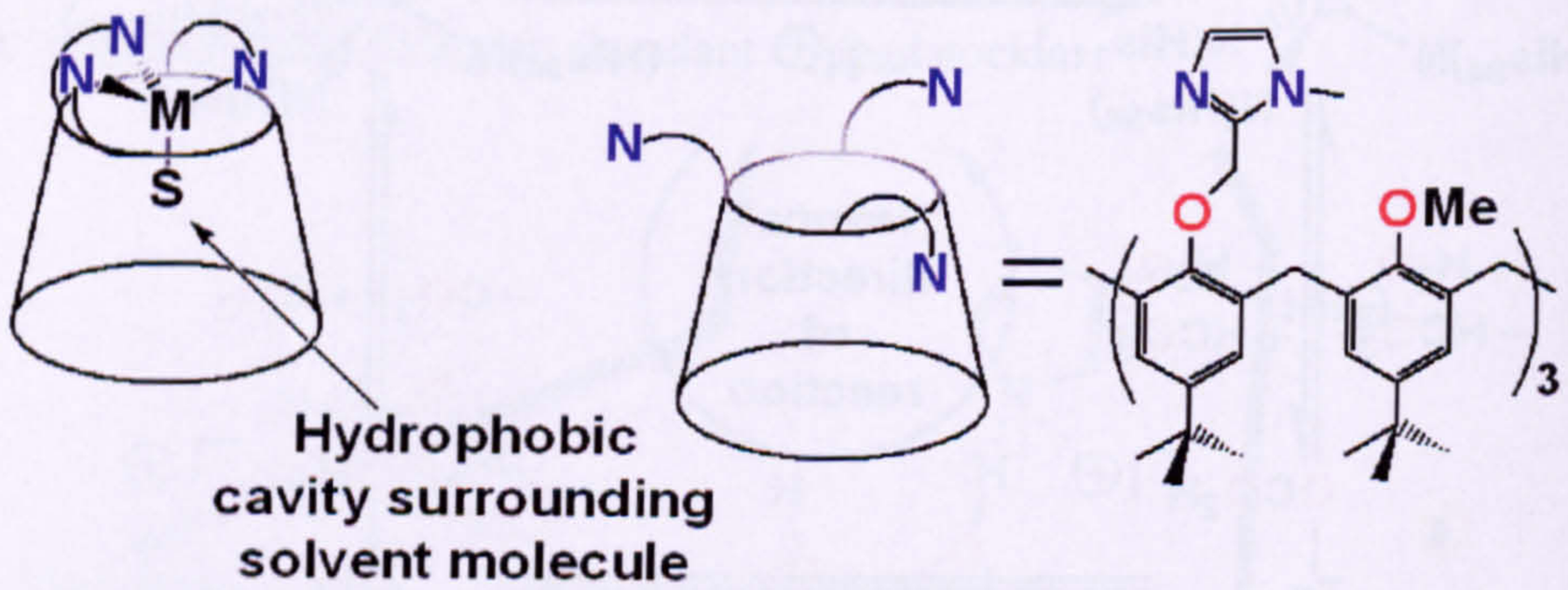

Figure 4.7: Funnel complexes prepared by Reinaud *et al.*[19]

Walton *et al.* have constructed a series of small molecule mimics of this enzyme, yielding some close approximations of certain features of the active site. The use of *tris*-imine ligands based on *cis,cis*-1,3,5-triaminocyclohexane gives a close approximation to the N_3 face-capping arrangement of the three histidine residues in HCA II. Use of rigid cinnamyl side chains also creates a hydrophobic pocket around the metal ion. This has allowed the observation of hydrogen-bonded solvent chains in the crystal structures of certain complexes.[21]

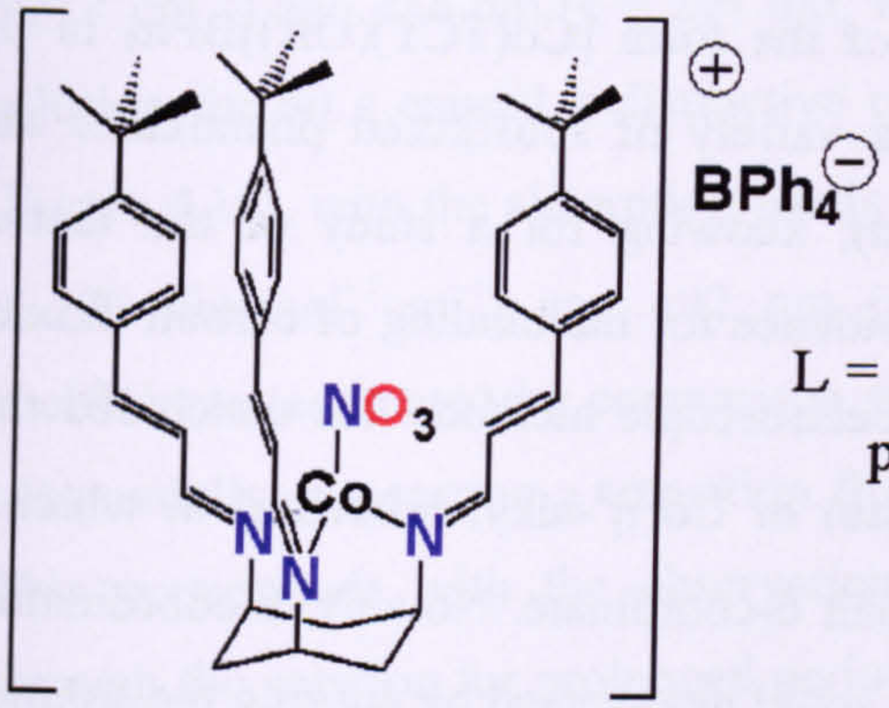

$[Co(L)(NO_3)]BPh_4$

L = *cis,cis*-1,3,5-tri[(4-*tert*-butylphenyl) propenylideneamino]cyclohexane

Figure 4.8: Model complex for formation of hydrogen-bonded solvent molecules.

Crystallisation of the complex cobalt (II) {*cis,cis*-1,3,5-*tris* [(4-*tert*-butyl-phenyl) propenylideneamino] cyclohexane} nitrate tetraphenylborate (Figure 4.8) from different mixtures of methanol and dichloromethane resulted in different structures. Use of a more methanol-rich mixture (9:1, *v/v*) gave a complex where three methanol molecules were directly bound to the cobalt centre, and the nitrate ion was held at the top of the cavity by hydrogen bonds to two of the methanol molecules (Figure 4.9). Recrystallisation of the complex from a less methanol-rich mixture (7:3, *v/v*) gave a structure with the nitrate ion and one methanol molecule directly bound to the cobalt centre, and two additional methanol molecules associated through hydrogen bonding. In both cases, the hydrogen-bonding network extends to an adjacent unit cell, resulting in the formation of pseudo-dimers.

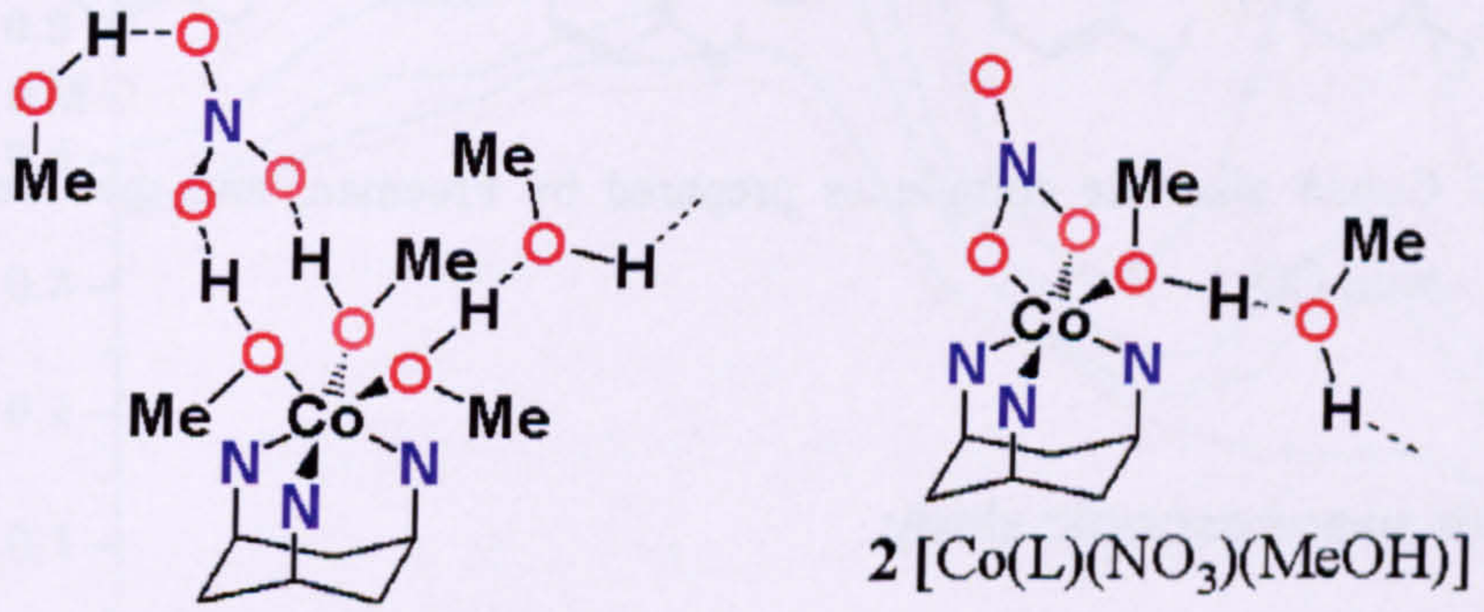

1 $[Co(L)(MeOH)_3](NO_3)(MeOH)_2(BPh_4)$

2 $[Co(L)(NO_3)(MeOH)](MeOH)_3(CH_2Cl_2)(BPh_4)$

Figure 4.9: Schematic representations of different modes of nitrate binding to cobalt centre, along with hydrogen-bonded solvent chains.

In his thesis,[22] Lusby described the use of zinc complexes immobilised in a polymer matrix as effective mimics of HCA II. Freeman reported the synthesis, and

reversible reaction of CO_2 with, complexes of the form $[Co(TCT)(OR)]BPh_4$ in his thesis (Figure 4.10).[23] The "R" group was a variety of substituted phenoxides and alkoxides (some of which were halogenated), allowing for a study of the factors affecting CO_2 binding to the cobalt centre. Evidence for the binding of carbon dioxide was provided by UV/vis, IR and ^1H NMR spectroscopic methods. He concluded that CO_2 inserted to form a Co(η^2-arylcarbononate) or Co(η^2-alkylcarbonate) in which a solvent molecule was also bound making cobalt 6-coordinate. Notably, a coordinating solvent was essential to reaction. The reaction could be reversed by purging the solution with argon or nitrogen. These studies have been continued during the course of this project to provide additional evidence for the assignment of the carbonated species and the presence of a bound solvent molecule.[24]

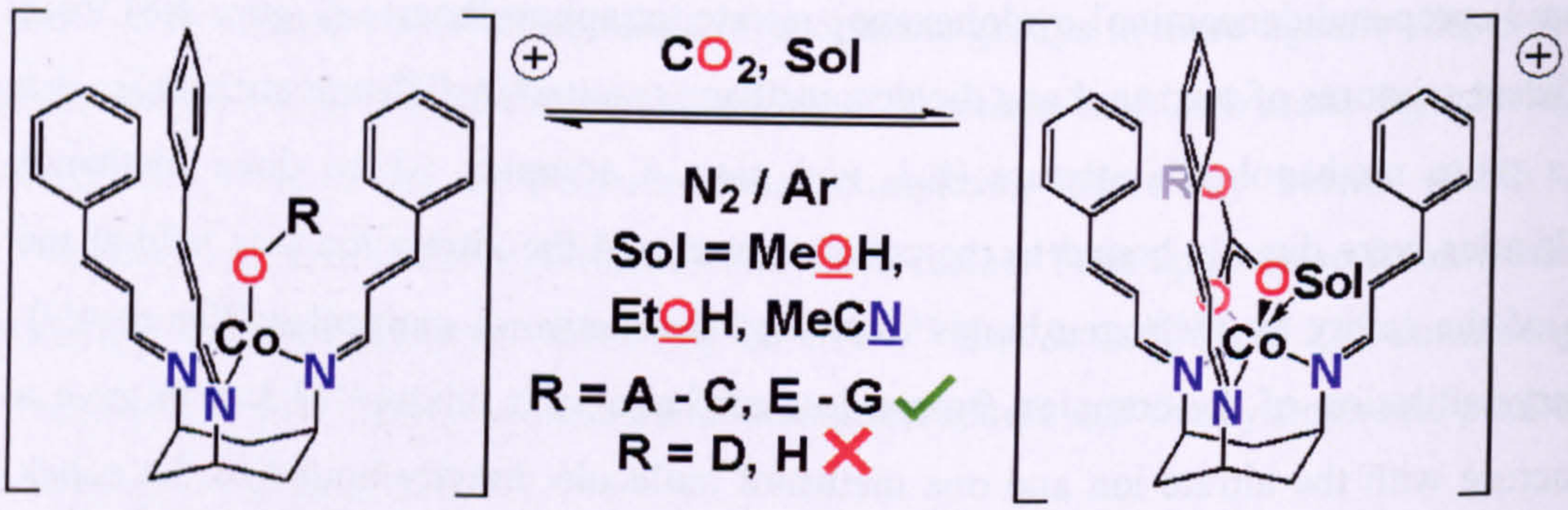

Figure 4.10: Cobalt alkoxide complexes prepared by Freeman, and their reactivity with CO_2.

4.2.2 UV/vis spectroscopic study

Freeman performed extensive UV/vis studies as part of his investigation of the reactivity of cobalt alkoxides with CO_2. The isolation of the complex $[Co(TCT)(OEt)]BPh_4$ in a pure form encouraged us to perform an additional study to show that its reaction with CO_2 is reversible, as for similar complexes. The complex was dissolved in a 9:1 mixture of dichloromethane and ethanol (at a concentration of 2.6×10^{-3} mol dm^{-3}) under an argon atmosphere, and the visible spectrum was recorded, showing absorption bands at 635 ($\varepsilon = 239$ dm^3 mol^{-1} cm^{-1}), 554 ($\varepsilon = 362$ dm^3

mol^{-1} cm^{-1}) and 486 nm (ε = 291 dm^3 mol^{-1} cm^{-1}) nm. Bubbling dry CO_2 through the solution for 60 s caused a distinctive change in the visible spectrum of the complex (Figure 4.10), with the absorption bands shifting to 550 (ε = 177 $dm^3mol^{-1}cm^{-1}$), 520 (ε = 173 $dm^3mol^{-1}cm^{-1}$) and 492 nm (sh) (ε = 158 $dm^3mol^{-1}cm^{-1}$); the extinction coefficients (estimated by comparison with those of the starting complex) are reduced substantially, suggesting a transition from four- to six-coordinate at the cobalt centre. This corresponds with the observations recorded by Freeman. Bubbling N_2 or Ar through the solution for prolonged periods causes the complex to lose CO_2, reverting to the ethoxide complex (Figure 4.11); note that the reverse reaction is slower than for $[Co(TCT)(OPh)]BPh_4$, and that a small amount of $[Co(TCT)Cl]BPh_4$ is formed, as can be seen from the slight shoulder around 593 nm on the spectra of the regenerated complex. Note that spectra of $[Co(TCT)(OEt)]BPh_4$ must be run in a dichloromethane / ethanol mixture, as the complex decomposes by hydrolysis in MeCN without EtOH present.

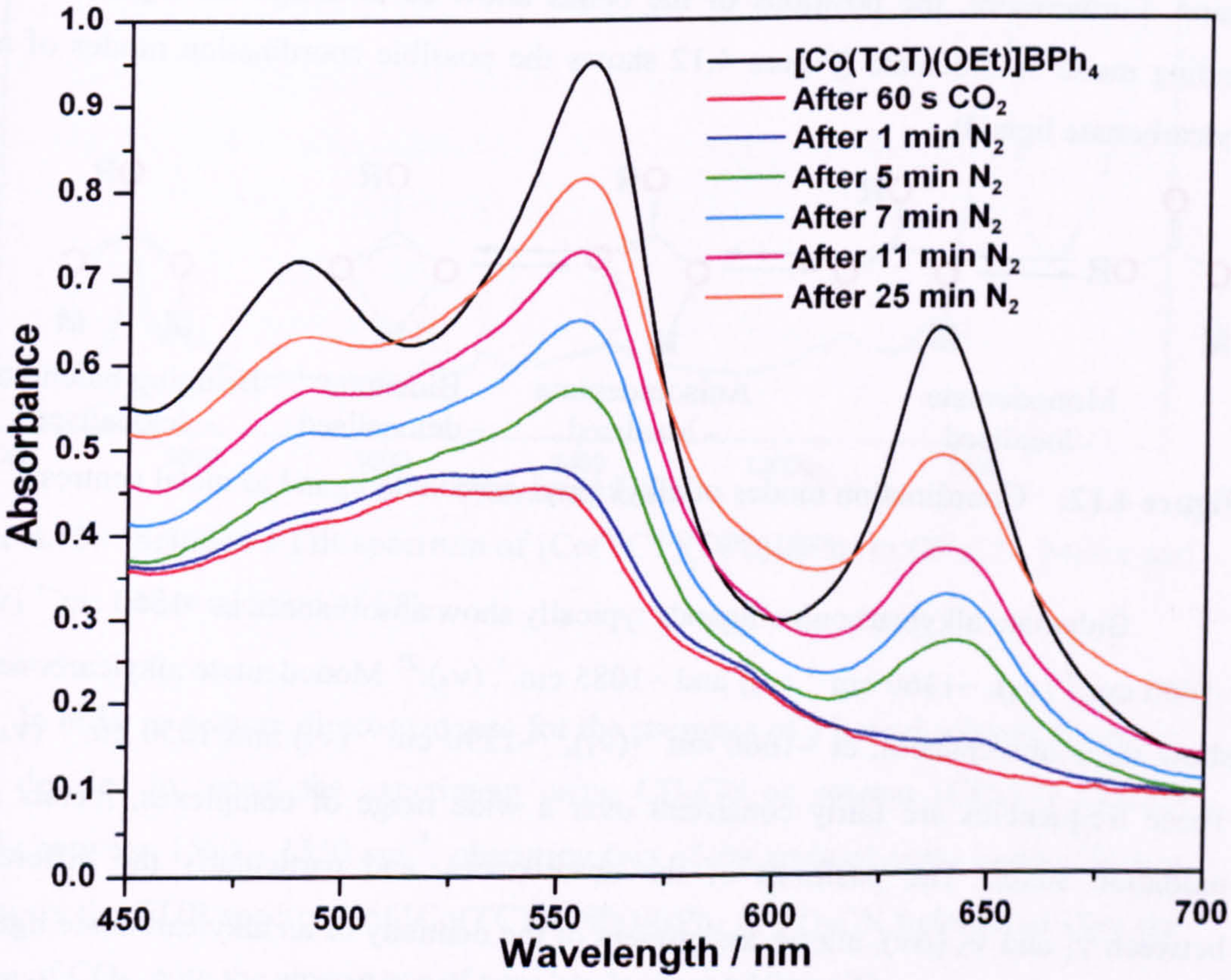

Figure 4.11: Visible spectra showing reversible reaction of $[Co(TCT)(OEt)]BPh_4$ with CO_2 in CH_2Cl_2/EtOH (9:1, *v*/*v*).

Although the UV/vis study does not in itself prove the identity of the carbonated product, it does provide strong evidence that the complex is six-coordinate, and confirms the reversibility of the reaction.

4.2.3 Solution FTIR spectroscopic study

FTIR spectroscopy of $[Co(TCT)(OPh)]BPh_4$ before and after reaction with CO_2, shows the emergence of absorption bands that can be assigned to an arylcarbonate ligand. The FTIR spectrum, run by Freeman, of the carbonated complex in CH_2Cl_2 / MeOH (9:1, *v/v*) shows bands at 1593, 1327 and 1093 cm^{-1}, which are assigned as arylcarbonate vibration modes. Freeman also acquired FTIR spectra monitoring the reaction of the complex with ^{18}O–labelled CO_2; the resulting shifts in the absorption frequencies of these bands relative to $C^{16}O_2$ were consistent with an arylcarbonate ligand. Furthermore, the positions of the bands allow us to assign the arylcarbonate binding mode as bidentate (Figure 4.12 shows the possible coordination modes of an arylcarbonate ligand).

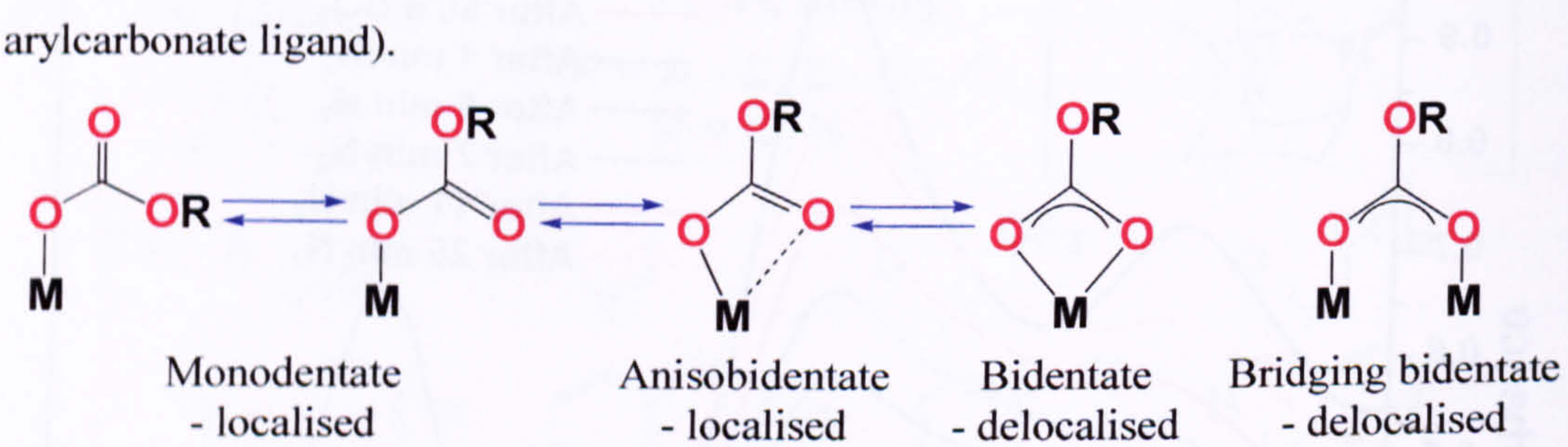

Figure 4.12: Coordination modes of alkyl / aryl-carbonate ligand to metal centres.[23]

Bidentate alkylcarbonate ligands typically show absorbances at ~1560 cm^{-1} (ν_1), ~1460 cm^{-1} (ν_2), ~1360 cm^{-1} (ν_3) and ~1085 cm^{-1} (ν_4).[25] Monodentate alkylcarbonates show three absorbances, at ~1660 cm^{-1} (ν_1), ~1290 cm^{-1} (ν_3) and 1050 cm^{-1} (ν_4).[26] These frequencies are fairly consistent over a wide range of complexes, metals and oxidation states. The positions of the absorbances, and particularly the difference between ν_1 and ν_3 ($\Delta\nu$), allows assignment of the denticity of an alkylcarbonate ligand: η^1 alkylcarbonate ligands typically have $\Delta\nu \geq 345$ cm^{-1}, η^2 alkylcarbonate ligands have $\Delta\nu \leq 227$ cm^{-1}, and μ_2-alkylcarbonate ligands have $\Delta\nu$ 294 – 325 cm^{-1}.[24(b,c)] The $\Delta\nu$ value of 265 cm^{-1} for the carbonated cobalt complexes under investigation here is much too low for a monodentate ligand, and below the range for μ^2-alkylcarbonate. Although

$\Delta\nu$ is above the range typical of bidentate alkylcarbonates, the positions of the bands make this the most likely coordination mode.

Since a coordinating solvent is crucial to the reaction (and the UV/vis study suggests the presence of a six-coordinate cobalt species), it is proposed that a molecule of solvent is directly bound to the cobalt centre, completing the coordination sphere. Although these experiments have provided strong support for the presence of a coordinated solvent molecule in the carbonated compound, direct spectroscopic evidence for the bound solvent is still lacking.

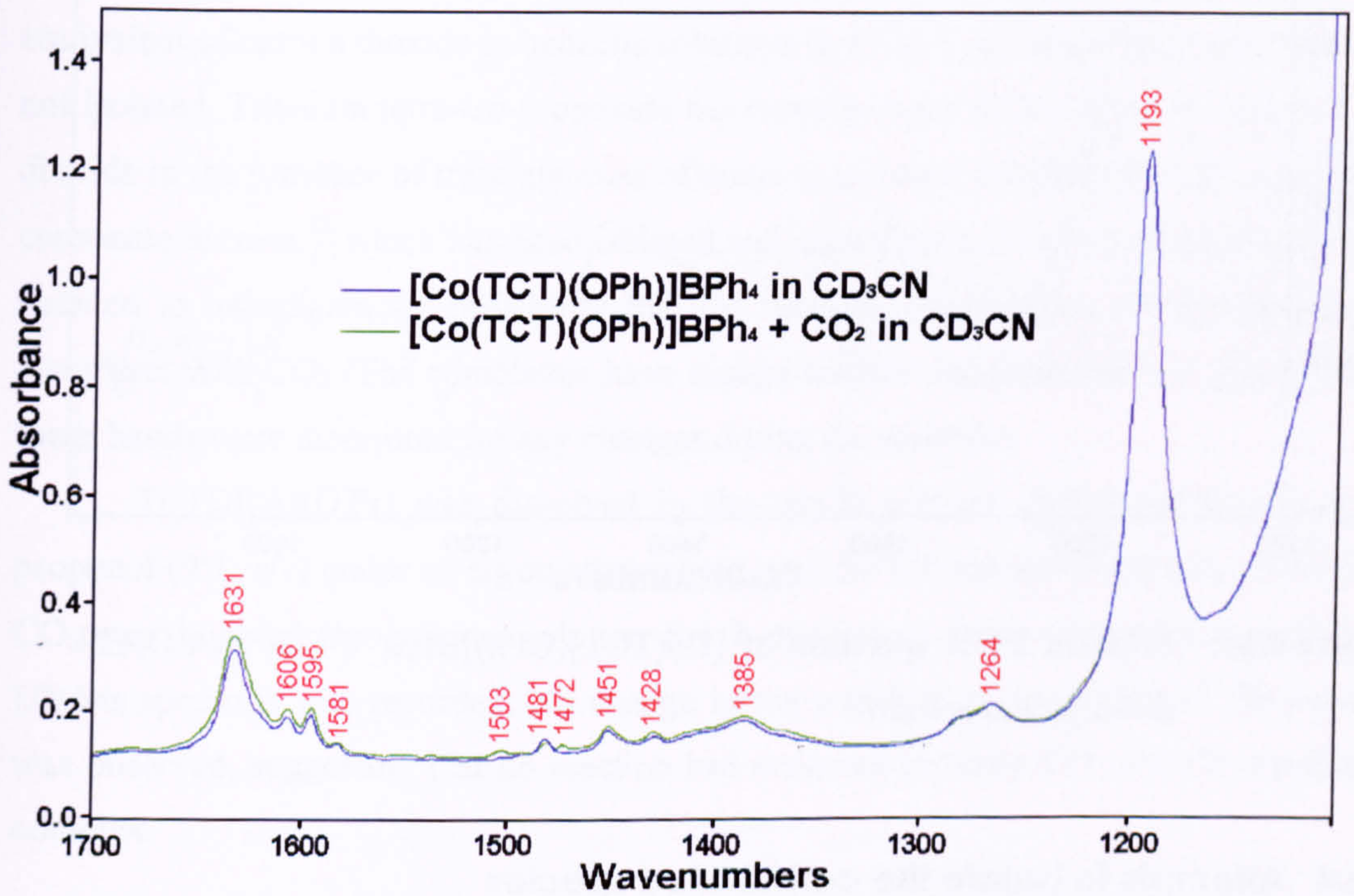

Figure 4.13: Solution FTIR spectrum of $[Co(TCT)(OPh)]BPh_4$ in CD_3CN, before and after addition of CO_2.

In order to acquire direct evidence for the presence of a bound solvent molecule, it was decided to repeat the experiment using CD_3CN as solvent (CH_3CN absorbs strongly between 1550 – 1350 cm^{-1}, obscuring two of the arylcarbonate bands). Figure 4.13 shows the FTIR spectrum of $[Co(TCT)(OPh)]BPh_4$ in CD_3CN before and after the addition of CO_2; note the emergence of new bands upon adding CO_2.

Subtracting the starting spectrum shows which absorption bands are due to the carbonated species (Figure 4.14). Very weak absorption bands assignable to arylcarbonate in $[Co(TCT)(\mu^2\text{-}O_2COPh)(\underline{N}CCD_3)]BPh_4$ are seen at 1503, 1363 and 1224 cm^{-1}; the fourth expected band (~1100 cm^{-1}) is not seen due to strong solvent

interference. The changes in two of the absorption frequencies of the arylcarbonate bands (1327 – 1363 cm^{-1} and 1593 – 1503 cm^{-1}) are of too great a magnitude to be caused by solvation effects alone, supporting the assumption that the complex contains a coordinated solvent molecule.

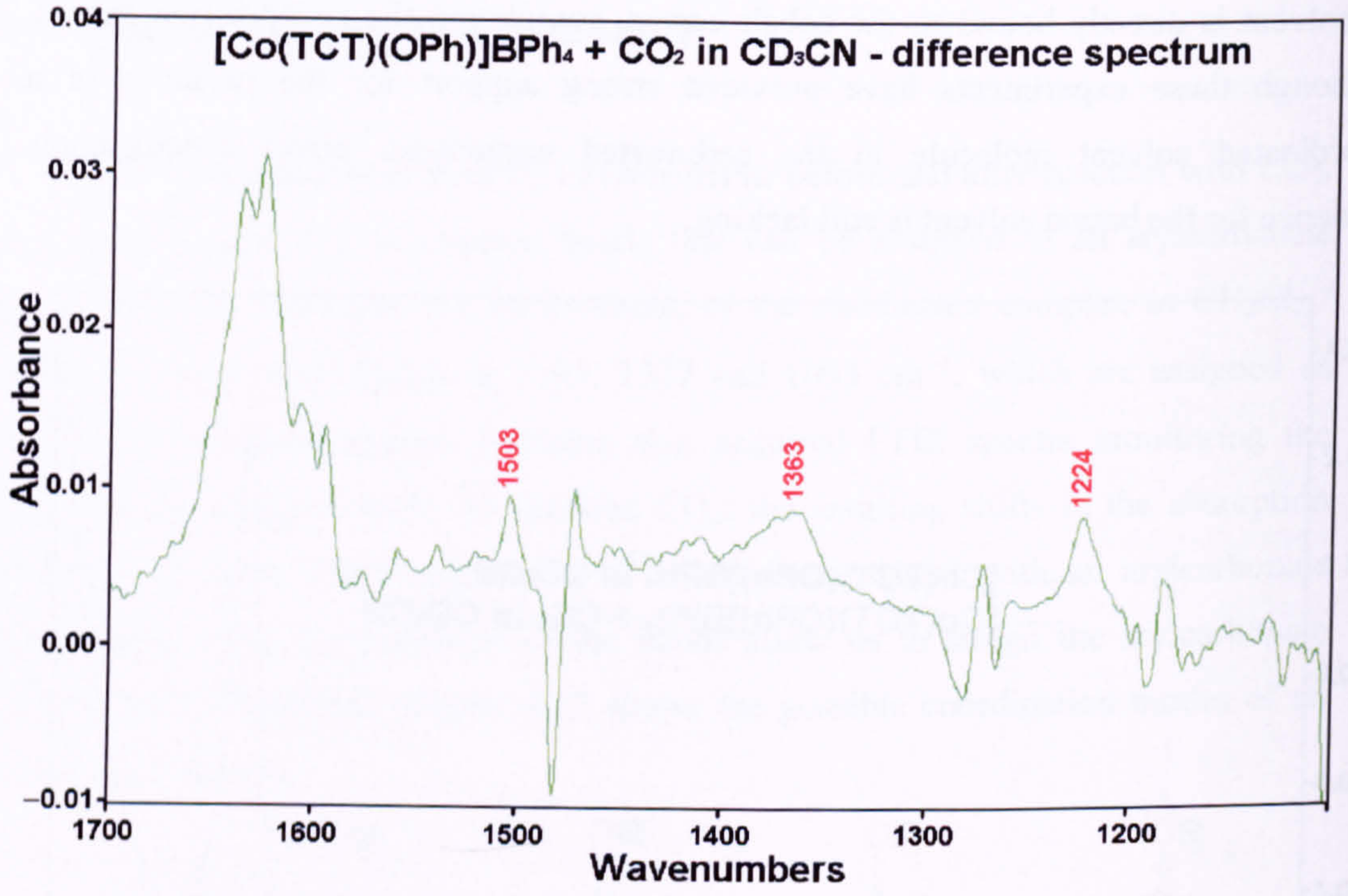

Figure 4.14: Solution FTIR spectrum of $[Co(TCT)(OPh)]BPh_4$ + CO_2 in CD_3CN – difference spectrum.

4.2.4 Attempts to isolate the carbonated species

Freeman made extensive efforts to isolate the carbonated species, which were all unsuccessful, resulting in isolation of the starting material. During the course of the FTIR study, it was noted that when CO_2 was bubbled through a concentrated solution of $[Co(TCT)(OPh)]BPh_4$ in CH_3CN, a purple precipitate formed, which re-dissolved upon bubbling argon through the solution, reversing the reaction. It was thought that the precipitate might be the carbonated species $[Co(TCT)(\mu^2\text{-}O_2COPh)(CH_3CN)]BPh_4$ in the solid state, with the lower solubility of the compound allowing its isolation. In order to investigate this possibility, a concentrated solution of $[Co(TCT)(OPh)]BPh_4$ in CH_3CN was left under an atmosphere of CO_2—the CO_2 was *not* bubbled through the solution—in a sealed, undisturbed vessel. After 1 week, small purple crystals had formed, and one of these was analysed by X-ray crystallography, with special care

taken to minimise exposure of the crystal to the atmosphere. It was found that the species formed was the previously identified μ^2-carbonate species, $\{[Co(TCT)]_2(\mu^2\text{-}CO_3)\}(BPh_4)_2$—presumably formed through hydrolysis by trace amounts of water—co-crystallised with a molecule of acetonitrile (Supplementary data, S7).

4.3 Attempted reaction of titanium alkoxides with CO_2

Titanium tetra-alkoxides were shown to react reversibly with one molar equivalent of carbon dioxide in benzene solutions in 1972,[27] although the products were not isolated. Titanium tetra-*iso*-propoxide has recently been shown to react with carbon dioxide in the presence of trace amounts of water to produce a tetranuclear *iso*-propoxo-carbonate species,[28] which has been isolated and crystallographically characterised. We decided to investigate the possibility that the titanium coordination complexes might also react with CO_2. The complexes have charge transfer bands in the UV region, and these bands were monitored for any changes during the reaction.

Ti(TDBA)(O^iPr) was dissolved in the mixed solvent dichloromethane / *iso*-propanol (9:1, *v/v*) under an argon atmosphere, and the UV/vis spectrum was recorded. CO_2 was bubbled through the solution for 2 minutes at room temperature, and the UV/vis spectrum was recorded. No change in the positions or intensities of the bands was observed, suggesting that no reaction had occurred between CO_2 and the titanium complex.

4.4 Attempted reaction of cobalt alkoxides with CO

Reaction between metal alkoxides and carbon monoxide has been observed in several systems, leading to the formation of the metallo-ester insertion product (Figure 4.15).[29] If a metal alkoxide complex has a vacant coordination site, then there is a possibility that this insertion reaction might take place.

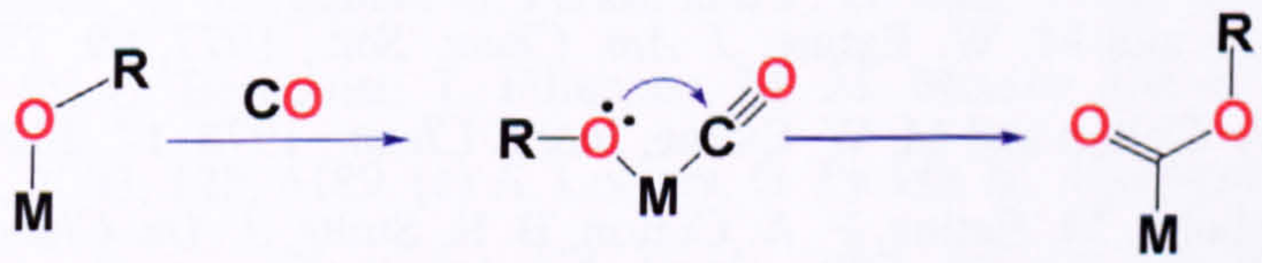

Figure 4.15: Insertion of CO into the M – O bond.

[Co(TCT)(OPh)]BPh_4 was dissolved in dichloromethane under an argon atmosphere, and the UV/vis spectrum was recorded. The solution was degassed and then placed under an atmosphere of CO; the solution was shaken and left overnight at room temperature, in the absence of light. The UV/vis spectrum showed no change, suggesting that there was no reaction with CO at room temperature. An additional experiment, using the mixed solvent dichloromethane / ethanol (9:1, *v/v*), also showed no evidence of reaction between CO and the cobalt complex.

4.5 Conclusions

- Freeman's original study of the reaction between cobalt alkoxides and CO_2 has been continued. Conclusive evidence for the presence of a bound solvent molecule in the carbonated product has been provided by FTIR spectra.
- The reaction between [Co(TCT)(OEt)]BPh_4 and CO_2 has been studied in more detail in light of the preparation of the ethoxide complex in a purer form, and the reversibility of the reaction has been demonstrated.
- Further attempts to isolate the carbonated products in the solid state have been unsuccessful.
- The cobalt alkoxides did not show any reactivity towards CO under the experimental conditions used.
- The complex Ti(TDBA)(O^{i}Pr), as an example of a neutral titanium complex, did not show reactivity towards CO_2 under the conditions used, although it is possible that altering the reaction conditions might influence the reactivity.

4.6 References:

1 T. Tsuda and T. Saegusa, *Inorg. Chem.*, 1972, **11**, 2561.

2 (a) M. H. Chisholm and M. Extine, *J. Chem. Soc., Chem. Commun.*, 1975, 438. (b) M. H. Chisholm and M. W. Extine, *J. Am. Chem. Soc.*, 1977, **99**, 782. (c) M. H. Chisholm, F. A. Cotton and M. W. Extine, *Inorg. Chem.*, 1978, **17**, 2000.

3 (a) M. H. Chisholm, M. Extine, F. A. Cotton, B. R. Stults, *J. Am. Chem. Soc.*, 1976, **98**, 4684. (b) M. H. Chisholm, F. A. Cotton, M. W. Extine and W. W. Reichert, *J. Am. Chem. Soc.*, 1978, **100**, 1727.

4 V. C. Arunasalam, I. Baxter, J. A. Darr, S. R. Drake, M. B. Hursthouse, K. M. A. Malik and D. M. P. Mingos, *Polyhedron*, 1998, **17**, 641.

5 M. Aresta, A. Dibenedetto and C. Pastore, *Inorg. Chem.*, 2003, **42**, 3256.

6 (a) M. Takimoto and M. Mori, *J. Am. Chem. Soc.*, 2001, **123**, 2895. (b) M. Takimoto and M. Mori, *J. Am. Chem. Soc.*, 2002, **124**, 10008.

7 M. Takimoto, Y. Nakamura, K. Kimura and M. Mori, *J. Am. Chem. Soc.*, 2004, ASAP article.

8 D. J. Darensbourg, M. W. Holtcamp, G. E. Struck, M. S. Zimmer, S. A. Niezgoda, P. Rainey, J. B. Robertson, J. D. Draper and J. H. Riebenspies, *J. Am. Chem. Soc.*, 1999, **121**, 107.

9 M. C. Cheng, E. B. Lobkovsky and G. W. Coates, *J. Am. Chem. Soc.*, 1998, **120**, 11018.

10 C. Bergquist, T. Fillebeen, M. M. Morlok and G. Parkin, *J. Am. Chem. Soc.*, 2003, **125**, 6189.

11 (a) L. Stryer, *'Biochemistry'*, W. H. Freeman and Company, 1995. (b) W. Kaim and B. Schwederski, *'Bioinorganic Chemistry: Inorganic Elements in the Chemistry of Life - An Introduction and Guide'*, Chapter 12, John Wiley & Sons, Chichester, 1994. (c) S. Lindskog, L. E. Henderson, K. K. Kannan, A. Liljas, P. O. Nyman, and B. Strandberg, *'The Enzymes'*, Chapter 21, ed. P. D. Boyer, Academic Press, 1971. (d) B. Greener, DPhil Thesis, University of York, 1997.

12 D. N. Silverman, S. Lindskog, *Acc. Chem. Res.*, 1988, **21**, 30.

13 J. E. Coleman, *Nature*, 1967, **214**, 193.

14 I. Bertini, C. Luchinat and G. Parigi *Solution NMR of Paramagnetic Molecules - Applications to Metallobiomolecules and Models*; Elsevier:, 2001.

15 (a) R. Walz, K. Weis, M. Ruf and H. Vahrenkamp, *Chem. Ber.-Recl.*, 1997, **130**, 975. (b) M. Ruf, F. A. Schell, R. Walz and H. Vahrenkamp, *Chem. Ber.-Recl.*, 1997, **130**, 101. (c) R. Alsfasser, M. Ruf, S. Trofimenko and H. Vahrenkamp, *Chem. Ber.-Recl.*, 1993, **126**, 703.

16 (a) A. S. Lipton, C. Bergquist, G. Parkin and P. D. Ellis, *J. Am. Chem. Soc.*, 2003, **125**, 3768. (b) C. Bergquist, T. Fillebeen, M. M. Morlok and G. Parkin, *J. Am. Chem. Soc.*, 2003, **125**, 6189. (c) A. Looney, G. Parkin, R. Alsfasser, M. Ruf and H. Vahrenkamp, *Angew. Chem.-Int. Ed. Engl.*, 1992, **31**, 92. (d) R. Alsfasser, S. Trofimenko, A. Looney, G. Parkin and H. Vahrenkamp, *Inorg. Chem.*, 1991, **30**, 4098.

17 B. Kersting, *Angew. Chem.-Int. Ed.*, 2001, **40**, 3987.

18 Co^{II} & Ni^{II}: O. Sénèque, M. Campion, M. Giorgi, Y. Le Mest and O. Reinaud, *Eur. J. Inorg. Chem.*, 2004, 1817.

19 (a) Cu^{I}: Y. Rondelez, O. Sénèque, M.-N. Rager, A. F. Duprat and O. Reinaud, *Chem. Eur. J.*, 2000, **6**, 4218; S. Blanchard, L. Le Clainche, M.-N. Rager, B. Chansou, J.-P. Tuchagues, A. F. Duprat, Y. Le Mest and O. Reinaud, *Angew. Chem.-Int. Edit.*, 1998, **37**, 2732. (b) Cu^{II}: L. Le Clainche, M. Giorgi and O. Reinaud, *Inorg. Chem.*, 2000, **39**, 3436.

20 (a) O. Sénèque, Y. Rondelez, L. Le Clainche, C. Inisan, M.-N. Rager, M. Giorgi and O. Reinaud, *Eur. J. Inorg. Chem.*, 2001, 2597. (b) O. Sénèque, M.-N. Rager, M. Giorgi and O. Reinaud, *J. Am. Chem. Soc.*, 2001, **123**, 8442. (c) O. Sénèque, M.-N. Rager, M. Giorgi and O. Reinaud, *J. Am. Chem. Soc.*, 2000, **122**, 6183.

21 C. J. Boxwell and P. H. Walton, *Chem. Commun.*, 1999, 1647.

22 P. J. Lusby, DPhil Thesis, University of York, 2000.

23 J. D. Freeman, DPhil Thesis, University of York, 2001.

24 S, J. Archibald, S. P. Foxon, J. D. Freeman, J. E. Hobson, R. N. Perutz and P. H. Walton, *J. Chem. Soc., Dalton Trans.*, 2002, 2797.

25 (a) T. V. Ashworth and E. Singleton, *J. Chem. Soc., Chem. Comm.*, 1976, 204. (b) M. Kato and T. Ito, *Inorg. Chem.*, 1985, **24**, 504. (c) M. Kato and T. Ito, *Bull. Chem. Soc. Jpn.*, 1986, **59**, 285. (d) T.Ito, K. Hamamoto, S. Kurishima and K. Osakada, *J. Chem. Soc., Dalton Trans.*, 1990, 1645.

26 (a) T. Tsuda, S. Sanada, K. Ueda and T. Saegusa, *Inorg. Chem.*, 1976, **15**, 2329. (b) R. J. Crutchley, J. Powell, R. Faggiani and C. J. L. Lock, Inorg. Chim. Acta, 1977, **24**, L15. (c) A. Immirzi and A. Musco, *Inorg. Chim. Acta*, 1977, **22**, L35. (d) T. Ishida, T. Hayashi, Y. Mizobe and M. Hidai, Inorg. Chem., 1992, 31, 4481. (e) M. Ruf, F. A. Schell, R. Walz and H. Vahrenkamp, *Chem. Ber.-Recueil*, 1997, **130**, 101. See also: 24 (b) & (c).

27 M. Hidai, T. Hikita and Y. Uchida, *Chem. Lett. Japan.*, 1972, 521.

28 R. Ghosh, M. Nethaji, and A. G. Samuelson, *Chem. Commun.*, 2003, 2556.

29 D. C. Bradley, R. C. Mehrotra, I. P. Rothwell, and A. Singh, 'Alkoxo and Aryloxo Derivatives of Metals', Academic Press, 2001.

Chapter 5: Future work

5. 1 Titanium catalysts

The titanium catalysts produced during the course of this project have shown promising activity for transesterification processes, although they are somewhat slower than the stannoxane catalysts reported by Otera *et al.*[1] (55 T.O. h^{-1} compared to 100 T.O. h^{-1} for the stannoxanes at the same temperature). Use of the sterically hindered TDBA ligand gave a complex that could retain its activity even when less rigorously dried solvents were used. Limitations of the catalysts include their general susceptibility to hydrolysis [with the exception of Ti(TDBA)(O^iPr)] and the fact that they would remain in the final product. Modification of the ligands to include polymerisable functions such as vinyl groups may be possible, allowing the catalysts to be fixed to a solid support (Figure 5.1).

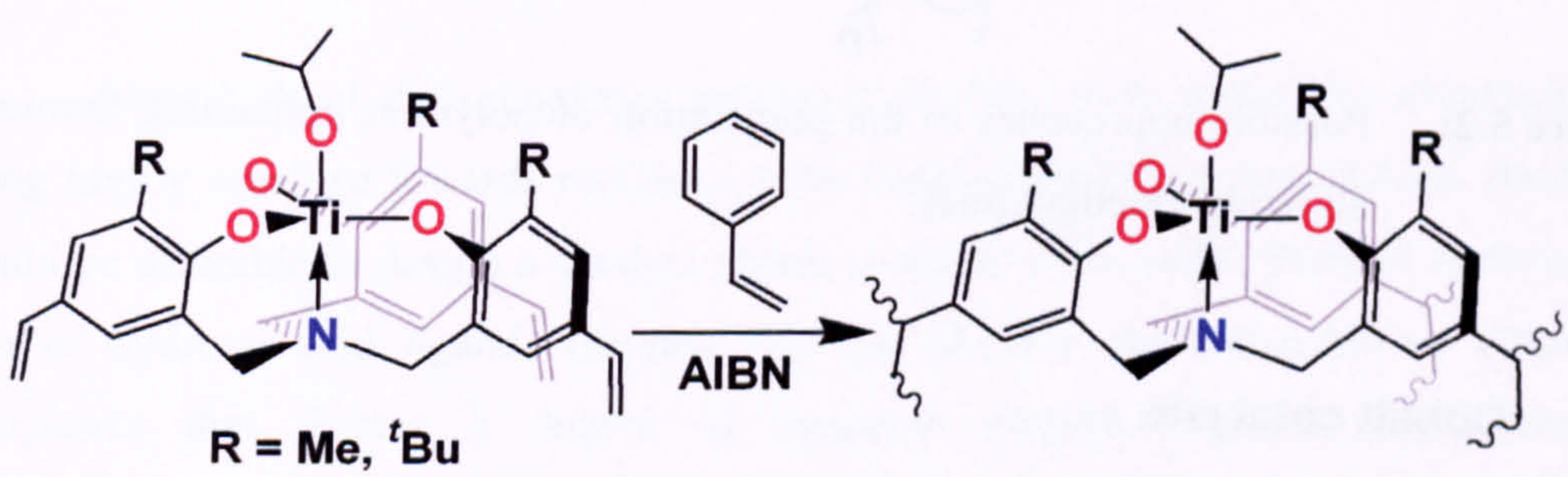

Figure 5.1: Modification of titanium coordination catalysts to enable immobilisation on a solid support.

An alternative approach to producing polymer-supported catalysts would be to abandon the drive toward well-defined homogeneous systems and focus on a simpler and direct attachment of titanium centres to a polymer. Reacting $Ti(OR)_4$ with a polymer containing phenol groups (such resins are commercially available) could potentially fix titanium centres to the polymer by phenolate bonds. Reaction of $Ti(OR)_4$ with one or more equivalents of 4-vinylphenol followed by polymerisation could also yield a polymer-fixed titanate species (Figure 5.2). This would give a less well-defined catalyst species, but would be much more simple to produce. The activity of such a catalyst would depend upon the accessibility of the titanium centres to the reactants. Attaching the titanium to a preformed polymer would allow for selection of the polymer

based on porosity, giving easy control over the macroscopic properties of the polymer (such as the diffusion rate within the polymer, which is dependent on the presence of appropriately-sized cavities), but at the expense of relatively little control over the precise coordination sphere of the titanate. Preforming a titanate species containing 4-vinylphenolate groups, followed by radical polymerisation, would allow some control over the degree of substitution at the titanium centre, but might not allow for good control over the macroscopic properties of the polymer.

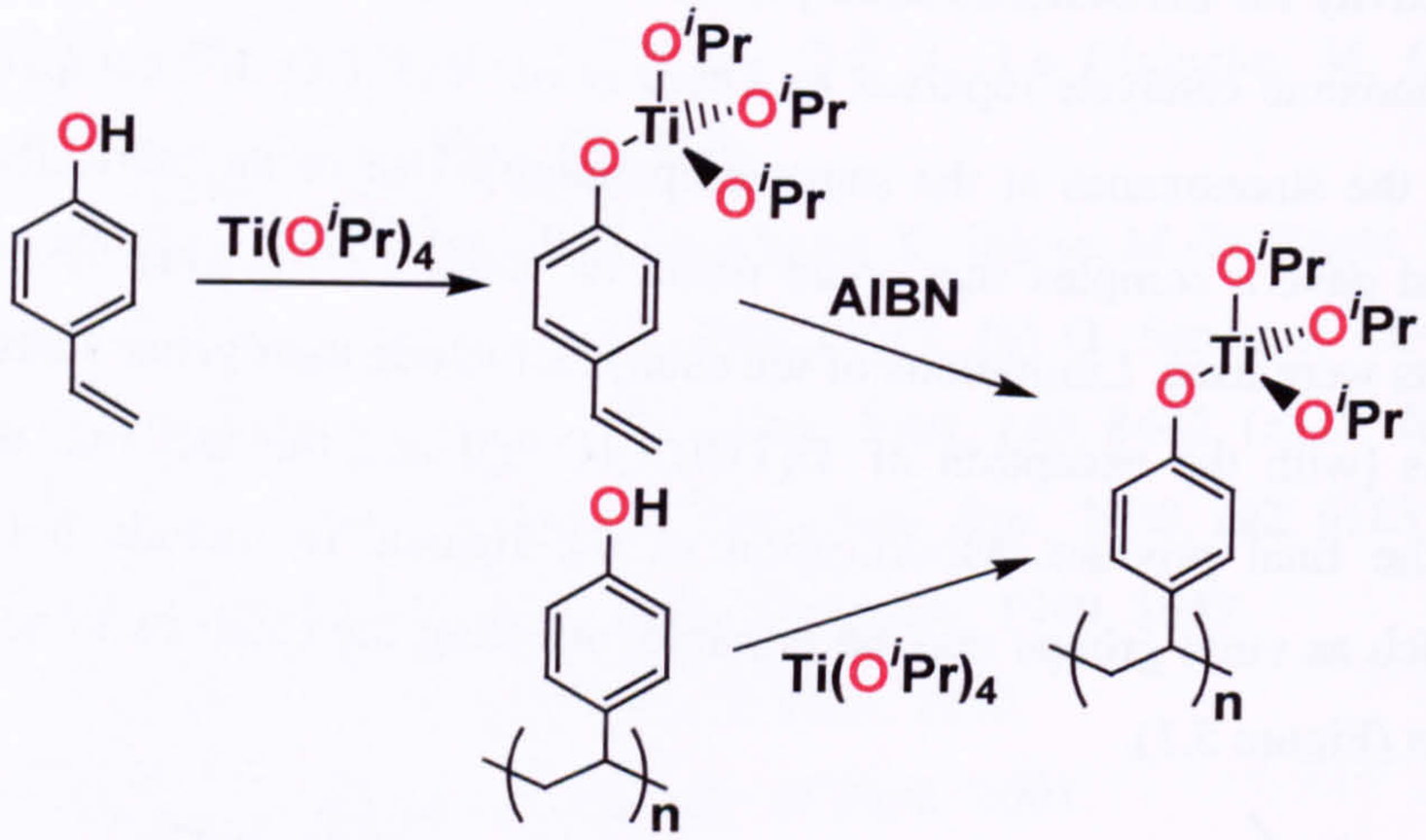

Figure 5.2: Possible approaches to the preparation of polymers containing titanium alkoxide functionalities.

5.2 Cobalt catalysts

Catalytic testing of the cobalt (II) alkoxide complexes has given the most satisfactory results in terms of raw activity for the transesterification reaction, though they are still slower than the stannoxane catalysts.[1] There are, however, a number of drawbacks associated with these catalysts, including their instability at high temperature, and the high cost of producing the ligand system. These problems could be overcome by modifying the TCT ligand to enable immobilisation of the complexes within a solid support, which would reduce the incorporation of cobalt into the product, and could improve the stability of the catalyst at high temperatures by imposing additional conformational rigidity upon the ligand. Lusby *et al.* successfully covalently incorporated cobalt and zinc complexes bearing a modified ligand into a polymer matrix, by the addition of vinyl groups in the *para* position of the cinnamyl groups (Figure 5.3).[2] A limitation to this strategy is that the macroscopic properties of the polymer must be suitable for diffusion of the substrates to occur rapidly; the polymer in

this case only needed to transport the small substrates CO_2 and H_2O, whereas large esters would be more difficult to transport efficiently, because of the steric crowding around the cobalt centre. This strategy would also be applicable to zinc (II) complexes.

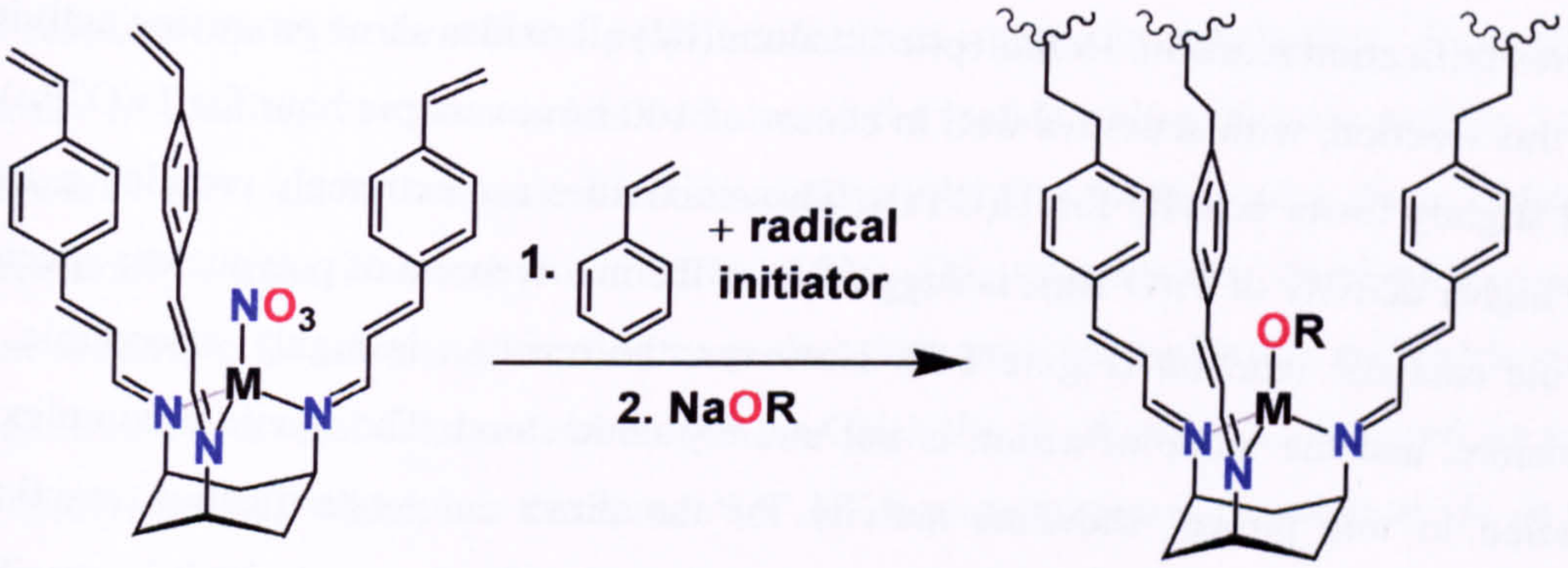

Figure 5.3: Proposed method for immobilising metal-TCT alkoxide complexes within a polystyrene support; method developed by Lusby *et al.*

5.3 Ligand design

Almost all of the complexes produced for this study suffer the drawback of being highly sensitive towards moisture at the catalyst operating temperature, hence it would be desirable to design a catalyst which could be more stable towards hydrolysis. Use of hydroxy acid ligands (Figure 5.4) has allowed the formation of titanium complexes that display a degree of moisture stability. Aldrich sell titanium *bis*(ammonium lactato)dihydroxide as a solution in water,[3] and Synetix use a polyesterification catalyst based on titanium with three citrate ligands.[4] The precise reason for the stability of these complexes is not fully established, but having groups which can donate additional electron density to the metal centre (without permanently blocking coordination sites) and / or groups which can stabilise the alkoxide ligand through hydrogen bonding, seem to be essential to their success as catalysts. It seems likely that exploration of ligand architectures that could provide these features would yield a new generation of moisture tolerant catalysts.

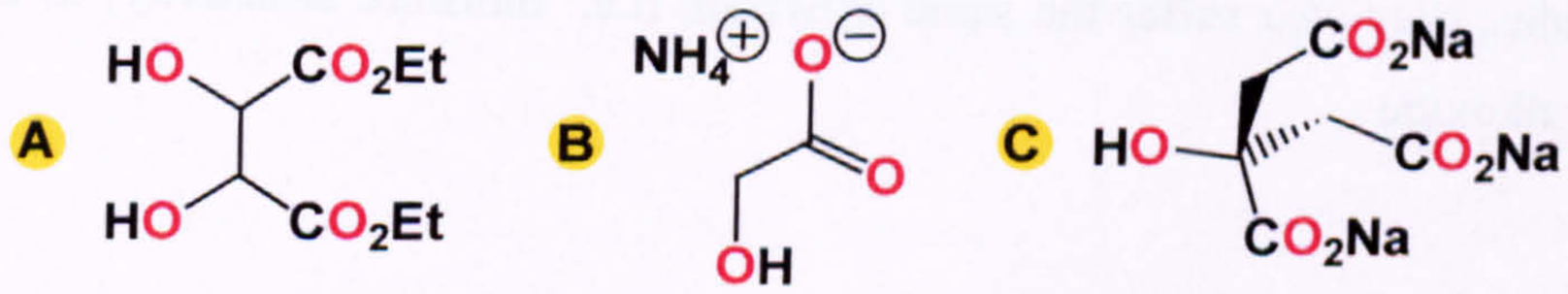

Figure 5.4: Hydroxy-acid derivatives used successfully in titanium chemistry; **A**: diethyl tartrate, **B**: ammonium lactate, **C**: sodium citrate.

5.4 Binuclear complexes

During the course of this project, little work has been carried out on the direct interesterification reaction. Homoleptic titanium (IV) alkoxides show promising activity for this reaction, with activities well in excess of 100 turnovers per hour for $Ti(O^nBu)_4$, and slightly lower activity for $Ti(O^iPr)_4$. These activities are extremely promising, and the higher activity of $Ti(O^nBu)_4$ is suggestive of the involvement of polynuclear species in the catalytic reaction (Figure 5.5). However, the reaction is highly susceptible to moisture, and the mode of action is not entirely understood. The titanium complexes studied in this project show no activity for the direct inter-esterification reaction, suggesting that mononuclear species are not responsible for the catalysis. It is possible that the active species is a transient, alkoxide-bridged, binuclear titanium compound, with two Lewis acid centres cooperating to enhance the reactivity, i.e.: double electrophilic activation.

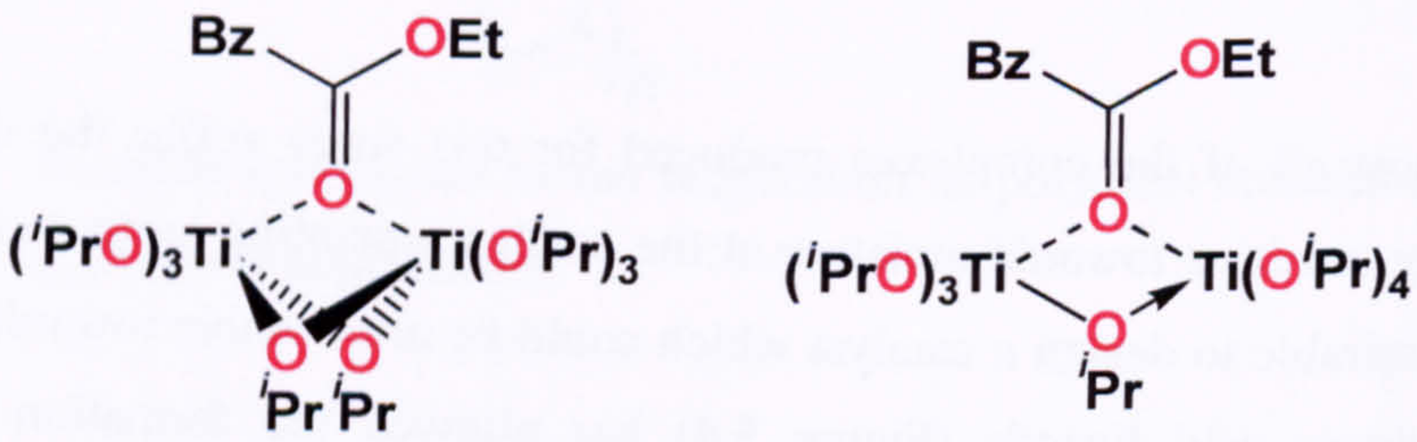

Figure 5.5: Possible intermediates in the transesterification and interesterification reactions, as catalysed by titanium tetra-alkoxides.

Having two electrophilic metal centres pre-arranged to activate the carbonyl centre should, in principle, give enhanced reactivity. This presents the challenge of how to go about rationally designing a binuclear complex. What ligands are suitable? How can the architecture of the end product be controlled, if at all? A large number of bimetallic alkoxide species are known, but most of these derive from simply mixing two different metal alkoxides in the appropriate ratio, and do not contain ligands other than alkoxides; they also suffer the same drawback (i.e.: moisture sensitivity) as any other metal alkoxide.

5.5 Lactide polymerisation

The use of metal alkoxides as lactide polymerisation catalysts is an active field of research due to the benefits of poly-lactides over conventional polymers.[5] Recently, a family of titanium compounds has been tested for lactide polymerisation activity,[6] two of which are used as transesterification catalysts in this thesis, and a third which is structurally almost identical to Ti(TDBA)(O^{i}Pr). This suggests that titanium alkoxides that are active for transesterification may also show activity for lactide polymerisation. Additionally, several catalysts developed by Chisholm *et al.* use ligands based on *tris*-pyrazolyl-borate,[7] which has the same *N*,*N*',*N*'' face-capping coordination mode as the TCT ligand. They reported that the magnesium catalysts were the most active, with the less active zinc catalysts being more robust towards moisture. It is possible that the cobalt and zinc alkoxides may also have potential for lactide polymerisation, where their cationic nature – and, therefore, increased Lewis acid character – could be an advantage in activating the carbonyl group.

5.6 References:

1 J. Otera, N. Dan-oh and H. Nozaki, *J. Org. Chem.*, 1991, **56**, 5307.

2 P. J. Lusby, DPhil Thesis, University of York, 2000.

3 Aldrich Handbook of Fine Chemicals and Laboratory Equipment, 2003 – 4, 1785.

4 M. G. Davidson and M. G. Partridge, *Chem. Br.*, 2002, **38** (7), 26.

5 B. J. O'Keefe, M. A. Hillmyer and W. B. Tolman, *J. Chem. Soc.-Dalton Trans.*, 2001, 2215.

6 Y. Kim, G. K. Jnaneshwara and J. G. Verkade, *Inorg. Chem.*, 2003, **42**, 1437.

7 (a) M. H. Chisholm, N. W. Eilerts, J. C. Huffman, S. S. Iyer, M. Pacold and K. Phomphrai, *J. Am. Chem. Soc.*, 2000, **122**, 11845. (b) M. H. Chisholm and N. W. Eilerts, *Chem. Commun.*, 1996, 853.

Chapter 6: Experimental

6.1 General considerations

Reagents were purchased from Aldrich, Fluka and Lancaster, and were generally used without further purification. TREN was purified by drying over sodium, distilled under vacuum and stored under argon. *o*-Anisidine was distilled under vacuum prior to use. Where dry, degassed solvents were required they were dried in the laboratory and stored under argon.[1] Dichloromethane and acetonitrile were dried by refluxing over calcium hydride for at least 24 h, and then distilled, under an argon atmosphere. Ethanol and methanol were dried by refluxing over magnesium and iodine and collected by distillation under an argon atmosphere. *iso*-Propanol and benzyl alcohol were dried over sodium and collected by distillation, under reduced pressure in the case of benzyl alcohol. Toluene, hexane and diethyl ether were refluxed over sodium-benzophenone ketyl and distilled under argon. Benzyl acetate, ethyl benzoate and ethyl phenyl acetate were refluxed over calcium hydride and distilled under vacuum. Other solvents were used as purchased from Fisher Scientific. Deuterated solvents for NMR spectroscopy were purchased from Aldrich and Goss Scientific Instruments Ltd. Dry gases (N_2, Ar, CO_2, CO) were supplied by BOC Gases PLC. Elemental analyses were performed by Elemental Microanalysis Ltd.

The syntheses of the titanium alkoxide and—where noted—cobalt alkoxide complexes were performed under rigorously anhydrous conditions in the absence of oxygen; Schlenk line techniques (using oven-dried glassware) and glove-boxes (Barrett's and MBraun) were used exclusively. The carousel reactor used in the catalytic investigations was supplied by Radleys Discovery Technologies; equipped with reflux head and gas inlet, using glass reaction tubes fitted with Teflon seals.

6.2 Instrumentation

Instruments for acquisition of data were as follows:

UV/vis spectroscopy: Perkin-Elmer Lambda 7 spectrophotometer.

FTIR spectroscopy: Unicam RS 10000-E spectrophotometer.

NMR spectroscopy:	JEOL 270 MHz (^{1}H and ^{13}C), Bruker AMX 300 MHz (^{1}H and ^{13}C), Bruker AMX 500 MHz (^{1}H, ^{13}C and ^{19}F) spectrometers as noted.
Gas chromatography:	Varian gas chromatograph with flame ionisation detector (FID).
Mass spectrometry:	MICROMASS Autospec – Double Focussing Magnetic Sector Instrument with EBE geometry, and Finnigan-MAT (Thermo Systems Inc.) LCQ – Atmospheric Pressure Ionisation Ion Trap Instrument.
X-ray crystallography:	Bruker Smart Apex diffractometer (see Appendix 3 for full details of diffraction and refinement methods).

6.3 Synthesis of ligand precursors

6.3.1 *Tris*(2-methoxyphenyl)amine[2]

2-Methoxyaniline (3.69 g, 30 mmol), 2-iodoanisole (16.3g, 70 mmol), K_2CO_3 (20.9 g, 151 mmol), 18-crown-6 (1.0 g, 4 mmol) and Cu powder (6.6 g, 100 mmol) were combined and dissolved / suspended in 1,2-dichlorobenzene (100 mL) and heated to 170°C under reflux conditions. After 48 h the mixture was cooled and the solids were separated by filtration. The solids were washed with CH_2Cl_2 (4 × 200 mL) and all filtrates were combined (dark brown solution). The solution was washed with dilute aqueous ammonia solution (3 × 100 mL), and equal an amount of water. The dark brown organic phase was dried over $MgSO_4$. The solids were removed by filtration, the solution was reduced in volume to 10 mL and hexane (50 mL) was added to precipitate a brown solid. The solid was separated and washed with hexane (50 mL). The filtrates were combined, reduced in volume to 10 mL, and hexane (50 mL) was added; the solution was decanted off and cooled to precipitate a second batch of product. All the solids were combined and recrystallised from ethanol / hexane (2:1). Yield: 7.55 g (22.5 mmol, 75%).

- ^{1}H NMR ($CDCl_3$, 300 MHz): δ 7.0 (m, 3H, arom), δ6.78 (m, 9H, arom), δ3.54 (s, 9H, OCH_3).

- Mass spectrum: [ESI] $m/z^+ = 336$ (M + 1).

6.3.2 *Cis,cis*-1,3,5-cyclohexane-*tris*(benzyl carbamate)[3]

Cis,cis-1,3,5-tricarboxylic acid cyclohexane (10 g, 46.3 mmol) was suspended in 300 mL benzene (previously dried over $MgSO_4$, then filtered) in a 1 L round-bottomed flask. To this was added, dropwise, 20 mL (14 g, 139 mmol) triethylamine with vigorous stirring, followed by 31 mL (38.3 g, 139 mmol) diphenyl phosphoryl azide. The mixture was stirred for 30 minutes at room temperature, then heated to reflux (65°C) and stirred for two hours (until all solid had dissolved), during which time the evolution of gas was observed. 16 mL (16.7 g, 154 mmol) benzyl alcohol was added slowly, and the mixture was stirred at reflux for 16 h, during which time a white precipitate formed. The solid was filtered off and washed with minimal chilled benzene and dried under vacuum. Yield: 8.90g (16.7 mmol, 36.2%).

- ^{1}H NMR (d_6-DMSO, 300 MHz): δ 7.34 (m, 15H, arom), 5.0 (s, 6H, OCH_2Ph), 3.06 (q, 3H, J = 7.1 Hz), 1.88 (br d, 3H, J = 8.2 Hz), 1.16 (q, 3H, J = 11 Hz).

6.3.3 *Cis,cis*-1,3,5-triaminocyclohexane.3HBr (TACH.3HBr)

cis,cis-1,3,5-cyclohexane-tris(benzyl carbamate) (8.9 g, 16.7 mmol) was placed in a 250 mL round-bottomed flask with a magnetic stirrer bar. To this was added 100 mL of a 30 wt% solution of HBr in acetic acid. The mixture was stirred at room temperature for two hours to give a fine powder, which was filtered over sintered glass (porosity 4) and then dried, under vacuum. The solid was then suspended in 300 mL diethyl ether and left stirring overnight. The ether was filtered off to leave a white powder, yield: 3.95g (10 .6 mmol, 63.4%).

- ^{1}H NMR (D_2O, 300 MHz): δ 3.49 (tt, 3H, J = 12.2 Hz, 3.8 Hz, HCNH$_2$), 2.46 (dt, 3H, J = 7.6 Hz, 3.8 Hz, CH_{eq}), 1.62 (q, 3H, J = 12.2 Hz, CH_{ax}).

6.3.4 *Cis,cis*-1,3,5-triaminocyclohexane.3CF_3SO_3H (TACH.3HOTf)

Cis,cis-1,3,5-cyclohexane-tris(benzyl carbamate) (18.9 g, 16.7 mmol) was dissolved in 100 mL trifluoroacetic acid in a 1 L round-bottomed flask, which was clamped securely in an ice bath. To this was added, slowly, with stirring, 25 mL trifluoromethanesulphonic acid via a pressure-equalised dropping funnel over 30 minutes. 350 mL Et_2O was added, and the mixture was stirred for 1 hour. The solid was separated by filtration, washed with chilled ether and dried in a dessicator overnight. The off-white solid was dissolved in 200 mL H_2O and filtered to remove insoluble material. Solvent was removed carefully on a rotary evaporator, and the solid was dried under reduced pressure. The solid was ground up, stirred with Et_2O to remove residual HOTf, filtered and dried first under vacuum and then in a dessicator. Yield: 9.72 g (16.8 mmol, 60% yield; 36 % overall yield from the starting acid).

- ^{1}H NMR (D_2O, 300 MHz): δ 3.49 (tt, 3H, J = 12.2 Hz, 3.8 Hz, *H*CNH_2), 2.46 (dt, 3H, J = 7.6 Hz, 3.8 Hz, CH_{eq}), 1.62 (q, 3H, J = 12.2 Hz, CH_{ax}).

6.3.5 Synthesis of benzyl-TACH ligand precursor[4,5]

Note that this ligand backbone contains a *tert*-butyl substituent on the benzyl group; this is to lower the solubility in water, allowing for more facile isolation of the free amine.

6.3.5 a *Cis,cis*-1,3,5-*tris*({4'-*tert*-butyl}benzylideneamino) cyclohexane (TBT)

TACH.3HOTf (4.64 g, 8 mmol) and NaOH (0.96 g, 24 mmol) were dissolved in 5 mL H_2O and 10 mL MeOH. To this was added a solution of 4-*tert*-butylbenzaldehyde (3.89 g, 24 mmol) in 15 mL MeOH, and the mixture was stirred vigorously overnight. Separation of the dense white precipitate, followed by recrystallisation from minimal hot ethanol, gave the desired product as white, needle-shaped crystals. Yield: 2.82 g (5.03 mmol, 63%).

- ^{1}H NMR ($CDCl_3$, 300 MHz): δ 8.3 (s, 3H, N=C*H*-Ar), 7.65 (d, 6H, C*H* arom), 7.4 (d, 6H, C*H* arom), 3.5 (t, 3H, N-CH_{ring}), 2.0 (q, 3H, CH_{ax}), 1.85 (d, 3H, CH_{eq}), 1.3 (s, 27H, C(CH_3)$_3$).
- Mass spectrum: [ESI] $m/z^+ = 562$.

6.3.5 b {r-1-[(Z)-{4'-*tert*-butyl}benzylideneamino]-3,5-diamino cyclohexane} $Ni^{II}(NO_3)_2$ [Ni(MBT)$(NO_3)_2$]

TBT (2.94 g, 5.24 mmol) was dissolved in 15 mL MeOH and 15 mL CH_2Cl_2. $[Ni(H_2O)_6](NO_3)_2$ (1.52 g, 5.24 mmol) was dissolved in 15 mL MeOH and 15 mL CH_2Cl_2. The two solutions were mixed together and stirred overnight, resulting in a turquoise solution. The solvent volume was reduced to 15 mL, and Et_2O (60 mL) was added to precipitate the product as a pale blue solid. The product was washed with 2 × 20 mL Et_2O and dried in a dessicator. Yield: 1.81 g (4.52 mmol, 86%).

6.3.5 c (1-{(4'-*tert*-butyl)benzylamino}-3,5-diaminocyclohexane) $Ni^{II}(NO_3)_2$ [Ni(BzTACH)$(NO_3)_2$]

Ni(MBT)$(NO_3)_2$ (1.81 g, 4.52 mmol) was dissolved in 400 mL MeOH and clamped in a salt water ice bath. $NaBH_4$ (0.86 g, 22.6 mmol) was added in portions, with stirring, over 30 min, during which time the solution became black. The solution was refluxed for 1 h, then the solvent volume was reduced to 120 mL and 300 mL water was added to quench the reaction. The complex was not isolated, and the resulting grey suspension was used directly in the demetallation step below.

6.3.5 d *Cis,cis*-1-{(4'-*tert*-butyl)benzylamino}-3,5-diamino cyclohexane (BzTACH)

Ni(BzTACH)$(NO_3)_2$ (4.52 mmol, assuming 100% yield from previous step) as a suspension in MeOH / H_2O, was treated with KCN (1.47 g, 22.6 mmol, 5 eq.) in portions over 30 min with continuous stirring. The reaction mixture was heated to reflux for 2 hours.

- ^{1}H NMR (CD_2Cl_2, 300 MHz): δ 7.4 (m, 4H, arom), 3.72 (s, 2H, N–C*H*$_2$–Ar), 2.6 (m, 3H), 2.1 (m, 3H), 1.24 (s, 9H, C(C*H*$_3$)$_3$), 0.9 (q, 3H).
- Mass spectrum: [ESI] $m/z^+ = 276$ [M + 1].

6.4 Synthesis of ligands

6.4.1 *Tris*{(2-hydroxy)phenyl}amine (TPA-H$_3$)[5]

Tris(2-methoxyphenyl)amine (6.44 g, 5.8 mmol) was dissolved in dry CH_2Cl_2 (150 mL) and cooled to –78°C. To this was added a solution of boron tribromide (14.94 g, 19.2 mmol) in 40 mL dry CH_2Cl_2 (40 mL) over 30 min. Evolution of white gas (HBr) was observed. The solution was stirred for 1 h and warmed to room temperature, then left stirring overnight. 200 mL H_2O was then added (evolution of gas) and the mixture was stirred for 30 min. The organic layer was separated, and the aqueous layer was washed with 3 × 50 mL Et_2O. All the organic residues were combined and dried over Na_2SO_4. Removal of solvent gave a brown solid which was recrystallised from acetone / hexane to give colourless crystals which were ground to a white solid and dried thoroughly under vacuum. Yield: 1.43 g (4.88 mmol, 84%).

- ^{1}H NMR ($CDCl_3$, 300 MHz): δ 7.07 (t, 3H, aryl), 6.9 (m, 9H, aryl), 5.26 (s, 3H, hydroxyl).
- ^{13}C NMR ($CDCl_3$, 300 MHz): δ 151.0, 134.5,127.4, 126.5, 122.0, 117.7.
- Mass spectrum: [ESI] $m/z^+ = 294$ (M + 1).

6.4.2 *Tris*{(2-hydroxy-3,5-dimethyl)benzyl}amine (TDMA-H$_3$)

Method 1:

Hexamethylenetetra-amine (3.80 g, 27.1 mmol), 2,4-dimethylphenol (15.0 mL, 124 mmol) and *para*-toluenesulphonic acid (0.10 g) were reacted together using the method described by Holmes *et al.*[6] Yield: 15.4 g (36.7 mmol, 67%). The product was further purified by recrystallisation from acetone / hexane to give colourless crystals which were ground to a white solid and dried in a dessicator.

- ^{1}H NMR ($CDCl_3$, 300 MHz): δ 6.84 (3H, s, aryl-*H*), 6.72 (3H, s, aryl-*H*), 3.57 (6H, s, N-C*H*$_2$-Ar), 2.17 (9H, s, C*H*$_3$), 2.14 (9H, s, C*H*$_3$).
- Mass spectrum: [ESI] $m/z^+ = 420$ (M^+).

Method 2:

Hexamethylenetetra-amine (0.94 g, 6.6 mmol), 2,4-dimethylphenol (10.0 g, 80 mmol) and 37% aqueous formaldehyde (2.3 mL, 28.4 mmol) were reacted together using the method described by Dargaville *et al.*[7] The product was recrystallised from acetone / hexane to give a white solid. Yield: 5.13 g (12.2 mmol, 45%).

6.4.3 *Tris*{(2-hydroxy-3,5-di-*tert*-butyl)benzyl}amine (TDBA-H$_3$)

Hexamethylenetetra-amine (0.47 g, 3.3 mmol), 2,4-di-*tert*-butylphenol (8.25 g, 40 mmol) and 37% aqueous formaldehyde (1.15 mL, 14.2 mmol) were reacted together using the method described by Kol *et al.*[8] (Note that their method was based on that of Dargaville *et al.*[7])The product was recrystallised from Et_2O / MeOH, resulting in a white solid. Yield: 6.36 g (9.5 mmol, 71%).

- ^{1}H NMR ($CDCl_3$, 270 MHz): δ 7.19 (s, 3H, C*H* arom), 7.16 (s, 3H, C*H* arom), 4.78 (s, 3H, C*H*H), 3.98 (s, 3H, CH*H*), 1.31 (s, 27H, C(C*H*$_3$)$_3$), 1.20 (s, 27H, C(C*H*$_3$)$_3$).
- Mass spectrum: [ESI] $m/z^+ = 672$ (M^+).

6.4.4 *Tris*{(2-benzylamino)ethylene}amine (H$_3$-Bz$_3$TREN)

Tris-(2-aminoethylene)-amine (TREN, 3.66 g, 25 mmol), benzaldehyde (7.96 g, 75 mmol) and $NaBH_4$ (3.6 g, 95 mmol) were reacted together using the method described by Verkade *et al.*[9] Yield: 6.88 g (16.5 mmol, 66%).

- ^{1}H NMR ($CDCl_3$, 300 MHz): δ 7.2 (m, 15H, CH arom), 3.71 (s, 6H, NC*H*$_2$Ph), 2.64 (t, 6H, C*H*$_2$), 2.55 (t, 6H, C*H*$_2$), 1.96 (br, 3H, N*H*).
- ^{13}C NMR ($CDCl_3$, 300 MHz): δ 140.4 (C_{ipso}, arom), 128.31 (C_{meta}, arom), 128.02 (C_{ortho}, arom), 126.78 (C_{para}, arom), 54. 37 (C benzyl), 53.99 (C_2 ethylene), 47.13 (C_1 ethylene).

- Mass spectrum: [ESI] $m/z^+ = 417.2$ (M + 1).

6.4.5 Attempted synthesis of *tris*{(2-mercapto-3,5-dimethyl)benzyl} amine (TDMMA-H_3)

Berreau *et al.* have recently reported the preparation of a zinc hydroxide complex with an N_2S_2 ligand, which was active as a transesterification catalyst.[10] The formation of a stable, monomeric zinc complex with the seemingly unsuitable sulfur ligands, combined with the high transesterification activity, led us to investigate the possibility of synthesising a titanium complex bearing thiolate donors in the supporting ligand. Replacing the hydroxy functions of TDMA with thiol groups would give a potential chelating ligand. Although the thiolate function is seemingly an unsuitable donor for titanium according to hard / soft donor rules, Bradley *et al.* reported the synthesis of titanium thiolates as early as 1967,[11] and the preparation and isolation of homoleptic titanium (IV) thiolates has been reported,[12] which suggests that carefully controlled reaction conditions should allow formation of the desired complex.

Reaction was attempted using 2,4-dimethylbenzenethiol with HMTA and formaldehyde under the same conditions as for the synthesis of TDMA-H_3 (i.e.: 48 h reflux at 400 K). The viscous yellow oil obtained was purified using the same work-up procedure as for TDMA-H_3. Characterisation was performed by mass spectrometry and ^{1}H NMR spectroscopy. Although mass spectrometry indicated the correct mass, ^{1}H NMR spectroscopy clearly showed that all of the original aromatic protons were still present. The product was assigned as a mixture of thioethers; attack had apparently taken place at the thiol function, not on the aromatic ring. This reaction was not pursued further, due to time constraints.

6.4.6 *Cis,cis*-1,3,5-*tris*(*E,E*-cinnamylideneamino)cyclohexane (TCT)

Method 1:[3]

TACH.3HBr (1.41 g, 3.8 mmol) and NaOH (459 mg, 11.4 mmol) in H_2O (15 mL) were stirred vigorously overnight with cinnamaldehyde (1.50 g, 11.4 mmol) in Et_2O (15 mL). The white precipitate was separated by filtration and washed with chilled Et_2O (3 × 20 mL). Removal of residual HBr was achieved by dissolving the TCT in

CH_2Cl_2 and washing 3 times with equal volume of deionised water. The solvent was removed on a rotary evaporator and the product was dried in a dessicator for 24 h. Yield: 1.49 g (3.15 mmol, 83%).

- ^{1}H NMR ($CDCl_3$, 270 MHz): δ 8.12 (t, 3H, imine), δ7.46 (m, 6H, aryl), δ7.34 (m, 9H, aryl), δ6.95 (s, 3H, alkene), δ6._4 (s, 3H, alkene), δ3.41 (m, 3H, C*H* ring), δ1.93 (m, 6H, CH_2, ring).
- Mass spectrum: [ESI] $m/z^+ = 472.3$.

Method 2 (solventless):[13]

TACH (0.23 g, 1.78 mmol) and cinnamaldehyde (0.71 g, 5.35 mmol) were ground together intermittently over 1 h using a mortar and pestle, during which time the mixture changed from a pale yellow solution to a sticky off-white solid. The reaction mixture was left overnight, then washed with chilled Et_2O (3 × 20 mL) and dried in a dessicator for 1 day. The white powder was washed with ether again and returned to the dessicator. Yield: 0.35 g (0.75 mmol, 42%).

6.4.7 Synthesis of *cis,cis*-1,3-*bis*-cinnamylideneamino-5-{(4-*tert*-butyl) benzylamino}cyclohexane (Cin$_2$BzTACH)[14]

BzTACH (112 mg, 407 μmol) and cinnamaldehyde (108 mg, 813 μmol) were dissolved in MeOH with a catalytic quantity of formic acid and heated to reflux with stirring for 18 h, with the solvent passing over activated 3 Å molecular sieves in a Soxhlet apparatus to remove water. The product was isolated as a brown, sticky oil. ^{1}H NMR suggested that the product had been formed, albeit with impurities, although mass spectral evidence did not support this.

6.4.8 *Cis,cis*-1,3-*bis*{(2-hydroxy-3,5-di-*tert*-butyl)benzylideneamino}-5-{(4-*tert*-butyl)benzylamino}cyclohexane ({^{t}Bu$_2$Sal-H}$_2$BzTACH)[5]

- Ligand sample supplied by Oliver Niemeier.
- Ligand prepared by refluxing BzTACH with 2 eq. of the salicylaldehyde in MeOH in a Soxhlet apparatus with activated 3 Å molecular sieves in thimble.

6.5 Synthesis of titanium complexes

6.5.1 Ti(TPA)(O^{i}Pr)

Tris(2-hydroxyphenyl)amine (TPA-H_3, 147 mg, 0.5 mmol) was dissolved in 10 ml CH_2Cl_2 and 2 mL ^{i}PrOH in a Schlenk tube. Ti(O^{i}Pr)$_4$ (142 mg, 0.5 mmol) was dissolved in 10 ml CH_2Cl_2 and 2 mL ^{i}PrOH in a separate Schlenk tube and added slowly by cannula to the solution of TPA-H_3, with stirring. The yellow solution that formed was left to stir for 2 h, then transferred to a clean Schlenk tube by cannula filter, and the solvent was removed under vacuum. The product was isolated as a yellow powder that contained ~3 equivalents of ^{i}PrOH even after extended drying under vacuum.

- ^{1}H NMR (C_6D_6, 300 MHz): δ 7.44 (d, 3H, C*H* arom), 6.90 (t, 3H, C*H* arom), 6.62 (d, 6H, C*H* arom), 4.86 (br, 1H, OC*H*Me$_2$), 1.41 (br, 6H, CH(C*H*$_3$)$_2$).
- Mass spectrum: [EI] m/z^+ = 397 ([Ti(TPA)(O^{i}Pr)]$^+$), 355 ([Ti(TPA)(OH)]$^+$), 338 ([Ti(TPA)]$^+$).

6.5.2 Ti(TDMA)(O^{i}Pr)

Ti(O^{i}Pr)$_4$ (220 mg, 0.76 mmol) was dissolved in 15 mL Et_2O. To this was added a solution of TDMA-H_3 (330 mg, 0.76 mmol) in 15 mL Et_2O, and the resulting yellow solution was stirred overnight and the volatiles were removed to give an orange solid, which was precipitated from cold Et_2O to give a yellow solid. Yield: 373 mg (0.71 mmol, 94%).

- ^{1}H NMR (C_6D_6, 500 MHz): δ 6.75 (s, 3H, arom), 6.45 (s, 3H, arom), 5.31 (hept, 1H, C*H*(CH$_3$)$_2$), 3.9 (br, methylene), 2.31 (br, methylene), 2.31 (s, 9H, CH$_3$), 2.13 (s, 9H, CH$_3$), 1.58 (d, 6H, CH$_3$).
- ^{13}C NMR (C_6D_6, 125.76 MHz): δ 160.5 (*C*O arom), 131.1 (C_{quat} arom), 129.3 (C_{quat} arom), 124.6 (*C*H arom), 124.1 (*C*H arom), 80 (CH alkoxide), 58.8 (CH_2), 25.6 (CH$_3$ alkoxide), 20.9 (CH$_3$ arom), 16.7 (CH$_3$ arom).
- UV/vis (CH_2Cl_2 / ^{i}PrOH, 9:1 *v/v*): λ_{max} / nm 326 (ε / dm^3 mol^{-1} cm^{-1} 1.02 × 10^4), 266 (2.51 × 10^4), 260 (2.6 × 10^4).

- Mass spectrum: [ESI] m/z^+ = 523 [Ti(TDMA)(O^{i}Pr)]$^+$, 505 [Ti(TDMA)(MeCN)]$^+$, 464 [Ti(TDMA)]$^+$.

  (MeCN added to mass spectrometry sample for conductance.)

6.5.3 Ti(TDBA)(O^{i}Pr)

$Ti(O^iPr)_4$ (200 mg, 0.7 mmol) was dissolved in 10 mL Et_2O. To this was added a solution of TDBA-H_3 (472 mg, 0.7 mmol) in 10 mL Et_2O, and the resulting yellow solution was stirred for 2 h. Removal of solvent afforded a yellow powder, and the product was obtained by recrystallisation from cold Et_2O. Yield: 500 mg (0.64 mmol, 92%).

- ^{1}H NMR (C_6D_6, 500 MHz): δ 7.43 (d, J = 2.4 Hz, 3H, arom), 6.8 (d, J = 2.3 Hz, 3H, arom), 5.45 (hept, 1H, J = 6.1 Hz, C*H*(CH$_3$)$_2$), 4.02 (d, 3H, J = 13.4 Hz, C*H*H), 2.6 (d, 3H, J = 13.5 Hz, CH*H*), 1.7 (d, 6H, J = 6.1 Hz, CH(C*H*$_3$)$_2$), 1.64 (s, 27H, C(C*H*$_3$)$_3$), 1.33 (s, 27H, C(C*H*$_3$)$_3$).
- ^{13}C NMR (C_6D_6, 125.76 MHz): δ 161.1 (*C*O arom), 142.6 (C_{quat} arom), 135.6 (C_{quat} arom), 124.5 (*C*H arom), 123.1 (*C*H arom), 79.8 (*C*H alkoxide), 59.3 (*C*H$_2$), 35.4 (C_{quat}), 34.5 (C_{quat}), 31.9 (*C*H$_3$), 29.9 (*C*H$_3$), 26.9 (*C*H$_3$).
- UV/vis (CH_2Cl_2 / ^{i}PrOH, 9:1 *v/v*): λ_{max} / nm 327 (ε / dm^3 mol^{-1} cm^{-1} 1.05 × 10^4), 266 (2.3 × 10^4), 260 (2.41 × 10^4).
- Mass spectrum: [ESI] m/z^+ = 776 [Ti(TDBA)(O^{i}Pr)]$^+$, 717 [Ti(TDBA)]$^+$.

6.5.4 [Ti({^{t}Bu$_2$Sal}$_2$BzTACH)(O^{i}Pr)]BPh$_4$

TiCl(O^{i}Pr)$_3$ (18.4 mg, 70.6 μmol as a 1 M solution in hexanes) in CH_2Cl_2 (30 mL) was added to a solution of ({^{t}Bu$_2$Sal-H}$_2$BzTACH) (50 mg, 70.6 μmol) and $NaBPh_4$ (24.2 mg, 70.6 μmol) in CH_2Cl_2 (30 mL) and EtOH (5 mL). The resulting yellow solution was stirred for 1 h, then transferred by cannula filter to remove solids. The solvent was removed to give an orange solid, which was extracted with CH_2Cl_2 (leaving a small quantity of white solid behind).

- ^{1}H NMR (CD_2Cl_2, 300 MHz): δ 8.4 (m, imine), 7.44 (d, C*H* arom), 7.35 (m, C*H* arom), 7.29 (m, BPh_4), 7.00 (t, BPh_4), 6.84 (t, BPh_4), 3.4 (q, C*H* ring), 2.18 (m, C*H* ring), 1.95 (m, C*H* ring, 1.40 (CH_3 ^{i}Pr), 1.28 (^{t}Bu).
- Mass spectrum: [ESI] m/z^+ = 812 ([Ti({^{t}Bu$_2$Sal}$_2$BzTACH)(O^{i}Pr)]$^+$).

6.5.5 $TiCl_3(O^nBu)$

Bradley *et al.* described the preparation of mixed titanium chloride / alkoxide compounds by simply mixing $TiCl_4$ and $Ti(OR)_4$ in the correct ratios.[15] Due to the strongly exothermic nature of the reaction, this procedure was performed in solution to allow for moderation of the heat produced.

$TiCl_4$ (5.7 g, 30 mmol) was added slowly to a stirred solution of $Ti(O^nBu)_4$ (3.4 g, 10 mmol) in toluene (30 mL). The solution was allowed to stir for 30 minutes and the solvent was removed under vacuum to give an off-white solid, which was pumped dry under vacuum. Yield: 8.9 g (39.1 mmol, 98%).
The product was used immediately in Reaction 6.5.6, below.

6.5.6 $Ti(Bz_3TREN)(O^nBu)$

H_3-Bz_3TREN (1.04 g, 2.5 mmol) was dissolved in 30 mL dry THF and cooled to –78°C using a dry ice / acetone bath. A 1.6 M solution of ^{n}BuLi in hexanes (4.7 mL, 7.5 mmol) was added slowly with stirring to give a deep purple solution. $TiCl_3(O^nBu)$ (568 mg, 2.5 mmol), dissolved in 30 mL dry THF, was added slowly to this solution, with stirring. The solution gradually changed through yellow to olive in colour, and was left stirring for 48 h. After this time, the solution was filtered by cannula, and the solvent was removed under vacuum to give an olive-green microcrystalline solid. The solid became waxy after several days, and was redissolved in toluene and filtered by cannula; removing the solvent under vacuum gave a grey solid. Yield: 577 mg (1.08 mmol, 43%).

- ^{1}H NMR (d_8-THF, 300 MHz): δ 7.37 (m, 6H, CH_{mcta} arom), 7.2 (m, 9H, C$H_{ortho,para}$ arom), 3.8 (s, 6H, NCH_2Ph), 3.46 (t, 2H, OCH_2), 2.56 (2 × t, 12H, NC_2H_4N), 1.4 (m, 4H, C_2H_4 alkoxide) 0.9 (t, 3H, CH_3).
- Mass spectrum: Inconclusive.

6.6 Synthesis of cobalt complexes

6.6.1 $[Co(TCT)(NO_3)]BPh_4$[16]

To a stirred solution of $[Co(H_2O)_6](NO_3)_2$ (466 mg, 16 mmol) and TCT (755 mg, 16 mmol) in 150 mL EtOH was added a solution of $NaBPh_4$ (548 mg, 16 mmol) in EtOH (40mL). The reaction mixture was stirred for 16 h, after which time a purple precipitate had formed. The purple solid was recovered by filtration and dried in a dessicator. Yield: 1.23 g (1.35 mmol, 81%).

- ^1H NMR (CD_2Cl_2, 300 MHz): δ 367.8 (br, $H_d/_c$), 328.2 (br, $H_c/_d$), 11.81 (br, H_e), 8.01 ($H_f/_j$), 7.79 (H_h), 7.61 (BPh_4^- *meta*), 7.35 (BPh_4^- *para*), 7.23 (BPh_4^- *ortho* + $H_g/_i$), 1.25 (H_b), -12(br, H_k). See Figure 6.1 for labelling scheme. Notes on acquisition: 2048 scans run, 0.2 s time delay between pulses.

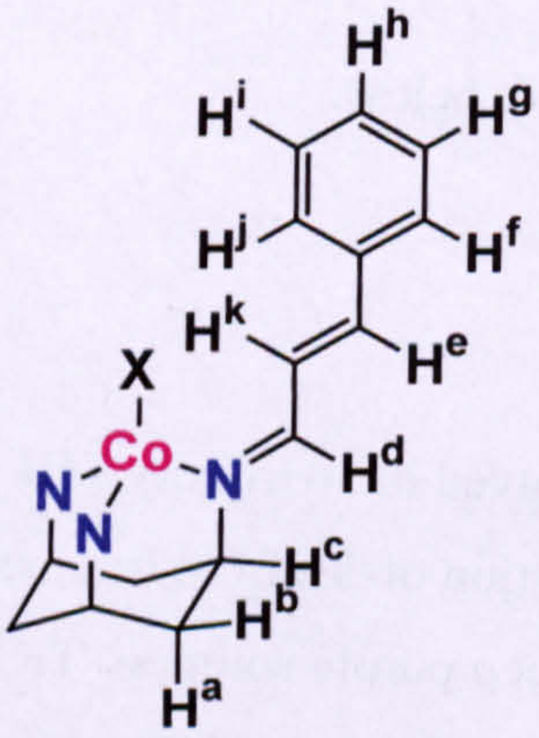

Figure 6.1:
Proton labels for $[Co(TCT)(X)]^+$.
X = Cl, NO_3

- UV/vis: λ_{max} / nm (CH_2Cl_2) 547.
- IR / cm^{-1}: [FTIR, KBr pressed disc] 3054, 3031, 3000, 2985, 2919, 1626, 1607, 1592, 1523, 1480, 1454, 1423, 1385, 1266, 1181, 1116, 1001, 751, 732, 705, 690, 609, 560, 514.
- Mass spectrum: [ESI] $m/z^+ = 592$ $[Co(TCT)(NO_3)]^+$.

6.6.2 $[Co(TCT)Cl]BPh_4$

To a stirred solution of $[Co(H_2O)_6](Cl)_2$ (95 mg, 4 mmol), TCT (200 mg, 4 mmol) and $NaBPh_4$ (140 mg, 4 mmol) were reacted together using the method described by Freeman[3] and Greener.[16] Yield: 280 mg (3.2 mmol, 79%).

- ^{1}H NMR (CD_2Cl_2, 300 MHz): δ 430 (br, $H_d/_c$), 393 (br, $H_c/_d$), 20.9 (s, H_e), 8.4 ($H_f/_j$), 7.9 (H_h), 7.7 (BPh_4 – H_{meta}), 7.2 (BPh_4 – H_{ortho}), 7.0 (sh, BPh_4 – H_{para}), 6.95 ($H_g/_i$), 1.5 (H_b), –3.2 (br, H_k), –24.5 (br, H_a). See Figure 6.1 for labelling scheme. Notes on acquisition: 2048 scans run, 0.2 s time delay between pulses.
- UV/vis: λ_{max} / nm (CH_2Cl_2) 593.
- IR / cm^{-1}: [FTIR, KBr pressed disc] 3056, 3031, 2999, 2985, 2920, 1630, 1607, 1594, 1482, 1451, 1426, 1404, 1271, 1175, 1125, 1000, 844, 749, 734, 706, 689, 614, 601, 561, 511.
- Mass spectrum: [ESI] m/z^+ = 565, 567 (3:1 relative intensity, ^{35}Cl / ^{37}Cl) $[Co(TCT)Cl]^+$.

6.6.3 [Co(TCT)(OEt)]BPh_4

$[Co(TCT)(NO_3)]BPh_4$ (250 mg, 0.27 mmol) was dissolved in CH_2Cl_2 (20 mL) in a Schlenk tube, and 1.9 mL of a solution of NaOEt in EtOH (19 mg NaOEt, 0.3 mmol, 1.1 eq.) was added with stirring. A colour change from dark-purple to mid-purple was noted. After 15 min the solution was filtered by cannula and the solvent was removed to produce a purple powder. Yield: 206 mg (0.23 mmol, 84%). Crystals suitable for X-ray diffraction were grown by slow evaporation of a concentrated solution of the complex in CH_2Cl_2 / EtOH in a glovebox under Ar.

- ^{1}H NMR (CD_2Cl_2 / d_6-EtOH, 300 MHz): δ 430 (br, $H_d/_c$), 374 (br, $H_c/_d$), 16.14 (H_e), 9.72 ($H_f/_j$), 9.41 (H_h), 7.32 ($H_g/_i$), 1.8 (H_b), –7 (H_k), –18 (H_a). See Figure 6.2 for labelling scheme. Notes on acquisition: 1024 scans run, 0.2 s delay between pulses.

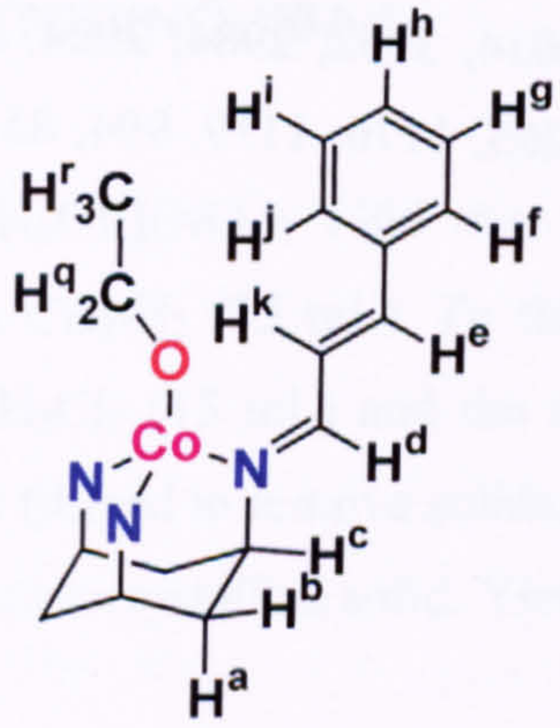

Figure 6.2:
Proton labels for $[Co(TCT)(OEt)]^+$.

- UV/vis: λ_{max} / nm (9 CH_2Cl_2 : 1 EtOH) 635 (ε / dm^3 mol^{-1} cm^{-1} 239), 554 (362), 486 (291).

- IR / cm^{-1}: [FTIR, KBr pressed disc] ν(CN) = 1628, ν(CC, aromatic) = 1604, ν(CC, alkenic) = 1593.
- Mass spectrum: [ESI] m/z^+ = 575 (M^+). High resolution FAB–MS was attempted for additional proof of structure, but the compound decomposed under these conditions.

6.6.4 [Co(TCT)(OPh)]BPh_4

[Co(TCT)Cl]BPh_4 (100 mg, 110 μmol) and NaOPh (40 mg, >1 eq.) were reacted together using the method described by Freeman.[3] Yield: 74 mg (78 μmol, 69%).

- ^{1}H NMR (CD_2Cl_2, 300 MHz): δ 367 (br, $H_{d/c}$), 366 (br, $H_{c/d}$), 37.35 ($H_{m/o}$), 19.05 (H_e), 9.39 ($H_{f/j}$), 9.13 (H_h), 7.7 (BPh_4 – H_{meta}), 7.1 (BPh_4 – H_{ortho} + $H_{g/i}$), 6.8 (BPh_4 – H_{para}), 1.42 (H_b), –6 (H_k), –9.75 (H_a), –31.4 (H_n), –39.5 ($H_{l/p}$). See Figure 6.3 for labelling scheme. Notes on acquisition: 1024 scans run, 0.2 s delay between pulses.

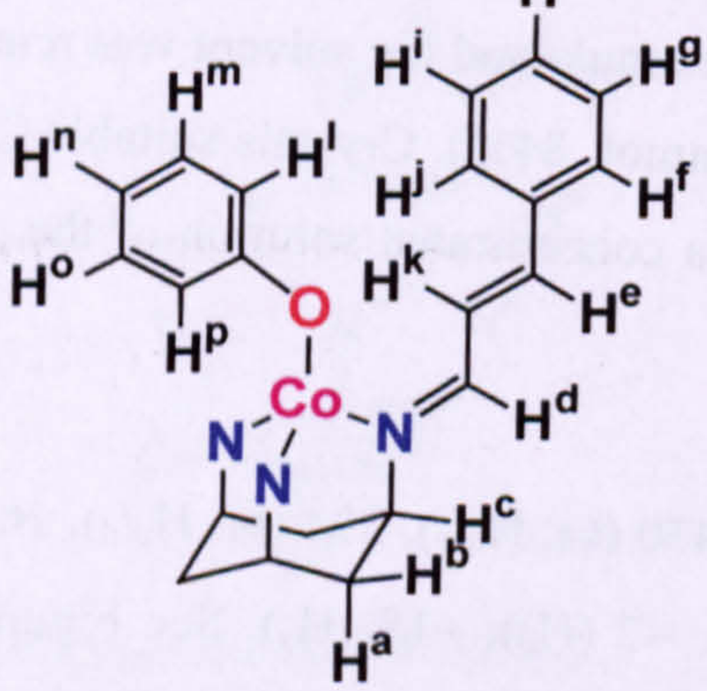

Figure 6.3:
Proton labels for $[Co(TCT)(OPh)]^+$.

- UV/vis: λ_{max} / nm (CH_2Cl_2) 645, 561, 507.
- IR / cm^{-1}: [FTIR, KBr pressed disc] 3056, 3034, 3002, 2984, 2924, 2849, 1628, 1605, 1592, 1480, 1451, 1426, 1401, 1281, 1265, 1176, 1119, 994, 851, 751, 733, 708, 690, 613, 558, 513.S
- Mass spectrum: [ESI] m/z^+ = 623 (M^+).

6.6.5 [Co(TCT)(OBz)]BPh_4

[Co(TCT)(NO_3)]BPh_4 (500 mg, 0.55 mmol) was dissolved in CH_2Cl_2 (20 mL) in a Schlenk tube, and NaOBz (0.57 mol, >1 eq., as a 1 M solution in BzOH) was added

with stirring. A slight colour change from dark-purple to mid-purple was noted. After 2 h the solution was filtered by cannula and the solvent was removed to produce an oily purple solid. Toluene was added, briefly producing a purple solution; after 15 min a purple solid settled out. The liquids were removed by cannula and the solid was dried under vacuum. Yield: 458 mg (0.48 mmol, 87%).

- ^{1}H NMR (CD_2Cl_2 / BzOH, 300 MHz): δ 375 (br, $H_d/_c$), 363 (br, $H_c/_d$), 20.3 (H_e), [14.53 ($H_l/_p$), 13.46 (H_n)], 10.05 ($H_f/_j$), 8.68 (H_h), 2.33 (H_b), –4.12 (H_k), –8.8 (br, H_a), [–9.5 ($H_m/_o$)]. See Figure 6.4 for labelling scheme. Notes on acquisition: 2048 scans run, 0.2 s delay between pulses.

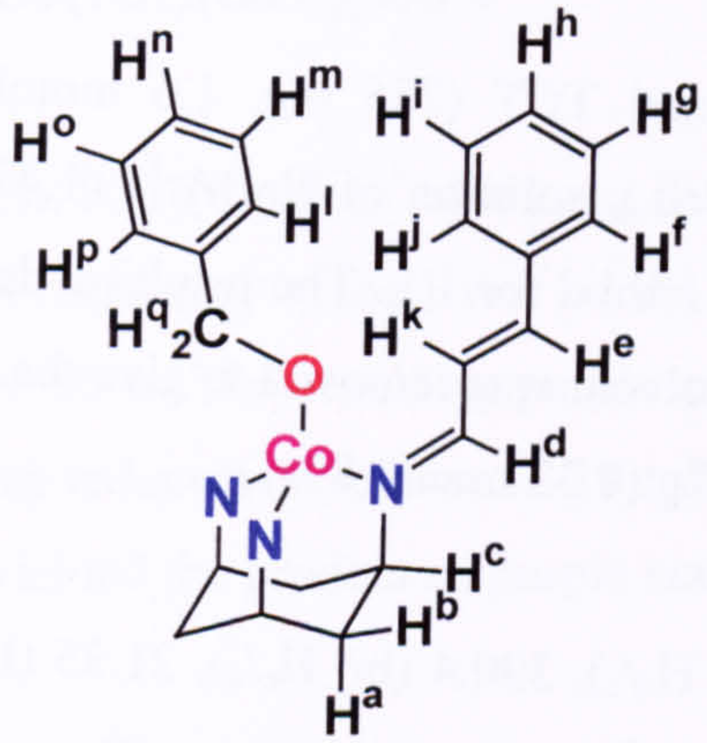

Figure 6.4:
Proton labels for $[Co(TCT)(OBz)]^+$.

- UV/vis: λ_{max} / nm (CH_2Cl_2) 639, 556, 488.
- IR / cm^{-1}: [FTIR, KBr pressed disc] 3058, 3031, 3002, 2983, 2923, 2793, 1953, 1882, 1819, 1700, 1629, 1603, 1595, 1480, 1454, 1427, 1383, 1360, 1267, 1204, 1177, 1122, 1002, 998, 961, 920, 896, 838, 748, 734, 707, 689, 614, 558, 513.
- Mass spectrum: [ESI] $m/z^+ = 637$ (M^+).

6.6.6 $[Co(TCT)(NO_3)]BAr^F_4$

$[Co(H_2O)_6](NO_3)_2$ (466 mg, 1.6 mmol) and TCT (755 mg, 1.6 mmol) were dissolved in CH_2Cl_2 (35 mL). To this was added a solution of $NaBAr^F_4$ (1.42 g, 1.6 mmol) in CH_2Cl_2 (15 mL) and the mixture was stirred for 1 h. The resulting purple solution was filtered to remove solids, and the solvent was removed to yield the product as a purple microcrystalline solid. Yield: 2.07 g (1.42 mmol, 89%).

- ^{1}H NMR (CD_2Cl_2, 300 MHz): δ 365.5 ($H_c/_d$), 20.83 (H_e), 11.75 ($H_f/_j$), 8.00 (H_h), 7.78 (s, $BAr^F_4{}^-$), 7.65 (s, $BAr^F_4{}^-$), 7.34, 7.22, 7.14, 1.25 (H_b), –12.14 (H_k), –24.5

(H_a). See Figure 6.1 for labelling scheme. Notes on acquisition: 1024 scans run, 0.2 s delay between pulses.

- UV/vis: λ_{max} / nm (CH_2Cl_2) 547 (br).
- IR / cm^{-1}: [FTIR, KBr pressed disc] 2965, 2927, 2854, 1630, 1596, 1385, 1358, 1281, 1172 (sh), 1162 (sh), 1124, 1001, 959, 886, 840, 805, 751, 713, 686, 671, 560, 514.
- Mass spectrum: [ESI] m/z^+ = 592.1 (M^+); 862.5, 863.3 (M^-, ^{10}B / ^{11}B).

6.6.7 [Co(TCT)Cl]BAr^F_4

$[Co(H_2O)_6](Cl)_2$ (381 mg, 1.6 mmol) and TCT (755 mg, 1.6 mmol) were dissolved in CH_2Cl_2 (50 mL). To this was added a solution of $NaBAr^F_4$ (1.42 g, 1.6 mmol) in CH_2Cl_2 (25 mL) and the mixture was stirred for 1 h. The resulting deep blue solution was filtered to remove solids, and the solvent was removed to give the product as a deep blue microcrystalline solid. Yield: 1.89 g (1.32 mmol, 89%).

- ^1H NMR (CD_2Cl_2, 300 MHz): δ 429.7 (br, $H_d/_c$), 390.4 (br, $H_c/_d$), 21.35 (H_e), 8.43 ($H_f/_j$), 7.95 (H_h), 7.70 (s, $BAr^F_4{}^-$), 7.55 (s, $BAr^F_4{}^-$), 6.93 ($H_g/_i$), 1.41 (H_b), –3.16 (br, H_a), –23.85 (br, H_k). See Figure 6.1 for labelling scheme. Notes on acquisition: 1024 scans run, 0.2 s delay between pulses.
- UV/vis: λ_{max} / nm (CH_2Cl_2) 593.
- IR / cm^{-1}: [FTIR, KBr pressed disc] 3049, 2965, 2931, 1630, 1607, 1596, 1358, 1277, 1177 (sh), 1124, 1001, 959, 890, 844, 805, 751, 717, 686, 671, 560, 514.
- Mass spectrum: [ESI] m/z^+ = 565, 567 (3:1 relative intensity, ^{35}Cl / ^{37}Cl) $[Co(TCT)Cl]^+$.

6.6.8 [Co(TCT)(OEt)]BAr^F_4

$[Co(TCT)(NO_3)]BAr^F_4$ (0.5 g, 0.34 mmol) was dissolved in CH_2Cl_2 (30 mL) in a Schlenk tube, and 2.5 mL of a solution of NaOEt in EtOH (25 mg NaOEt, 0.35 mmol, 1.1 eq.) was added with stirring. A slight change in colour was noted as for the corresponding BPh_4 compound. After 10 min the solution was filtered by cannula and the solvent was removed to give a red / purple microcrystalline solid, with a small

amount of brown impurity on the side of the Schlenk tube; the product was readily separated using a spatula. Yield: 385 mg (0.27 mmol, 78%).

- ^{1}H NMR (CD_2Cl_2 / d_6-EtOH, 300 MHz): δ 423 (br, $H_d/_c$), 371 (br, $H_c/_d$), 15.85 (H_e), 9.77 ($H_f/_j$), 9.38 (H_h), 7.15 ($H_g/_i$), 1.8 (H_b), –9 (H_k), –20 (H_a). See Figure 6.2 for labelling scheme. Notes on acquisition: 2048 scans run, 0.2 s delay between pulses.
- UV/vis: λ_{max} / nm (9 CH_2Cl_2 : 1 EtOH): 638, 558, 491.
- Mass spectrum: not acquired (Section 6.8).

6.6.9 [Co(TCT)(OPh)]BAr^F_4

[Co(TCT)(Cl)]BAr^F_4 (161 mg, 0.113 mmol) was dissolved in CH_2Cl_2 (30 mL), and NaOPh (30 mg, > 1eq.) was added and the mixture was protected from light and stirred for 16 h. The resulting purple solution was filtered to remove solids and the filtrate was reduced in volume to 10 mL. Diffusion of cyclohexane (100 mL) into the solution yielded the product as purple needle-shaped crystals. Yield: 87 mg (0.59 mmol, 52%).

- ^{1}H NMR (CD_2Cl_2, 300 MHz): δ 383 (br, H_d / H_c), 381 (br, H_c / H_d), 38 (s, $H_m/_o$), 19.05 (s, H_e), 9.48 (s, $H_f/_j$), 9.23 (br, H_h), 7.75 (s, $BAr^F_4^-$), 7.56 (s, $BAr^F_4^-$), 7.1 (s, $H_g/_i$), 1.25 (s, H_b), –6 (br, H_k), –8.95 (s, H_a), –32.4 (s, H_n), –40.5 (br, $H_l/_p$). See Figure 6.3 for labelling scheme. Notes on acquisition: 2048 scans run, 0.2 s delay between pulses.
- IR / cm^{-1}: [FTIR, KBr pressed disc] 3064, 3029, 2963, 2930, 2903, 1627, 1606, 1594, 1491, 1479, 1451, 1355, 1278, 1163, 1125, 998, 890, 841, 803, 750, 714, 682, 672, 557, 513.
- Mass spectrum: not acquired (Section 6.8).
- Elemental analysis; found% (calculated%) for $C_{71}H_{50}N_3OF_{24}BCo$: C, 57.51 (57.35), H, 3.57 (3.39), N, 2.56 (2.83).

6.6.10 [Co({^{t}Bu$_2$Sal}$_2$BzTACH)]

To a stirred solution of $[Co(H_2O)_6](NO_3)_2$ (29.1 mg, 100 μmol) in 25 mL MeOH was added a solution of {^{t}Bu$_2$Sal-H}$_2$BzTACH in 25 mL MeOH. The solution was stirred and became a dark green / brown colour in < 30 s. The mixture was stirred overnight to ensure complete reaction. Filtration to remove solids followed by removal of solvent gave the product as a dark brown solid. Crude yield: 69 mg (89 μmol, 89%). The compound was purified by flash column chromatography (15 × 2 cm column, grade III neutral alumina, solvent: dry, degassed MeOH, column run under pressure of Ar).

Note: yield based on Co({^{t}Bu$_2$Sal}$_2$BzTACH), may have attached solvent molecule.

- ^{1}H NMR (CD_2Cl_2, 300 MHz): δ 7.36 (m, N=C*H*), 7.23 (m, aromatic), 7.1 (m, aromatic), 2.0 (m, C*H* ring)1.93 (C*H* ring), 1.3 (m, *t*Bu).
- Mass spectrum: [ESI] m/z^+ = 764.4 (M^+).

6.7 Synthesis of zinc complexes

6.7.1 [Zn(TCT)(NO$_3$)]BPh$_4$

Previously synthesised by Greener, method of Lusby adapted.[17]

$[Zn(H_2O)_6](NO_3)_2$ (0.27 g, 0.89 mmol) in MeOH (25 mL) was added via cannula to a solution of TCT (0.42 g, 0.89 mmol) in CH_2Cl_2 (50 mL) under Ar. The pale yellow solution was stirred for 1 h, then filtered by cannula to a solution of $NaBPh_4$ (306 mg, 0.89 mmol) in MeOH (25 mL). The solution was filtered by cannula and the solvent was removed to give a white powder. Yield: 0.65 g (0.71 mmol, 80%).

Note: the synthesis was previously carried out under normal atmosphere, but formation of insoluble white solid (presumed to be the carbonate-bridged dimer, $[Zn(TCT)]_2(\mu^2\text{-}CO_3)(BPh_4)_2$) has been observed on occasion.

- ^{1}H NMR (CD_2Cl_2, 270 MHz): δ 7.95 (3H, d, J_{HH} = 10 Hz, H_d), 7.59 (6H, m, H_g/$_i$), 7.49 (8H, m, BPh_4^-), 7.33 (11H, m, 8 BPh_4^- + H_k), 7.07 – 6.86 (16H, m, H_f/$_j$ + H_h + H_e + 4 BPh_4^-). See Figure 6.5 for labelling scheme.

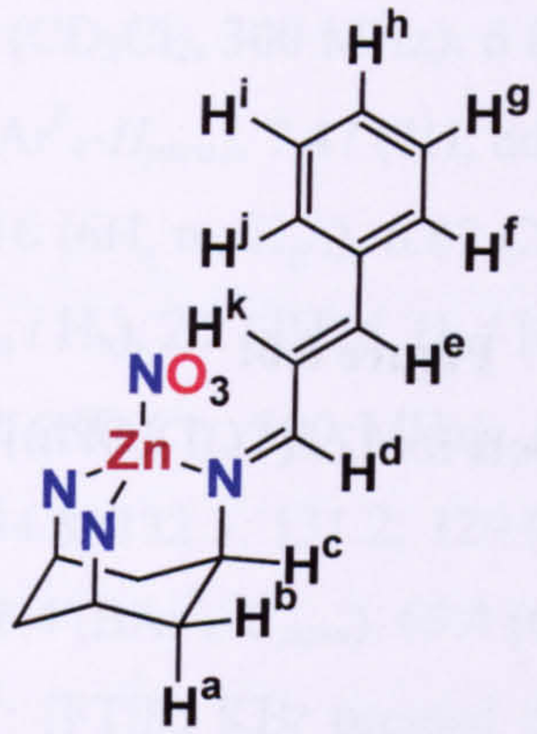

Figure 6.5:

Proton labels for $[Zn(TCT)(NO_3)]^+$.

- IR / cm^{-1}: [FTIR, KBr pressed disc] 3057, 3031, 3000, 2985, 2923, 1952, 1887, 1822, 1630, 1607, 1596, 1480, 1454, 1431, 1404, 1365, 1273, 1177, 1123, 1078, 1032, 1001, 962, 920, 901, 847, 751, 736, 709, 690, 613, 602, 560, 514
- Mass spectrum [ESI]: $m/z^+ = 597$ ($[Zn(TCT)(NO_3)]^+$).

6.7.2 $[Zn(TCT)(OPh)]BPh_4$

Mass spectral evidence previously reported by Freeman.

$[Zn(TCT)(NO_3)]BPh_4$ (50 mg, 54.5 μmol) dissolved in CH_2Cl_2 (50 mL) was stirred for 4 h with $NaOPh.3H_2O$ (30 mg, an excess) in the absence of light. Solids were removed by filtration, the solvent volume reduced to 10 mL and cyclohexane (50 mL) added to precipitate the product as an off-white solid. Yield: 46.2 mg (48.7 μmol, 89%).

- ^1H NMR (CD_2Cl_2, 270 MHz): δ 7.99 (3H, d, J_{HH} = 5 Hz, H_d), 7.44 (3H, dd, J_{HH} = 8.5 Hz, 5 Hz, H_k), 7.39 (m, 11H, $H_{f/j} + H_h + H_{m/o}$), 7.31 (8H, q, J_{HH} = 4 Hz, BPh_4^-), 7.25 (3H, d, J_{HH} = 8.5 Hz, H_e), 7.2 (6H, d, J_{HH} = 4 Hz, $H_{g/i}$), 7.08 (8H, t, J_{HH} = 4 Hz, BPh_4^-), 6.93 (4H, t, J_{HH} = 4 Hz, BPh_4^-), 6.87 (2H, d, J_{HH} = 4 Hz, $H_{l/p}$), 6.8 (1H, t, J_{HH} = 4 Hz, H_n), 3.99 (3H, s, H_c), 2.27 (3H, d, J_{HH} = 8 Hz, H_a / H_b), 2.03 (3H, d, J_{HH} = 8 Hz, H_b / H_a).See Figure 6.6 for labelling scheme.
- IR / cm^{-1}: [FTIR, KBr pressed disc] 3053, 3038, 3006, 2984, 2921, 2849, 1638, 1628, 1607, 1595, 1483, 1450, 1424, 1401, 1290, 1267, 1175, 1127, 1008, 749, 736, 705, 685, 614, 558, 512.
- Mass spectrum: [ESI] m/z^+ = 628 / 630 / 632 (M^+, correct Zn isotope ratio).

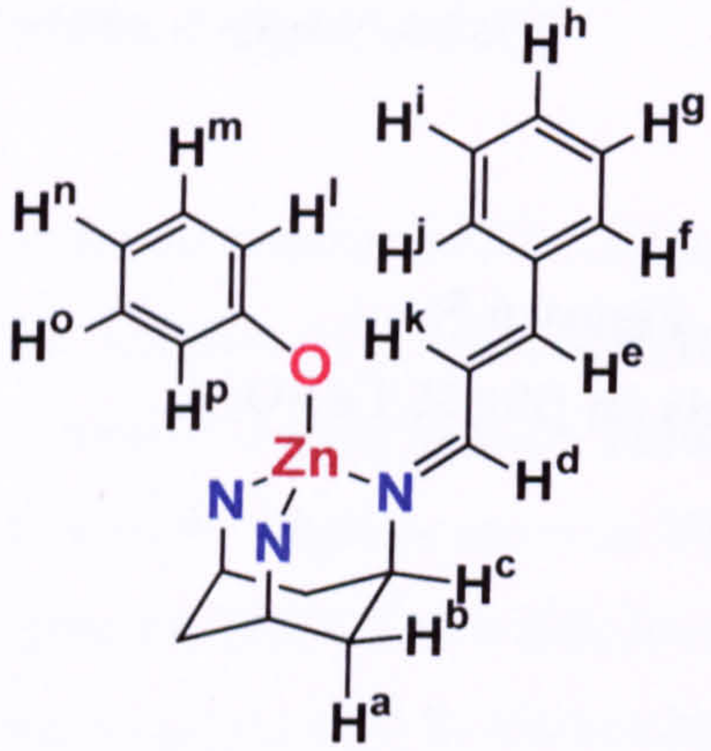

Figure 6.6:

Proton labels for $[Zn(TCT)(OPh)]^+$.

6.7.3 $[Zn(TCT)(NO_3)]BAr^F_4$

$[Zn(H_2O)_6](NO_3)_2$ (735 mg, 2.46 mmol) in MeOH (50 mL) was added dropwise to a solution of TCT (1.16 g, 2.46 mmol) in CH_2Cl_2 (50 mL). The pale yellow solution was stirred for 1 h, then a solution of $NaBAr^F_4$ (2.18 g, 2.46 mmol) in MeOH (50 mL) was added dropwise with stirring. The solvent was removed to give an oily solid, which was washed with hexane and recrystallised from CH_2Cl_2 / cyclohexane. The product was isolated as an off-white solid. Yield: 4.48 g (3.06 mmol, 62.3%).

- ^1H NMR (CD_2Cl_2, 300 MHz): δ 8.2 (3H, d, J_{HH} = 10.5 Hz, H_d), 7.7 (8H, s, BAr^F_4-H_{ortho}), 7.6 (6H, m, H_g/$_i$), 7.57 (4H, s, BAr^F_4-H_{para}), 7.5 (9H, m, H_f/$_j$ + H_h), 7.4 (3H, d, J_{HH} = 17.2 Hz, H_k), 7.05 (3H, dd, H_e), 4.2 (3H, s, H_c), 2.4 (3H, d, H_a / H_b), 2.2 (3H, d, H_b / H_a). See Figure 6.5 for labelling scheme.
- Mass spectrum: not acquired (Section 6.8).

6.7.4 $[Zn(TCT)(OPh)]BAr^F_4$

$[Zn(TCT)(NO_3)]BAr^F_4$ (400 mg, 0.27 mmol) dissolved in CH_2Cl_2 (50 mL) was stirred overnight with $NaOPh.3H_2O$ (60 mg, an excess) in the absence of light. Solids were removed by filtration, the solvent volume reduced to 5 mL and cyclohexane (50 mL) added to precipitate the product as an off-white solid. Yield: 360 mg (0.24 mmol, 89%).

- ^{1}H NMR (CD_2Cl_2, 300 MHz): δ 8.15 (3H, d, H_d), 7.73 (8H, br s, $BAr^F{}_4$-*H*$_{ortho}$), 7.56 (4H, s, $BAr^F{}_4$-*H*$_{para}$), 7.47 (3H, dd, H_k), 7.4 (3H, m, H_e), 7.27 (11H, m, H_f/$_j$ + H_h + 2 H_m/$_o$), 7.16 (6H, m, H_g/$_i$), 6.87 (2H, d, H_l/$_p$), 6.77 (1H, t, H_n), 4.17 (3H, s, H_c), 2.4 (3H, d, H_a / H_b), 2.2 (3H, d, H_b / H_a). See Figure 6.6 for labelling scheme.
- ^{13}C NMR (CD_2Cl_2, 300 MHz): δ 170, 163 (m, $BAr^F{}_4$-*C*$_{ipso}$),152.5, 135.7 ($BAr^F{}_4$-*C*$_{ortho}$), 134.8, 132.3, 131.2, 129.9 ($BAr^F{}_4$-*C*$_{meta}$), 129.6, 127 3, 124.7 (*C*F_3), 123.7, 120.8, 118.4 ($BAr^F{}_4$-*C*$_{para}$), 65.4 (*C*N-cyclohexyl), 38.1 (*C*-cyclohexyl).
- IR / cm^{-1}: [FTIR, KBr pressed disc] 3069, 3028, 2938, 2905, 1636, 1629, 1610, 1595, 1495, 1483, 1454, 1401, 1357, 1289 (sh), 1281, 1163, 1133, 1121 (sh), 1005, 961, 935, 920, 890, 842, 748, 711, 685, 674, 562, 513.
- Mass spectrum: not acquired (Section 6.8).

6.8 Preparation of $NaBAr^F{}_4$[18]

1,2-dibromoethane (1.5 mL) was added to Mg (5 g) in dry Et_2O (75 mL) under Ar. (Note: exothermic reaction). The mixture was cooled in an ice bath and 1-bromo-3,5-(trifluoromethyl)benzene (50 mL, 129.6 mmol) in dry Et_2O (150 mL) added *slowly* via a pressure-equalised dropping funnel (note: exothermic reaction). $NaBF_4$ (3.4 g, 32.4 mmol) was added to the dark brown solution, which was left stirring for 1 h, then heated to 313 K overnight. The mixture was washed by slow addition to a solution of Na_2CO_3 (74 g) in H_2O (note: vigorous reaction), then filtered through celite. The aqueous layer was separated and washed with Et_2O (3 × 25 mL). The ether fractions were combined, dried over Na_2SO_4 for 2 h and filtered through activated charcoal 3 times. Solvent was removed under reduced pressure, producing a yellow / brown solid, which was finely ground and washed with minimal cold CH_2Cl_2 to give a yellow powder. Yield: 20.03 g (22.6 mmol, 70%).

Note: The anion has been observed to contaminate subsequent mass spectrum samples for extended periods. Consequently, only the first two compounds submitted for analysis ([Co(TCT)X]$BAr^F{}_4$, where X = Cl, NO_3) were characterised by this method.

6.9 Catalytic experiments

6.9.1 Sample procedure for titanium-catalysed interesterification

2-Phenyl acetic acid ethyl ester (32.84 g, 0.02 mol) and benzyl acetate (30.04 g, 0.02 mol) were heated to 383 K, with stirring, in a 2-necked round-bottomed flask with condenser attached. $Ti(O^nBu)_4$ (3.4 g, 0.01 mol, 5 mol%) was added to the esters (yellow colour observed) and samples (~ 1.5 mL) were withdrawn from the reaction mixture at 30 s intervals over the course of 10 min. The samples were immediately placed in sample tubes with 1 M HCl (0.5 mL) in an ice bath to prevent further reaction. ^1H NMR spectroscopy provided initial confirmation of production of 2-phenyl acetic acid benzyl ester and ethyl acetate, with kinetic analysis performed by gas chromatography (200 μL sample, + 100 μL ethyl benzoate internal standard in 10 mL acetone). The GC integrals were evaluated, and a linear regression program was used to calculate reaction rate.

6.9.2 Sample procedure for cobalt-catalysed transesterification

Ethyl benzoate (3.0 g, 20 mmol), benzyl alcohol (21.63 g, 200 mmol) and $[Co(TCT)(OPh)]BPh_4$ were sealed under Ar with a condenser. The vessel was removed from the glovebox and immediately attached to an argon supply. The reactants were heated to 353 K in the absence of light with stirring under a steady flow of argon. Samples were withdrawn by syringe at 30 min intervals over 6 h. Analysis was performed by gas chromatography (samples prepared as for titanium-catalysed reaction, but with ethyl phenyl acetate as internal standard).

6.10 CO_2 sequestration experiments[19]

6.10.1 Reversible reaction of CO_2 with [Co(TCT)(OEt)]BPh_4

A solution of [Co(TCT)(OEt)]BPh_4 (10 mg, 11 μmol) in the mixed solvent [9 CH_2Cl_2 : 1 EtOH] *v/v* (5 mL) was placed in a UV/vis cell under argon (sealed with a Young's tap), and the visible spectrum was recorded. A stream of CO_2 was passed though the solution for 60 s, and the new visible spectrum recorded. Nitrogen was bubbled through the solution and visible spectra were recorded at intervals of 1, 5, 7, 11 and 25 min. Absorption bands of the carbonated reaction product λ / nm: 492(sh), 520, 550.

6.10.2 Reaction of CO_2 with [Co(TCT)(OPh)]BPh_4 in CD_3CN

A solution of [Co(TCT)(OPh)]BPh_4 (25 mg, 27 μmol) in CD_3CN (2 mL) was placed in a Schlenk tube under argon, and the FTIR spectrum recorded. A stream of CO_2 was passed through the solution for 60 s, and the new FTIR spectrum recorded. The difference spectrum was calculated showing bands at 1503, 1363 and 1224 cm^{-1}, with a possible band at 1472 cm^{-1} (solvent cut-off is < 1110 cm^{-1}). *Note: precipitation of solid was observed upon addition of CO_2; the solid redissolved after conversion to starting material.*

6.11 References

1 D. D. Perrin, W. L. F. Armarego, Purification of Laboratory Chemicals, Pergamon Press, 1988.

2 R. J. Bushby, D. R. McGill, K. M. Ng and N. Taylor, *J. Mater. Chem.*, 1997, **7**, 2343.

3 J. D. Freeman, DPhil Thesis, University of York, 2001.

4 E. A. Lewis, DPhil Thesis, University of York, 2002.

5 A. K. Nairn, DPhil Thesis, University of York, 2001.

6 A. Chandrasekeran, Roberta O. Day and Robert R. Holmes, *J. Am. Chem. Soc.*, 2000, **122**, 1066.

7 T. R. Dargaville. P. J. De Bruyn, A. S. C. Lim, M. G. Looney, A. C. Potter, D. H. Solomon and X. Zhang, *J. Polym. Sci., Part A: Polym. Chem.*, 1997, **35**, 1389.

8 M. Kol, M. Shamis, I. Goldberg, Z. Goldschmidt, S. Alfi, E. Ḥayut-Salant, *Inorg. Chem.Commun.*, 2001, **4**, 177.

9 A. A. Naiini, W. M. P. B. Menge and J. G. Verkade, *Inorg. Chem.*, 1991, **30**, 5009.

10 L. M. Berreau *et al.*, *Chem. Commun.*, not yet in press

11 D. C. Bradley and P. A. Hammersley, *J. Chem. Soc. A*, 1967, 1894.

12 (a) M. Bochmann, I. Hawkins and L. M. Wilson, *J. Chem. Soc., Chem. Commun.*, 1988, 344. (b) C. J. Carmalt, C. W. Dinnage, I. P. Parkin, A. J. P. White and D. J. Williams, *J. Chem. Soc., Dalton Trans.*, 2001, 2554. (c) For a review, see: D. W. Stephan and T. T. Nadasdi, *Coord. Chem. Rev.*, 1996, **147**, 147.

13 For a recent review of solventless reactions, see: G. W. V. Cave, C. L. Raston and J. L. Scott, *Chem. Commun.*, 2001, 2159.

14 Walton, Archibald *et al.*, unpublished results.

15 D. C. Bradley, D. C. Hancock and W. Wardlaw, *J. Chem. Soc.*, 1952, 2773.

16 B. Greener, DPhil Thesis, University of York, 1997.

17 P. J. Lusby, DPhil Thesis, University of York, 2000.

18 (a) M. Brookhart, B. Grant and A. F. Volpe Jr., *Organometallics*, 1992, **11**, 3920; (b) H. Nishida, N. Takada, M. Yoshimura, T. Sonoda and H. Kobayashi, *Bull. Chem. Soc. Jpn.*, 1984, **57**, 2600.

19 S, J. Archibald, S. P. Foxon, J. D. Freeman, J. E. Hobson, R. N. Perutz and P. H. Walton, *J. Chem. Soc., Dalton Trans.*, 2002, 2797.

Appendix – Selected crystallographic data

Experimental details for the collection of crystal structure data are listed individually for each compound. Diffraction data were collected at 115 K on a Bruker Smart Apex diffractometer with Mo-K_α radiation (λ = 0.71073 Å) using a SMART CCD camera. An Oxford Cryosystems Cryostream probe was used to maintain the required sample temperature. Diffractometer control, data collection and initial unit cell determination was performed using SMART.[1] Frame integration and unit-cell refinement software was carried out with the SAINT+[2] software. Absorption correction was applied using SADABS[3] (v2.03, Sheldrick). Structures were solved by direct methods using SHELXS-97[4] and refined by full-matrix least squares using SHELXL-97.[5] All non-hydrogen atoms were refined anisotropically. Hydrogen atoms were placed using a "riding model" and included in the refinement at calculated positions. Solvent systems used for growing crystals are noted in Chapter 2 and Chapter 6, under the descriptions for each compound.

Acknowledgements:

The crystal structures of $[Co(TCT)(OEt)]BPh_4 \cdot ½$ EtOH and $[Co(TCT)(OPh)]BAr^F_4$ were solved by Dr. Stephen J. Archibald of the University of Hull. The structures of $[Co(TCT)(NO_3)]BAr^F_4 \cdot CH_2Cl_2 \cdot 1½\ c\text{-}C_6H_{12}$, $[Co(TCT)Cl]BAr^F_4$, $\{[Co(TCT)]_2(\mu\text{-}CO_3)\}(BPh_4)_2 \cdot CH_3CN$, $[Zn(TCT)(NO_3)]BAr^F_4 \cdot CH_2Cl_2$, $[Zn(TCT)(OPh)]BPh_4 \cdot ½\ c\text{-}C_6H_{12}$ and $[Zn(TCT)(OPh)]BAr^F_4 \cdot c\text{-}C_6H_{12}$ were solved by Dr. Adrian Whitwood of the University of York.

A1 Crystal data and structure refinement for $[Co(TCT)(NO_3)]BAr^F_4 \cdot CH_2Cl_2 \cdot 1½\ c\text{-}C_6H_{12}$

Identification code	phw0325m
Empirical formula	$C_{75}H_{65}BCl_2CoF_{24}N_4O_3$
Formula weight	1666.95
Temperature	115(2) K
Wavelength	0.71073 Å
Crystal system	Monoclinic
Space group	$P2_1/n$
Unit cell dimensions	a = 13.3665(5) Å α = 90°
	b = 16.1561(6) Å β = 96.6100(10)°
	c = 35.1452(13) Å γ = 90°
Volume	7539.2(5) $Å^3$
Z	4
Density (calculated)	1.469 Mg / m^3
Absorption coefficient	0.408 mm^{-1}
F(000)	3396
Crystal size	0.26 × 0.18 × 0.09 mm^3
Theta range for data collection	1.17 to 25.06°
Index ranges	$-12 \le h \le 15, -19 \le k \le 19, -41 \le l \le 37$
Reflections collected	42509
Independent reflections	13315 [*R*(int) = 0.0395]
Completeness to theta = 25.06°	99.7 %
Absorption correction	Semi-empirical from equivalents
Max. and min. transmission	0.960 and 0.828
Refinement method	Full-matrix least-squares on F^2
Data / restraints / parameters	13315 / 0 / 1072
Goodness-of-fit on F^2	1.021
Final *R* indices [$I > 2$ sigma (I)]	$R1 = 0.0533$, $wR2 = 0.1405$
R indices (all data)	$R1 = 0.0889$, $wR2 = 0.1659$
Largest diff. peak and hole	0.889 and –0.609 $e.Å^{-3}$

Table A1.1: Bond lengths (/ Å) and angles (/ °) for $[Co(TCT)(NO_3)]BAr^F{}_4 \cdot CH_2Cl_2 \cdot 1½\ c\text{-}C_6H_{12}$.

B(1)–C(19)	1.636(4)	**B(1)–C(1)**	1.637(4)
B(1)–C(13)	1.638(4)	**B(1)–C(7)**	1.640(4)
C(1)–C(6)	1.394(4)	**C(1)–C(2)**	1.400(4)
C(2)–C(3)	1.387(4)	**C(2)–H(2)**	0.9500
C(3)–C(4)	1.374(5)	**C(3)–C(25)**	1.502(5)
C(4)–C(5)	1.383(5)	**C(4)–H(4)**	0.9500
C(5)–C(6)	1.395(4)	**C(5)–C(26)**	1.495(5)
C(6)–H(6)	0.9500	**C(7)–C(12)**	1.395(4)
C(7)–C(8)	1.397(4)	**C(8)–C(9)**	1.389(4)
C(8)–H(8)	0.9500	**C(9)–C(10)**	1.385(4)
C(9)–C(27)	1.492(4)	**C(10)–C(11)**	1.385(4)
C(10)–H(10)	0.9500	**C(11)–C(12)**	1.392(4)
C(11)–C(28)	1.493(5)	**C(12)–H(12)**	0.9500
C(13)–C(14)	1.393(4)	**C(13)–C(18)**	1.402(4)
C(14)–C(15)	1.388(4)	**C(14)–H(14)**	0.9500
C(15)–C(16)	1.385(4)	**C(15)–C(29)**	1.506(5)
C(16)–C(17)	1.387(4)	**C(16)–H(16)**	0.9500
C(17)–C(18)	1.385(4)	**C(17)–C(30)**	1.493(4)
C(18)–H(18)	0.9500	**C(19)–C(20)**	1.394(4)
C(19)–C(24)	1.405(4)	**C(20)–C(21)**	1.395(4)
C(20)–H(20)	0.9500	**C(21)–C(22)**	1.385(5)
C(21)–C(31)	1.487(4)	**C(22)–C(23)**	1.390(5)
C(22)–H(22)	0.9500	**C(23)–C(24)**	1.390(4)
C(23)–C(32)	1.492(5)	**C(24)–H(24)**	0.9500
C(25)–F(1)	1.330(4)	**C(25)–F(2)**	1.330(4)
C(25)–F(3)	1.345(5)	**C(26)–F(4)**	1.192(7)
C(26)–F(5A)	1.219(8)	**C(26)–F(6)**	1.317(8)
C(26)–F(5)	1.324(8)	**C(26)–F(4A)**	1.362(8)
C(26)–F(6A)	1.363(9)	**C(27)–F(8)**	1.334(4)
C(27)–F(7)	1.335(4)	**C(27)–F(9)**	1.350(4)
C(28)–F(11)	1.298(4)	**C(28)–F(10)**	1.316(4)

C(28)–F(12)	1.356(4)	C(29)–F(15A)	1.224(13)
C(29)–F(14)	1.263(10)	C(29)–F(13A)	1.288(10)
C(29)–F(15)	1.308(8)	C(29)–F(14A)	1.325(10)
C(29)–F(13)	1.343(10)	C(30)–F(17)	1.307(4)
C(30)–F(16)	1.323(4)	C(30)–F(18)	1.331(4)
C(31)–F(21)	1.309(4)	C(31)–F(20)	1.311(4)
C(31)–F(19)	1.320(4)	C(32)–F(24)	1.282(4)
C(32)–F(23)	1.299(4)	C(32)–F(22)	1.338(5)
C(33)–N(1)	1.283(4)	C(33)–C(34)	1.443(4)
C(33)–H(33)	0.9500	C(34)–C(35)	1.341(4)
C(34)–H(34)	0.9500	C(35)–C(36)	1.471(5)
C(35)–H(35)	0.9500	C(36)–C(37)	1.380(5)
C(36)–C(41)	1.395(5)	C(37)–C(38)	1.380(5)
C(37)–H(37)	0.9500	C(38)–C(39)	1.376(7)
C(38)–H(38)	0.9500	C(39)–C(40)	1.365(7)
C(39)–H(39)	0.9500	C(40)–C(41)	1.386(6)
C(40)–H(40)	0.9500	C(41)–H(41)	0.9500
C(42)–N(2)	1.285(4)	C(42)–C(43)	1.437(4)
C(42)–H(42)	0.9500	C(43)–C(44)	1.339(4)
C(43)–H(43)	0.9500	C(44)–C(45)	1.455(4)
C(44)–H(44)	0.9500	C(45)–C(50)	1.388(5)
C(45)–C(46)	1.394(5)	C(46)–C(47)	1.389(5)
C(46)–H(46)	0.9500	C(47)–C(48)	1.365(6)
C(47)–H(47)	0.9500	C(48)–C(49)	1.390(6)
C(48)–H(48)	0.9500	C(49)–C(50)	1.373(5)
C(49)–H(49)	0.9500	C(50)–H(50)	0.9500
C(51)–C(52)	1.334(5)	C(51)–C(71)	1.435(4)
C(51)–H(51)	0.9500	C(52)–C(53)	1.464(5)
C(52)–H(52)	0.9500	C(53)–C(54)	1.389(5)
C(53)–C(58)	1.390(5)	C(54)–C(55)	1.393(5)
C(54)–H(54)	0.9500	C(55)–C(56)	1.373(6)
C(55)–H(55)	0.9500	C(56)–C(57)	1.375(6)
C(56)–H(56)	0.9500	C(57)–C(58)	1.377(5)
C(57)–H(57)	0.9500	C(58)–H(58)	0.9500

C(59)–N(1)	1.483(4)	C(59)–C(60)	1.525(5)
C(59)–C(64)	1.532(5)	C(59)–H(59)	1.0000
C(60)–C(61)	1.532(4)	C(60)–H(60A)	0.9900
C(60)–H(60B)	0.9900	C(61)–N(2)	1.490(4)
C(61)–C(62)	1.524(4)	C(61)–H(61)	1.0000
C(62)–C(63)	1.530(4)	C(62)–H(62A)	0.9900
C(62)–H(62B)	0.9900	C(63)–N(3)	1.484(4)
C(63)–C(64)	1.529(4)	C(63)–H(63)	1.0000
C(64)–H(64A)	0.9900	C(64)–H(64B)	0.9900
C(65)–C(68)	1.514(6)	C(65)–C(66)	1.522(6)
C(65)–H(65A)	0.9900	C(65)–H(65B)	0.9900
C(66)–C(70)	1.526(6)	C(66)–H(66A)	0.9900
C(66)–H(66B)	0.9900	C(67)–C(70)	1.509(6)
C(67)–C(69)	1.532(6)	C(67)–H(67A)	0.9900
C(67)–H(67B)	0.9900	C(68)–C(69)	1.522(6)
C(68)–H(68A)	0.9900	C(68)–H(68B)	0.9900
C(69)–H(69A)	0.9900	C(69)–H(69B)	0.9900
C(70)–H(70A)	0.9900	C(70)–H(70B)	0.9900
C(71)–N(3)	1.279(4)	C(71)–H(71)	0.9500
C(74)–C(76)#1	1.504(6)	C(74)–C(75)	1,518(6)
C(74)–H(74A)	0.9900	C(74)–H(74B)	0.9900
C(75)–C(76)	1.509(6)	C(75)–H(75A)	0.9900
C(75)–H(75B)	0.9900	C(76)–C(74)#1	1.504(6)
C(76)–H(76A)	0.9900	C(76)–H(76B)	0.9900
C(77)–Cl(1)	1.729(10)	C(77)–Cl(2)	1.829(12)
C(77)–H(77A)	0.9900	C(77)–H(77B)	0.9900
C(78)–Cl(3)	1.717(10)	C(78)–Cl(4)	1.727(13)
C(78)–H(78A)	0.9900	C(78)–H(78B)	0.9900
Co(1)–O(2)	2.000(2)	Co(1)–N(1)	2.035(3)
Co(1)–N(2)	2.040(3)	Co(1)–N(3)	2.043(3)
Co(1)–O(1)	2.328(2)	N(4)–O(3)	1.223(4)
N(4)–O(1)	1.252(3)	N(4)–O(2)	1.288(3)
C(19)–B(1)–C(1)	112.6(2)	C(19)–B(1)–C(13)	102.1(2)

C(1)–B(1)–C(13)	112.8(2)	C(19)–B(1)–C(7)	112.6(2)
C(1)–B(1)–C(7)	103.7(2)	C(13)–B(1)–C(7)	113.4(2)
C(6)–C(1)–C(2)	115.9(3)	C(6)–C(1)–B(1)	122.2(3)
C(2)–C(1)–B(1)	121.7(3)	C(3)–C(2)–C(1)	121.9(3)
C(3)–C(2)–H(2)	119.1	C(1)–C(2)–H(2)	119.1
C(4)–C(3)–C(2)	121.2(3)	C(4)–C(3)–C(25)	119.9(3)
C(2)–C(3)–C(25)	118.8(3)	C(3)–C(4)–C(5)	118.4(3)
C(3)–C(4)–H(4)	120.8	C(5)–C(4)–H(4)	120.8
C(4)–C(5)–C(6)	120.4(3)	C(4)–C(5)–C(26)	119.9(3)
C(6)–C(5)–C(26)	119.8(3)	C(1)–C(6)–C(5)	122.2(3)
C(1)–C(6)–H(6)	118.9	C(5)–C(6)–H(6)	118.9
C(12)–C(7)–C(8)	116.0(3)	C(12)–C(7)–B(1)	121.8(3)
C(8)–C(7)–B(1)	121.8(3)	C(9)–C(8)–C(7)	122.3(3)
C(9)–C(8)–H(8)	118.8	C(7)–C(8)–H(8)	118.8
C(10)–C(9)–C(8)	120.7(3)	C(10)–C(9)–C(27)	120.1(3)
C(8)–C(9)–C(27)	119.2(3)	C(11)–C(10)–C(9)	118.1(3)
C(11)–C(10)–H(10)	120.9	C(9)–C(10)–H(10)	120.9
C(10)–C(11)–C(12)	120.9(3)	C(10)–C(11)–C(28)	118.3(3)
C(12)–C(11)–C(28)	120.8(3)	C(11)–C(12)–C(7)	122.0(3)
C(11)–C(12)–H(12)	119.0	C(7)–C(12)–H(12)	119.0
C(14)–C(13)–C(18)	115.7(3)	C(14)–C(13)–B(1)	122.3(3)
C(18)–C(13)–B(1)	121.2(3)	C(15)–C(14)–C(13)	121.9(3)
C(15)–C(14)–H(14)	119.0	C(13)–C(14)–H(14)	119.0
C(16)–C(15)–C(14)	121.7(3)	C(16)–C(15)–C(29)	119.2(3)
C(14)–C(15)–C(29)	119.1(3)	C(15)–C(16)–C(17)	117.2(3)
C(15)–C(16)–H(16)	121.4	C(17)–C(16)–H(16)	121.4
C(18)–C(17)–C(16)	121.1(3)	C(18)–C(17)–C(30)	118.9(3)
C(16)–C(17)–C(30)	120.0(3)	C(17)–C(18)–C(13)	122.4(3)
C(17)–C(18)–H(18)	118.8	C(13)–C(18)–H(18)	118.8
C(20)–C(19)–C(24)	115.7(3)	C(20)–C(19)–B(1)	122.3(3)
C(24)–C(19)–B(1)	121.1(3)	C(19)–C(20)–C(21)	122.5(3)
C(19)–C(20)–H(20)	118.7	C(21)–C(20)–H(20)	118.7
C(22)–C(21)–C(20)	120.5(3)	C(22)–C(21)–C(31)	120.9(3)
C(20)–C(21)–C(31)	118.6(3)	C(21)–C(22)–C(23)	118.3(3)

C(21)–C(22)–H(22)	120.8	C(23)–C(22)–H(22)	120.8
C(24)–C(23)–C(22)	120.7(3)	C(24)–C(23)–C(32)	118.5(3)
C(22)–C(23)–C(32)	120.8(3)	C(23)–C(24)–C(19)	122.2(3)
C(23)–C(24)–H(24)	118.9	C(19)–C(24)–H(24)	118.9
F(1)–C(25)–F(2)	106.8(3)	F(1)–C(25)–F(3)	106.4(3)
F(2)–C(25)–F(3)	105.4(3)	F(1)–C(25)–C(3)	112.9(3)
F(2)–C(25)–C(3)	112.5(3)	F(3)–C(25)–C(3)	112.4(3)
F(4)–C(26)–F(5A)	127.2(6)	F(4)–C(26)–F(6)	111.6(11)
F(5A)–C(26)–F(6)	57.0(12)	F(4)–C(26)–F(5)	110.5(10)
F(5A)–C(26)–F(5)	42.4(12)	F(6)–C(26)–F(5)	99.2(6)
F(4)–C(26)–F(4A)	45.6(12)	F(5A)–C(26)–F(4A)	105.1(10)
F(6)–C(26)–F(4A)	138.5(6)	F(5)–C(26)–F(4A)	69.8(6)
F(4)–C(26)–F(6A)	51.4(11)	F(5A)–C(26)–F(6A)	109.9(10)
F(6)–C(26)–F(6A)	63.7(5)	F(5)–C(26)–F(6A)	134.8(6)
F(4A)–C(26)–F(6A)	95.1(5)	F(4)–C(26)–C(5)	113.8(5)
F(5A)–C(26)–C(5)	118.3(5)	F(6)–C(26)–C(5)	109.9(4)
F(5)–C(26)–C(5)	110.9(5)	F(4A)–C(26)–C(5)	111.4(5)
F(6A)–C(26)–C(5)	114.2(4)	F(8)–C(27)–F(7)	106.4(3)
F(8)–C(27)–F(9)	104.9(3)	F(7)–C(27)–F(9)	106.3(3)
F(8)–C(27)–C(9)	112.6(3)	F(7)–C(27)–C(9)	113.6(3)
F(9)–C(27)–C(9)	112.5(3)	F(11)–C(28)–F(10)	111.6(4)
F(11)–C(28)–F(12)	103.4(3)	F(10)–C(28)–F(12)	102.1(3)
F(11)–C(28)–C(11)	114.6(3)	F(10)–C(28)–C(11)	112.9(3)
F(12)–C(28)–C(11)	111.2(3)	F(15A)–C(29)–F(14)	126.4(10)
F(15A)–C(29)–F(13A)	108.1(12)	F(14)–C(29)–F(13A)	28.0(9)
F(15A)–C(29)–F(15)	70.2(11)	F(14)–C(29)–F(15)	111.0(8)
F(13A)–C(29)–F(15)	129.3(6)	F(15A)–C(29)–F(14A)	110.6(10)
F(14)–C(29)–F(14A)	72.8(8)	F(13A)–C(29)–F(14A)	99.1(7)
F(15)–C(29)–F(14A)	44.4(6)	F(15A)–C(29)–F(13)	32.1(13)
F(14)–C(29)–F(13)	105.1(9)	F(13A)–C(29)–F(13)	80.4(8)
F(15)–C(29)–F(13)	100.0(7)	F(14A)–C(29)–F(13)	132.3(8)
F(15A)–C(29)–C(15)	113.1(7)	F(14)–C(29)–C(15)	114.1(6)
F(13A)–C(29)–C(15)	112.9(6)	F(15)–C(29)–C(15)	113.6(5)
F(14A)–C(29)–C(15)	112.0(6)	F(13)–C(29)–C(15)	111.8(5)

F(17)–C(30)–F(16)	106.7(3)	**F(17)–C(30)–F(18)**	105.6(3)
F(16)–C(30)–F(18)	104.9(3)	**F(17)–C(30)–C(17)**	113.0(3)
F(16)–C(30)–C(17)	113.9(3)	**F(18)–C(30)–C(17)**	111.9(3)
F(21)–C(31)–F(20)	107.8(3)	**F(21)–C(31)–F(19)**	104.1(3)
F(20)–C(31)–F(19)	105.0(3)	**F(21)–C(31)–C(21)**	113.2(3)
F(20)–C(31)–C(21)	113.7(3)	**F(19)–C(31)–C(21)**	112.2(3)
F(24)–C(32)–F(23)	110.0(3)	**F(24)–C(32)–F(22)**	104.4(4)
F(23)–C(32)–F(22)	101.8(3)	**F(24)–C(32)–C(23)**	113.9(3)
F(23)–C(32)–C(23)	114.2(3)	**F(22)–C(32)–C(23)**	111.6(3)
N(1)–C(33)–C(34)	125.4(3)	**N(1)–C(33)–H(33)**	117.3
C(34)–C(33)–H(33)	117.3	**C(35)–C(34)–C(33)**	119.8(3)
C(35)–C(34)–H(34)	120.1	**C(33)–C(34)–H(34)**	120.1
C(34)–C(35)–C(36)	125.5(3)	**C(34)–C(35)–H(35)**	117.2
C(36)–C(35)–H(35)	117.2	**C(37)–C(36)–C(41)**	118.7(3)
C(37)–C(36)–C(35)	122.7(3)	**C(41)–C(36)–C(35)**	118.6(3)
C(36)–C(37)–C(38)	120.6(4)	**C(36)–C(37)–H(37)**	119.7
C(38)–C(37)–H(37)	119.7	**C(39)–C(38)–C(37)**	120.3(4)
C(39)–C(38)–H(38)	119.9	**C(37)–C(38)–H(38)**	119.9
C(40)–C(39)–C(38)	120.0(4)	**C(40)–C(39)–H(39)**	120.0
C(38)–C(39)–H(39)	120.0	**C(39)–C(40)–C(41)**	120.2(4)
C(39)–C(40)–H(40)	119.9	**C(41)–C(40)–H(40)**	119.9
C(40)–C(41)–C(36)	120.2(4)	**C(40)–C(41)–H(41)**	119.9
C(36)–C(41)–H(41)	119.9	**N(2)–C(42)–C(43)**	127.3(3)
N(2)–C(42)–H(42)	116.3	**C(43)–C(42)–H(42)**	116.3
C(44)–C(43)–C(42)	118.2(3)	**C(44)–C(43)–H(43)**	120.9
C(42)–C(43)–H(43)	120.9	**C(43)–C(44)–C(45)**	129.0(3)
C(43)–C(44)–H(44)	115.5	**C(45)–C(44)–H(44)**	115.5
C(50)–C(45)–C(46)	118.5(3)	**C(50)–C(45)–C(44)**	122.7(3)
C(46)–C(45)–C(44)	118.8(3)	**C(47)–C(46)–C(45)**	120.2(4)
C(47)–C(46)–H(46)	119.9	**C(45)–C(46)–H(46)**	119.9
C(48)–C(47)–C(46)	120.3(4)	**C(48)–C(47)–H(47)**	119.8
C(46)–C(47)–H(47)	119.8	**C(47)–C(48)–C(49)**	120.1(4)
C(47)–C(48)–H(48)	120.0	**C(49)–C(48)–H(48)**	120.0
C(50)–C(49)–C(48)	119.8(4)	**C(50)–C(49)–H(49)**	120.1

C(48)–C(49)–H(49)	120.1	C(49)–C(50)–C(45)	121.1(4)
C(49)–C(50)–H(50)	119.5	C(45)–C(50)–H(50)	119.5
C(52)–C(51)–C(71)	118.4(3)	C(52)–C(51)–H(51)	120.8
C(71)–C(51)–H(51)	120.8	C(51)–C(52)–C(53)	128.4(3)
C(51)–C(52)–H(52)	115.8	C(53)–C(52)–H(52)	115.8
C(54)–C(53)–C(58)	118.8(3)	C(54)–C(53)–C(52)	118.3(3)
C(58)–C(53)–C(52)	122.9(3)	C(53)–C(54)–C(55)	120.8(4)
C(53)–C(54)–H(54)	119.6	C(55)–C(54)–H(54)	119.6
C(56)–C(55)–C(54)	119.1(4)	C(56)–C(55)–H(55)	120.4
C(54)–C(55)–H(55)	120.4	C(55)–C(56)–C(57)	120.7(4)
C(55)–C(56)–H(56)	119.6	C(57)–C(56)–H(56)	119.6
C(56)–C(57)–C(58)	120.2(4)	C(56)–C(57)–H(57)	119.9
C(58)–C(57)–H(57)	119.9	C(57)–C(58)–C(53)	120.3(4)
C(57)–C(58)–H(58)	119.8	C(53)–C(58)–H(58)	119.8
N(1)–C(59)–C(60)	112.5(3)	N(1)–C(59)–C(64)	109.1(3)
C(60)–C(59)–C(64)	110.6(3)	N(1)–C(59)–H(59)	108.2
C(60)–C(59)–H(59)	108.2	C(64)–C(59)–H(59)	108.2
C(59)–C(60)–C(61)	115.4(3)	C(59)–C(60)–H(60A)	108.4
C(61)–C(60)–H(60A)	108.4	C(59)–C(60)–H(60B)	108.4
C(61)–C(60)–H(60B)	108.4	H(60A)–C(60)–H(60B)	107.5
N(2)–C(61)–C(62)	111.0(2)	N(2)–C(61)–C(60)	110.2(2)
C(62)–C(61)–C(60)	111.8(3)	N(2)–C(61)–H(61)	107.9
C(62)–C(61)–H(61)	107.9	C(60)–C(61)–H(61)	107.9
C(61)–C(62)–C(63)	114.2(3)	C(61)–C(62)–H(62A)	108.7
C(63)–C(62)–H(62A)	108.7	C(61)–C(62)–H(62B)	108.7
C(63)–C(62)–H(62B)	108.7	H(62A)–C(62)–H(62B)	107.6
N(3)–C(63)–C(64)	111.6(3)	N(3)–C(63)–C(62)	109.6(2)
C(64)–C(63)–C(62)	111.0(3)	N(3)–C(63)–H(63)	108.2
C(64)–C(63)–H(63)	108.2	C(62)–C(63)–H(63)	108.2
C(63)–C(64)–C(59)	114.9(3)	C(63)–C(64)–H(64A)	108.6
C(59)–C(64)–H(64A)	108.6	C(63)–C(64)–H(64B)	108.6
C(59)–C(64)–H(64B)	108.6	H(64A)–C(64)–H(64B)	107.5
C(68)–C(65)–C(66)	112.3(4)	C(68)–C(65)–H(65A)	109.1
C(66)–C(65)–H(65A)	109.1	C(68)–C(65)–H(65B)	109.1

C(66)–C(65)–H(65B)	109.1	**H(65A)–C(65)–H(65B)**	107.9
C(65)–C(66)–C(70)	111.6(4)	**C(65)–C(66)–H(66A)**	109.3
C(70)–C(66)–H(66A)	109.3	**C(65)–C(66)–H(66B)**	109.3
C(70)–C(66)–H(66B)	109.3	**H(66A)–C(66)–H(66B)**	108.0
C(70)–C(67)–C(69)	111.0(4)	**C(70)–C(67)–H(67A)**	109.4
C(69)–C(67)–H(67A)	109.4	**C(70)–C(67)–H(67B)**	109.4
C(69)–C(67)–H(67B)	109.4	**H(67A)–C(67)–H(67B)**	108.0
C(65)–C(68)–C(69)	111.0(4)	**C(65)–C(68)–H(68A)**	109.4
C(69)–C(68)–H(68A)	109.4	**C(65)–C(68)–H(68B)**	109.4
C(69)–C(68)–H(68B)	109.4	**H(68A)–C(68)–H(68B)**	108.0
C(68)–C(69)–C(67)	111.7(4)	**C(68)–C(69)–H(69A)**	109.3
C(67)–C(69)–H(69A)	109.3	**C(68)–C(69)–H(69B)**	109.3
C(67)–C(69)–H(69B)	109.3	**H(69A)–C(69)–H(69B)**	107.9
C(67)–C(70)–C(66)	111.0(4)	**C(67)–C(70)–H(70A)**	109.4
C(66)–C(70)–H(70A)	109.4	**C(67)–C(70)–H(70B)**	109.4
C(66)–C(70)–H(70B)	109.4	**H(70A)–C(70)–H(70B)**	108.0
N(3)–C(71)–C(51)	127.1(3)	**N(3)–C(71)–H(71)**	116.5
C(51)–C(71)–H(71)	116.5	**C(76)#1–C(74)–C(75)**	110.8(4)
C(76)#1–C(74)–H(74A)	109.5	**C(75)–C(74)–H(74A)**	109.5
C(76)#1–C(74)–H(74B)	109.5	**C(75)–C(74)–H(74B)**	109.5
H(74A)–C(74)–H(74B)	108.1	**C(76)–C(75)–C(74)**	111.4(4)
C(76)–C(75)–H(75A)	109.4	**C(74)–C(75)–H(75A)**	109.4
C(76)–C(75)–H(75B)	109.4	**C(74)–C(75)–H(75B)**	109.4
H(75A)–C(75)–H(75B)	108.0	**C(74)#1–C(76)–C(75)**	111.5(4)
C(74)#1–C(76)–H(76A)	109.3	**C(75)–C(76)–H(76A)**	109.3
C(74)#1–C(76)–H(76B)	109.3	**C(75)–C(76)–H(76B)**	109.3
H(76A)–C(76)–H(76B)	108.0	**Cl(1)–C(77)–Cl(2)**	105.4(5)
Cl(1)–C(77)–H(77A)	110.7	**Cl(2)–C(77)–H(77A)**	110.7
Cl(1)–C(77)–H(77B)	110.7	**Cl(2)–C(77)–H(77B)**	110.7
H(77A)–C(77)–H(77B)	108.8	**Cl(3)–C(78)–Cl(4)**	116.1(7)
Cl(3)–C(78)–H(78A)	108.3	**Cl(4)–C(78)–H(78A)**	108.3
Cl(3)–C(78)–H(78B)	108.3	**Cl(4)–C(78)–H(78B)**	108.3
H(78A)–C(78)–H(78B)	107.4	**O(2)–Co(1)–N(1)**	112.12(10)
O(2)–Co(1)–N(2)	138.69(10)	**N(1)–Co(1)–N(2)**	98.61(10)

O(2)–Co(1)–N(3)	109.72(10)	**N(1)–Co(1)–N(3)**	94.33(10)
N(2)–Co(1)–N(3)	94.12(10)	**O(2)–Co(1)–O(1)**	59.02(9)
N(1)–Co(1)–O(1)	91.88(9)	**N(2)–Co(1)–O(1)**	94.35(9)
N(3)–Co(1)–O(1)	168.63(9)	**C(33)–N(1)–C(59)**	116.5(3)
C(33)–N(1)–Co(1)	132.7(2)	**C(59)–N(1)–Co(1)**	110.80(19)
C(42)–N(2)–C(61)	114.8(3)	**C(42)–N(2)–Co(1)**	134.7(2)
C(61)–N(2)–Co(1)	110.45(18)	**C(71)–N(3)–C(63)**	115.5(3)
C(71)–N(3)–Co(1)	132.6(2)	**C(63)–N(3)–Co(1)**	111.85(19)
O(3)–N(4)–O(1)	123.6(3)	**O(3)–N(4)–O(2)**	120.6(3)
O(1)–N(4)–O(2)	115.7(3)	**N(4)–O(1)–Co(1)**	85.48(17)
N(4)–O(2)–Co(1)	99.73(18)		

Symmetry transformations used to generate equivalent atoms:

1 – x, –y + 1, –z + 1

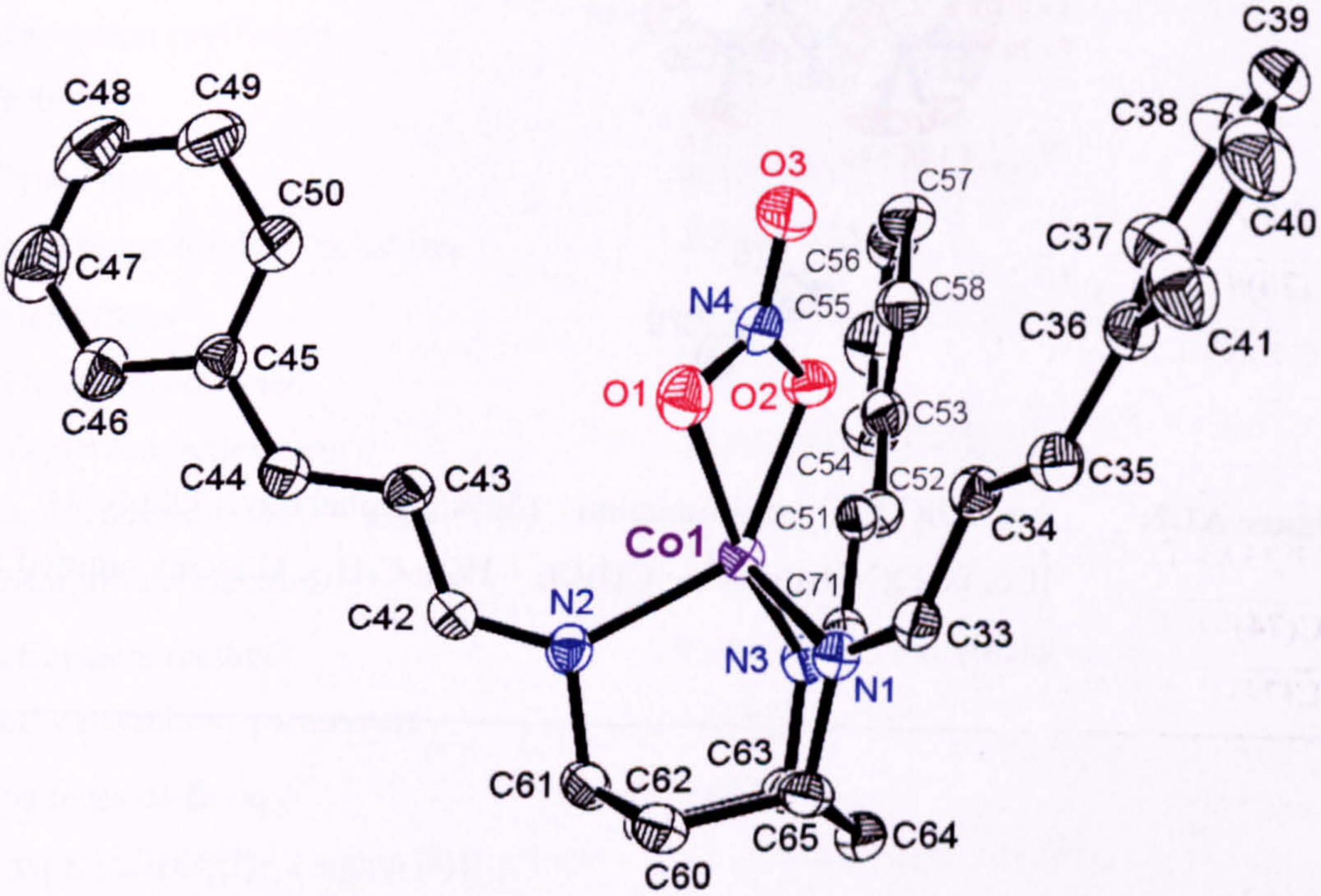

Figure A1.1: An ORTEP[6] representation (30% probability ellipsoids) of $[Co(TCT)(NO_3)]BAr^F{}_4 \cdot CH_2Cl_2 \cdot 1\frac{1}{2}\ c\text{-}C_6H_{12}$, cation only, H atoms omitted for clarity.

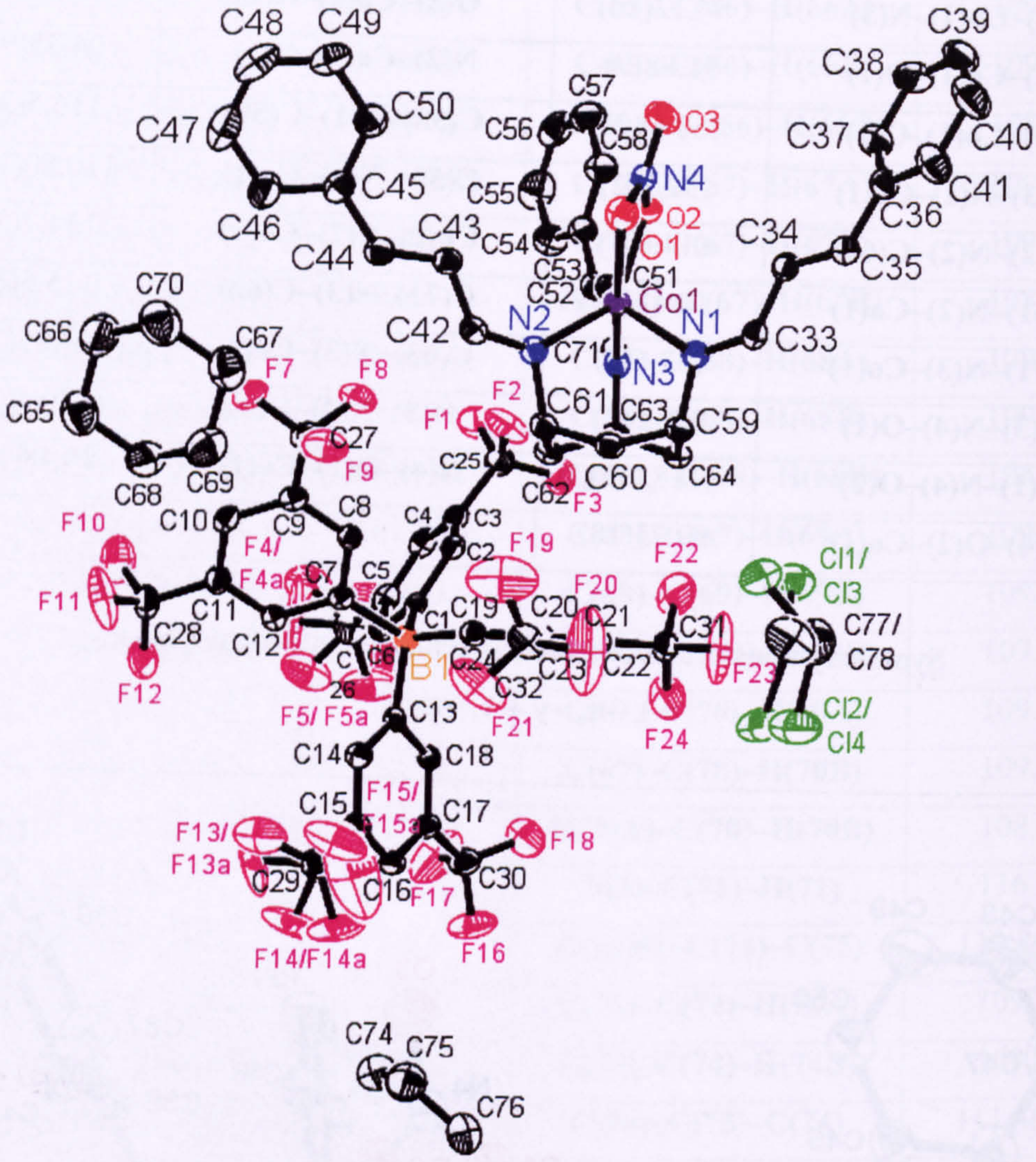

Figure A1.2: An ORTEP representation (30% probability ellipsoids) of $[Co(TCT)(NO_3)]BAr^F{}_4 \cdot CH_2Cl_2 \cdot 1½\ c\text{-}C_6H_{12}$, H atoms omitted for clarity.

A2 Crystal data and structure refinement for [Co(TCT)Cl]BAr^F_4

Identification code	phw0328m	
Empirical formula	$C_{65}H_{45}BClCoF_{24}N_3$	
Formula weight	1429.23	
Temperature	115(2) K	
Wavelength	0.71073 Å	
Crystal system	Triclinic	
Space group	$P\bar{1}$	
Unit cell dimensions	a = 10.063(2) Å	α = 97.365(5)°
	b = 13.421(3) Å	β = 95.966(5)°
	c = 24.709(5) Å	γ = 103.401(4)°
Volume	3188.6(11) $Å^3$	
Z	2	
Density (calculated)	1.489 Mg / m^3	
Absorption coefficient	0.424 mm^{-1}	
$F(000)$	1442	
Crystal size	0.18 × 0.14 × 0.10 mm^3	
Theta range for data collection	0.84 to 25.06°	
Index ranges	$-11 \le h \le 11, -15 \le k \le 15, -29 \le l \le 19$	
Reflections collected	18277	
Independent reflections	11192 [R(int) = 0.0267]	
Completeness to theta = 25.06°	99.2 %	
Absorption correction	None	
Refinement method	Full-matrix least-squares on F^2	
Data / restraints / parameters	11192 / 0 / 910	
Goodness-of-fit on F^2	1.045	
Final R indices [$I > 2$ sigma (I)]	$R1$ = 0.0428, w$R2$ = 0.1034	
R indices (all data)	$R1$ = 0.0652, w$R2$ = 0.1178	
Largest diff. peak and hole	0.529 and –0.365 e.$Å^{-3}$	

Table A2.1: Bond lengths (/ Å) and angles (/ °) for $[Co(TCT)Cl]BAr^{F}_{4}$.

B(1)–C(42)	1.636(4)	**B(1)–C(50)**	1.641(4)
B(1)–C(58)	1.643(4)	**B(1)–C(34)**	1.649(4)
C(1)–N(1)	1.490(3)	**C(1)–C(6)**	1.526(4)
C(1)–C(2)	1.536(4)	**C(1)–H(1)**	1.0000
C(2)–C(3)	1.529(4)	**C(2)–H(2A)**	0.9900
C(2)–H(2B)	0.9900	**C(3)–N(2)**	1.486(3)
C(3)–C(4)	1.0000	**C(4)–C(5)**	1.530(4)
C(4)–H(4A)	0.9900	**C(4)–H(4B)**	0.9900
C(5)–N(3)	1.489(3)	**C(5)–C(6)**	1.530(4)
C(5)–H(5)	1.0000	**C(6)–H(6A)**	0.9900
C(6)–H(6B)	0.9900	**C(7)–N(1)**	1.289(3)
C(7)–C(8)	1.437(4)	**C(7)–H(7)**	0.9500
C(8)–C(9)	1.332(4)	**C(8)–H(8)**	0.9500
C(9)–C(10)	1.455(4)	**C(9)–H(9)**	0.9500
C(10)–C(15)	1.392(4)	**C(10)–C(11)**	1.393(4)
C(11)–C(12)	1.391(4)	**C(11)–H(11)**	0.9500
C(12)–C(13)	1.373(4)	**C(12)–H(12)**	0.9500
C(13)–C(14)	1.385(4)	**C(13)–H(13)**	0.9500
C(14)–C(15)	1.376(4)	**C(14)–H(14)**	0.9500
C(15)–H(15)	0.9500	**C(16)–N(2)**	1.287(3)
C(16)–C(17)	0.9500	**C(17)–C(18)**	1.339(4)
C(17)–H(17)	0.9500	**C(18)–C(19)**	1.465(4)
C(18)–H(18)	0.9500	**C(19)–C(20)**	1.386(4)
C(19)–C(24)	1.397(4)	**C(20)–C(21)**	1.387(4)
C(20)–H(20)	0.9500	**C(21)–C(22)**	1.378(4)
C(21)–H(21)	0.9500	**C(22)–C(23)**	1.380(4)
C(22)–H(22)	0.9500	**C(23)–C(24)**	1.385(4)
C(23)–H(23)	0.9500	**C(24)–H(24)**	0.9500
C(25)–N(3)	1.286(3)	**C(25)–C(26)**	1.436(4)
C(25)–H(25)	0.9500	**C(26)–C(27)**	1.341(4)
C(26)–H(26)	0.9500	**C(27)–C(28)**	1.460(4)
C(27)–H(27)	0.9500	**C(28)–C(29)**	1.385(4)

C(28)–C(33)	1.389(4)	C(29)–C(30)	1.383(5)
C(29)–H(29)	0.9500	C(30)–C(31)	1.357(5)
C(30)–H(30)	0.9500	C(31)–C(32)	1.380(4)
C(31)–H(31)	0.9500	C(32)–C(33)	1.386(4)
C(32)–H(32)	0.9500	C(33)–H(33)	0.9500
C(34)–C(35)	1.398(3)	C(34)–C(39)	1.402(3)
C(35)–C(36)	1.393(3)	C(35)–H(35)	0.9500
C(36)–C(37)	1.390(4)	C(36)–C(40)	1.496(4)
C(37)–C(38)	1.386(4)	C(37)–H(37)	0.9500
C(38)–C(39)	1.397(3)	C(38)–C(41)	1.485(4)
C(39)–H(39)	0.9500	C(40)–F(1)	1.337(3)
C(40)–F(3)	1.341(3)	C(40)–F(2)	1.351(3)
C(41)–F(4)	1.326(3)	C(41)–F(6)	1.334(3)
C(41)–F(5)	1.341(3)	C(42)–C(47)	1.392(4)
C(42)–C(43)	1.397(4)	C(43)–C(44)	1.390(4)
C(43)–H(43)	0.9500	C(44)–C(45)	1.389(4)
C(44)–C(48)	1.497(4)	C(45)–C(46)	1.383(4)
C(45)–H(45)	0.9500	C(46)–C(47)	1.393(4)
C(46)–C(49)	1.501(4)	C(47)–H(47)	0.9500
C(48)–F(7)	1.330(3)	C(48)–F(8)	1.337(3)
C(48)–F(9)	1.346(3)	C(49)–F(11A)	1.203(10)
C(49)–F(12A)	1.235(6)	C(49)–F(10)	1.272(5)
C(49)–F(11)	1.333(10)	C(49)–F(10A)	1.404(7)
C(49)–F(12)	1.422(6)	C(50)–C(55)	1.398(4)
C(50)–C(51)	1.399(3)	C(51)–C(52)	1.390(4)
C(51)–H(51)	0.9500	C(52)–C(53)	1.383(4)
C(52)–C(56)	1.498(4)	C(53)–C(54)	1.385(4)
C(53)–H(53)	0.9500	C(54)–C(55)	1.394(4)
C(54)–C(57)	1.490(4)	C(55)–H(55)	0.9500
C(56)–F(15)	1.331(3)	C(56)–F(13)	1.335(3)
C(56)–F(14)	1.345(3)	C(57)–F(18)	1.259(6)
C(57)–F(17A)	1.261(9)	C(57)–F(16A)	1.261(6)
C(57)–F(17)	1.281(10)	C(57)–F(16)	1.401(6)
C(57)–F(18A)	1.405(7)	C(58)–C(63)	1.396(4)

C(58)–C(59)	1.402(3)	**C(59)–C(60)**	1.398(4)
C(59)–H(59)	0.9500	**C(60)–C(61)**	1.384(4)
C(60)–C(64)	1.487(4)	**C(61)–C(62)**	1.373(4)
C(61)–H(61)	0.9500	**C(62)–C(63)**	1.394(4)
C(62)–C(65)	1.498(4)	**C(63)–H(63)**	0.9500
C(64)–F(21)	1.319(3)	**C(64)–F(20)**	1.338(3)
C(64)–F(19)	1.344(3)	**C(65)–F(22)**	1.321(4)
C(65)–F(24)	1.322(3)	**C(65)–F(23)**	1.342(4)
Cl(1)–Co(1)	2.2208(8)	**Co(1)–N(1)**	2.000(2)
Co(1)–N(3)	2.010(2)	**Co(1)–N(2)**	2.018(2)
C(42)–B(1)–C(50)	109.6(2)	**C(42)–B(1)–C(58)**	111.3(2)
C(50)–B(1)–C(58)	109.1(2)	**C(42)–B(1)–C(34)**	107.3(2)
C(50)–B(1)–C(34)	109.4(2)	**C(58)–B(1)–C(34)**	110.1(2)
N(1)–C(1)–C(6)	109.8(2)	**N(1)–C(1)–C(2)**	110.4(2)
C(6)–C(1)–C(2)	112.0(2)	**N(1)–C(1)–H(1)**	108.2
C(6)–C(1)–H(1)	108.2	**C(2)–C(1)–H(1)**	108.2
C(3)–C(2)–C(1)	114.7(2)	**C(3)–C(2)–H(2A)**	108.6
C(1)–C(2)–H(2A)	108.6	**C(3)–C(2)–H(2B)**	108.6
C(1)–C(2)–H(2B)	108.6	**H(2A)–C(2)–H(2B)**	107.6
N(2)–C(3)–C(4)	110.1(2)	**N(2)–C(3)–C(2)**	110.4(2)
C(4)–C(3)–C(2)	111.2(2)	**N(2)–C(3)–H(3)**	108.3
C(4)–C(3)–H(3)	108.3	**C(2)–C(3)–H(3)**	108.3
C(3)–C(4)–C(5)	114.2(2)	**C(3)–C(4)–H(4A)**	108.7
C(5)–C(4)–H(4A)	108.7	**C(3)–C(4)–H(4B)**	108.7
C(5)–C(4)–H(4B)	108.7	**H(4A)–C(4)–H(4B)**	107.6
N(3)–C(5)–C(4)	110.5(2)	**N(3)–C(5)–C(6)**	110.6(2)
C(4)–C(5)–C(6)	110.9(2)	**N(3)–C(5)–H(5)**	108.3
C(4)–C(5)–H(5)	108.3	**C(6)–C(5)–H(5)**	108.3
C(1)–C(6)–C(5)	114.8(2)	**C(1)–C(6)–H(6A)**	108.6
C(5)–C(6)–H(6A)	108.6	**C(1)–C(6)–H(6B)**	108.6
C(5)–C(6)–H(6B)	108.6	**H(6A)–C(6)–H(6B)**	107.5
N(1)–C(7)–C(8)	125.1(3)	**N(1)–C(7)–H(7)**	117.5
C(8)–C(7)–H(7)	117.5	**C(9)–C(8)–C(7)**	120.8(3)

C(9)–C(8)–H(8)	119.6	C(7)–C(8)–H(8)	119.6
C(8)–C(9)–C(10)	127.1(3)	C(8)–C(9)–H(9)	116.4
C(10)–C(9)–H(9)	116.4	C(15)–C(10)–C(11)	118.4(3)
C(15)–C(10)–C(9)	122.3(3)	C(11)–C(10)–C(9)	119.3(3)
C(12)–C(11)–C(10)	120.4(3)	C(12)–C(11)–H(11)	119.8
C(10)–C(11)–H(11)	119.8	C(13)–C(12)–C(11)	120.1(3)
C(13)–C(12)–H(12)	119.9	C(11)–C(12)–H(12)	119.9
C(12)–C(13)–C(14)	120.2(3)	C(12)–C(13)–H(13)	119.9
C(14)–C(13)–H(13)	119.9	C(15)–C(14)–C(13)	119.8(3)
C(15)–C(14)–H(14)	120.1	C(13)–C(14)–H(14)	120.1
C(14)–C(15)–C(10)	121.2(3)	C(14)–C(15)–H(15)	119.4
C(10)–C(15)–H(15)	119.4	N(2)–C(16)–C(17)	124.2(3)
N(2)–C(16)–H(16)	117.9	C(17)–C(16)–H(16)	117.9
C(18)–C(17)–C(16)	121.1(3)	C(18)–C(17)–H(17)	119.4
C(16)–C(17)–H(17)	119.4	C(17)–C(18)–C(19)	127.5(3)
C(17)–C(18)–H(18)	116.3	C(19)–C(18)–H(18)	116.3
C(20)–C(19)–C(24)	118.5(3)	C(20)–C(19)–C(18)	119.2(3)
C(24)–C(19)–C(18)	122.3(3)	C(19)–C(20)–C(21)	120.8(3)
C(19)–C(20)–H(20)	119.6	C(21)–C(20)–H(20)	119.6
C(22)–C(21)–C(20)	120.1(3)	C(22)–C(21)–H(21)	120.0
C(20)–C(21)–H(21)	120.0	C(21)–C(22)–C(23)	120.1(3)
C(21)–C(22)–H(22)	120.0	C(23)–C(22)–H(22)	120.0
C(22)–C(23)–C(24)	120.0(3)	C(22)–C(23)–H(23)	120.0
C(24)–C(23)–H(23)	120.0	C(23)–C(24)–C(19)	120.6(3)
C(23)–C(24)–H(24)	119.7	C(19)–C(24)–H(24)	119.7
N(3)–C(25)–C(26)	123.0(3)	N(3)–C(25)–H(25)	118.5
C(26)–C(25)–H(25)	118.5	C(27)–C(26)–C(25)	122.9(3)
C(27)–C(26)–H(26)	118.6	C(25)–C(26)–H(26)	118.6
C(26)–C(27)–C(28)	126.1(3)	C(26)–C(27)–H(27)	117.0
C(28)–C(27)–H(27)	117.0	C(29)–C(28)–C(33)	117.5(3)
C(29)–C(28)–C(27)	120.5(3)	C(33)–C(28)–C(27)	121.9(3)
C(30)–C(29)–C(28)	121.3(3)	C(30)–C(29)–H(29)	119.4
C(28)–C(29)–H(29)	119.4	C(31)–C(30)–C(29)	120.6(3)
C(31)–C(30)–H(30)	119.7	C(29)–C(30)–H(30)	119.7

C(30)–C(31)–C(32)	119.4(3)	C(30)–C(31)–H(31)	120.3
C(32)–C(31)–H(31)	120.3	C(31)–C(32)–C(33)	120.2(3)
C(31)–C(32)–H(32)	119.9	C(33)–C(32)–H(32)	119.9
C(32)–C(33)–C(28)	120.9(3)	C(32)–C(33)–H(33)	119.6
C(28)–C(33)–H(33)	119.6	C(35)–C(34)–C(39)	115.8(2)
C(35)–C(34)–B(1)	120.3(2)	C(39)–C(34)–B(1)	123.8(2)
C(36)–C(35)–C(34)	122.8(2)	C(36)–C(35)–H(35)	118.6
C(34)–C(35)–H(35)	118.6	C(37)–C(36)–C(35)	120.5(2)
C(37)–C(36)–C(40)	119.8(2)	C(35)–C(36)–C(40)	119.6(2)
C(38)–C(37)–C(36)	117.8(2)	C(38)–C(37)–H(37)	121.1
C(36)–C(37)–H(37)	121.1	C(37)–C(38)–C(39)	121.5(2)
C(37)–C(38)–C(41)	119.4(2)	C(39)–C(38)–C(41)	119.1(2)
C(38)–C(39)–C(34)	121.6(2)	C(38)–C(39)–H(39)	119.2
C(34)–C(39)–H(39)	119.2	F(1)–C(40)–F(3)	106.8(2)
F(1)–C(40)–F(2)	105.8(2)	F(3)–C(40)–F(2)	105.2(2)
F(1)–C(40)–C(36)	113.1(2)	F(3)–C(40)–C(36)	112.9(2)
F(2)–C(40)–C(36)	112.5(2)	F(4)–C(41)–F(6)	105.9(2)
F(4)–C(41)–F(5)	105.3(2)	F(6)–C(41)–F(5)	104.7(2)
F(4)–C(41)–C(38)	113.3(2)	F(6)–C(41)–C(38)	113.7(2)
F(5)–C(41)–C(38)	113.2(2)	C(47)–C(42)–C(43)	116.0(2)
C(47)–C(42)–B(1)	124.2(2)	C(43)–C(42)–B(1)	119.8(2)
C(44)–C(43)–C(42)	122.6(3)	C(44)–C(43)–H(43)	118.7
C(42)–C(43)–H(43)	118.7	C(45)–C(44)–C(43)	120.0(3)
C(45)–C(44)–C(48)	121.1(2)	C(43)–C(44)–C(48)	119.0(3)
C(46)–C(45)–C(44)	118.7(3)	C(46)–C(45)–H(45)	120.6
C(44)–C(45)–H(45)	120.6	C(45)–C(46)–C(47)	120.5(3)
C(45)–C(46)–C(49)	119.6(3)	C(47)–C(46)–C(49)	119.9(3)
C(42)–C(47)–C(46)	122.2(3)	C(42)–C(47)–H(47)	118.9
C(46)–C(47)–H(47)	118.9	F(7)–C(48)–F(8)	106.5(2)
F(7)–C(48)–F(9)	105.5(3)	F(8)–C(48)–F(9)	106.3(2)
F(7)–C(48)–C(44)	112.7(2)	F(8)–C(48)–C(44)	112.9(3)
F(9)–C(48)–C(44)	112.3(2)	F(11A)–C(49)–F(12A)	115.3(8)
F(11A)–C(49)–F(10)	61.1(4)	F(12A)–C(49)–F(10)	125.7(7)
F(11A)–C(49)–F(11)	31.0(9)	F(12A)–C(49)–F(11)	132.5(7)

F(10)–C(49)–F(11)	107.0(7)	F(11A)–C(49)–F(10A)	105.6(7)
F(12A)–C(49)–F(10A)	102.6(6)	F(10)–C(49)–F(10A)	41.7(4)
F(11)–C(49)–F(10A)	76.3(7)	F(11A)–C(49)–F(12)	72.7(7)
F(12A)–C(49)–F(12)	47.1(4)	F(10)–C(49)–F(12)	101.6(5)
F(11)–C(49–F(12)	100.4(6)	F(10A)–C(49)–F(12)	135.2(4)
F(11A)–C(49)–C(46)	112.8(6)	F(12A)–C(49)–C(46)	111.7(3)
F(10)–C(49)–C(46)	118.1(3)	F(11)–C(49)–C(46)	113.7(6)
F(10A)–C(49)–C(46)	107.7(4)	F(12)–C(49)–C(46)	114.1(3)
C(55)–C(50)–C(51)	115.1(2)	C(55)–C(50)–B(1)	121.2(2)
C(51)–C(50)–B(1)	123.5(2)	C(52)–C(51)–C(50)	122.6(2)
C(52)–C(51)–H(51)	118.7	C(50)–C(51)–H(51)	118.7
C(53)–C(52)–C(51)	120.9(2)	C(53)–C(52)–C(56)	120.5(2)
C(51)–C(52)–C(56)	118.6(2)	C(52)–C(53)–C(54)	118.1(2)
C(52)–C(53)–H(53)	120.9	C(54)–C(53)–H(53)	120.9
C(53)–C(54)–C(55)	120.4(2)	C(53)–C(54)–C(57)	120.0(2)
C(55)–C(54)–C(57)	119.5(2)	C(54)–C(55)–C(50)	122.8(2)
C(54)–C(55)–H(55)	118.6	C(50)–C(55)–H(55)	118.6
F(15)–C(56)–F(13)	106.9(2)	F(15)–C(56)–F(14)	106.5(2)
F(13)–C(56)–F(14)	105.9(2)	F(15)–C(56)–C(52)	112.5(2)
F(13)–C(56)–C(52)	113.1(2)	F(14)–C(56)–C(52)	111.5(2)
F(18)–C(57)–F(17A)	129.3(6)	F(18)–C(57)–F(16A)	57.5(5)
F(17A)–C(57)–F(16A)	113.0(7)	F(18)–C(57)–F(17)	110.7(6)
F(17A)–C(57)–F(17)	28.5(8)	F(16A)–C(57)–F(17)	125.5(5)
F(18)–C(57)–F(16)	102.4(5)	F(17A)–C(57)–F(16)	74.0(6)
F(16A)–C(57)–F(16)	47.2(5)	F(17)–C(57)–F(16)	98.9(6)
F(18)–C(57)–F(18A)	49.5(4)	F(17A)–C(57)–F(18A)	98.9(6)
F(16A)–C(57)–F(18A)	104.4(6)	F(17)–C(57)–F(18A)	71.2(6)
F(16)–C(57)–F(18A)	137.5(4)	F(18)–C(57)–C(54)	115.4(3)
F(17A)–C(57)–C(54)	112.6(5)	F(16A)–C(57)–C(54)	115.8(4)
F(17)–C(57)–C(54)	116.2(5)	F(16)–C(57)–C(54)	111.0(3)
F(18A)–C(57)–C(54)	110.3(3)	C(63)–C(58)–C(59)	115.9(2)
C(63)–C(58)–B(1)	120.3(2)	C(59)–C(58)–B(1)	123.7(2)
C(60)–C(59)–C(58)	121.7(3)	C(60)–C(59)–H(59)	119.2
C(58)–C(59)–H(59)	119.2	C(61)–C(60)–C(59)	120.6(2)

C(61)–C(60)–C(64)	118.8(2)	**C(59)–C(60)–C(64)**	120.6(2)
C(62)–C(61)–C(60)	118.9(2)	**C(62)–C(61)–H(61)**	120.6
C(60)–C(61)–H(61)	120.6	**C(61)–C(62)–C(63)**	120.3(3)
C(61)–C(62)–C(65)	120.0(2)	**C(63)–C(62)–C(65)**	119.6(3)
C(62)–C(63)–C(58)	122.6(2)	**C(62)–C(63)–H(63)**	118.7
C(58)–C(63)–H(63)	118.7	**F(21)–C(64)–F(20)**	106.8(2)
F(21)–C(64)–F(19)	106.2(2)	**F(20)–C(64)–F(19)**	104.1(2)
F(21)–C(64)–C(60)	114.1(2)	**F(20)–C(64)–C(60)**	112.4(2)
F(19)–C(64)–C(60)	112.6(2)	**F(22)–C(65)–F(24)**	108.0(3)
F(22)–C(65)–F(23)	104.5(3)	**F(24)–C(65)–F(23)**	104.8(3)
F(22)–C(65)–C(62)	113.5(2)	**F(24)–C(65)–C(62)**	113.0(3)
F(23)–C(65)–C(62)	112.3(3)	**N(1)–Co(1)–N(3)**	97.41(9)
N(1)–Co(1)–N(2)	97.95(9)	**N(3)–Co(1)–N(2)**	93.66(9)
N(1)–Co(1)–Cl(1)	119.93(7)	**N(3)–Co(1)–Cl(1)**	121.31(7)
N(2)–Co(1)–Cl(1)	120.67(6)	**C(7)–N(1)–C(1)**	117.5(2)
C(7)–N(1)–Co(1)	131.88(19)	**C(1)–N(1)–Co(1)**	110.60(16)
C(16)–N(2)–C(3)	118.2(2)	**C(16)–N(2)–Co(1)**	129.82(19)
C(3)–N(2)–Co(1))	111.62(16)	**C(25)–N(3)–C(5)**	118.2(2)
C(25)–N(3)–Co(1)	130.35(19)	**C(5)–N(3)–Co(1)**	111.45(16)

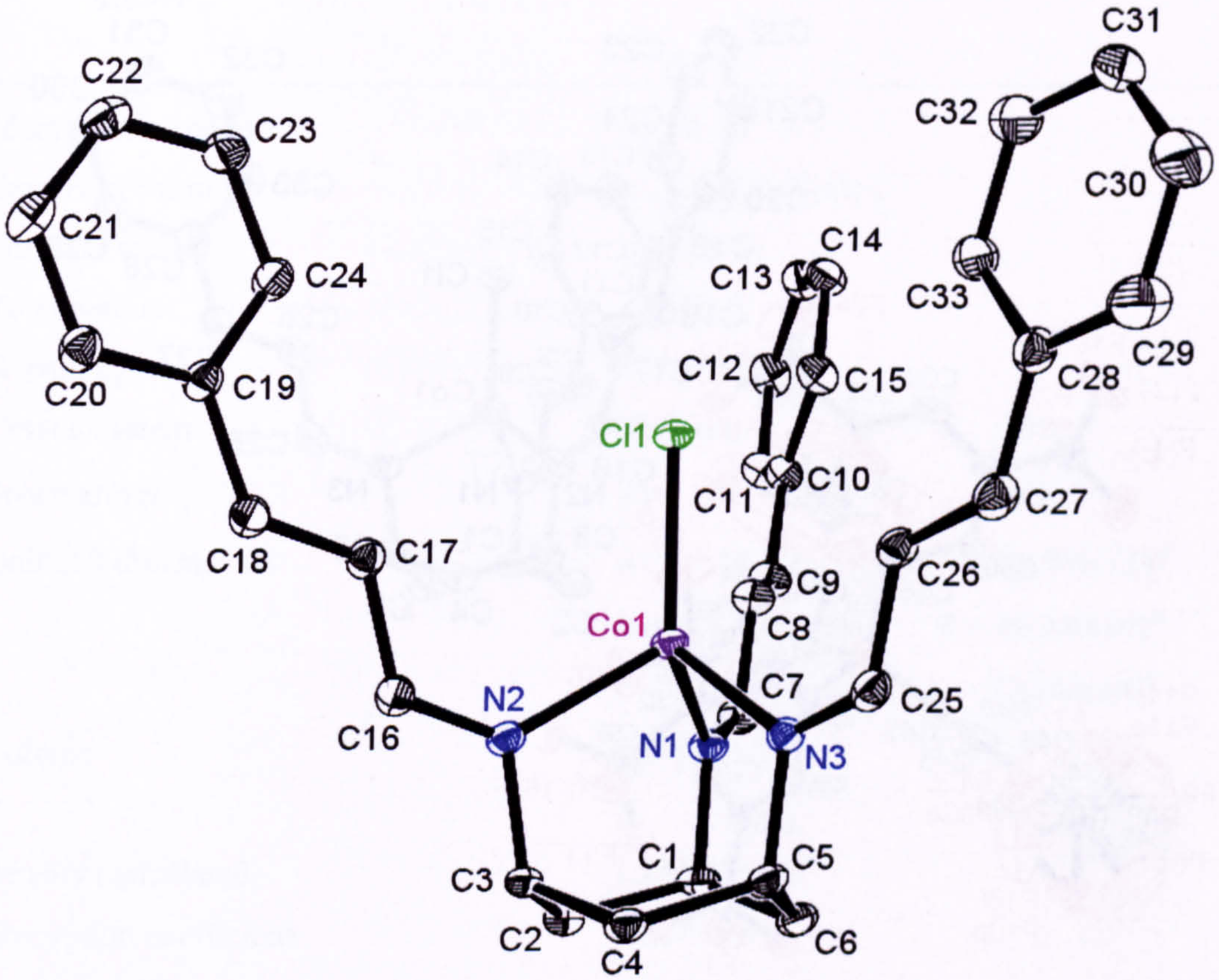

Figure A2.1: An ORTEP representation (30% probability ellipsoids) of $[Co(TCT)Cl]BAr^{F}_{4}$, cation only, H atoms omitted for clarity.

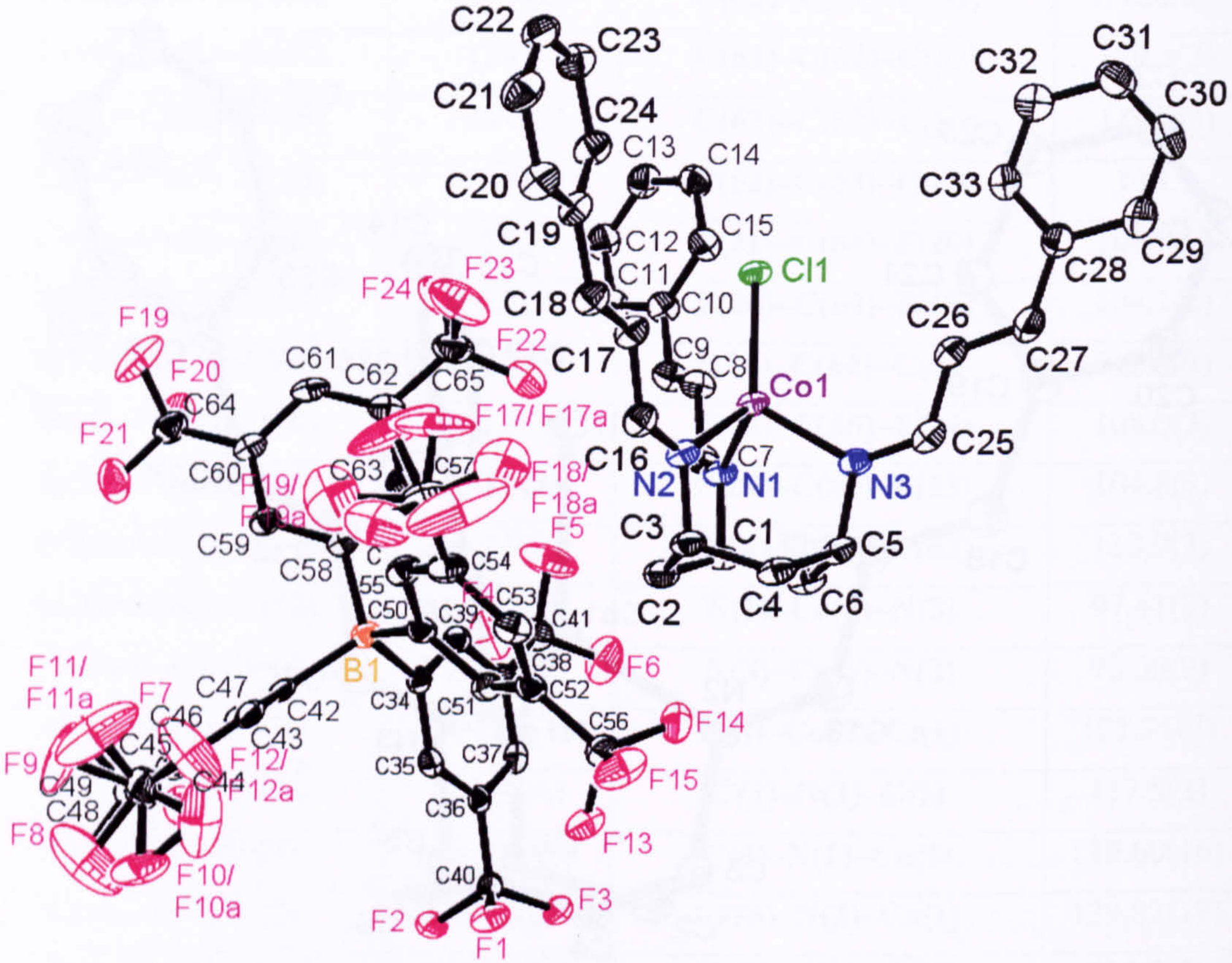

Figure A2.2: An ORTEP representation (30% probability ellipsoids) of $[Co(TCT)Cl]BAr^{F}_{4}$, H atoms omitted for clarity.

A3 Crystal data and structure refinement for $[Co(TCT)(OEt)]BPh_4 \cdot ½ EtOH$

Identification code	sja60_01	
Empirical formula	$C_{60}H_{61}BCoN_3O_{1.5}$	
Formula weight	917.86	
Temperature	150(2) K	
Wavelength	0.71073 Å	
Crystal system	Triclinic	
Space group	$P\bar{1}$	
Unit cell dimensions	a = 11.053(2) Å	α = 65.866(12)°
	b = 15.812(3) Å	β = 86.349(14)°
	c = 16.503(3) Å	γ = 72.640(14)°
Volume	2506.6(8) $Å^3$	
Z	2	
Density (calculated)	1.216 Mg / m^3	
Absorption coefficient	0.387 mm^{-1}	
F(000)	972	
Crystal size	0.18 × 0.12 × 0.07 mm^3	
Theta range for data collection	2.50 to 30.00°	
Index ranges	$-15 \le h \le 15, -22 \le k \le 22, -23 \le l \le 23$	
Reflections collected	47525	
Independent reflections	14596 [*R*(int) = 0.1698]	
Completeness to theta = 30.00°	99.8 %	
Refinement method	Full-matrix least-squares on F^2	
Data / restraints / parameters	14596 / 2 / 600	
Goodness-of-fit on F^2	0.972	
Final *R* indices [$I > 2$ sigma (I)]	$R1 = 0.0901$, $wR2 = 0.2216$	
R indices (all data)	$R1 = 0.2087$, $wR2 = 0.2510$	
Extinction coefficient	0.0146(14)	
Largest diff. peak and hole	0.676 and –0.541 $e.Å^{-3}$	

Table A3.1: Bond lengths (/ Å) and angles (/ °) for $[Co(TCT)(OEt)]BPh_4 \cdot ½ EtOH$.

C(1)–N(1)	1.506(6)	**C(1)–C(6)**	1.521(7)
C(1)–C(2)	1.522(8)	**C(2)–C(3)**	1.531(8)
C(3)–N(2)	1.477(6)	**C(3)–C(4)**	1.541(7)
C(4)–C(5)	1.509(8)	**C(5)–N(3)**	1.482(6)
C(5)–C(6)	1.531(8)	**C(7)–N(1)**	1.295(7)
C(7)–C(8)	1.444(7)	**C(8)–C(9)**	1.349(8)
C(9)–C(10)	1.465(7)	**C(10)–C(11)**	1.377(8)
C(10)–C(15)	1.397(8)	**C(11)–C(12)**	1.391(8)
C(12)–C(13)	1.338(9)	**C(13)–C(14)**	1.368(9)
C(14)–C(15)	1.392(7)	**C(16)–N(2)**	1.291(7)
C(16)–C(17)	1.440(7)	**C(17)–C(18)**	1.328(8)
C(18)–C(19)	1.472(7)	**C(19)–C(20)**	1.378(9)
C(19)–C(24)	1.395(9)	**C(20–C(21)**	1.388(8)
C(21)–C(22)	1.388(10)	**C(22)–C(23)**	1.388(10)
C(23)–C(24)	1.378(8)	**C(25)–N(3)**	1.281(7)
C(25)–C(26)	1.444(8)	**C(26)–C(27)**	1.314(8)
C(27)–C(28)	1.489(9)	**C(28)–C(29)**	1.380(10)
C(28)–C(33)	1.399(10)	**C(29)–C(30)**	1.402(10)
C(30)–C(31)	1.348(14)	**C(31)–C(32)**	1.341(14)
C(32)–C(33)	1.398(11)	**C(34)–O(1)**	1.224(10)
C(34)–C(35)	1.518(11)	**C(36)–C(37)**	1.402(8)
C(36)–C(41)	1.410(7)	**C(36)–B(1)**	1.646(8)
C(37)–C(38)	1.387(9)	**C(38)–C(39)**	1.382(9)
C(39)–C(40)	1.379(9)	**C(40)–C(41)**	1.365(8)
C(42)–C(43)	1.403(7)	**C(42)–C(47)**	1.423(8)
C(42)–B(1)	1.634(9)	**C(43)–C(44)**	1.376(8)
C(44)–C(45)	1.387(9)	**C(45)–C(46)**	1.378(8)
C(46)–C(47)	1.382(8)	**C(48)–C(49)**	1.372(8)
C(48)–C(53)	1.393(8)	**C(48)–B(1)**	1.661(7)
C(49)–C(50)	1.422(8)	**C(50)–C(51)**	1.359(10)
C(51)–C(52)	1.367(10)	**C(52)–C(53)**	1.394(8)
C(54)–C(59)	1.391(8)	**C(54)–C(55)**	1.420(8)

C(54)–B(1)	1.644(8)	C(55)–C(56)	1.381(8)
C(56)–C(57)	1.402(9)	C(57)–C(58)	1.371(8)
C(58)–C(59)	1.401(8)	Co(1)–O(1)	1.867(4)
Co(1)–N(1)	2.014(4)	Co(1)–N(3)	2.019(4)
Co(1)–N(2)	2.027(4)	O(1S)–C(1S)	1.484(16)
C(1S)–C(2S)	1.526(16)		
N(1)–C(1)–C(6)	110.3(4)	N(1)–C(1)–C(2)	109.0(4)
C(6)–C(1)–C(2)	111.7(4)	C(1)–C(2)–C(3)	114.0(4)
N(2)–C(3)–C(2)	110.8(4)	N(2)–C(3)–C(4)	109.8(4)
C(2)–C(3)–C(4)	111.1(4)	C(5)–C(4)–C(3)	114.3(4)
N(3)–C(5)–C(4)	111.2(4)	N(3)–C(5)–C(6)	109.0(4)
C(4)–C(5)–C(6)	113.0(5)	C(1)–C(6)–C(5)	114.9(4)
N(1)–C(7)–C(8)	121.8(5)	C(9)–C(8)–C(7)	122.4(5)
C(8)–C(9)–C(10)	123.6(5)	C(11)–C(10)–C(15)	118.3(5)
C(11)–C(10)–C(9)	121.7(5)	C(15)–C(10)–C(9)	120.0(5)
C(10)–C(11)–C(12)	119.9(6)	C(13)–C(12)–C(11)	121.2(6)
C(12)–C(13)–C(14)	120.6(5)	C(13)–C(14)–C(15)	119.4(5)
C(14)–C(15)–C(10)	120.5(5)	N(2)–C(16)–C(17)	123.4(5)
C(18)–C(17)–C(16)	122.1(6)	C(17)–C(18)–C(19)	126.8(6)
C(20)–C(19)–C(24)	118.6(5)	C(20)–C(19)–C(18)	122.6(5)
C(24)–C(19)–C(18)	118.7(5)	C(19)–C(20)–C(21)	121.3(6)
C(22)–C(21)–C(20)	119.9(7)	C(21)-C(22)–C(23)	118.9(6)
C(24)–C(23)–C(22)	121.0(6)	C(23)–C(24)–C(19)	120.3(6)
N(3)–C(25)–C(26)	124.5(5)	C(27)–C(26)–C(25)	121.1(5)
C(26)–C(27)–C(28)	124.9(6)	C(29)–C(28)–C(33)	120.4(7)
C(29)–C(28)–C(27)	121.9(6)	C(33)–C(28)–C(27)	117.6(7)
C(28)–C(29)–C(30)	118.4(8)	C(31)–C(30)–C(29)	120.5(10)
C(32)–C(31)–C(30)	121.9(9)	C(31)–C(32)–C(33)	120.2(9)
C(32)–C(33)–C(28)	118.6(9)	O(1)–C(34)–C(35)	116.1(7)
C(37)–C(36)–C(41)	113.8(5)	C(37)–C(36)–B(1)	126.9(5)
C(41)–C(36)–B(1)	119.2(5)	C(38)–C(37)–C(36)	122.8(5)
C(39)–C(38)–C(37)	120.7(6)	C(40)–C(39)–C(38)	118.3(5)
C(41)–C(40)–C(39)	120.4(5)	C(40)–C(41)–C(36)	124.0(6)

C(43)–C(42)–C(47)	113.7(5)	**C(43)–C(42)–B(1)**	126.2(5)
C(47)–C(42)–B(1)	120.1(5)	**C(44)–C(43)–C(42)**	123.5(5)
C(43)–C(44)–C(45)	120.9(6)	**C(46)–C(45)–C(44)**	117.9(6)
C(45)–C(46)–C(47)	120.9(6)	**C(46)–C(47)–C(42)**	122.9(5)
C(49)–C(48)–C(53)	115.5(5)	**C(49)–C(48)–B(1)**	125.6(5)
C(53)–C(48)–B(1)	118.7(5)	**C(48)–C(49)–C(50)**	121.5(6)
C(51)–C(50)–C(49)	121.0(6)	**C(50)–C(51)–C(52)**	118.8(5)
C(51)–C(52)–C(53)	119.8(6)	**C(48)–C(53)–C(52)**	123.3(6)
C(59)–C(54)–C(55)	114.6(5)	**C(59)–C(54)–B(1)**	125.2(5)
C(55)–C(54)–B(1)	120.1(5)	**C(56)–C(55)–C(54)**	122.7(6)
C(55)–C(56)–C(57)	120.6(6)	**C(58)–C(57)–C(56)**	118.1(5)
C(57)–C(58)–C(59)	120.7(6)	**C(54)–C(59)–C(58)**	123.2(5)
C(42)–B(1)–C(54)	112.4(4)	**C(42)–B(1)–C(36)**	111.2(4)
C(54)–B(1)–C(36)	105.9(4)	**C(42)–B(1)–C(48)**	107.4(4)
C(54)–B(1)–C(48)	108.6(4)	**C(36)–B(1)–C(48)**	111.3(4)
O(1)–Co(1)–N(1)	115.11(19)	**O(1)–Co(1)–N(3)**	122.96(18)
N(1)–Co(1)–N(3)	97.41(17)	**O(1)–Co(1)–N(2)**	125.82(19)
N(1)–Co(1)–N(2)	91.76(18)	**N(3)–Co(1)–N(2)**	96.51(17)
C(7)–N(1)–C(1)	117.6(4)	**C(7)–N(1)–Co(1)**	129.2(4)
C(1)–N(1)–Co(1)	112.5(3)	**C(16)–N(2)–C(3)**	117.8(4)
C(16)–N(2)–Co(1)	129.2(4)	**C(3)–N(2)–Co(1)**	112.8(3)
C(25)–N(3)–C(5)	119.1(4)	**C(25)–N(3)–Co(1)**	130.1(3)
C(5)–N(3)–Co(1)	110.9(3)	**C(34)–O(1)–Co(1)**	136.8(5)
O(1S)–C(1S)–C(2S)	125.4(16)		

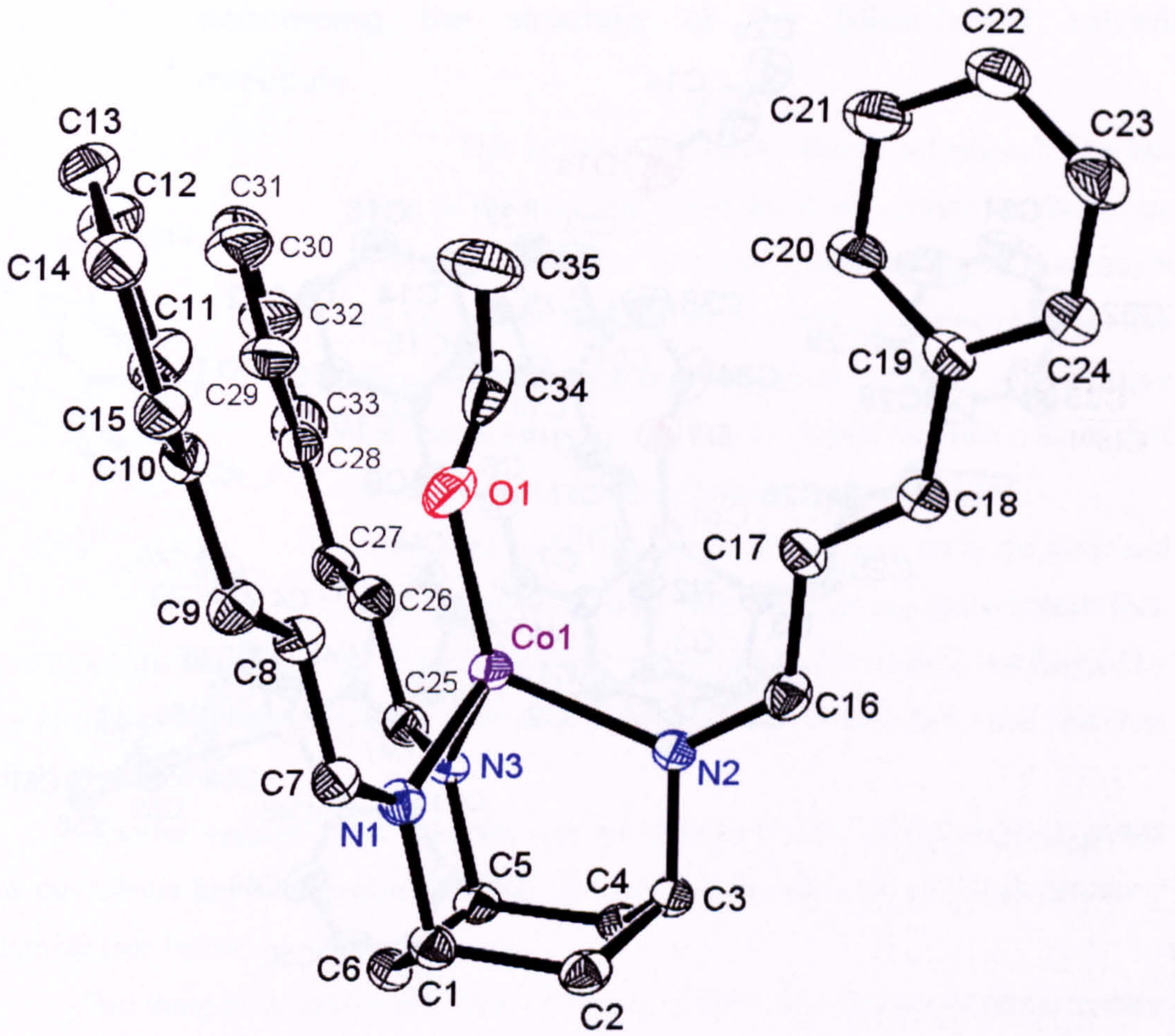

Figure A3.1: An ORTEP representation (30% probability ellipsoids) of $[Co(TCT)(OEt)]^+$, H atoms omitted for clarity.

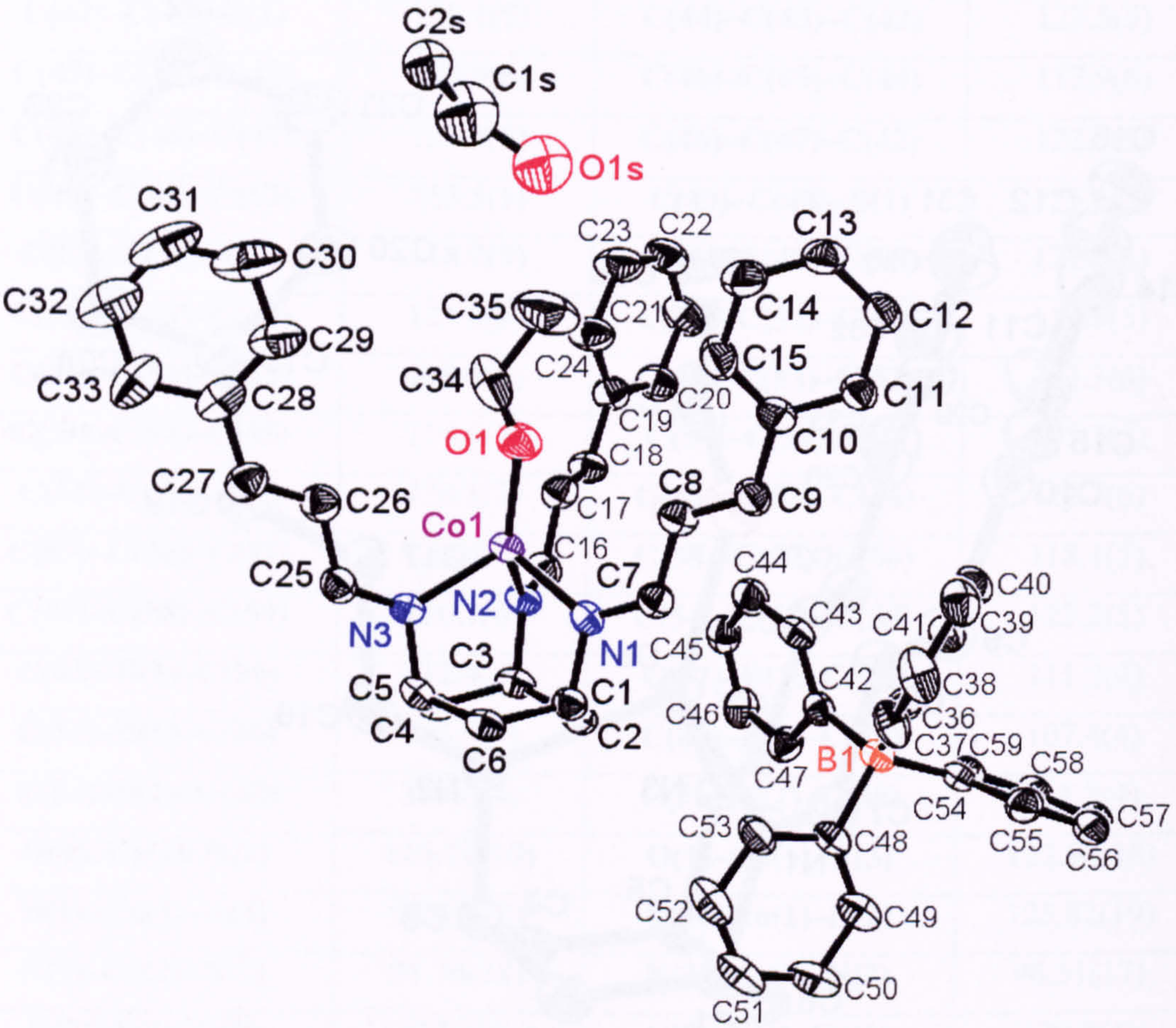

Figure A3.2: An ORTEP representation (30% probability ellipsoids) of $[Co(TCT)(OEt)]BPh_4 \cdot ½$ EtOH, H atoms omitted for clarity.

A3 a Personal communication from Dr. Stephen J. Archibald – concerning the structure of the [disordered] solvent molecule.

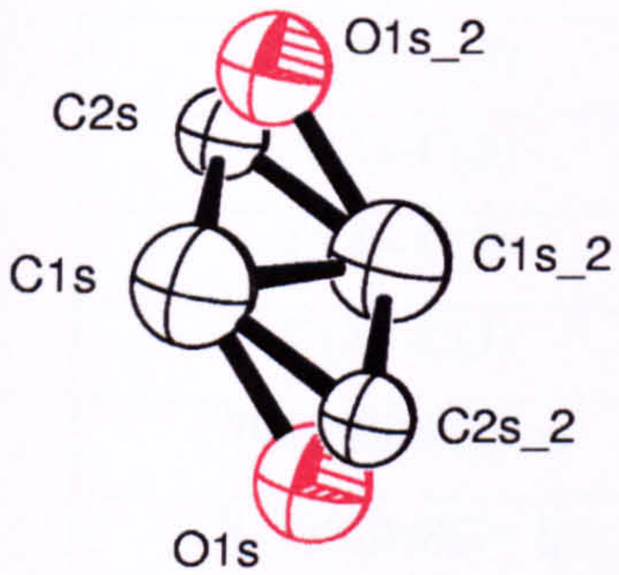

This is the model of the disordered ethanol. The first thing is: the max shift is not due to the solvent but the cobalt. A very large number of cycles (as in hundreds) were run at the time to get the structure to converge—which it does—but after that the first cycle always gives a shift of –0.013. There does not seem to be any way to change this (the overall shift is 0.00) but any other suggestions are welcome.

The main problem with this data set is the poor and weak nature of the data. The very high R_{int} value reflects this. The problems flagged by the checking software relate to this. The shift is not flagged by the checking software which has a larger threshold for these (max shift / esd less than ±0.05 is permitted).

Another version of the data file with the additional restraint (solvent) suggested for the solvent has been prepared. More changes can be made for the final version if required (see below).

One thing to be said is that data has been collected on a number of these crystals and the sample given were all of low quality and weak diffractors. To obtain the solution / refinement and to satisfactorily model the disordered solvent was gratifying.

Problems flagged by checkcif and platon data check

Potentially serious: The R_{int} value exceeds the limit of 0.20 (but only just).

Ratio of observed to unique reflections is low (24%).

One way to solve these problems would be to exclude some of the high angle data and cut it back from the $2\theta = 70°$ initially collected out to. This would increase the percentage of observed reflections (for example the data beyond 65 or 60° could be removed).

Stephen Archibald.

A4 Crystal data and structure refinement for [Co(TCT)(OPh)]BAr^F_4

Identification code	sja3_02
Empirical formula	$C_{71}H_{50}BCoF_{24}N_3O$
Formula weight	1486.88
Temperature	150(2) K
Wavelength	0.71073 Å
Crystal system	triclinic
Space group	$P\bar{1}$
Unit cell dimensions	a = 10.1059(14) Å α = 74.071(10)°
	b = 13.7856(18) Å β = 78.478(11)°
	c = 26.066(4) Å γ = 76.473(11)°
Volume	3359.2(8) $Å^3$
Z	2
Density (calculated)	1.470 Mg / m^3
Absorption coefficient	0.369 mm^{-1}
F(000)	1506
Crystal size	0.1 × 0.2 × 0.2 mm^3
Theta range for data collection	2.27 to 30.00°
Index ranges	$-13 \le h \le 14, -19 \le k \le 19, -36 \le l \le 36$
Reflections collected	56852
Independent reflections	19540 [*R*(int) = 0.1154]
Completeness to theta = 30.00°	99.6 %
Refinement method	Full-matrix least-squares on F^2
Data / restraints / parameters	19540 / 0 / 910
Goodness-of-fit on F^2	0.708
Final *R* indices [$I > 2$ sigma (I)]	$R1 = 0.0563$, $wR2 = 0.1214$
R indices (all data)	$R1 = 0.1745$, $wR2 = 0.1504$
Largest diff. peak and hole	0.685 and –0.675 $e.Å^{-3}$

Table A4.1: Bond lengths (/ Å) and angles (/ °) for [Co(TCT)(OPh)]BAr^F_4.

Co(1)–O(1)	1.875(2)	**Co(1)–N(1)**	2.000(3)
Co(1)–N(3)	2.007(3)	**Co(1)–N(2)**	2.017(3)
O(1)–C(34)	1.329(4)	**N(2)–C(16)**	1.290(4)
N(2)–C(3)	1.486(4)	**N(3)–C(25)**	1.294(4)
N(3)–C(5)	1.473(4)	**C(4)–C(3)**	1.528(5)
C(4)–C(5)	1.540(5)	**C(5)–C(6)**	1.533(4)
C(2)–C(3)	1.523(4)	**C(2)–C(1)**	1.525(5)
C(9)–C(8)	1.339(4)	**C(9)–C(10)**	1.464(5)
N(1)–C(7)	1.283(4)	**N(1)–C(1)**	1.473(4)
C(25)–C(26)	1.423(5)	**C(16)–C(17)**	1.421(5)
C(8)–C(7)	1.424(5)	**C(17)–C(18)**	1.340(5)
C(1)–C(6)	1.530(5)	**C(18)–C(19)**	1.464(6)
C(34)–C(35)	1.394(5)	**C(34)–C(39)**	1.397(5)
F(4)–C(47)	1.336(4)	**F(3)–C(46)**	1.336(4)
C(41)–C(40)	1.395(4)	**C(41)–C(42)**	1.398(4)
F(1)–C(46)	1.354(4)	**C(45)–C(44)**	1.397(4)
C(45)–C(40)	1.406(4)	**C(40)–B(1)**	1.653(5)
C(43)–C(44)	1.379(5)	**C(43)–C(42)**	1.393(5)
F(5)–C(47)	1.311(4)	**C(47)–F(6)**	1.336(4)
C(47)–C(44)	1.486(5)	**C(39)–C(38)**	1.381(5)
C(37)–C(36)	1.369(7)	**C(37)–C(38)**	1.377(6)
C(42)–C(46)	1.473(5)	**C(35)–C(36)**	1.384(6)
C(11)–C(12)	1.402(6)	**C(11)–C(10)**	1.409(5)
C(46)–F(2)	1.346(4)	**C(10)–C(15)**	1.383(5)
C(12)–C(13)	1.351(7)	**C(26)–C(27)**	1.336(5)
C(56)–C(57)	1.402(4)	**C(56)–C(61)**	1.413(4)
C(56)–B(1)	1.640(5)	**C(64)–C(69)**	1.398(4)
C(64)–C(65)	1.400(4)	**C(64)–B(1)**	1.649(5)
C(13)–C(14)	1.391(6)	**C(27)–C(28)**	1.451(5)
C(48)–C(49)	1.394(5)	**C(48)–C(53)**	1.400(4)
C(48)–B(1)	1.643(5)	**C(14)–C(15)**	1.384(5)
C(28)–C(33)	1.373(5)	**C(28)–C(29)**	1.386(5)

C(33)–C(32)	1.394(6)	**C(29)–C(30)**	1.378(6)
C(24)–C(19)	1.392(7)	**C(24)–C(23)**	1.394(7)
C(20)–C(19)	1.371(7)	**C(20)–C(21)**	1.388(9)
C(23)–C(22)	1.398(10)	**F(22)–C(71)**	1.291(4)
C(58)–C(59)	1.383(4)	**C(58)–C(57)**	1.393(4)
C(58)–C(62)	1.483(5)	**C(61)–C(60)**	1.385(4)
C(67)–C(68)	1.371(4)	**C(67)–C(66)**	1.398(5)
C(69)–C(68)	1.396(4)	**C(59)–C(60)**	1.388(5)
C(66)–C(65)	1.385(4)	**C(66)–C(70)**	1.482(5)
C(68)–C(71)	1.481(5)	**C(60)–C(63)**	1.498(4)
C(71)–F(23)	1.333(4)	**C(71)–F(24)**	1.356(4)
F(17)–C(63)	1.335(4)	**F(18)–C(63)**	1.333(4)
F(16)–C(63)	1.341(4)	**C(49)–C(50)**	1.396(5)
F(14)–C(62)	1.293(4)	**F(13)–C(62)**	1.302(4)
F(20)–C(70)	1.323(4)	**C(52)–C(51)**	1.381(5)
C(52)–C(53)	1.399(5)	**C(52)–C(55)**	1.488(5)
F(19)–C(70)	1.284(4)	**F(15)–C(62)**	1.324(5)
C(70)–F(21)	1.274(4)	**C(55)–F(12)**	1.306(5)
C(55)–F(10)	1.335(5)	**C(55)–F(11)**	1.343(5)
C(51)–C(50)	1.382(5)	**C(50)–C(54)**	1.484(6)
C(31)–C(30)	1.358(6)	**C(31)–C(32)**	1.361(6)
C(54)–F(7)	1.297(5)	**C(54)–F(9)**	1.306(5)
C(54)–F(8)	1.325(5)	**C(22)–C(21)**	1.360(11)
O(1)–Co(1)–N(1)	123.61(10)	**O(1)–Co(1)–N(3)**	114.88(11)
N(1)–Co(1)–N(3)	95.06(11)	**O(1)–Co(1)–N(2)**	124.43(11)
N(1)–Co(1)–N(2)	97.56(11)	**N(3)–Co(1)–N(2)**	94.19(11)
C(34)–O(1)–Co(1)	129.0(2)	**C(16)–N(2)–C(3)**	119.0(3)
C(16)–N(2)–Co(1)	129.5(2)	**C(3)–N(2)–Co(1)**	111.3(2)
C(25)–N(3)–C(5)	119.5(3)	**C(25)–N(3)–Co(1)**	127.5(2)
C(5)–N(3)–Co(1)	113.0(2)	**C(3)–C(4)–C(5)**	114.3(3)
N(3)–C(5)–C(6)	110.7(2)	**N(3)–C(5)–C(4)**	110.5(3)
C(6)–C(5)–C(4)	110.0(3)	**C(3)–C(2)–C(1)**	115.0(3)
C(8)–C(9)–C(10)	125.8(4)	**C(7)–N(1)–C(1)**	120.2(3)

C(7)–N(1)–Co(1)	127.5(2)	C(1)–N(1)–Co(1)	112.20(18)
N(3)–C(25)–C(26)	122.5(3)	N(2)–C(16)–C(17)	123.6(3)
C(9)–C(8)–C(7)	122.0(3)	C(18)–C(17)–C(16)	122.0(4)
N(1)–C(1)–C(2)	111.3(3)	N(1)–C(1)–C(6)	109.4(3)
C(2)–C(1)–C(6)	111.2(3)	C(17)–C(18)–C(19)	127.6(5)
C(1)–C(6)–C(5)	114.4(3)	N(2)–C(3)–C(2)	111.4(2)
N(2)–C(3)–C(4)	110.7(3)	C(2)–C(3)–C(4)	110.3(3)
N(1)–C(7–)C(8)	122.2(3)	O(1)–C(34)–C(35)	119.5(3)
O(1)–C(34)–C(39)	122.4(3)	C(35)–C(34)–C(39)	118.1(3)
C(40)–C(41)–C(42)	122.5(3)	C(44)–C(45)–C(40)	122.8(3)
C(41)–C(40)–C(45)	115.5(3)	C(41)–C(40)–B(1)	123.4(3)
C(45)–C(40)–B(1)	121.0(3)	C(44)–C(43)–C(42)	118.7(3)
F(5)–C(47)–F(6)	105.7(3)	F(5)–C(47)–F(4)	106.6(3)
F(6)–C(47)–F(4)	104.9(3)	F(5)–C(47)–C(44)	114.5(3)
F(6)–C(47)–C(44)	111.9(3)	F(4)–C(47)–C(44)	112.4(3)
C(43)–C(44)–C(45)	120.2(3)	C(43)–C(44)–C(47)	119.1(3)
C(45)–C(44)–C(47)	120.7(3)	C(38)–C(39)–C(34)	120.6(4)
C(36)–C(37)–C(38)	119.2(4)	C(43)–C(42)–C(41)	120.4(3)
C(43)–C(42)–C(46)	118.0(3)	C(41)–C(42)–C(46)	121.6(3)
C(36)–C(35)–C(34)	120.2(4)	C(12)–C(11)–C(10)	119.1(4)
F(3)–C(46)–F(2)	105.5(3)	F(3)–C(46)–F(1)	105.2(3)
F(2)–C(46)–F(1)	105.6(3)	F(3)–C(46)–C(42)	114.1(3)
F(2)–C(46)–C(42)	112.4(3)	F(1)–C(46)–C(42)	113.1(3)
C(15)–C(10)–C(11)	118.8(4)	C(15)–C(10)–C(9)	122.7(3)
C(11)–C(10)–C(9)	118.4(4)	C(37)–C(38)–C(39)	120.6(4)
C(13)–C(12)–C(11)	120.8(4)	C(27)–C(26)–C(25)	122.8(3)
C(57)–C(56)–C(61)	113.6(3)	C(57)–C(56)–B(1)	122.0(3)
C(61)–C(56)–B(1)	124.2(3)	C(69)–C(64)–C(65)	115.4(3)
C(69)–C(64)–B(1)	124.5(3)	C(65)–C(64)–B(1)	120.0(3)
C(12)–C(13)–C(14)	120.8(4)	C(26)–C(27)–C(28)	126.9(3)
C(49)–C(48)–C(53)	115.6(3)	C(49)–C(48)–B(1)	124.4(3)
C(53)–C(48)–B(1)	120.0(3)	C(15)–C(14)–C(13)	119.2(5)
C(33)–C(28)–C(29)	117.3(4)	C(33)–C(28)–C(27)	122.7(3)
C(29)–C(28)–C(27)	120.0(3)	C(56)–B(1)–C(48)	109.8(2)

C(56)–B(1)–C(64)	110.4(3)	**C(48)–B(1)–C(64)**	107.3(3)
C(56)–B(1)–C(40)	111.8(3)	**C(48)–B(1)–C(40)**	109.3(3)
C(64)–B(1)–C(40)	108.1(2)	**C(28)–C(33)–C(32)**	120.8(4)
C(10)–C(15)–C(14)	121.3(4)	**C(30)–C(29)–C(28)**	121.9(4)
C(19)–C(24)–C(23)	121.3(6)	**C(37)–C(36)–C(35)**	121.2(4)
C(19)–C(20)–C(21)	121.1(8)	**C(20)–C(19)–C(24)**	118.8(5)
C(20)–C(19)–C(18)	119.4(6)	**C(24)–C(19)–C(18)**	121.8(5)
C(24)–C(23)–C(22)	117.6(7)	**C(59)–C(58)–C(57)**	120.6(3)
C(59)–C(58)–C(62)	118.9(3)	**C(57)–C(58)–C(62)**	120.4(3)
C(60)–C(61)–C(56)	123.4(3)	**C(68)–C(67)–C(66)**	118.1(3)
C(68)–C(69)–C(64)	121.8(3)	**C(58)–C(59)–C(60)**	117.8(3)
C(65)–C(66)–C(67)	120.0(3)	**C(65)–C(66)–C(70)**	120.4(3)
C(67)–C(66)–C(70)	119.6(3)	**C(67)–C(68)–C(69)**	121.5(3)
C(67)–C(68)–C(71)	119.3(3)	**C(69)–C(68)–C(71)**	119.1(3)
C(58)–C(57)–C(56)	123.7(3)	**C(61)–C(60)–C(59)**	120.9(3)
C(61)–C(60)–C(63)	121.6(3)	**C(59)–C(60)–C(63)**	117.5(3)
F(22)–C(71)–F(23)	108.3(3)	**F(22)–C(71)–F(24)**	104.6(3)
F(23)–C(71)–F(24)	101.2(3)	**F(22)–C(71)–C(68)**	115.0(3)
F(23)–C(71)–C(68)	113.9(3)	**F(24)–C(71)–C(68)**	112.5(3)
C(66)–C(65)–C(64)	123.2(3)	**C(48)–C(49)–C(50)**	122.7(3)
F(18)–C(63)–F(17)	106.7(3)	**F(18)–C(63)–F(16)**	105.6(3)
F(17)–C(63)–F(16)	105.2(3)	**F(18)–C(63)–C(60)**	113.9(3)
F(17)–C(63)–C(60)	112.6(3)	**F(16)–C(63)–C(60)**	112.2(3)
C(51)–C(52)–C(53)	119.9(3)	**C(51)–C(52)–C(55)**	122.3(3)
C(53)–C(52)–C(55)	117.8(4)	**C(52)–C(53)–C(48)**	122.5(3)
F(21)–C(70)–F(19)	108.4(4)	**F(21)–C(70)–F(20)**	103.2(4)
F(19)–C(70)–F(20)	101.0(4)	**F(21)–C(70)–C(66)**	114.2(3)
F(19)–C(70)–C(66)	114.9(3)	**F(20)–C(70)–C(66)**	113.8(3)
F(14)–C(62)–F(13)	108.9(4)	**F(14)–C(62)–F(15)**	102.0(3)
F(13)–C(62)–F(15)	102.4(4)	**F(14)–C(62)–C(58)**	115.7(3)
F(13)–C(62)–C(58)	114.3(3)	**F(15)–C(62)–C(58)**	112.1(4)
F(12)–C(55)–F(10)	107.3(4)	**F(12)–C(55)–F(11)**	105.9(4)
F(10)–C(55)–F(11)	105.1(3)	**F(12)–C(55)–C(52)**	114.2(3)
F(10)–C(55)–C(52)	112.0(4)	**F(11)–C(55)–C(52)**	111.7(3)

C(52)–C(51)–C(50)	119.2(3)	**C(51)–C(50)–C(49)**	120.1(3)
C(51)–C(50)–C(54)	120.0(3)	**C(49)–C(50)–C(54)**	119.9(4)
C(30)–C(31)–C(32)	120.3(4)	**F(7)–C(54)–F(9)**	108.4(5)
F(7)–C(54)–F(8)	103.8(4)	**F(9)–C(54)–F(8)**	104.0(4)
F(7)–C(54)–C(50)	114.7(3)	**F(9)–C(54)–C(50)**	112.4(3)
F(8)–C(54)–C(50)	112.8(4)	**C(31)–C(30)–C(29)**	119.5(4)
C(31)–C(32)–C(33)	120.1(4)	**C(21)–C(22)–C(23)**	121.6(7)
C(22)–C(21)–C(20)	119.4(8)		

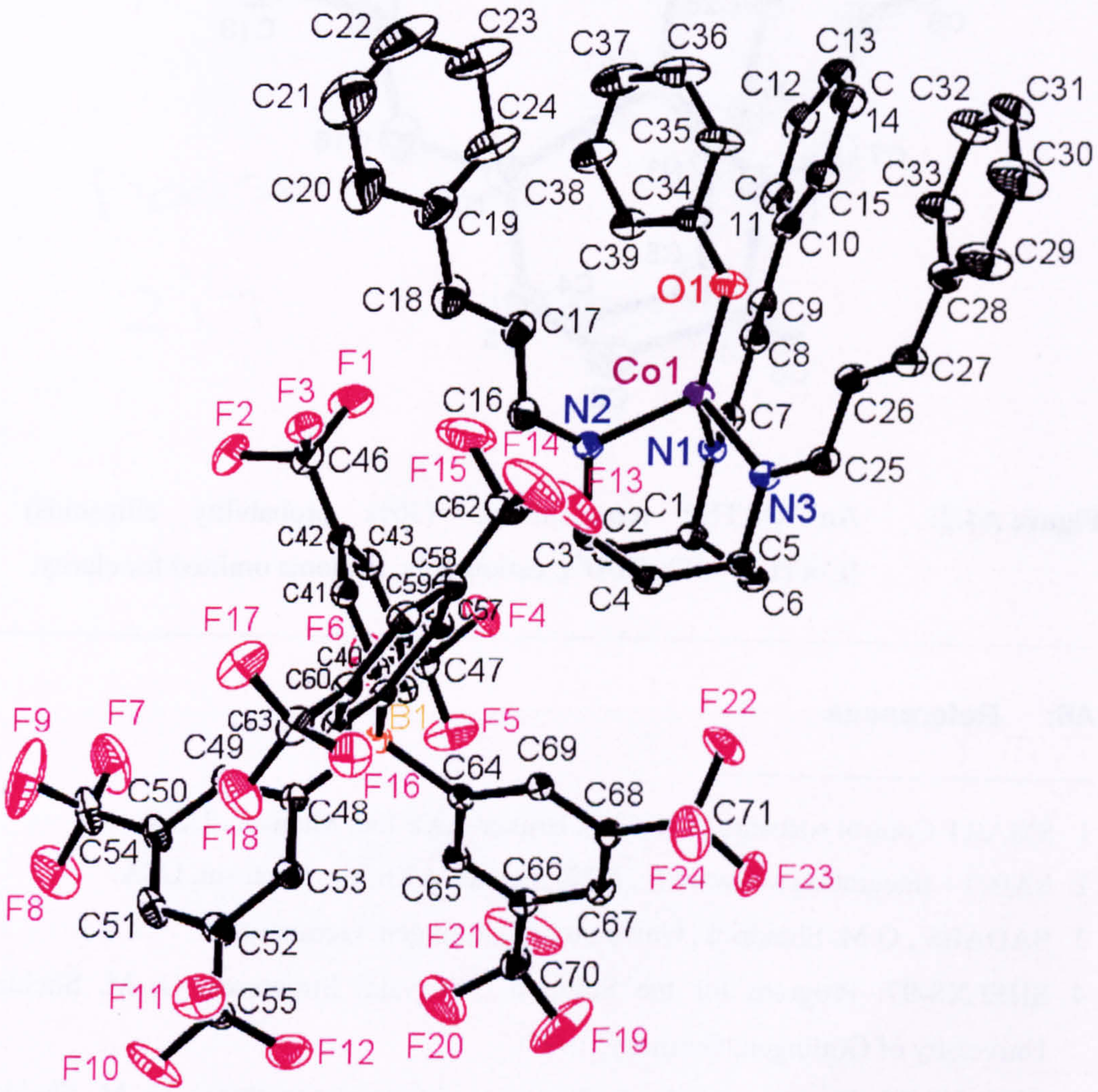

Figure A4.1: An ORTEP representation (30% probability ellipsoids) of $[Co(TCT)(OPh)]BAr^{F}_{4}$, H atoms omitted for clarity.

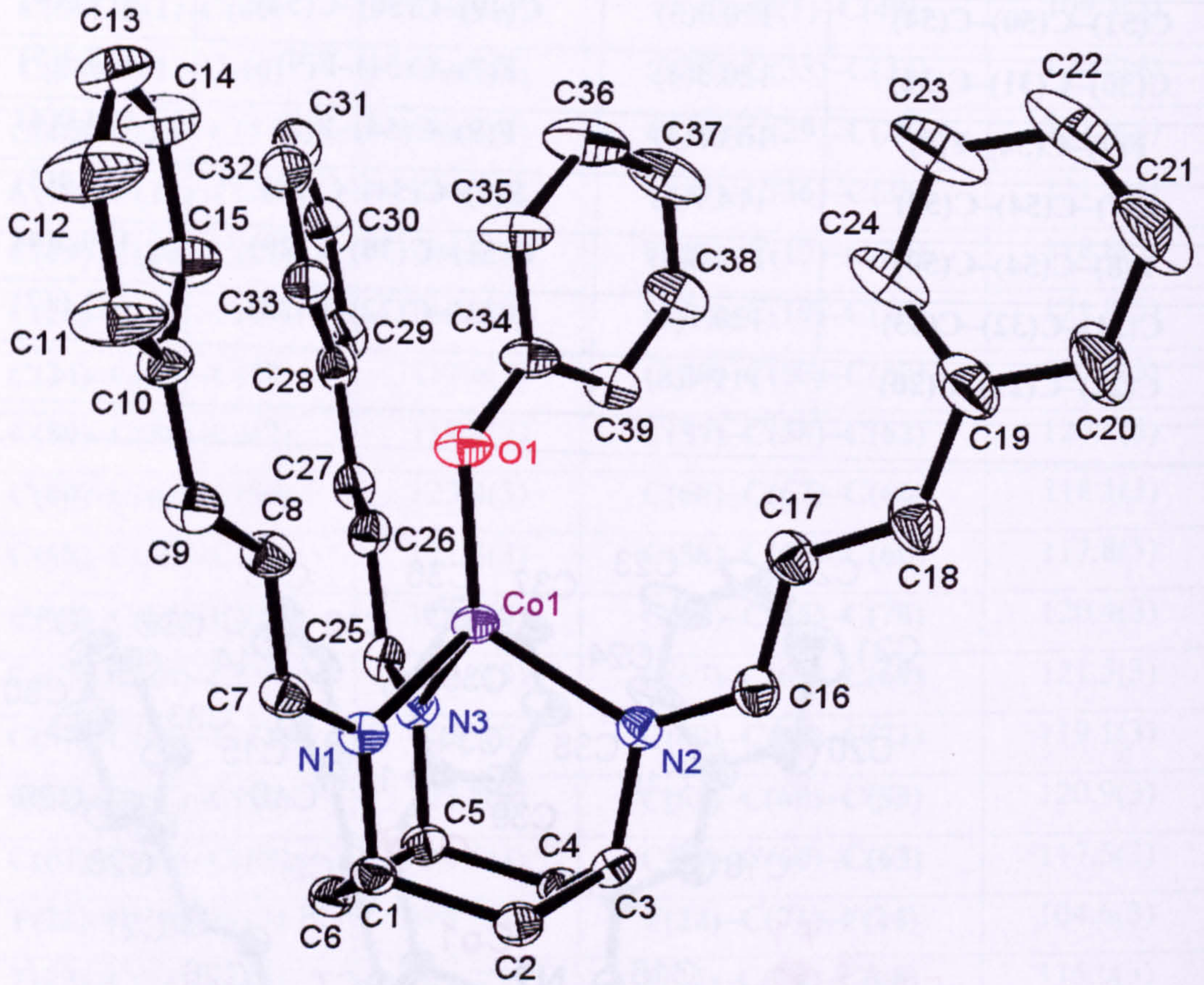

Figure A4.2: An ORTEP representation (30% probability ellipsoids) of $[Co(TCT)(OPh)]BAr^{F}_{4}$, cation only, H atoms omitted for clarity.

A5: References

1 SMART Control software (v. 5.625), Bruker-AXS Inc, Madison, USA.

2 SAINT+ Integration software (v. 6.22), Bruker-AXS Inc, Madison, USA.

3 SADABS , G.M. Sheldrick, University of Göttingen, Germany.

4 SHELXS-97: Program for the Solution of Crystal Structures, G. M. Sheldrick, University of Göttingen, Germany, 1997

5 SHELXL-97: Program for the Refinement of Crystal Structures, G. M. Sheldrick, University of Göttingen, Germany, 1997.

6 C. K. Johnson, 1976, ORTEP-11, *A FORTRAN Thermal-Ellipsoid Plot Program*, Report ORNL-5138, Oak Ridge National Laboratory, Oak Ridge, Tennessee.

Publications

"Preparation of cationic cobalt phenoxide and ethoxide complexes and their reversible reaction with carbon dioxide", Stephen J. Archibald, Simon P. Foxon, Jonathan D. Freeman, James E. Hobson, Robin N. Perutz and Paul H. Walton, *J. Chem. Soc., Dalton Trans.*, 2002, 2797 – 2799.

Pages 218 – 220 (numbered as presented in journal).

DALTON COMMUNICATION

Preparation of cationic cobalt phenoxide and ethoxide complexes and their reversible reaction with carbon dioxide

Stephen J. Archibald,[a] Simon P. Foxon,[b] Jonathan D. Freeman,[b] James E. Hobson,[b] Robin N. Perutz*[b] and Paul H. Walton*[b]

[a] *Department of Chemistry, University of Hull, Cottingham Road, Hull, England HU6 7RX*
[b] *Department of Chemistry, University of York, Heslington, York, England Y010 5DD. E-mail: phw2@york.ac.uk*

Received 13th May 2002, Accepted 12th June 2002
First published as an Advance Article on the web 21st June 2002

The complexes [Co(TCT)(OR)]BPh_4 (R = Et, Ph; TCT = *cis*,*cis*-1,3,5-tris(cinnamylideneamino)cyclohexane) have been prepared and characterised by X-ray diffraction; in coordinating solvents both complexes react reversibly with carbon dioxide to form organocarbonate complexes.

Metal alkoxide complexes find use in a variety of reactions, including ring-opening polymerisation of lactides,[1] transesterification,[2] and copolymerisation of carbon dioxide and epoxides.[3] In addition, recent work on modelling the active site of horse liver alcohol dehydrogenase has involved the synthesis of monomeric zinc alkoxides.[4] Monomeric, cationic metal alkoxide complexes are difficult to isolate due to potential hydride abstraction,[5] formation of bridged alkoxy metal species, and the tendency of other anions to coordinate to the metal ion to give neutral complexes. We have previously reported evidence that the monomeric complex [Co^{II}(TCT)(OEt)]BPh_4 catalyses the decomposition of dialkylpyrocarbonates.[6] Here we report the analogous cobalt(II) phenoxide complex, and show that both complexes react reversibly with CO_2. We also report the isolation and structure of the cobalt ethoxide — the first structure of a monomeric, cationic cobalt(II) alkoxide.

[Co(TCT)(OPh)]BPh_4 (**1**) and [Co(TCT)(OEt)]BPh_4 (**2**) were prepared in good yield by stirring a dichloromethane solution of [Co(TCT)Cl]BPh_4 with solid $NaOPh{\cdot}3H_2O$, and [Co(TCT)(NO_3)]BPh_4 with a solution of NaOEt in ethanol, respectively (eqns. (1) and (2), Scheme 1). The complexes could also be

$$[Co(TCT)Cl]BPh_4 \xrightarrow[CH_2Cl_2]{NaOPh} [Co(TCT)(OPh)]BPh_4 \quad (1)$$
1

$$[Co(TCT)(NO_3)]BPh_4 \xrightarrow[CH_2Cl_2]{NaOEt/EtOH} [Co(TCT)(OEt)]BPh_4 \quad (2)$$
2

TCT =

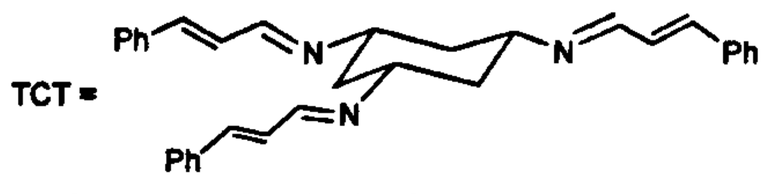

Scheme 1 Synthesis of Co–TCT complexes.

prepared by addition of phenol or ethanol to a solution of [Co(TCT)(OH)]BPh_4. Both complexes are stable to air in the solid state.†

The crystal structure of **2** is shown in Fig. 1.‡ In both, the cobalt adopts a C_{3v} coordination geometry, with the three nitrogen atoms of the TCT ligand capping one face of the metal. The fourth coordination site is occupied by the aryloxide/alkoxide group, which is bound *via* the oxygen atom. The C–O vector of the ethoxide group is directed between two of the cinnamyl arms, and "*trans*" to the third. The cinnamyl arms of the TCT ligand create a hydrophobic pocket that encapsulates the aryloxide/alkoxide group. There are no contacts less than 4.4 Å between the aromatic rings of the TCT and phenoxide ligands in **1**, nor are there any contacts less than

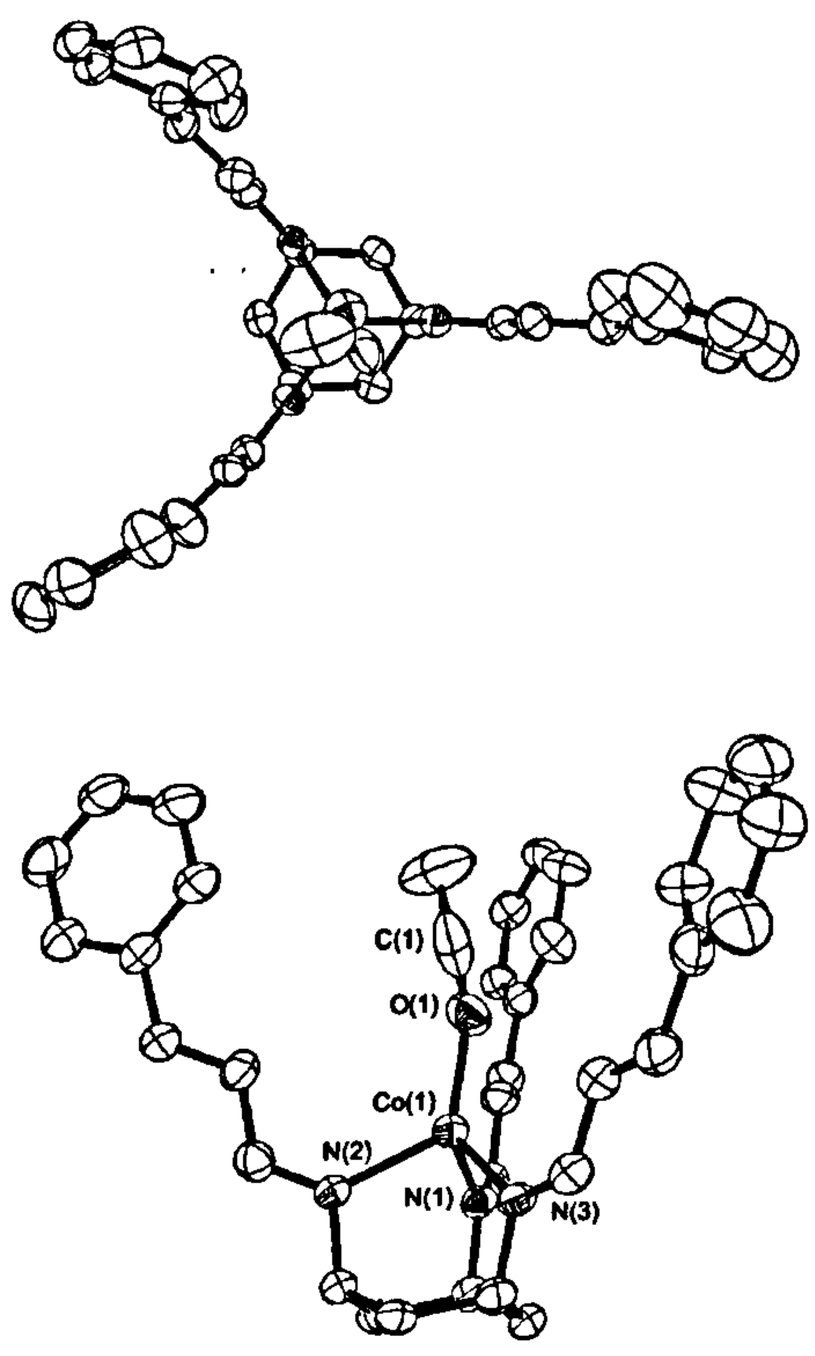

Fig. 1 ORTEP[10] (50% probability ellipsoids) views of **2**. Selected bond lengths/Å: Co–O 1.867(4), Co–N1 2.014(4), Co–N2 2.027(4), Co–N3 2.019(4); Bond angles/°: O–Co–N1 115.1(2), O–Co–N2 125.8(2), O–Co–N3 123.0(2), Co–O–C1 136.8(5). BPh_4^- and H atoms deleted for clarity.

4.7 Å between the cations, indicating that there are no π–π interactions.

The visible spectrum of **1** in dichloromethane (Fig. 2a) shows absorptions at 507, 523 (sh), 561 and 641 nm. The bands are shifted by less than 1 nm upon changing the solvent to [9CH_2Cl_2 : 1MeOH] v/v or [9CH_2Cl_2 : 1EtOH] v/v. On dissolving **1** in CH_3CN, the band previously at λ = 507 nm shifts to λ = 517 nm, but the remaining bands are hardly affected. The insensitivity of the spectrum to solvent, and the absorption coefficients (450–600 $dm^3\ mol^{-1}\ cm^{-1}$), suggest that the absorptions are predominantly due to d–d transitions.

A dichloromethane solution of **1** showed no colour change or alteration in its visible spectrum after passing a stream of carbon dioxide through it for extended periods. When a stream of carbon dioxide (99.995%) was passed through a solution of **1** dissolved in the mixed solvent [9CH_2Cl_2 : 1MeOH] v/v, an immediate colour change from reddish-purple to orange

DOI: 10.1039/b204560e

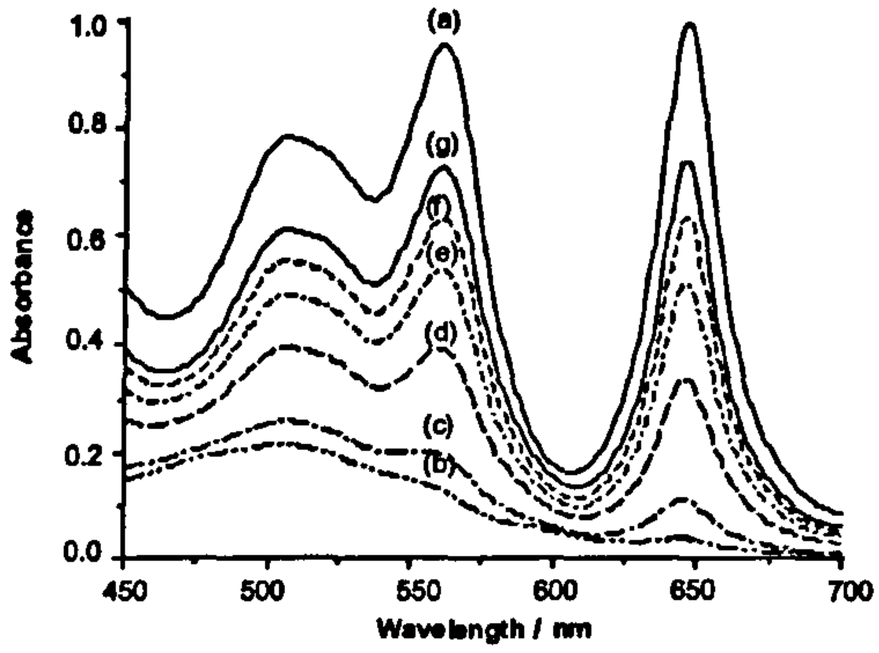

Fig. 2 UV/vis spectra showing (a) **1** under N_2 initially, (b) CO_2 bubbled for 60 s, (c)–(g) N_2 bubbled for 30, 45, 60, 90 and 120 s.

occurred, which could be monitored by visible spectroscopy (Fig. 2). The structure of the visible spectrum changes dramatically, and the intensities of the absorptions decrease substantially after reaction with carbon dioxide (Fig. 2b). The new spectrum exhibits absorptions at 471 nm (sh), 501 nm, 556 nm (sh) and 644 nm. Reaction is still observed on stirring with a partial pressure of only 10 Torr CO_2. Upon passing a stream of inert gas (N_2 or Ar) through the carbonated solution, the colour reverted to reddish-purple, and the original visible spectrum for **1** was obtained (Figs. 2c–g). The carbonated species **3**, when protected from light, does not decolourise in solution over extended periods.

IR spectra show the appearance of bands at 1327 and 1093 cm^{-1} upon reaction with carbon dioxide. Other bands shift slightly (Fig. 3b,d) and a further new band may be present at

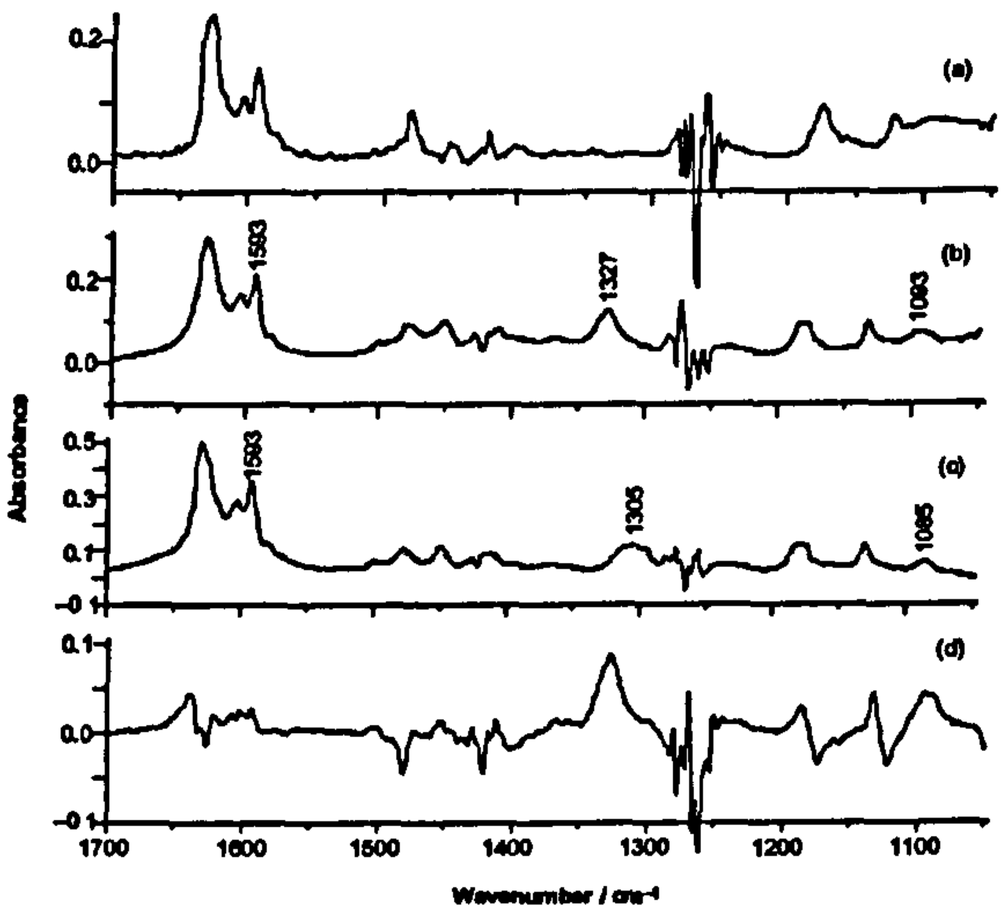

Fig. 3 Solution ([$9CH_2Cl_2$: 1MeOH] v/v) FTIR spectra of **1** (a) before CO_2, (b) after $C^{16}O_2$, (c) after $C^{18}O_2$, (d) b − a. The regions 1250–1280 and 1390–1440 cm^{-1} are noisy due to strong solvent absorption.

1593 cm^{-1}, but is masked by a precursor band. The IR spectrum after $C^{18}O_2$ exposure (Fig. 3c) shows that the absorption at 1327 cm^{-1} shifts to 1305 cm^{-1}, and the absorption at 1093 cm^{-1} shifts to 1085 cm^{-1}.

The IR spectrum of **3** correlates very well with three of the four bands characteristic of bidentate organocarbonate complexes (≈1560 cm^{-1}, ≈1460 cm^{-1}, ≈1360 cm^{-1} and ≈1085 cm^{-1}).[7] The solvent "cut-off" region observed between 1440–1390 cm^{-1} could have obscured a fourth band. An analogous experiment in CD_3CN instead of CH_2Cl_2–MeOH gave bands at 1503, 1363 and 1224 cm^{-1}, and a possible band at 1472 cm^{-1}. (Solvent cut-off is < 1110 cm^{-1}.) For both solvents the IR data are consistent with a bidentate organocarbonate complex, but a monodentate complex cannot be excluded. There is already extensive documentation for the conversion of alkyl/aryloxides and their precursors to alkyl/arylcarbonate complexes, but the facile reversible reaction with CO_2 at room temperature is remarkable.[7,8] A very recent paper describes the reaction of CO_2 and cobalt(II) perchlorate with a dinucleating ligand in MeOH–CH_3CN to form a dicobalt methylcarbonato complex. A methoxide complex is a presumed intermediate.[9]

Evidence which shows that CO_2 inserts reversibly into the Co–O bond of complex **2** as well as **1** is provided by visible spectroscopy.§ A solution of **2** in the mixed solvent [$9CH_2Cl_2$: 1EtOH] v/v shows a change in the visible spectrum after a stream of carbon dioxide is passed through it for 60 s. The solution progressively regains its original spectrum as a stream of Ar is passed through it.

The requirement for a coordinating solvent (S = MeOH/EtOH/CH_3CN) and the change in the IR spectrum from CH_2Cl_2–MeOH to CD_3CN indicate that solvent is coordinated in the product. A coordinating solvent may facilitate the bidentate coordination of phenylcarbonate to form a six-coordinate cobalt(II) complex from a pseudo-tetrahedral one. The reduced absorption coefficient of **3** compared to **1** is consistent with an octahedral geometry for **3**. We therefore assign the orange carbonated product **3** as [Co(TCT)(S)(η^2-O_2COPh)]BPh_4 (Scheme 2). Attempts to isolate **3** were unsuccessful. All

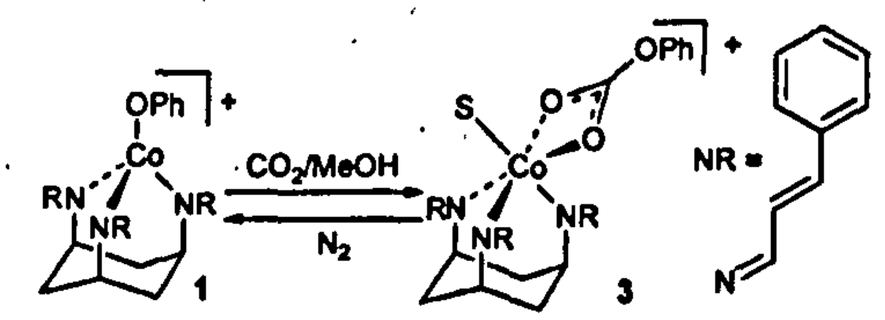

Scheme 2 Reversible reaction of **1** with CO_2.

attempts at crystallization yielded **1**. Evaporating the solvent with a stream of carbon dioxide also led to formation of **1**.

These studies demonstrate that monomeric cationic alkoxides and aryloxides of cobalt(II) may be isolated with the aid of suitable co-ligands that offer steric protection and a hydrophobic environment. The reversibility of the reaction with CO_2 offers potential for the development of a carbon dioxide sequestration catalyst. Studies by others of metal alkoxide complexes reacting with carbon dioxide show similarities to the work described here. The importance of an auxiliary ligand for coordination sphere expansion has been demonstrated by Saegusa's work on copper complexes.[8e] Furthermore complexes **1** and **3** resemble Vahrenkamp's Zn(Tp) complexes most closely in structure although the two systems differ in their activity towards carbon dioxide.[8e]

We wish to acknowledge EPSRC, BG Technology and Synetix for their financial support. We also wish to thank P. Elliot and N. Jasim for experimental assistance, and T. Dransfield for mass spectrometry.

Notes and references

† Complex **1** — [Co(TCT)Cl]BPh_4 (0.100 g, 0.11 mmol) was dissolved in CH_2Cl_2 (20 mL). NaOPh (0.050 g, 0.43 mmol) was added, and the mixture was stirred. Within 10 minutes the solution had turned purple. The mixture was left stirring overnight to ensure complete reaction. The solids were filtered off, the solution volume reduced to ≈10 mL, and cyclohexane (20 mL) added to give a reddish-purple precipitate. The liquid was filtered off, and the solid dried *in vacuo*. Yield: 74 mg (0.078 mmol, 69%). Crystals suitable for X-ray diffraction were formed as cyclohexane diffused into a solution of **1** in CH_2Cl_2. Elemental analysis: C: 79.71; H: 6.49; N: 4.19% (calculated for $C_{63}H_{58}N_3CoOB$: C: 80.24; H: 6.21; N: 4.46%). UV/vis: λ_{max}/nm (CH_2Cl_2) 641 (ε/dm^3 mol^{-1} cm^{-1} 600), 561 (530), 523 (sh), 507 (450). IR/cm^{-1}: [DRIFT] 8200 (br), 6250 (br), 4000 (br), d–d transitions; [FTIR] ν(CN) = 1625; ν(CC, aromatic) = 1602; ν(CC, alkenic) = 1590. Mass spectrum: [ESMS] m/z^+ = 623 (M^+); [HRFABMS] m/z^+ = 623.2345 (calculated for $C_{39}H_{38}N_3CoO$: 623.2347, difference = 0.2 mDa).

Complex **2** — [Co(TCT)(NO_3)]BPh_4 (0.50 g, 0.55 mmol) was dissolved in CH_2Cl_2 (30 mL) in a Schlenk tube under argon. To this was

added 3.75 mL of a solution of NaOEt in EtOH (37.5 mg, 0.55 mmol NaOEt); the resulting mixture was shaken for 15 minutes during which time a slight colour change was noted (dark purple to mid-purple). The solution was transferred through a cannula filter to a clean Schlenk tube, and the volatiles removed *in vacuo* to give a purple powder. Yield: 365 mg (0.41 mmol, 74%). Crystals suitable for X-ray diffraction were grown by slow evaporation of a concentrated solution of the complex in CH_2Cl_2/EtOH in a glovebox. UV/vis: λ_{max}/nm ($9CH_2Cl_2$: 1EtOH) 635 (ε/dm^3 mol^{-1} cm^{-1} 239), 554 (362), 486 (291). IR/cm^{-1}: [FTIR] ν(CN) = 1628, ν(CC, aromatic) = 1604, ν(CC, alkenic) = 1593. Mass spectrum: [ESMS] m/z^+ = 575 (M^+).

‡ Crystal structure determination of complex $(1)_2(C_6H_{12})_2(CH_2Cl_2)_3$. $C_{141}H_{146}B_2Cl_6Co_2N_6O_2$, M = 2308.2, triclinic, space group $P\bar{1}$, a = 18.31(3), b = 22.022(11), c = 17.219(6) Å, α = 98.97(4), β = 92.61(7), γ = 67.78(5)°, V = 6348 Å^3, T = 150 K, Z = 2, D_c = 1.208 Mg m^{-3}, μ(Mo-Kα) = 0.71069 mm^{-1}, F(000) = 2432, 12510 reflections measured, 11978 unique (R_{int} = 0.10152) which were used in all calculations. $R1$ = 0.0642 on $F > 4\sigma(F)$, $wR2$ = 0.2534 (all data).

Crystal structure determination of complex **2**·0.5(EtOH). $C_{60}H_{61}N_3CoO_{1.5}B$, M = 917.86, triclinic, space group $P\bar{1}$, a = 11.053(2), b = 15.812(3), c = 16.503(3) Å, α = 65.866(12), β = 86.349(14), γ = 72.640(14)°, V = 2506.6(8) Å^3, T = 150(2) K, Z = 2, D_c = 1.216 Mg m^{-3}, μ(Mo-Kα) = 0.387 mm^{-1}, F(000) = 972, 47525 reflections measured, 14596 unique (R_{int} = 0.1698) which were used in all calculations. $R1$ = 0.0901 on $F > 2\sigma(F)$, $wR2$ = 0.2510 on all data. CCDC reference numbers 185609 and 185610. See http://www.rsc.org/suppdata/dt/b2/b204560e/ for crystallographic data in CIF or other electronic format.

§ Reaction of **2** with CO_2: A solution of **2** (10 mg, 11 μmol) in 5 mL of the mixed solvent [$9CH_2Cl_2$: 1 EtOH] v/v was placed in a UV/vis cell under argon, and the visible spectrum recorded. A stream of CO_2 was passed through the solution for 60 s, and the new visible spectrum recorded. Nitrogen was bubbled through the solution and visible spectra were recorded at intervals of 1, 5, 7, 11 and 25 min. Absorption bands of reaction product of **2** with CO_2 λ/nm: 492(sh), 520, 550.

1 B. J. O'Keefe, M. A. Hillmyer and W. B. Tolman, *J. Chem. Soc., Dalton Trans.*, 2001, 2215.
2 J. Otera, *Chem. Rev.*, 1993, **93**, 1447.
3 (*a*) D. J. Darensbourg, M. W. Holtcamp, G. E. Struck, M. S. Zimmer, S. A. Niezgoda, P. Rainey, J. B. Robertson, J. D. Draper and J. H. Reibenspies, *J. Am. Chem. Soc.*, 1999, **121**, 107; (*b*) M. C. Cheng, E. B. Lobkovsky and G. W. Coates, *J. Am. Chem. Soc.*, 1998, **120**, 11018.
4 (*a*) R. Walz, K. Weis, M. Ruf and H. Vahrenkamp, *Chem. Ber./Rec.*, 1997, **130**, 975; (*b*) C. Bergquist and G. Parkin, *Inorg. Chem.*, 1999, **38**, 422.
5 R. Walz and H. Vahrenkamp, *Inorg. Chim. Acta*, 2001, **314**, 139.
6 B. Greener and P. H. Walton, *J. Chem. Soc., Dalton Trans.*, 1997, 3733.
7 (*a*) T. V. Ashworth and E. Singleton, *J. Chem. Soc., Chem. Commun.*, 1976, 204; (*b*) M. Kato and T. Ito, *Bull. Chem. Soc. Jpn.*, 1986, **59**, 285; (*c*) T. Ito, K. Hamamoto, S. Kurishima and K. Osakada, *J. Chem. Soc., Dalton Trans.*, 1990, 1645.
8 (*a*) T. Tsuda and T. Saegusa, *Inorg. Chem.*, 1972, **11**, 2561; T. Tsuda, S. Sanada, K. Ueda and T. Saegusa, *Inorg. Chem.*, 1976, **15**, 2329; (*b*) A. Immirzi and A. Musco, *Inorg. Chim. Acta*, 1977, **22**, L35; (*c*) R. J. Crutchley, J. Powell, R. Faggiani and C. J. L. Lock, *Inorg. Chim. Acta*, 1977, **24**, L15; (*d*) M. H. Chisholm, F. A. Cotton, M. W. Extine and W. W. Reichert, *J. Am. Chem. Soc.*, 1978, **100**, 1727; (*e*) M. Ruf, F. A. Schell, R. Walz and H. Vahrenkamp, *Chem. Ber./Rec.*, 1997, **126**, 703; (*f*) V. C. Arunasalam, I. Baxter, J. A. Darr, S. R. Drake, M. B. Hursthouse, K. M. A. Malik and D. M. P. Mingos, *Polyhedron*, 1998, **17**, 641.
9 Y. Dussart, C. Harding, P. Dalgaard, C. McKenzie, R. Kadirvelraj, V. McKee and J. Nelson, *J. Chem. Soc., Dalton Trans.*, 2002, 1704.
10 M. N. Burnett and C. K. Johnson, ORTEP3, Report ORNL-6895, Oak Ridge National Laboratory, Oak Ridge, TN, 1996.

Definitions

List of abbreviations:

Symbol:	Definition:		Context: (where appropriate)
A	Absorbance	(dimensionless)	UV / vis
A^{con}	contact coupling constant		NMR
A^{pc}	pseudo-contact coupling constant		NMR
Å	Ångstrom(s)	(1×10^{-10} m)	
Ac	acetyl	($-C(O)CH_3$)	
AIBN	Azo-*bis*-*Iso*-ButyroNitrile		
allyl	($-CH_2-CH=CH_2$)		
Ar	[generic] aryl		
Ar^F	3,5-bis(trifluoromethyl)phenyl		
arom	aromatic		NMR
Asp_x	Aspartate / aspartic acid residue (position in subscript)		
B	magnetic field		NMR
BINOL	BINaphthOL		
br	broad [peak]		NMR, IR
^{n}Bu	*n*-butyl	(n-C_4H_9)	
^{t}Bu	*tert*-butyl	($-C(CH_3)_3$)	
Bz	benzyl	($-CH_2Ph$)	
Bze	benzoate	($-OC(O)Ph$)	
BzTACH	*cis,cis*-1,3-diamino-5-{(4-tert-butyl)benzylamino} cyclohexane		
β	2nd atom in hydrocarbon chain		
c-	*cyclo*-		
CI	Chemical Ionisation		MS
cm^{-1}	wavenumbers		
COSY	COrrelation SpectroscopY		NMR
18-crown-6	1,4,7,10,13,16-hexa-oxo-cyclooctadecane, c-$[C_2H_4O]_6$		
Cy	cyclohexyl	(c-C_6H_{11})	
Cys_x	cysteine residue (position in subscript)		

d	doublet	NMR
d^n	d-electron configuration	
d_n	number of deuterium atoms incorporated [in solvent]	NMR
D	dextra-rotatory	
dcm	dichloromethane (CH_2Cl_2)	
dd	doublet of doublets	NMR
dt	doublet of triplets	NMR
DET	Di-Ethyl Tartrate	
DMSO	DiMethyl SulfOxide ($CH_3S(O)CH_3$)	
δ	chemical shift / parts per million	NMR
or	slight positive / negative charge	
or	4^{th} atom in hydrocarbon chain	
δ^{con}	contact contribution to chemical shift	
δ^{pc}	pseudo-contact contribution to chemical shift	
EI	Electron Impact ionisation	MS
ESI	Electro-Spray Ionisation	MS
Et	ethyl ($-C_2H_5$)	
EtOH	ethanol (C_2H_5OH)	
ε	extinction coefficient	UV / vis
or	5^{th} atom in hydrocarbon chain	
et al.	and co-workers / others	
FAB	Fast Atom Bombardment	FAB
FID	Flame Ionisation Detector	GC
or	Free Induction Decay	NMR
FTIR	Fourier-Transform Infra-Red [spectroscopy]	
g	gram(s)	
g_e	free electron "g" value	NMR
$g_{\parallel}$	component of "g" parallel to a given axis	NMR
$g_{\perp}$	component of "g" perpendicular to a given axis	NMR
$\bar{g}$	"g" averaged over all orientations	NMR
γ_I	nuclear magnetogyric ratio	NMR
γ_S	electronic magnetogyric ratio	NMR
GC	Gas Chromatography	
Glu_x	glutamate / glutamic acid residue (position in subscript)	
η	hapticity / denticity	ligands

h	hour(s)		
h	Planck constant		
ħ	$h / 2\pi$		
HCA	Human Carbonic Anhydrase		
His_x	histidine residue (position in subscript)		
HMTA	Hexa-Methylene-Tetra-Amine ($C_6H_{12}N_4$, atropine)		
HS	high spin [electron configuration]		
Hz	Hertz	(s^{-1})	
in situ	in reaction vessel / without isolation		
IR	Infra-Red [spectroscopy]		
J	proton-proton coupling	(Hz)	NMR
k	Boltzmann constant		
K	Kelvin		
K_{eq}	equilibrium constant		
λ	wavelength		
λ_{max}	absorption maximum		UV / vis
L	litre(s)		
<u>or</u>	levo-rotatory		
LA	diLActide		
LADH	Liver Alcohol DeHydrogenase [enzyme]		
Ln	generic lanthanide (La – Lu)		
LS	low spin [electron configuration]		
m	[complex] multiplet		NMR
M	moles per litre (mol L^{-1})		
μ_x	number of metal centres bridged		ligands
μ_0	permeability of a vacuum		
μ_B	magnetic field strngth		NMR
MBT	Mono-(4-*tert*-butyl)Benzylidene-Tach		
Me	methyl	($-CH_3$)	
MeOH	methanol	(CH_3OH)	
Mes	mesityl	($2,4,6-(CH_3)_3-C_6H_2$)	
meso	R,S [dilactide]		
min	minute(s)		
MOCVD	Metal Oxide Chemical Vapour Deposition		
mol	mole(s)		

MS	Mass Spectrometry	
m / z	mass-to-charge ratio	MS
NAD	Nicotinamide Adenine Dinucleotide	
nm	nanometre(s)	
NMR	Nuclear Magnetic Resonance [spectroscopy]	
nOeSY	nuclear Overhauser effect SpectroscopY	NMR
ν	stretching mode	IR
OTf	triflate (CF_3SO_3-)	
ω	position of double bond in fatty acid chain	
ω_0	spectral density	NMR
PET	Poly(Ethylene Terephthalate)	
Ph	phenyl	
pK_a	$-\log_{10}$[association constant]	
PLA	Poly(diLActide)	
^{i}Pr	*iso*-propyl (-$CH(CH_3)_2$)	
proTACH	TCT	
Ψ	generic symbol for an electronic wavefunction	
R	alkyl or aryl	
ρ	spin density [at nucleus]	NMR
s	second(s)	
or	singlet	NMR
S	[total] spin quantum number	
Sal	generic salicyl group, as component of imine	
Ser_x	serine residue (position in subscript)	
sh	shoulder	UV / vis
t	triplet	NMR
T	temperature	
TACH	*cis,cis*-1,3,5-triaminocyclohexane	
TBT	*cis,cis*-1,3,5-*tris*(benzylideneamino)cyclohexane	
TCT	*cis,cis*-1,3,5-*tris*(*E,E*-cinnamylideneamino)cyclohexane	
TDBA-H_3	*tris*(2-hydroxy-3,5-di-*tert*-butyl-benzyl)amine	
TDBA	deprotonated form of TDBA-H_3 (coordinated to titanium)	
TDMA-H_3	*tris*(2-hydroxy-3,5-dimethyl-benzyl)amine	
TDMA	deprotonated form of TDMA-H_3 (coordinated to titanium)	
tert / ^{t}	tertiary	

TPA-H_3	*tris*(2-hydroxy-phenyl)amine	
TPA	deprotonated form of TPA-H_3 (coordinated to titanium)	
Thr_x	threonine residue (position in subscript)	
T.O.F.	turnover frequency	
Trp_x	tryptophan residue (position in subscript)	
TREN	*tris*(2-aminoethyl)amine	
τ_c	correlation time	NMR
UV/vis	ultra-violet / visual [spectroscopy]	
Val_x	valine residue (position in subscript)	
VT	Variable Temperature	NMR
v/v	volume by volume	
$X^{(-)}$	generic negative ion, usually a halide	
°	degrees	

Journal abbreviations:

· *Acc. Chem. Res.*	Accounts of Chemical Research
· *Angew. Chem., Int. Ed. Eng.*	Angewandte Chemie, International Edition in English
· *Angew. Makromol. Chem.*	Die Angewandte Makromolekulare Chemie
· *Ann.*	Annalen(?)
· *Ann. Chem.*	Annalen der Chemie - Justus Liebig
· *Aust. J. Chem.*	Australian Journal of Chemistry
· *Biochemistry*	Biochemistry
· *Bull. Chem. Soc. Jpn.*	Bulletin of the Chemical Society of Japan
· *Chem. Abstr.*	Chemical Abstracts
· *Chem. Ber.-Recl.*	Chemische Berichte-Recueil
· *Chem. Br.*	Chemistry in Britain
· *Chem. Commun.*	Chemical Communications
· *Chem. Eur. J.*	Chemistry: a European Journal
· *Chem. Lett.*	Chemistry Letters
· *Chem. Lett. Japan.*	Chemistry Letters, Japanese (?)
· *Chem. Rev.*	Chemical Reviews
· *Coord. Chem. Rev.*	Coordination Chemistry Reviews
· *Faraday Discuss.*	Faraday Discussions
· *FEBS Lett.*	Federation of European Biochemical Societies Letters
· *Helv. Chim. Acta*	Helvetica Chimica Acta
· *Ind. Eng. Chem.*	Industrial and Engineering Chemistry
· *Inorg. Chem.*	Inorganic Chemistry
· *Inorg. Chem. Commun.*	Inorganic Chemistry Communications
· *Inorg. Chim. Acta*	Inorganica Chimica Acta
· *J. Am. Chem. Soc.*	Journal of the American Chemical Society
· *J. Chem. Soc.*	Journal of the Chemical Society
· *J. Chem. Soc., Chem. Comm.*	Journal of the Chemical Society, Chemical Communications
· *J. Chem. Soc., Dalton Trans.*	Journal of the Chemical Society, Dalton Transactions
· *J. Ind. Chem. Soc.*	Journal of the Indian Chemical Society

· *J. Inorg. Biochem.*	Journal of Inorganic Biochemistry
· *J. Mag. Res.*	Journal of Magnetic Resonance
· *J. Mater. Chem.*	Journal of Materials Chemistry
· *J. Org. Chem.*	Journal of Organic Chemistry
· *J. Organomet. Chem.*	Journal of Organometallic Chemistry
· *J. Phys. Chem. B*	Journal of Physical Chemistry B
· *J. Polym. Sci., Part A: Polym. Chem.*	Journal of Polymer Science Part A: Polymer Chemistry
· *Nature*	Nature (London)
· *New J. Chem.*	New Journal of Chemistry
· *Organometallics*	Organometallics
· *Polyhedron*	Polyhedron
· *Polymer*	Polymer
· *Polym. Bull.*	Polymer Bulletin
· *Polym. J.*	Polymer Journal
· *Research (London)*	Research (London)
· *Russ. J. Inorg. Chem.*	Russian Journal of Inorganic Chemistry
· *Science*	Science
· *Synth. React. Inorg. Met.-Org. Chem.*	Synthesis and Reactivity in Inorganic and Metal-Organic Chemistry
· *Synthesis*	Synthesis
· *Tetrahedron*	Tetrahedron
· *Tetrahedron Lett.*	Tetrahedron Letters